

# **Theoretical Studies on Noise Techniques for Measuring Physics Parameters of Accelerator Driven Systems**

*By*

**Y. S. Rana**

**Enrolment No: PHYS01200704022**

**Bhabha Atomic Research Centre, Mumbai**

*A thesis submitted to the*

*Board of Studies in Physical Sciences*

*In partial fulfillment of requirements*

*For the Degree of*

**DOCTOR OF PHILOSOPHY**

*Of*

**HOMI BHABHA NATIONAL INSTITUTE**



**March, 2013**


# Homi Bhabha National Institute

## Recommendations of the Viva Voce Board


As members of the Viva Voce Board, we certify that we have read the dissertation prepared by **Yeshpal Singh Rana** entitled "*Theoretical studies on noise techniques for measuring physics parameters of accelerator driven systems*" and recommend that it may be accepted as fulfilling the dissertation requirement for the Degree of Doctor of Philosophy.

  
Chairman- **Professor B. N. Jagatap**

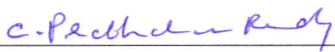
Date: 31/01/2014

  
Guide / Convener- **Professor S. B. Degweker**

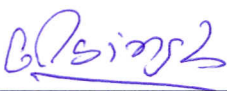
Date: 31/01/2014

  
Member 1- **Professor Y. S. Mayya**

Date: 31/01/2014

  
Member 2- **Professor C. P. Reddy**

Date: 31/01/2014

  
External Examiner- **Professor Om Pal Singh**

Date: 31/01/2014

External Examiner- **Professor Om Pal Singh**

Final approval and acceptance of this dissertation is contingent upon the candidate's submission of the final copies of the dissertation to HBNI.

I hereby certify that I have read this dissertation prepared under my direction and recommend that it may be accepted as fulfilling the dissertation requirement.

Date: 31/01/2014

Place: Mumbai



Professor S. B. Degweker

(Guide)

## STATEMENT BY AUTHOR

This dissertation has been submitted in partial fulfillment of requirements for an advanced degree at Homi Bhabha National Institute (HBNI) and is deposited in the Library to be made available to borrowers under rules of the HBNI.

Brief quotations from this dissertation are allowable without special permission, provided that accurate acknowledgement of source is made. Requests for permission for extended quotation from or reproduction of this manuscript in whole or in part may be granted by the Competent Authority of HBNI when in his or her judgment the proposed use of the material is in the interests of scholarship. In all other instances, however, permission must be obtained from the author.



**Y. S. Rana**

# DECLARATION

I, hereby declare that the investigation presented in the thesis has been carried out by me. Whenever contributions of others are involved, every efforts is made to indicate this clearly with due reference to the literature and acknowledge of collaborative research and discussions. The work is original and has not been submitted earlier as a whole or in part for a degree / diploma at this or any other Institution / University.



**Y. S. Rana**

# DECLARATION

I, hereby declare that the minor corrections suggested by one of the examiners have been incorporated.



**Dr. S.B. Degweker**

**(Guide)**

## **To my parents**

**Who always gave top priority to my education and taught me the value of hard work.**

# ACKNOWLEDGEMENTS

First of all I would like to express my deep and sincere gratitude to my thesis supervisor and teacher, Dr. S.B. Degweker for his invaluable guidance, constant encouragement and keen interest. I am also thankful to him for his patience during technical discussions and clarifying my doubts all through these years.

I sincerely thank Dr. Kanchhi Singh, Head, Research Reactor Services Division who has always encouraged and motivated me. I am also grateful to Shri R.C. Sharma, Director, Reactor Group and Shri V.K. Raina (Ex. Director, Reactor Group) for their support and encouragement. Thanks are due to all the members of RPNE Section for the help rendered by them.

I thank the members of the doctoral committee Prof. P. Mohankrishnan (Ex. Chairman), Prof. B.N. Jagtap (Chairman), Prof. Y.S. Mayya (Member) and Prof. C.P. Reddy (Member) for their critical review and suggestions during the progress review and pre-synopsis viva-voce.

Thanks are also due to Dr. H.P. Gupta, Dr. R.S. Modak, Dr. Amar Sinha and Dr. P. Satyamoorthy who taught me during the course work.

I thank my friends Shri Sohrab Abbas and Shri Jitendra Bahadur of SSPD, BARC and Shri Rajeev Kumar of RPDD, BARC for their help during writing of the thesis.

Finally, I would like to thank my wife Ruchi for her exceptional care, personal support and great patience throughout these years. I am thankful to my son Harshvardhan for bearing my absence during weekends and on holidays.

# CONTENTS

	<b>Page</b>
<b>Synopsis</b> .....	1
<b>List of Figures</b> .....	17
<b>List of Tables</b> .....	23
<b>Chapter 1: Introduction and Overview</b> .....	24
1.1. ADS: A historical background.....	25
1.2. Present interest in ADS.....	26
1.2.1. Waste transmutation.....	27
1.2.2. Thorium utilization.....	29
1.3. The external neutron source.....	31
1.3.1. The spallation source.....	31
1.4. Physics studies in ADS: A review.....	32
1.4.1. Theoretical studies .....	32
1.4.2. Experimental studies.....	36
<b>Chapter 2: Reactor Noise in Traditional Reactors and ADS</b> .....	38
2.1. Noise in critical reactors.....	38
2.1.1. Experimental methods.....	38
2.1.1.1. Rossi alpha technique.....	39
2.1.1.2. Feynman alpha (variance to mean ratio) technique.....	40
2.1.1.3. Correlation function and power spectral density methods...	40
2.1.1.4. Other methods.....	42
2.1.2. Basics of noise theory of critical reactors.....	42
2.1.2.1. Kolmogorov forward equation.....	44
2.1.2.2. Kolmogorov backward equation.....	45

2.1.2.3. The Bartlett formula.....	46
2.1.2.4. Space energy dependence.....	47
2.1.2.5. The Langevin approach.....	48
2.2. Review of noise theories in ADS.....	53
2.2.1. Early studies on theory of reactor noise in ADS .....	53
2.2.2. Studies with periodic pulses.....	54
2.2.3. Studies with non-Poisson sources.....	55
<b>Chapter 3: Finite Pulses and Correlations between Different Pulses.....</b>	<b>60</b>
3.1. The doubly stochastic Poisson point process.....	61
3.2. Correlated Gaussian pulsed source.....	61
3.2.1. Rossi alpha formula.....	62
3.2.2. The variance to mean ratio.....	64
3.2.3. The ACF and PSD.....	65
3.3. Effect of finite spread of source pulse.....	68
3.3.1. The Rossi alpha formula .....	68
3.4. Numerical results .....	77
3.5. Conclusion.....	78
<b>Chapter 4: Theory of Reactor Noise in ADS with Delayed Neutrons.....</b>	<b>81</b>
4.1. No correlation between different pulses. ....	81
4.1.1. The variance to mean ratio (Feynman alpha) formula .....	81
4.1.2. The two time probability density (Rossi alpha) formula.....	91
4.1.3. Numerical Results.....	95
4.2. Correlation between different pulses. ....	96
4.2.1. The two time probability density (Rossi alpha) formula.....	96
4.2.2. The variance to mean ratio (Feynman alpha) formula .....	101

4.2.3. Numerical Results.....	105
4.3. Conclusion.....	107
Appendix I. Additional terms in the Feynman alpha formula due to prompt- delayed and delayed-delayed correlations .....	110
Appendix II. Additional terms in the Rossi alpha formula due to prompt-delayed and delayed-delayed correlations.....	111
<b>Chapter 5: The Langevin Approach to Reactor Noise in ADS.....</b>	<b>121</b>
5.1. The Langevin theory of noise measurements. ....	122
5.1.1. Un-correlated delta pulsed source .....	122
5.1.2. Correlated finite pulsed source including delayed neutrons .....	128
5.2. Conclusion.....	136
<b>Chapter 6: Simulation of Noise Experiments in Sub-critical Systems by Diffusion Theory based Analogue Monte Carlo.....</b>	<b>137</b>
6.1. Analytical diffusion theory kernels.....	139
6.1.1. Infinite medium kernel.....	139
6.1.2. Finite medium kernel: Method of images for bare homogenous reactor.....	140
6.2. Finite difference diffusion theory kernels .....	142
6.3. Modal effects in noise experiments.....	144
6.4. Results.....	150
6.5. Conclusion.....	153
Appendix I. Derivation of flux at the boundary of a mesh .....	154
<b>Chapter 7: Summary and Conclusions.....</b>	<b>166</b>
<b>References.....</b>	<b>169</b>
<b>List of Publications.....</b>	<b>183</b>

# SYNOPSIS

In recent years, Accelerator Driven Systems (ADSs) have attracted worldwide attention due to their superior safety characteristics as compared to critical reactors and their potential to incinerate Minor Actinides (MAs) and transmute Long Lived Fission Products (LLFPs). In a critical reactor, the number of neutrons produced by fission is exactly balanced by the number lost by leakage and absorption in various materials in the reactor. This balance is responsible for maintaining reactor power at any desired level. In sub-critical reactors, the number of neutrons produced by fission is less than that lost by leakage and absorption and hence, such reactors need an external neutron supply in order to maintain a constant power level. This external supply of neutrons comes from the interaction of a high energy proton beam with a heavy atom nucleus such as lead through a process known as spallation.

Such systems, first proposed for production of fissile material, were not pursued mainly due to the technological difficulties associated with building the required high power (about 1 GeV energy and few hundred mA current) proton accelerators, and developing suitable targets and windows which could withstand the severe thermal and radiation environment associated with such high power beams. The other reason was that uranium prices did not increase significantly so as to make accelerator breeding economically attractive. In the mid nineties, the Nobel laureate Carlo Rubia proposed ADSs for energy production using thorium fuel in a self sustaining cycle and requiring relatively modest power accelerators (about 1 GeV energy and 10 mA current). This initiated a renewed interest in sub-critical systems, and has presently caught the attention of the world for the equally important role of nuclear waste transmutation.

Indian interest in ADS is primarily related to the planned utilization of our large thorium reserves for future nuclear energy generation. Thorium has an added advantage that it produces much less quantities of long-lived radioactive wastes as compared to uranium.

The main R&D efforts are related to development of accelerator technologies leading to construction of a high energy high current accelerator. A major effort is also directed towards target and window technologies. Basic research activities in the area of the sub-critical reactor physics include new measurements and evaluations of nuclear data both at traditional reactor energies as well as at high energies, development of computer codes for describing the interaction of high energy protons with targets, and new Monte Carlo codes for predicting the properties of the sub-critical cores including the effects of fuel burn-up. Theoretical studies on new and more suitable definitions of parameters such as sub-critical reactivity, reactivity worth and the parameter  $k_s$  in addition to  $k_{eff}$  are being carried out. Considerable theoretical and experimental effort is being devoted to developing methods for measuring and monitoring the sub-criticality of an ADS. The fission power in an ADS is directly proportional to the neutron source strength and inversely proportional to the degree of sub-criticality. To get a high power, the sub-criticality should be low. However if the reactor is operated too close to criticality, it may go critical due to addition of reactivity during operating transients such as xenon decay or decay of  $\text{Pa}^{233}$  to  $\text{U}^{233}$ . Thus, sub-critical reactivity is an important parameter from the point of view of ADS operation. It decides not only the accelerator current that will be required to produce the desired power but also the margin of safety available. Measurement and continuous monitoring of this parameter in operating ADS reactors will be an essential safety requirement.

Several low power experiments (Kitamura et al., 2004; Kloosterman and Rugama, 2005) have been performed for evaluating various methods (deterministic as well as stochastic) for

measuring the sub-critical reactivity in ADS. The well known pulsed neutron method and a recently proposed method viz., the source jerk method are the deterministic methods that have been studied in these experiments. There have also been suggestions regarding use of noise techniques for monitoring the sub-criticality of ADS (Behringer and Wydler, 1999; Carta and D'Angelo, 1999; Munoz-Cobo et al., 2001). Similar experiments are planned to be carried out in the Purnima sub-critical facility at BARC.

Noise methods have long been used for measurement of reactor kinetics parameters and as diagnostic tools for monitoring the health of a nuclear power plant. It is conceivable that noise techniques would find similar applications in ADS. For this reason, theoretical and experimental studies on ADS noise methods have appeared since the late nineties. The earliest theoretical studies on various noise techniques for ADS (Pazsit and Yamane, 1998; Kuang and Pazsit, 2000; Behringer and Wydler, 1999) assumed that the neutron producing source events in an ADS form a Stationary Poisson Point Process (SPPP). Each such event (spallation) was assumed to produce neutrons with a large multiplicity distribution.

However, the principal difference between critical reactor noise and ADS noise is due to the statistical properties of the source. Unlike the source due to radioactive decay present in ordinary reactors, the accelerator produced neutron source in an ADS cannot be assumed to be a Poisson process. Moreover, the source may be pulsed. It was first pointed out by Degweker (2000, 2003) that a new theoretical approach is required to describe noise in ADS.

In the present thesis, we discuss theoretical work aimed at developing noise methods for measurement of the sub-criticality in the light of the new theoretical approach mentioned above. The scope and content of the theory has been considerably expanded by us (Degweker and Rana, 2007; Rana and Degweker, 2009; Degweker and Rana, 2011; Rana

and Degweker, 2011). A diffusion theory based analogue Monte Carlo method (Rana, Singh and Degweker, 2013) has been developed for simulating the noise experiments planned at BARC. These are the new results presented in this thesis. The thesis is divided into seven chapters as elaborated below.

## **1. Introduction and Overview**

Chapter I is a brief introduction to the ADS concept. The concept of ADS and its evolution over the years is discussed. A survey of the theoretical and experimental studies on such systems is presented.

## **2. Reactor Noise in Traditional Reactors and ADS**

Chapter II gives a general introduction to the subject of reactor noise and presents an overview of theoretical methods employed for studying the subject. The Kolmogorov forward and backward equations are discussed and the probability generating function method for obtaining their solutions is described. The Bartlett formula for source dependent problems is presented. A discussion on the space dependent effects in reactor noise is included as also the theoretical approaches to this problem. The Langevin method, which is an alternative theoretical approach for studying reactor noise problems, is discussed.

Measurement of the variance to mean ratio in counting intervals, the Rossi alpha function, the Auto Correlation Function (ACF) or the Cross Correlation Function (CCF), of the number of counts in one or two detectors, or in the frequency domain, the Power Spectral Density (PSD) or the Cross Power Spectral Density (CPSD) are some of the commonly used experimental methods for noise analysis. The theory is used to obtain expressions for these quantities which include various parameters such as the sub-critical reactivity, delayed neutron fraction and neutron lifetime. The parameters are extracted by fitting measured

quantities to these expressions. A discussion of various experimental procedures used for analyzing reactor noise and the connection of the theory with these procedures for extracting reactor physics parameters is also included.

This is followed by a review of the various theoretical studies on Reactor Noise in ADS. The earliest theoretical studies on various noise techniques for ADS (Pazsit and Yamane, 1998; Kuang and Pazsit, 2000; Behringer and Wydler, 1999) did not account for either periodic pulsed source or for its non-Poisson character. By a Poisson source we mean that the arrival times of protons or ions (and therefore the injection times of neutron bunches) constitute a stochastic Poisson point process. For such sources, the Bartlett formula is valid whether the source is stationary as in ordinary radioactive sources or even if it is pulsed, with finite or infinitesimal width.

On the other hand if the arrival times do not constitute a Poisson point process, the previously described and commonly used theoretical approaches such as the Kolmogorov forward equation or the Bartlett formula are inapplicable and we call such sources as non-Poisson sources. These features were considered by Degweker (2000, 2003) treating the individual pulses as Dirac delta functions, uncorrelated with one another. In these papers, it was shown that reactor noise in ADS is different from that in critical or radioactive source driven sub-critical systems due to non-Poisson character of the periodically pulsed source. Various noise descriptors, such as Rossi alpha, Feynman alpha (or variance to mean), PSD and CPSD were derived.

The method developed for treating non-Poisson sources consisted of obtaining the probability generating function (pgf) of detected counts for a single neutron injected in a source free medium. Using the multiplicative property of pgfs for different source events, the pgf for the case of an arbitrary source was obtained. This property is due to the

independent propagation of chains initiated by different source neutrons and is a consequence of the linear character of the neutron transport and multiplication.

A similar treatment was subsequently used by Ballester & Munoz Cobo (2005a). Using a space dependent model the authors derived CPSD for sub-critical assemblies driven by external non-Poisson source. The results were validated (Ballester & Munoz Cobo, 2005b) against the data gathered in MUSE-4 experiments to investigate the application of the Feynman-alpha method using an external pulsed source as a sub-criticality level monitoring technique. They also made an attempt to study the influence of the non-Poisson nature of the pulsed source. Pazsit et al. (2005) and Kitamura et al. (2005) included periodic pulsing but with a Poisson source. They considered the pulse to be of finite width of rectangular and Gaussian shapes and also included the effect of delayed neutrons.

### **3. Finite Pulses and Correlations between Different Pulses**

In Chapter III, we extend the scope of the earlier papers (Degweker, 2000, 2003) to include the possibility of correlations between different pulses and finite pulses of different shapes. A possible reason for the non-Poisson nature of the source is identified as being due to fluctuations in the beam current. Measurements of the number of protons per shot during the TARC experiments (Abanades et al., 2002) clearly show that the fluctuations in the current are much too large so as to be described by a Poisson distribution.

At any instant of time, the probability per unit time for a spallation (neutron producing reaction) event to occur is taken to be proportional to the instantaneous proton (ion) current  $I(t)$  at that time.  $I(t)$  itself is treated as a stochastic process which is moreover having a periodic modulation corresponding to the pulsed nature of the proton (ion) beam. The source is thus treated as a doubly stochastic Poisson point process. Each pulse can have any shape but calculations are done for the two commonly occurring shapes – rectangular and

Gaussian. Thus, this approach allows us to extend the earlier formulation based on delta function pulses to take care of finite pulses as well as correlations between different pulses. The development in this chapter is restricted to the case of prompt neutrons only.

Expressions for  $v/m$ , Rossi alpha, ACF and PSD are obtained for the cases of Gaussian and rectangular pulses. The correlations in the source fluctuations introduce additional terms which could confuse interpretation of alpha measurements by the variance method. The Rossi alpha and PSD methods might perform better in this case. The finiteness of the pulse width introduces small corrections to the formulae for delta function pulses.

#### **4. Theory of Reactor Noise in ADS with Delayed Neutrons**

In Chapter IV, we develop the theory further to include delayed neutrons and derive Feynman alpha and Rossi alpha formulae by considering the source to consist of periodic pulses (delta functions) with non-Poisson statistics, but without correlations between different pulses. By carrying out calculations of the Feynman alpha and Rossi alpha for typical experimental parameters, it is shown that the delayed neutron effects become important in those situations where the prompt and delayed neutron timescales are not very distinct and the formulae derived by us would serve as corrections even on prompt neutron timescales. The derived formulae provide important corrections for delayed neutron effects to the formulae obtained earlier.

We find that in addition to the terms due to source and fission chain correlations, the formulae contain periodic variations in the uncorrelated terms. The terms representing neutron chain correlations in the formulae have forms similar to that given in the literature and have been expressed by us in terms of the properties of the zero power transfer function. The term due to source correlations is different from that appearing in recently published formulae because of the non-Poisson character of accelerator-based sources.

An analysis of the results of experiments in the KUCA facility (Pazsit et al., 2005) using our formulae also clearly shows the presence of a source contribution to the Feynman  $Y$  function. Such a contribution is not expected for D-D or D-T sources since neutron production in these reactions is in singlets (i.e., there is no bunching) and can be explained due to the non-Poisson character of the ion beam. In the absence of delayed neutrons, the expressions reduce to the form derived in an earlier paper (Degweker, 2003), as they should.

Subsequently, we also include correlations between different source pulses. It is assumed that source can be described as a periodic sequence of delta function non-Poisson pulses, with exponential correlations. Feynman alpha and Rossi alpha formulae are derived for such a source taking into account the effect of delayed neutrons.

Calculation of the Rossi alpha formula for typical experimental parameters shows that if the external source fluctuations are correlated with correlation times greater than or of the order of the prompt neutron decay times, it will be difficult to use methods such as Rossi alpha.

It is therefore important to study the current fluctuation statistics of ion beams from accelerators, either theoretically or experimentally.

## **5. The Langevin Approach to Reactor Noise in ADS**

Behringer and Wydler (1999) considered the Langevin approach for ADS noise, but they used a modified Schottky prescription to include the Noise Equivalent Source (NES) for source fluctuations. This formulation is valid only for Poisson sources. Thus the pulsed non-Poisson character of the source is not brought out in their paper. Another paper based on the Langevin approach for ADS noise is due to Pazsit and Arzhanov (1999). They however have presented a treatment using the Langevin approach in the context of power reactor ADS noise.

In Chapter V, we develop the Langevin approach to reactor noise in ADS. Apart from being simpler, the Langevin approach allows treatment of feedback effects arising in ADS with significant power as well as other noise sources if any. We examine if it is possible to treat zero power neutron fluctuations in an ADS with non-Poisson source using this formulation. We show that this is possible and for this purpose, the external source fluctuations cannot be treated only as an NES or only as an external parametric fluctuation but rather as a combination of an internal noise described by the Schottky formula and as an external fluctuating function. This way, non-Poisson sources of all kinds can be treated.

We first demonstrate, for two models of the source studied by us earlier, that it is possible to obtain the correct expressions for various noise descriptors using the Langevin approach with Schottky prescription for fission, detector, and capture events but with a separate treatment for ADS source fluctuations. In both these cases we show that our earlier results by the more rigorous method are reproduced. The demonstration is important as it fixes the recipes required for treating a new system (ADS, in this case) using the heuristic Langevin approach.

The method is then applied to treat the more general problem of zero power ADS noise viz., correlated non-Poisson pulsed sources with finite pulse width including delayed neutrons. The rather complicated nature of this problem makes the calculations by the pgf method wholly intractable and this necessitates the use of a simpler approach. We find that the Langevin method fits the bill. We obtain the PSD of the noise as the Langevin method is simplest to use in the frequency domain. This is the main new result presented in this chapter.

## **6. Simulation of Noise Experiments in Sub-critical Systems by Diffusion Theory Based Analogue Monte Carlo**

Various low power experiments are being planned (Rasheed et al., 2010) to be carried out at Bhabha Atomic Research Centre (BARC) with the aim of demonstrating pulsed neutron and noise methods for measuring the sub-critical reactivity of ADS. One of the aims of the experiments would be to verify the theory of reactor noise in ADS developed by us and interpret the results in terms of the theory. The system planned is a natural uranium sub-critical assembly moderated by water or high density polyethylene. The maximum  $k_{eff}$  of such a system is expected to be about 0.9. At such a low value of  $k_{eff}$ , noise experiments for determining alpha are likely to face difficulties in interpretation due to modal contamination effects at such low values of the  $k_{eff}$ . By the time the higher modes have died out and the fundamental mode decay of the correlation sets in, very few correlated counts remain and the background noise dominates. However, for both types of experiments it is possible to select certain detector positions where the modal contamination of many of the higher modes immediately above the fundamental mode can be eliminated.

As part of the planning of the experiments, a simulation of the kind of results that might be expected with different detector locations and counting and analyzing setups is necessary, particularly in view of the difficulty mentioned above. Simulations with standard code packages (MCNP, 1987; MONALI 1991) are not appropriate because of several non-analogue features built into such codes. These need to be modified into completely analogue simulation codes. Munoz Cobo et al. (2001) coupled the high energy code LAHET with another Monte Carlo code MCNP-DSP and simulated cross power spectral density between the proton current signal and a neutron detector signal for a typical fast energy amplifier configuration. While LAHET simulates the spallation process and transport of charged

particles, MCNP-DSP is used to simulate the counting statistics from neutrons counters. Pozzi et al. (2012) have developed a variant of MCNP, called MCNP-PoliMi. The code can simulate correlated statistics of neutrons and photons. It can also handle the effect of delayed neutrons. However, completely analogue computations are very time consuming. There have been attempts to remedy (Máté Szieberth and Gergely Klujber, 2010) some of these problems by special methods of correcting tallies which give not only the correct value of the first moment but also of the second moment. The simulation is still having many time reducing features and takes less time compared to purely analogue simulations.

But the purpose of simulations of proposed experiments is often not to obtain the ‘correct’ value of say the variance to mean ratio but rather to obtain the kind of results that are expected. For example one may be interested in knowing the magnitude of this quantity for given values of system parameters such as  $k_{eff}$ , detection efficiency etc., and how it compares with the background random noise for a given counting time or the magnitude of the space dependent effects, delayed neutron contributions and dead time effects that invariably appear in the experiment. All this is possible only if the simulation is completely analogue and, as mentioned above, such simulation requires long computing times.

In Chapter VI, we describe an analogue Monte Carlo code developed by us for carrying out such simulations. The simulator generates a detailed time history of counts in the detector so that any method of analysis can be carried out. Since analogue MC takes very long computing time, instead of carrying out a simulation to yield results equivalent to transport theory, we attempt to reproduce results equivalent to few-group diffusion theory, which requires much less time. While few-group diffusion theory may not be as accurate as exact MC simulations, it will be adequate for the purpose mentioned above. Moreover, it is always possible to substitute the diffusion equivalent simulation with a transport equivalent

simulation in regions where diffusion theory is not valid. We discuss the basic theory of the simulation method and some results of our simulations. We describe some simple reactor models for which analytical diffusion kernels can be used very effectively to get some of the required results. We also describe a numerical approach based on the finite differenced diffusion equation which is applicable to more general situations.

The few group diffusion theory based analogue MC code for simulating reactor noise experiments is used to study the problem of suitable location (at the intersection of the zeros of the symmetric modes) of the neutron detectors to avoid contamination due to contribution from higher modes. A simplified model of one of the proposed Purnima sub-critical assemblies is used for the purpose of the study. We simulate the ACF and Feynman alpha experiments. The value of alpha obtained from the simulation agrees well with the value obtained from the analytical solution for the geometry. The simulations show that proper location of detectors gives an almost single exponential (fundamental mode) response making alpha measurements by the noise methods possible even in deeply sub-critical systems.

## **7. Summary and Conclusions**

Chapter VII gives a brief summary of the results presented in the thesis and the main conclusions drawn.

Reactor noise in ADS is different from ordinary reactors due to the different statistical characteristics of the driving source. Since Reactor Noise techniques are potential candidates for sub-criticality measurement / monitoring of ADSs, it is important that these are put on a sound theoretical footing. A beginning was made in this direction by Degweker through two pioneering papers (Degweker, 2000, 2003) in which the individual pulses are treated as

Dirac delta functions, uncorrelated with one another. The theory treated all neutrons as prompt.

In this thesis we (Degweker and Rana, 2007; Rana and Degweker, 2009; Degweker and Rana, 2011; Rana and Degweker, 2011) present developments carried out to include the effects of finite pulses, delayed neutrons and correlations between different pulses of the source. Formulae for Rossi alpha, Feynman alpha (or variance to mean), PSD and CPSD have been derived. While much of the work is based on the probability generating function approach, for the more complicated problems, we have successfully developed the simpler, though somewhat heuristic, Langevin approach to ADS noise theory. A novel method (Rana, Singh and Degweker, 2013) for simulating noise experiments (planned to be carried out at BARC) using diffusion based analogue Monte Carlo, and some interesting results on the spatial dependence of noise in ADS, thus obtained, are also discussed in the thesis.

## **References:**

**Abanades A. et al. (2002)**, “Results from the TARC experiment: spallation neutron phenomenology in lead and neutron-driven nuclear transmutation by adiabatic resonance crossing”, *Nuclear Instrumental Methods* **A478**, 577

**Abderahim A.H. (2005)**, “Myrrha Project – ADS Related R&D and Nuclear Data”, *DAE-BRNS National Workshop on Nuclear Data for Reactor Technology and Fuel Cycle*, March 7-10, Mumbai

**Ballester D. and Munoz-Cobo J. L. (2005a)**, “Feynman-Y Function for a Sub-critical Assembly with Intrinsic Spontaneous Fissions Driven by External Pulsed Sources,” *Annals of Nuclear Energy*, **32**, 493

- Ballester D., Munoz-Cobo J. L. and Kloosterman J.L. (2005b)**, “On the applicability of the pulsing Feynman-a method: Validation with MUSE,” *Annals of Nuclear Energy*, **32**, 1476
- Behringer K. and Wydler P. (1999)** “On the Problem of Monitoring Neutron Parameters of the Fast Energy Amplifier”, *Annals of Nuclear Energy* **26**, 1131
- Carta M. and D’Angelo A. (1999)**, “Sub-criticality-level evaluation in Accelerator- Driven Systems by harmonic modulation of the external source”, *Nucl. Sci. Engg.*, **133**, 282
- Degweker S.B. (2000)** “Some Variants of the Feynman Alpha Method in Critical and Accelerator Driven Sub-critical Systems”, *Annals of Nuclear Energy* **27**, 1245
- Degweker S.B. (2003)** “Reactor Noise in Accelerator Driven Systems”, *Annals of Nuclear Energy*, **30**, 223
- Degweker S.B. and Rana Y.S. (2007)**, “Reactor Noise in Accelerator Driven Systems-II”, *Annals of Nuclear Energy* **34(6)**, 463
- Degweker S.B. and Rana Y.S. (2011)**, “The Langevin Approach to Reactor Noise in Accelerator Driven Systems”, *Nucl. Sci. Engg.* **169**, 296
- Rasheed K. K. et al. (2010)**, “Proposed Experiments at BARC with Natural Uranium- Light Water Sub-critical Assembly Driven by 14 Mev Neutrons”, *ADS benchmark CRP, 4th RCM, Mumbai, India, 22-26 February*
- Kitamura Y. et al. (2004)** “Experimental investigation of variance-to-mean formula for periodic and pulsed neutron source” *Annals of Nuclear Energy* **31**, 163
- Kitamura Y. et al. (2005)**, “Calculation of the Pulsed Feynman and Rossi-Alpha Formulae with Delayed Neutrons,” *Annals of Nuclear Energy* **32**, 671
- Kloosterman J.L. and Rugama Y. (2005)**, “Feynman- $\alpha$  Measurements on the Fast Critical Zero-Power Reactor MASURCA”, *Progress in Nuclear Energy* **46(2)**, 111

**Kuang Z.F. and Pazsit I. (2000)**, “A Quantitative Analysis of the Feynman- and Rossi-Alpha Formulas with Multiple Emission Sources”, *Nucl. Sci. Engg.* **136**

**Máté Szieberth and Gergely Klujber (2010)**, “Monte Carlo simulation of neutron noise measurements”, *ADS benchmark CRP, 4th RCM, Mumbai, India, 22-26 February*

**“MCNP — A General Monte Carlo N-Particle Transport Code”**, *Report LA-UR-03-1987*

**“MONALI – Rev.1, A Monte Carlo code for analyzing fuel assemblies of nuclear reactors”**, *Report BARC-1543 (1991)*

**Munoz Cobo J.L. et al. (2001)** “Sub-critical Reactivity Monitoring in Accelerator Driven Systems”, *Annals of Nuclear Energy* **28**, 1519

**Pal, L., (1958)** “On the theory of stochastic processes in nuclear reactors”, *II Nuovo Cimento* **7 (Suppl.)**, 25-42

**Pazsit I. and Yamane Y. (1998)**, “The variance to mean ratio in sub-critical systems driven by a spallation source”, *Annals Nuclear Energy* **25**, 667

**Pazsit I. and V. Arzhanov (1999)**, “Theory of Neutron Noise Induced by Source Fluctuations in Accelerator Driven Sub-critical Reactors”, *Annals of Nuclear Energy* **26** 1371

**Pazsit I. et al. (2005)**, “Calculation of the Pulsed Feynman-Alpha Formulae and Their Experimental Verification”, *Annals of Nuclear Energy* **32**, 986

**Pozzi, S. A. et al. (2012)**, “MCNPX-PoliMi for nuclear nonproliferation applications,” *Nucl. Instr. Meth. A*, **694(2)** 119

**Rana Y.S. and Degweker S.B. (2009)**, “Feynman Alpha and Rossi Alpha Formulae with Delayed Neutrons for Sub-critical Reactors Driven by Pulsed Non-Poisson Sources”, *Nucl. Sci. Engg.* **162**, 117

**Rana Y.S. and Degweker S.B. (2011)**, “Feynman-Alpha and Rossi-Alpha Formulas with Delayed Neutrons for Subcritical Reactors Driven by Pulsed Non-Poisson Sources with Correlation Between Different Pulses”, *Nucl. Sci. Engg.* **169**, 98

**Rana Y.S., Singh Arun and Degweker S.B. (2013)**, “Diffusion Theory Based Analogue Monte Carlo for Simulating Noise Experiments in sub-critical Systems”, *Nucl. Sci. Eng.*, **174**, 245

**Saleh, B.**, “Photoelectron Statistics”, *Springer, Berlin* (1978)

**Van Kampen N.G. (1983)** “Stochastic Processes in Physics and Chemistry”, *North Holland, Amsterdam*

**Williams, M.M.R. (1974)**, “Random Processes in Nuclear Reactors”, *Pergamon Press, Oxford*

# LIST OF FIGURES

		Page
2.1	Variation of the $v/m$ with inverse of the decay constant. The points are based on the experimental results presented by Pazsit et al. (2005). In the graph (a) we show a power law fit while in (b) we show a quadratic fit. While both fits are equally good, the power obtained is not 2 as is expected on the assumption of a Poisson source. The quadratic fit passes through the origin and the linear term indicates a non-Poisson source contribution.	59
3.1	Variation of different terms of the Rossi alpha formula [Eq. (3.8)] with $\tau$ . B, C, D, and E refer to the second, the third, the fourth and the sum of the second and fourth terms, respectively. The three sets of graphs (a)–(c) are for $\beta \ll \alpha$ , $\beta \approx \alpha$ and $\beta \gg \alpha$ respectively.	79
3.2	Comparison of the (uncorrelated part) Rossi alpha formula for delta function and rectangular shaped pulses. The two are identical except close to an integral multiple of the pulse period. In the former we get a sharp cusp whereas for the latter we get a smooth curve in these regions.	80
4.1	Variation of different terms of the $v/m$ formula with the length of the counting interval. The parameters used to plot the graphs are listed under set 1 in table 4.1. (a) Fission chain contribution on prompt neutron lifetime scale; (b) Fission chain contribution on delayed neutron lifetime scale; the contribution of delayed neutrons is to be noticed; (c) Contribution due to source correlations; (d) Oscillatory term due to the periodicity of the source.	112

- 4.2 Variation of different terms of the  $v/m$  formula with the length of the counting interval. The parameters used to plot the graphs are listed under set 2 in table 4.1. (a) Fission chain contribution on prompt neutron lifetime scale; (b) Fission chain contribution on delayed neutron lifetime scale; this being a heavy water reactor case, the two scales can be seen overlapping; (c) Contribution due to source correlations; (d) Oscillatory term due to the periodicity of the source. 113
- 4.3 Variation of different terms of the  $v/m$  formula with the length of the counting interval. The parameters used to plot the graphs are listed under set 3 in table 4.1. (a) Fission chain contribution on prompt neutron lifetime scale; (b) Fission chain contribution on delayed neutron lifetime scale; again this being a heavy water reactor case, the two scales can be seen overlapping, also the magnitude is more than that in Fig. 4.2 because of lesser sub-criticality level; (c) Contribution due to source correlations; (d) Oscillatory term due to the periodicity of the source. 114
- 4.4 Variation of different terms of the Rossi Alpha formula with delay time. The parameters used to plot the graphs are listed under set 1 in table 4.1. (a) on prompt neutron lifetime scale; (b) on delayed neutron lifetime scale; (c) term arising due to source correlations. 115
- 4.5 Variation of different terms of the Rossi Alpha formula with delay time. The parameters used to plot the graphs are listed under set 2 in table 4.1. (a) on prompt neutron lifetime scale; (b) on delayed neutron lifetime scale. 116
- 4.6 Variation of different terms of the Rossi Alpha formula with delay time. The parameters used to plot the graphs are listed under set 3 in table 4.1. (a) on prompt neutron lifetime scale; (b) on delayed neutron lifetime scale. 116

- 4.7 Counting gate system for Rossi alpha measurements. The first count 117  
occurs in the interval  $dt$  around  $t=0$  and the second in the interval  $d\tau$  around  $t=\tau$ . The last source pulse that contributes to the counts occurs at  $t_0$  and the ones prior to this will occur at  $t_0-1/f$ ,  $t_0-2/f$ , ... etc.  $t_0$  is a random variable and has equal probability of occurrence between  $\tau-1/f$ ,  $\tau$ . Correspondingly, the earlier pulse will lie between  $\tau-2/f$  and  $\tau-1/f$  and so on.
- 4.8 Variation of different terms of the Rossi alpha formula (Eq. 4.50) 117  
with  $\tau$  on prompt neutron lifetime scale. The parameters used to plot the graphs are listed under set 1 in Table 4.2 corresponding to light water systems. Also shown is the Rossi alpha function oscillates with time and has a decaying part in the beginning which later on becomes non-decaying. The correlated component (due to fission chain, source multiplicity and correlations in the source fluctuations) of Rossi alpha function falls exponentially. The contribution of the fourth term of the Rossi alpha function i.e. oscillating part of the term arising due to correlations in the source fluctuations is rather small to be significant in this case.
- 4.9 Variation of different terms of the Rossi alpha formula with  $\tau$ . The graphs 118  
a-c are for  $\zeta \ll \alpha$ ,  $\zeta \sim \alpha$  and  $\zeta \gg \alpha$  respectively. If  $\zeta \sim \alpha$  or  $\zeta \ll \alpha$ , it is likely that noise experiments might yield  $\zeta$  which may be mistaken for  $\alpha$ ! Only in the case of  $\zeta \gg \alpha$  i.e. where source fluctuations can be treated as white do we get Rossi alpha which will give correct  $\alpha$ . Fig. 4.9 (d) shows contribution to Rossi alpha due to correlations in the source fluctuations

and that due to source multiplicity plus fission chain. The parameters used to plot the graphs are listed under set 2 in Table 4.2 corresponding to heavy water systems.

- 4.10 Counting gate system for  $\nu/m$  measurements. The counting interval is  $[0, T]$ . The last source pulse that contributes to the counts occurs at  $t_0$  and the ones prior to this will occur at  $t_0 - 1/f$ ,  $t_0 - 2/f$ , ...etc.  $t_0$  is a random variable and has equal probability of occurrence between  $T - 1/f$ ,  $T$ . Correspondingly, the earlier pulse will lie between  $T - 2/f$  and  $T - 1/f$  and so on. 119
- 4.11 Variation of total and different terms of the  $\nu/m$  formula with the length of the counting interval. The parameters used to plot the graphs are listed under set 1 in Table 4.2. (a) On prompt neutron life time scale. It is seen that the  $\nu/m$  appears to saturate and hence use of formula with only prompt neutrons may be adequate for analyzing the experimental results. (b) On delayed neutron life time scale; the contribution of delayed neutrons is however seen. 119
- 4.12 Variation of total and different terms of the  $\nu/m$  formula with the length of the counting interval. The parameters used to plot the graphs are listed under set 3 in Table 4.2 corresponding to heavy water systems. Here the prompt and delayed scales are not very distinct and corrections due to delayed neutron terms will be necessary for analyzing experimental results. (a) On short life time scale. (b) On delayed neutron life time scale. 120
- 6.1 The problem of determining the potential (to the left of the plane P) due to a positive charge  $+q$  near the conducting plane P which is earthed can be 157

- solved by adding an image charge  $-q$  at an equal distance behind the plane.
- 6.2 On the left we show the case of a single plane boundary with the medium on the left and vacuum on the right. A single negative image source on the right at the same distance from the boundary as the original source reproduces the zero flux boundary condition on B. For the two dimensional case shown on the right, we need three image sources to reproduce the zero flux boundary condition on B and BB. 158
- 6.3 Mesh arrangement in finite differencing scheme. 158
- 6.4 (a) Plot of the auto covariance of the count rate with the time separation with symmetrically placed detectors at the zeros of the first symmetric harmonics. After removing the first point, the single exponential fit is almost exact and gives a value of alpha close to the expected value. (b) Plot of the variance to mean ratio with the counting interval length with symmetrically placed detectors at the zeros of the first symmetric harmonics. 159
- 6.5 (a) Plot of the auto covariance of the count rate with the time separation with symmetrically placed detectors at the zeros of the first symmetric harmonics with inclusion of delayed neutrons. Note that the auto covariance reaches an approximately constant value after 1 ms due to delayed neutrons. (b) Plot of the auto covariance of the count rate with the time separation with symmetrically placed detectors at the zeros of the first symmetric harmonics after subtracting the delayed neutron contribution. The exponential fit is good and gives a value of alpha close to the expected value. 160

- 6.6 (a) Plot of the auto covariance of the count rate with the time separation 161  
with detectors placed symmetrically but away from the zeros of the first symmetric harmonics. The exponential fit is not good nor does it give a value of alpha close to the expected value. (b) Plot of the auto covariance of the count rate with the time separation with detectors placed at the zeros of the first symmetric harmonics but in a single quadrant. The exponential fit is not good nor does it give a value of alpha close to the expected value.
- 6.7 (a) Plot of the auto covariance of the count rate with the time separation 162  
with symmetrically placed detectors at the zeros of the first symmetric harmonics as simulated by few group diffusion theory based analogue Monte Carlo code with coarse mesh size. (b) Plot of the auto covariance of the count rate with the time separation with symmetrically placed detectors at the zeros of the first symmetric harmonics as simulated by few group diffusion theory based analogue Monte Carlo code with fine mesh size.
- 6.8 (a) Plot of the variance to mean ratio with the counting interval length 163  
with symmetrically placed detectors at the zeros of the first symmetric harmonics as simulated by few group diffusion theory based analogue Monte Carlo code with coarse mesh size. (b) Plot of the variance to mean ratio with the counting interval length with symmetrically placed detectors at the zeros of the first symmetric harmonics as simulated by few group diffusion theory based analogue Monte Carlo code with fine mesh size.
- 6.9 Plot of the variance to mean ratio with the counting interval length with 164  
symmetrically placed detectors at the zeros of the first symmetric

harmonics- a comparison of the results obtained by analytical diffusion theory based kernels and simulation (for fine mesh structure) by few group diffusion theory based analogue Monte Carlo code.

6.10	Variance to mean ratios for non-paralyzable dead-times of 2 and 4 micro seconds	164
6.11	Variance to mean ratios for paralyzable dead-times of 2 and 4 micro seconds	165

## LIST OF TABLES

	<b>Page</b>
4.1	Numerical parameters used to plot Figures (4.1) through (4.6). 108
4.2	Numerical parameters used to plot Figures (4.8), (4.9), (4.11) and 4.12). 109
6.1	Bare homogeneous reactor: geometrical and nuclear data. 156
6.2	Comparison of various parameters obtained using analytical kernel and finite difference kernels with exact values. 157

## Introduction and Overview

Accelerator Driven Systems (ADSs) are being studied around the world for energy production using thorium and for nuclear waste transmutation. Such systems are attractive due to their superior safety characteristics as super criticality related accidents can be avoided in a well designed ADS. India also has a program on R & D of ADS which includes development of technologies for high energy high current accelerators, targets and windows and the basic research activities in the area of reactor physics.

One of the important issues related with the operation of an ADS is measurement and monitoring of its sub-criticality. Studies are being carried out around the world towards developing suitable methods for the purpose. Among the various methods proposed for this purpose, there have been suggestions (Behringer and Wydler, 1999; Carta and D'Angelo, 1999; Munoz-Cobo et al., 2001) regarding use of noise techniques. A considerable amount of theoretical work has been carried out towards understanding Reactor Noise in ADS (Pazsit and Yamane, 1998a,b; Kuang and Pazsit, 2000; Behringer and Wydler, 1999; Degweker, 2000, 2003). The theoretical formulation of Degweker (2000, 2003) is different in so far as it treats the ADS source as a non-Poisson source, which is a major departure from conventional reactor noise theory.

Various experimental studies (Soule et al., 2004; Carl-Magnus Persson et al., 2005) at low power have been carried out for evaluating both deterministic as well as stochastic methods for measuring the sub-critical reactivity in ADS. Similar experiments are planned (Rasheed et al., 2010) to be carried out in the upcoming Purnima sub-critical facility at BARC as a part of

the Indian program on R & D of ADS. Apart from demonstrating pulsed neutron and noise methods for measuring the sub-critical reactivity of ADS, the experiments aim to verify the theory of reactor noise in ADS mentioned above, and to interpret the results in terms of the theory.

The work described in the thesis generally relates to the problem of sub-criticality measurement by the noise technique and also in particular to the proposed experimental program of the Purnima sub-critical facility. The thesis extends the scope and content of the theory of noise in ADS (Degweker and Rana, 2007, 2011; Rana and Degweker, 2009, 2011). The thesis also describes the development of a diffusion theory based analogue Monte Carlo code (Rana et al., 2013) for simulating the noise experiments being planned at Purnima.

### **1.1 ADS: A historical background**

The earliest suggestion of using accelerator produced neutrons for breeding fissile material from fertile isotopes (referred to as electronuclear breeding) can be traced back to Glenn Seaborg around 1940. However, due to requirements of high energy and high current accelerators it did not pick up. The discovery of the spallation process (Goeckerman and Perlman, 1948) opened up the possibility of producing fissile material on large scale. Around 1950, USA started the program of Materials Testing Accelerator (MTA) [Van Atta C.M., 1977] for producing fissile materials  $\text{Pu}^{239}$  and  $\text{U}^{233}$  from fertile materials. The program was finally terminated around 1954 with the discovery of large uranium reserves in the United States. Other countries such as Canada also performed theoretical studies on the subject (Bartholomew, 1965). A project proposal called Intense Neutron Generator (ING) was made in 1960s. Feasibility studies on electronuclear breeding were also performed in Russia in 1970s (Davidenko, 1970).

Another application of accelerator based neutron sources was for nuclear waste transmutation. The idea was to convert long lived sources of radio-toxicity (Plutonium, Minor Actinides, Long Lived Fission Fragments) into stable or short lived materials. Steinberg et al. (1964) carried out the earliest transmutation studies in thermal reactors having high neutron flux. Subsequent studies (Gregory and Steinberg, 1967; Claiborne, 1972; Beaman and Aitken, 1976; Croff et al., 1980; Steinberg et al., 1979) on the subject investigated transmutation in liquid-metal fast breeder reactors (LMFBR's) and accelerator based enrichers and transmuters.

More recently, Bowman (1992) and Venneri et al. (1993) carried out studies on Accelerator-Driven Transmutation of Waste (ATW) at Los Alamos. The proposed sub-critical system was designed to transmute both fission products and higher actinides using a thermal neutron flux of about  $10^{16}$  n/cm<sup>2</sup>/sec. Another recent development has been the TARC (Transmutation by Adiabatic Resonance Crossing) experiment (Abanades et al. 2002) at CERN for demonstration of transmutation of Tc<sup>99</sup> and I<sup>129</sup> by using the high resonance cross sections of the nuclides and the Adiabatic Resonance Crossing principle.

## **1.2 Present interest in ADS**

There has been an increased interest in recent years in the use of accelerator based neutron sources to drive sub-critical blankets for the purposes of thorium utilization and waste transmutation [referred to as accelerator driven system (ADS)], particularly after the proposals from the CERN group led by Carlo Rubia. The fast energy amplifier (Rubia, C. et al. 1995) is one of their proposed designs for power production using thorium. The proposal is based on much lower power accelerator (a proton cyclotron with 1 GeV -12.5 mA beam) than the earlier ones. Lead acts as spallation target, coolant and radiation shield. The beam window, which separates the vacuum in accelerator from the reactor vessel (RV), is cooled

by lead whose circulation in the RV is maintained by natural convection. The reactor does not have control rods and the power is controlled by varying the proton beam current. Initially, the system was proposed as a sub-critical device for power production using thorium fuel in a self sustaining cycle. During operation, thorium gets converted into  $U^{233}$  which compensates for decrease in reactivity due to depletion of initial fissile material and build up of fission products. Thus, long cycles of operation are possible after which the full core is replaced; the fuel being replaced with (Th- $U^{233}$ ) MOX from second cycle onwards. Presently, fast ADS systems cooled by liquid lead or lead bismuth eutectic (LBE) and driven by low power accelerators (as in the energy amplifier) are being studied primarily for waste transmutation.

As a consequence of the renewed interest in ADS, several countries (Abderrahim et al. 2001; Kapoor, 2001; Mukaiyama et al., 2001; Gohar and Smith, 2010; Shvedov et al. 1997) have drawn roadmaps for development of ADS. India has also a program (Kapoor, 2001) for development of ADS which, besides waste transmutation, aims at thorium utilization for nuclear power production. We present a brief discussion of the work being carried out in these two areas.

### **1.2.1 Waste transmutation**

Considering long term safety, IAEA has defined six classes of radioactive waste (IAEA, 2009). The spent nuclear fuel, generated as a result of nuclear power production, falls in the class of High Level Waste (HLW). This HLW can broadly be divided into two categories:

1. The TRUs, which include Plutonium and Minor Actinides (Am, Cm and Np), form about 1% (Nifenecker et al., 2001) of the spent fuel of a typical PWR. These nuclides are formed by neutron capture reactions in the fuel and have long half lives (24000 years for  $Pu^{239}$ ).

2. Fission Fragments (FFs) form about 4% (Nifenecker et al., 2001) of the spent fuel and, based on their half lives, are divided into two categories namely Long Lived Fission Fragments (LLFFs) having half lives of more than 1000 years e.g.  $\text{Tc}^{99}$ ,  $\text{I}^{129}$  and Medium Lived Fission Fragments (MLFFs) e.g.  $\text{Sr}^{90}$ ,  $\text{Cs}^{137}$  having half lives of about 30 years.

The degree of potential risk associated with HLW is represented in terms of a quantity known as radio-toxicity. It is defined (IAEA, 2002) as “the activity or quantity of radio-nuclides in spent fuel or HLW multiplied by their effective dose coefficients accounting for radiation and tissue weighting factors by ingestion, inhalation and absorption”.

During first few hundred years after its discharge, the major contribution to the radio-toxicity of spent fuel is from short-lived fission products ( $\text{Cs}^{137}$  and  $\text{Sr}^{90}$ ), and subsequently from TRUs (NEA-OECD, 2004). Since the fission products have larger mobility compared to actinides, waste management strategies to reduce the long term risk from the MAs should also consider long lived fission products such as  $\text{I}^{129}$ ,  $\text{Tc}^{99}$  and  $\text{Cs}^{135}$ .

The conventional method of waste management is its storage in deep geological repositories. An alternate method for waste management is partitioning (separation of long lived radio-nuclides from the HLW by a chemical process) and transmutation (IAEA-TRS 435, 2004).

### ***Transmutation in Fast Reactors***

Average cross sections of MAs for typical thermal and fast spectrums indicate that fission to capture ratio is higher for the latter (NEA-OECD, 1999). Thus, incineration of MAs is more efficient in fast systems. Though, LLFPs have high capture cross sections in thermal systems, from neutron economy point of view, it is favorable to use fast systems for their transmutation. Several studies (NEA-OECD, 2002; Wakabayashi, 1997; Tommasi, 1995;

Bays et al., 2009; Ackerman, 1997) have been carried out on recycling of Pu and MAs in fast reactors. The addition of minor actinides adversely affects reactor safety parameters such as effective delayed neutron fraction, Doppler coefficient and coolant void coefficient of reactivity in a liquid-metal cooled reactor. This puts a constraint on the quantity of TRUs to be loaded in critical fast reactors (Wakabayashi, 1997; Tommasi, 1995; Bays et al., 2009).

### ***Transmutation in ADS***

Based on the foregoing discussions it is clear that critical reactors loaded with a large fraction of MA fuel will be difficult to operate safely. Accelerator Driven Systems (ADS) have been proposed (Bowman, 1992; Rubia et al., 1995) to address the safety issues.

Since an ADS is always in sub-critical state, criticality related accidents can be avoided in a well designed system. Moreover, the response of an ADS to insertion of reactivity is much more benign than that due to similar insertions in a critical reactor; the ADS clearly has an advantage in that it can be loaded with considerably larger MA fuel than a fast reactor, without the need to add any fertile component, and therefore has a much higher rate of incineration over that in fast reactors.

### **1.2.2 Thorium utilization**

Thorium fuel cycles drew a lot of attention in the 1970s (IAEA TECDOC 1319; Rosenthal, 1970; Haubenreich and Engel, 1970; Beck and Pincock, 2011) due to limited uranium reserves estimated at that time. However, due to various reasons, including discovery of new uranium reserves (Van Atta, 1977), the programs did not pick up and came to a stop. India has continued its efforts in this direction; an example being work for the design and development of the Advanced Heavy Water Reactor (AHWR). The reason for this is of

course its large thorium reserves and the unique three stage nuclear power programme (Kakodkar, 2008).

### ***Self sustaining thorium cycles in ADS***

The ADS designs, proposed by Rubia et al. (1995) and Bowman (1992) for energy production using thorium and nuclear waste transmutation, initiated new interest in thorium utilization around the world. Since then, lot of studies on the subject (Bowman, 2011; Nuttin et al., 2012; Coates and Parks, 2010; Cheol Ho Pyeon et al., 2011; Bergelson et al., 2007; Lindley and Parks, 2012; Juraj Breza et al., 2010; Si Shengyi, 2009; Adonai Herrera-Martínez et al., 2007; Degweker, 2001a), both with respect to critical and sub-critical systems, have been carried out.

Studies on self sustaining thorium cycles in ADS have been carried out by Rubia et al. (1995), Bowman (1997), Furukawa et al. (1997) and subsequently by Kadi and Adonai (2006), Bowman (2000), Degweker (2001b). The studies show that thorium-uranium cycle, which is not easily self sustaining in critical reactors due to low burn-ups achievable, is much easier to sustain in ADS.

### ***Once through cycles***

The reprocessing of spent fuel in a thorium-uranium cycle is associated with high costs due to  $U^{232}$  contamination. In-situ breeding and burning of  $U^{233}$  is an attractive alternative. Bowman and coworkers have studied (Bowman and Venneri, 1993; Bowman, 1997, 2000) molten salt systems in once through mode. Other fuel systems in fast and thermal spectrum cycles have also been studied (Cisneros et al., 2012; Szuta and Wojciechowski, 2010). Studies on PHWR and fast spectrum ADS by Degweker et al. (2001b, 2010) show that such systems can be

operated in once through cycle with an initial seed fuel which can be natural uranium in PHWRs and plutonium in fast reactors.

### **1.3 The external neutron source**

Due to the requirements of high source strengths of about  $10^{15}$ - $10^{18}$  n/s, radioactive neutron sources (based on  $\alpha, n$  and  $\gamma, n$  reactions) cannot be used for driving the sub-critical reactor. The neutron sources based on high energy deuteron beams (Ridikas and Mitting, 1998) have the major drawback of causing very strong activation of accelerator structures. Electron accelerators can produce high neutron source strengths (Devan et al., 2006; Gohar et al., 2004; Beller, 2004) and are compact in size. However, the energy efficiency of an electron based source is rather low (Nifenecker et al., 2003). There have been proposals (Gohar et al., 2004; Beller, 2004; Brolley and Vertes, 2004) regarding use of electron LINAC based neutron sources in experimental or research ADS facilities. Another source that has been used for experimental systems is the D-D or D-T fusion based neutron generator. For driving a sub-critical power reactor, spallation seems to be the best practical method for producing neutrons.

#### **1.3.1 The spallation source**

Spallation refers to interaction of high energy (typically about 1 GeV) protons with target nuclei (Nifenecker et al., 2003). Due to very high energy (small d'Broglie wavelength) of the projectile, it can be treated as classical particle. The proton interacts with individual nucleons which in turn collide with other nucleons and a cascade develops. Some of these nucleons may escape from the nucleus. These nucleons have high energies and may cause further spallation reactions in other nuclei of the target. This stage is commonly referred to as intranuclear cascade. At energies below 150 MeV, the classical description does not hold and a quantum mechanical treatment is required to describe this pre-equilibrium stage. Finally the

nucleus reaches equilibrium and decays by emitting neutrons and protons through evaporation process or by fission. The spectrum of neutrons emitted during this stage is similar to the fission. There is however a high energy tail in the overall spallation spectrum due to neutrons emitted in the intra-nuclear cascade

The distribution of the residual nuclei, called the spallation products, and the number of emitted neutrons depends on the target nuclei and the energy of the incident particle. For a given target, the number of emitted neutrons increases with energy of the projectile. The number of neutrons emitted per unit energy however increases with proton energy up to about 1-2 GeV and decreases subsequently. The reason is that at low energies, the particle loses much of its energy to electronic excitations while at higher energies other non-productive reactions such as neutral pion production start dominating. The number of neutrons produced per unit energy is an important quantity since it is related with the energy gain of an ADS. Experimental studies (Andriamonje et al., 1995) have been carried out in this regard.

The possible spallation targets are lead, bismuth, thorium, uranium, tantalum and tungsten. Due to very high heat deposition density by proton beam (about few kW/cc) and very high radiation damage (about 100 DPA or more per year), circulating liquid targets are preferred. Thus, liquid lead and lead-bismuth eutectic (LBE) are considered to be the main choice for the purpose. The proposed MYRHHA facility (Abderrahim, 2005) in Belgium will use liquid LBE as spallation target.

## **1.4 Physics studies in ADS: A review**

### **1.4 .1 Theoretical studies**

#### ***Computer codes and nuclear data***

Simulation of Accelerator Driven Systems (ADS) can be conveniently divided into two parts: one involving description of the interaction of high energy protons with the target and the

other involving the low energy ( $< \sim 10$  MeV) neutronics of the sub-critical core. The quantities of interest obtained in the first part are the number of spallation neutrons produced per proton and their spectrum, the heat deposited in the target and the distribution of the spallation products. LAHET, FLUKA and CASCADE (Prael and Madland, 2000; Ferrari and Sala, 1996; Kumawat and Barashenkov, 2005) are examples of the codes used for the interaction of high energy protons with the target. The core neutronics codes on the other hand are expected to perform calculations for criticality, sub-critical multiplication, power distribution, neutron transport, fuel burn-up, fission products evolution and finally kinetics for discussing transients and safety. Multi-group transport/ diffusion theory codes (Sa. Kondo et al., 1992; Suzuki et al., 2005; Singh et al., 2009, 2011) and continuous energy Monte Carlo codes (Catsaros et al., 2009; Ghosh and Degweker, 2004) for reactor physics analysis fall in this category.

Unlike critical reactors (fast or thermal), neutron energies in an ADS can extend up to hundreds of MeV. Nuclear data for nuclides involved in the thorium-uranium cycle and for minor actinides are also not as well developed as for the uranium cycle. This requires augmentation of existing nuclear data files. Experimental and theoretical studies (Sugawara et al., 2011; Koning et al., 2007) with regard to measurement of cross sections, sensitivity/uncertainty analysis and extension of existing nuclear data files are being carried out by various groups. In this respect, a neutron Time of Flight (nTOF) facility (Abbondanno et al., 2002) has been constructed at CERN and has become operational since 2002.

### ***Degree of sub-criticality and ADS power***

For commercial applications such as electricity generation, waste transmutation and fissile material breeding, the power of an ADS is an important quantity. While in critical reactors the maximum power is decided by the heat removal capacity of the coolant system, the

fission power in an ADS is directly proportional to the external neutron source strength and inversely proportional to the degree of sub-criticality of the core (Nifenecker et al., 2003). Thus, for a given source strength (which is proportional to the proton beam current), the power output can be maximized by minimizing the sub-criticality level. However, at small sub-criticality levels, there are chances of reactor attaining criticality due to reactivity addition under operating transients such as xenon decay or decay of  $\text{Pa}^{233}$  to  $\text{U}^{233}$ . The sub-criticality level should thus be decided based on a balance between requirements of proton current and margin of safety available. The power distribution in an ADS is also different from that in critical reactors and depends on the degree of sub-criticality (Rubia et al., 1995).

### ***Source multiplication and $k_s$ concept***

In a sub-critical finite system, the number of secondary neutrons due to a neutron created at the center will not be the same as that due to a neutron created at the boundary. This has led to the concept of source multiplication factor  $k_s$  (Gandini and Salvatores, 2002) which is defined as the ratio of number of fission neutrons produced to the total number of neutrons produced due to fission and external source. In other words, the number of fission neutrons produced with external source  $S_0$  present is given as:

$$S_0 / (1/k_s - 1) \text{ n/s}$$

We also know that the number of fission neutrons produced in a sub-critical system (characterized by multiplication factor  $k_{eff}$ ) with external source of strength  $S_0$  is given as:

$$S_0 \phi^* / (1/k_{eff} - 1) \text{ n/s}$$

Here,  $\phi^*$  is the ratio of average importance of source neutrons to that of fission neutrons and is commonly known as source importance factor.

Equating the above expressions, the importance of external source can be obtained as:

$$\phi^* = \left( \frac{1}{k_{eff}} - 1 \right) / \left( \frac{1}{k_s} - 1 \right)$$

The  $k_s$  value depends on the properties of the reactor core and characteristics (position, energy) of the external source as it is obtained by solving transport equation with external source.  $k_{eff}$  together with the source importance factor gives us information about reactor power and its level of sub-criticality. The source multiplication factor  $k_s$  can directly be used to obtain reactor power but is not very useful as a measure of departure from criticality.

### ***New definitions of various reactor parameters***

The neutron flux in a sub-critical core is peaked at the centre and falls exponentially as one moves away from the core (Andriamonje et al., 1995). Thus, the usual procedure of deriving reactor kinetics equations i.e. using solution of an adjoint criticality equation as a weighting function cannot be used due to the presence of higher modes. Various suggestions (Gandini, 1997; Gandini and Salvatores, 2002; Sandra Dulla et al., 2006; Kobayashi, 2005; Makai, 2008) have been made in this regard. Depending on the choice of weighting function, new definitions of reactor parameters have been introduced such as  $K_{sub}$  (Gandini, 1997; Gandini and Salvatores, 2002) and  $k_s$  (Sandra Dulla et al., 2006) but it still remains an open question to define a proper weighting function which fits in the framework of conventional reactor parameters.

### ***Studies related to measurement of parameters***

The sub-critical reactivity is an important parameter from the point of view of ADS operation. It decides the accelerator current that will be required to produce the desired power as well as the margin of safety available. Measurement and continuous monitoring of this parameter in operating ADS reactors will be an essential safety requirement. Theoretical and

experimental studies (Abderahim, 2005; Soule et al., 2004; Carl-Magnus Persson et al., 2005; Baeten et al., 2010) are being carried out around the world for developing suitable methods for this purpose. Noise techniques have also been suggested (Behringer and Wydler, 1999; Carta and D'Angelo; 1999 Munoz Cobo et al., 2001) for monitoring the sub-criticality of ADS. Since noise methods do not require any perturbation of the system, they might be more suitable for the purpose (Degweker and Rana, 2007). The earliest theoretical studies on various noise techniques for ADS (Pazsit and Yamane, 1998a, b; Kuang and Pazsit, 2000; Behringer and Wydler, 1999) assumed the neutron producing source events in an ADS to form a Stationary Poisson Point Process (SPPP) with each such event (spallation) producing neutrons with a large multiplicity distribution. A new theoretical approach considering periodic pulsing and non-Poisson character of the source was proposed by Degweker (2000, 2003). The theory has, since then, been considerably expanded by us and forms a major part of this thesis (Degweker and Rana, 2007, 2011; Rana and Degweker, 2009, 2011).

#### **1.4 .2 Experimental studies**

In order to develop suitable methods for measurement and monitoring the sub-criticality of ADS, low power experiments (Andriamonje et al., 1995; Soule et al., 2004; Carl-Magnus Persson et al., 2005; Kitamura et al., 2006; Imel et al., 2004) have been carried out. Other parameters pertaining to operation of a future ADS have also been studied/planned in FEAT and TRADE experiments (Andriamonje et al, 1995; Imel et al, 2004). Recently the Guinevere experimental facility in Belgium has become operational (Billebaud et al., 2009). Experiments aimed towards measurement and monitoring of sub-criticality and evolution of procedures for operation of an ADS are planned in the facility.

### ***Pulsed Neutron Source (PNS) experiments***

By studying the prompt neutron decay after a neutron pulse insertion in a sub-critical system, it is possible to determine the reactivity of the core. The methods used for analyzing a PNS experiment are slope fit method (Keepin, 1965) and area ratio method (Sjostrand, 1956). MUSE experiments (Soule et al., 2004) show that space and energy effects may introduce some bias in the results and detailed computer simulations should be used to take into account the spatial and spectral effects. The PNS experiments in YALINA (Carl-Magnus Persson et al., 2005) were found in good agreement with those obtained by Monte Carlo calculations. The experiments showed that the slope fit method gives better results compared to area ratio and source jerk methods. However, when applied to deep sub-criticalities, it may be difficult to find the correct slope.

### ***Noise experiments***

Noise methods using Rossi alpha, Feynman alpha and CPSD have been studied in MUSE experiments (Soule et al., 2004). The Rossi alpha and Feynman alpha methods were found suitable for low sub-criticalities. CPSD measurements demonstrated the inference of alpha through the break frequency. Rossi alpha measurements have been carried out at the Kyoto University Critical Assembly (KUCA) by using a D–T pulsed neutron source (Kitamura et al., 2006). Since the authors used a solution technique that is based on the Laplace transform, the formula derived by them contains infinite series expansion structure of the oscillating term. Therefore, it was difficult to fit the formula to the experimental data and only the correlated term was used to extract the value of alpha. Similar experiments for demonstrating pulsed neutron and noise methods for sub-criticality measurement are planned in the upcoming Purnima facility at the Bhabha Atomic Research Centre (BARC), India.

### **Reactor Noise in Traditional Reactors and ADS**

The subject of reactor noise has been studied for a long time – indeed it is as old as reactor physics itself. Reactor noise methods are important in the sense that one can obtain dynamic information from measurements at steady state. The subject can broadly be divided in two parts viz., zero power reactor noise and power reactor noise. Zero power reactor noise arises due to the inherently random interactions of neutrons with nuclei and the fission chain multiplication produced correlations and is used to measure kinetic parameters such as prompt neutron lifetime and reactivity. A number of theoretical and experimental techniques have been developed for the purpose. Power reactor noise on the other hand studies the neutronic and other fluctuations associated with vibration of fuel and control rods due to turbulent coolant flow, voids and temperature fluctuations, and is used for online monitoring of the health of the power plant. The recent interest in accelerator driven sub-critical systems (ADS) and the necessity of monitoring their degree of sub-criticality has created a renewed interest in noise methods. In this chapter, we review the subject of noise in critical reactors. We also present a review of noise theories in ADS. We consider only zero power systems in this thesis.

#### **2.1 Noise in critical reactors**

##### **2.1.1 Experimental methods**

The output of a detector, monitoring the neutron population of a reactor in its steady state, will have fluctuations around a mean value and is referred to as noise. The experimental

methods in reactor noise aim at getting information about reactor kinetics parameters by analyzing such fluctuations. Number of experimental methods (Williams, 1974; Saito, 1979) have been developed and are reviewed in the following section.

### 2.1.1.1 Rossi alpha technique

Bruno Rossi (1944) observed that, due to the presence of fission chains, critical assemblies are self modulated and could be used for measurement of prompt neutron decay time. The method is based on measurement of the probability  $P(t_2|t_1)dt_2$  of detecting a neutron between times  $t_2$  and  $t_2 + dt_2$  given that there has been a detection at some earlier time  $t_1$ . Theoretical analysis (Orndoff, 1957; Babala, 1967) shows that in the point model,

$$P(t_2|t_1)dt_2 = N_0 + \frac{\varepsilon \overline{\nu(\nu-1)}}{2\overline{\nu}^2} \alpha \frac{k_p^2}{(1-k_p)^2} e^{-\alpha\tau}$$

where  $\tau = t_2 - t_1$ ,  $N_0$  is the average count rate,  $k_p$  is the prompt neutron multiplication factor,  $\alpha$  is prompt neutron decay constant,  $\varepsilon$  is detector efficiency,  $\overline{\nu}$  and  $\overline{\nu(\nu-1)}$  are first and second moments of number of fission neutrons respectively.

The experimental procedure was first developed by Orndoff (1957) and was based on continuous registration of delayed coincidences of counts. The author made measurements of  $\alpha$  on Godiva (a  $U^{235}$  based bare critical assembly) and its plutonium equivalent. Another procedure proposed by Brunson (1957) measured time interval distribution between successive counts. The experimental procedure developed by Stribel (1963) was based on multi-channel analyzer wherein neutron counts were used to trigger a channel sweep. However, the measurements did not agree with the Rossi alpha formula. Later on Babala (1967) derived expression for  $P(t_2|t_1)dt_2$  for the experimental procedure adopted by Stribel (1963) and showed that the difference was due to smaller amplitude of the exponential term.

### 2.1.1.2 Feynman alpha (variance to mean ratio) technique

This method was proposed by Feynman et al. (1956) and was used by the authors to measure the second moment of the number of neutrons in thermal fission of  $U^{235}$ . The method consists of measuring number of counts in a time interval  $\Delta t$ . The number of counts in  $\Delta t$  is measured repeatedly and used to calculate the variance and the mean. The ratio  $v/m$  is plotted as a function of  $\Delta t$ . By fitting the plot to an expression for  $v/m$  (Bennett, 1960), information about the reactor kinetic parameters can be obtained.

$$\frac{v}{m} = 1 + \frac{2\varepsilon v(v-1)}{v^2} \sum_{i=1}^{J+1} Y_i \left( 1 - \frac{1 - e^{-\alpha_i t}}{\alpha t} \right)$$

where  $J$  is the number of delayed neutron groups and  $Y_i = A_i G(\alpha_i) / \alpha_i$ .  $G(s)$  is the zero power transfer function and  $A_i$  and  $\alpha_i$  are its residues and poles respectively. Subsequently, Albrecht (1962) carried out  $v/m$  measurements and analyzed the results in two group structure of delayed neutrons. It was concluded that the effect of delayed neutrons should be considered in measurement of prompt neutron lifetime.

### 2.1.1.3 Correlation function and power spectral density methods

The most commonly used techniques in reactor noise analysis are based on Auto Correlation Function (ACF) and Power Spectral Density (PSD) methods. The ACF of a fluctuating signal  $N(t)$  is defined as:

$$\phi_{NN}(\tau) = \lim_{T \rightarrow \infty} \frac{1}{2T} \int_{-T}^T N(t)N(t+\tau)dt$$

If one considers correlation between two different noise signals (e.g. neutron density and detector current), the function is called Cross Correlation Function (CCF).

For zero power reactor noise, the expression for ACF is related to reactor kinetics parameters as follows (Williams, 1974):

$$\phi_{NN}(\tau) = \varepsilon \lambda_f \bar{N} \left[ \delta(\tau) + \frac{1}{2} \sum_i Y_i \alpha_i e^{-\alpha_i |\tau|} \right]$$

where the first term is due to the detector noise and the second term is due to fission chain correlations.

For small values of  $\tau$ , the main contribution comes from the prompt neutrons and accordingly the above expression for ACF can be approximated as:

$$\phi_{NN}(\tau) = \varepsilon \lambda_f \bar{N} \left[ \delta(\tau) + \frac{\varepsilon \nu (\nu - 1)}{\bar{\nu}^2} \frac{e^{-\alpha_1 \tau}}{2\Lambda(\beta - \rho)} \right]$$

Dragt (1966a) analyzed current from ion chamber by ACF and was able to evaluate reactor kinetics parameters with high accuracy.

The PSD is defined as the Fourier Transform of ACF and is a measure of the power of the noise signal per unit of frequency. Similarly, the Fourier transform of CCF is called Cross Power Spectral Density (CPSD).

$$\phi_{NN}(\omega) = \int_{-\infty}^{\infty} \phi_{NN}(\tau) e^{-i\omega\tau} d\tau$$

Performing the Fourier transform we obtain:

$$\phi_{NN}(\omega) = \varepsilon \lambda_f \bar{N} \left( 1 + \sum_i \frac{Y_i \alpha_i^2}{\alpha_i^2 + \omega^2} \right)$$

In the neighborhood of  $\alpha_1$ , the above expression can be approximated to the form:

$$\phi_{NN}(\omega) = A + \frac{B}{\alpha^2 + \omega^2}$$

Kinetic parameters have been determined (Kuramoto et al., 2007) in IPEN/MB-01 research reactor by PSD technique. Suzuki (1966) suggested a method of measuring absolute power of

a reactor by PSD measurements. Due to increase in sensitivity of the measurements at low powers, it was suggested that the method can be implemented in research reactors.

At high frequencies, the contribution of detector noise (the first term) increases and the PSD measurements become difficult. The two detector covariance method suggested by Nomura (1966) does not have the first term and overcomes this difficulty. Such measurements (Rugama et al., 2003) in MASURCA at CEA showed better results compared to those obtained by single detector PSD analysis due to low signal to noise ratio in the latter coming from strong inherent spontaneous fission source.

#### **2.1.1.4 Other methods**

A variant of Feynman-Y technique has been proposed by Bennett (1960) and is commonly referred to as Bennett variance technique. Based on computation of variance from cross-correlation of count rates in two successive time intervals, the author derived an expression for variance to mean ratio which does not diverge as reactor approaches criticality. Similar to correlation function method, a method based on polarity correlation function has been proposed (Veltman and Kwakernaak, 1961; Dragt, 1966b). Other methods for measurement of prompt neutron decay constant include the interval distributions method (Babala, 1966) and the dead time method (Srinivasan, 1967; Srinivasan and Sahni, 1967). The  $Cf^{252}$  method was developed and studied intensively by Mihalcz (1974, 1990) for measuring degree of sub-criticality.

#### **2.1.2 Basics of noise theory of critical reactors**

The inherent neutron noise in a low power reactor can be considered theoretically as a Markov process. Markov processes are the stochastic processes which are characterized by the fact that the conditional probability of a system being in a certain state at a certain time

$t_n$ , given that it was in some state at an earlier time  $t_{n-1}$ , is uniquely determined and does not depend on its state prior to  $t_{n-1}$ . If  $P_1(X, t)$  is the probability of the system being in state  $X$  at time  $t$  and  $P_{1|1}(X_2, t_2 | X_1, t_1)$  is the transition probability of the system going from state  $X_1$  at time  $t_1$  to the state  $X_2$  at time  $t_2$ , all other states can be determined as follows:

$$P_1(X_2, t_2) = \sum_{X_1} P_{1|1}(X_2, t_2 | X_1, t_1) P_1(X_1, t_1)$$

Thus, the Markov processes are completely described by the two probability functions  $P_1(X, t)$  and  $P_{1|1}(X_2, t_2 | X_1, t_1)$ . It can be shown that these probabilities are related through what is known as the Chapman Kolmogorov equation:

$$P_{1|1}(X_2, t_2 | X_1, t_1) = \sum_X P_{1|1}(X_2, t_2 | X, t) P_{1|1}(X, t | X_1, t_1)$$

A Markov process is called homogeneous if the transition probability  $P_{1|1}(X_2, t_2 | X_1, t_1)$  depends only on the time difference  $\tau = t_2 - t_1$ . For such processes, if it can be assumed that for small  $\tau$  the transition probability can be written as follows:

$$T_\tau(X_2 | X_1) = \delta(X_2 - X_1) - W(X_2 | X_1) \tau + O(\tau)$$

then the Chapman Kolmogorov equation can be written (Van Kampen, 1983) as a differential equation in time as given below.

$$\frac{\partial}{\partial \tau} T_\tau(X_2 | X_1) = \sum_X \left[ W(X_2 | X) T_\tau(X | X_1) - W(X | X_2) T_\tau(X_2 | X_1) \right]$$

This equation is known as the Master equation and is a statement of gain-loss for the probability of a state.

At zero power, there are no feedback effects and we get a linear equation. Starting with Chapman Kolmogorov equation and using probability balance equations, ‘forward’ and ‘backward’ equations can be derived for a point reactor model (Arcipiani and Pacilio, 1980).

### 2.1.2.1 Kolmogorov forward equation

This approach was first used by Courant and Wallace (1947) who derived expressions for standard deviation by considering distributed sources in a reactor whose power was assumed to be either steady or changing periodically. Subsequent studies on the subject were carried out by Matthes (1962), Norelli et al. (1975), Dalfes (1966), Pazsit (1987) and Degweker (1994). In the point model (Arcipiani and Pacilio, 1980; Dalfes, 1966; Norelli et al. 1975), one writes the probability equation for state of the reactor at time  $t + \Delta t$  in terms of its state at time  $t$ .

We start with the Chapman-Kolmogorov equation:

$$P(n, t | m, s) = \sum_l P(n, t | l, \tau) P(l, \tau | m, s)$$

and set  $\tau = t - dt$  for deriving the forward equation.

$$\begin{aligned} P(N, t + dt) &= \lambda_c(N+1)dtP(N+1) + \sum_{\nu} \lambda_f(N-\nu+1)dt p(\nu)P(N-\nu+1) \\ &+ SdtP(N-1, t) + [1 - \{(\lambda_f + \lambda_c)N + S\}dt]P(N, t) \end{aligned}$$

where  $S$  is the source strength,  $\lambda_c$ ,  $\lambda_f$  are the capture, fission probabilities per neutron per unit time and  $p(\nu)$  is the probability that a fission reaction produces  $\nu$  neutrons. Expanding the term on the LHS up to first order in  $dt$ , we can obtain the following equation:

$$\begin{aligned} \frac{dP(N, t)}{dt} &= \lambda_c(N+1)P(N+1) + \sum_{\nu} \lambda_f(N-\nu+1)p(\nu)P(N-\nu+1) \\ &+ SP(N-1, t) - \{(\lambda_f + \lambda_c)N + S\}P(N, t) \end{aligned}$$

We define the probability generating function (pgf) as:

$$F(x, t) = \sum_N P(N, t) x^N$$

We can rewrite the above equation in terms of the pgf as follows:

$$\frac{\partial F(x, t)}{\partial t} = [\lambda_c(1 - x) + \lambda_f(f(x) - x)] \frac{\partial F(x, t)}{\partial x} + S(x - 1)F(x, t)$$

Various moments are obtained by successive differentiation with respect to  $x$  and setting  $x = 1$ .

Using forward equation approach in point model, Norelli et al. (1975) set up reactor kinetics equations and obtained analytical solutions for different cases. Dalfes (1966) derived expressions for correlation function and PSD of detector output for a subcritical reactor driven by a Poisson source.

### 2.1.2.2 Kolmogorov backward equation

The backward equation approach was first used by Pal (1958) and Bell (1965) and has been significantly developed by Matthes (1966), Munoz-Cobo and Verdu (1987) and Pazsit (1987). In the point model (Arcipiani and Pacilio, 1980), one writes the probability equation for state of the reactor at time  $t$  given its state at some earlier time  $s$ . The Chapman-Kolmogorov equation is written with the intermediate time point  $s + ds$  considering all the possible processes in the interval  $ds$ .

For deriving the backward equation, we choose  $\tau = s + ds$  &  $m=1$

$$\begin{aligned} P(n, t | m, s) &= \lambda_c m ds P(n, t | m-1, s+ds) + \lambda_f m ds \sum_{\nu} p(\nu) P(n, t | m+\nu-1, s+ds) \\ &+ S ds P(n, t | m+1, s+ds) + [1 - \{m(\lambda_f + \lambda_c) + S\} ds] P(n, t | m, s+ds) \end{aligned}$$

$$\begin{aligned} -\frac{dP}{ds} &= \lambda_c m P(n, t | m-1, s) + \lambda_f m \sum_{\nu} p(\nu) P(n, t | m+\nu-1, s) \\ &+ S P(n, t | m+1, s) - \{m(\lambda_f + \lambda_c) + S\} P(n, t | m, s) \end{aligned}$$

The equation for the pgf is obtained by multiplying by  $x^n$  and summing over  $n$

$$-\frac{\partial F(x, t | m, s)}{\partial s} = \lambda_c m F(x, t | m-1, s) + \lambda_f m \sum_{\nu} p(\nu) F(x, t | m+\nu-1, s) + S F(x, t | m+1, s) - \{m(\lambda_f + \lambda_c) + S\} F(x, t | m, s)$$

Suppose  $m=1$  and  $S=0$  i.e. a single initial neutron in a source free medium. The above equation then becomes

$$-\frac{\partial F(x, t | 1, s)}{\partial s} = \lambda_c + \lambda_f \sum_{\nu} p(\nu) F^{\nu}(x, t | 1, s) - (\lambda_f + \lambda_c) F(x, t | 1, s)$$

where we have used the following relation due to of independence of chains

$$F(x, t | m, s) = F^m(x, t | 1, s)$$

By considering a multivariate joint distribution for neutrons and detector counts and following Kolmogorov forward equation approach, Pacilio et al. (1976) developed a unified theory of reactor neutron noise analysis techniques.

In the space energy dependent formulation, discussed below, the backward equation is almost invariably used due to its simplicity. This equation closely resembles the adjoint neutron transport equation.

### 2.1.2.3 The Bartlett formula

The normal procedure for deriving moments of any observable (say detector counts) in a multiplying medium with an external source consists of either writing forward Master equation with source or using the backward Master equation approach. In this method, first the backward Master equation is solved to find the pgf due to a single particle. The pgf for the case of external source is then obtained by using the Bartlett formula (Bartlett, 1955).

Suppose we have a Poisson source switched at time  $s$ . There can be  $k$  source events ( $k = 1, 2, \dots, \infty$ ) at  $t_1, t_2, \dots, t_k$  with probability:

$$\frac{[S(t-s)]^k}{k!} \exp\{-S(t-s)\} \frac{dt_1}{(t-s)} \dots \frac{dt_k}{(t-s)}$$

The pgf from each of these events is  $F(x, t | 1, t_i)$  and that due to all the  $k$  events can be written (using the property of independence of neutron behavior) as follows:

$$F(x, t | 1, t_1) F(x, t | 1, t_2) \dots F(x, t | 1, t_k)$$

Multiplying the two expressions and summing over all possibilities of source events, we get the resultant pgf.

$$\begin{aligned} F_S(x, t | 1, \tau) &= \exp\{-S(t-s)\} \sum_{k=0}^{\infty} \int_s^t dt_1 \dots \int_s^t dt_k \frac{S^k}{k!} dt_1 \dots dt_k F(x, t | 1, t_1) F(x, t | 1, t_2) \dots F(x, t | 1, t_k) \\ &= \exp \left[ S \int_s^t \{F(x, t | 1, \tau) - 1\} d\tau \right] \end{aligned}$$

For a steady source, the lower limit can be taken to be  $-\infty$ .

#### 2.1.2.4 Space energy dependence

The earliest space dependent theory was developed by Pal (1958) who obtained an integral equation for pgf  $G(z, R, t_f; r, v, t)$  of number of neutrons in some region  $R$  of the reactor at time  $t_f$  starting from a single neutron at time  $t$  in region  $r$  with velocity  $v$ . The author also derived equations for first and second moments. Bell (1965) developed integro-differential equation for  $G$ . Dropping the explicit dependence of  $G$  on  $R$  and  $t_f$ , the equation can be written as follows:

$$\begin{aligned} -\frac{\partial G}{\partial t} &= \Omega \cdot \nabla G - \Sigma G + \Sigma_s \int f(E, \Omega \rightarrow E', \Omega') G(z, r, \Omega', E', t) d\Omega' dE' \\ &\quad + \Sigma_f F \left( \int \frac{\chi(E')}{4\pi} G(z, r, \Omega', E', t) d\Omega' dE' \right) \end{aligned}$$

It was shown by the author that the equation is adjoint to the Boltzman transport equation. Asymptotic solutions for sub-critical and super-critical systems were obtained and found to be consistent with physical arguments. Matthes showed that the space-energy dependent

backward equation is adjoint to the transport equation. Munoz-Cobo and Verdu (1987) derived stochastic transport equation including delayed neutrons. They obtained expressions for Feynman Y function and studied the effect of delayed neutrons on it.

Based on probability distribution of neutrons in phase cells, Matthes (1962) developed the forward equation for space-energy dependence. He derived ACF formula for output of a detector placed in a reactor. Pazsit (1987) derived forward and backward equations from a single equation representing Markovian property of the process. The author however pointed out the difficulties in getting higher order moments. Degweker (1994) developed a new formalism for describing the stochastic neutron transport by the forward approach. The formalism is based on the probability of having  $N$  neutrons in the entire reactor with each neutron lying in a phase space cell located at any point in phase space. It was shown that the first moment of the equation is the usual transport equation for the singlet density while higher moments yield equations for the doublet and higher multiplet densities.

#### **2.1.2.5 The Langevin approach**

The Langevin method for studying reactor noise problems was introduced in the point model by Cohn (1960) and was applied to space dependent problems by Moore (1964) and has been developed considerably by Sheff and Albrecht (1966), Ackasu and Osborn (1966) and Saito (1967). The method looks upon reactor noise as being the response of a linear system to a random source commonly referred to as the noise equivalent source (NES). The equations of the linear system are the usual kinetics equations for the variables referring to the mean values while the noise characteristics of the NES are determined by the so called Schottky prescription. Let us consider a simple point model with one group of delayed neutrons and a detector. The Langevin equations giving the neutron number ( $N$ ), the number of precursors ( $C$ ) and the detection rate ( $D$ ) are given by

$$\frac{dN}{dt} = [\lambda_f \bar{\nu}_p - (\lambda_c + \lambda_d)] N + \mu_c \bar{C} + \bar{\nu}_s S + s_N(t) \quad (2.1)$$

$$\frac{dC}{dt} = \lambda_f \bar{\nu}_d N - \mu_c \bar{C} + s_C(t) \quad (2.2)$$

$$\frac{dZ}{dt} = D(t) = \lambda_d N + s_D(t) \quad (2.3)$$

where  $\lambda_f, \lambda_c, \lambda_d$  are probabilities per unit time of fission, capture, detection respectively,  $\mu_c$  is delayed neutron precursor decay constant,  $\nu_s$  is the number of neutrons in each source event,  $\nu_p$  is number of prompt neutrons,  $\nu_d$  is number of delayed neutrons,  $D$  is the detection rate,  $Z$  is the number of counts accumulated in a detector over a time  $t$  and  $s_N, s_C, s_D$  are noise equivalent sources for neutrons, delayed neutron precursors and detection respectively.

The NES is a white noise whose magnitude is determined by the Schottky prescription. According to this, each of the processes such as absorption, fission, source, etc contribute a white noise to the NES. The contribution of the power spectral density of the NES due to each of these reactions is given by  $\overline{q^2 m}$  where  $q$  is the change in the number of particles (corresponding to that equation, neutrons, precursors etc) in one reaction and  $m$  is the mean reaction rate of that reaction. Similarly, the cross power spectral density between NES for two different particles has a contribution given by  $\overline{q_i q_j m}$  where  $q_i$  and  $q_j$  are the change in the number of particles of type  $i$  and  $j$  in the reaction and  $m$  is the mean reaction rate of that reaction (Cohn, 1960). Using this prescription, we can write the following statistical properties for the NES terms of Eqs. (2.1) – (2.3)

$$\langle s_N(t) \rangle = \langle s_C(t) \rangle = \langle s_D(t) \rangle = 0 \quad (2.4)$$

$$\langle s_N(t) s_N(t') \rangle = [(\lambda_c + \lambda_d) \bar{N}(t) + \lambda_f (\bar{\nu}_p - 1)^2 \bar{N}(t) + \mu_c \bar{C}(t) + \bar{\nu}_s^2 \bar{S}(t)] \delta(t - t') \quad (2.5)$$

$$\langle s_C(t) s_C(t') \rangle = [\lambda_f \bar{\nu}_d^2 \bar{N}(t) + \mu_c \bar{C}(t)] \delta(t - t') \quad (2.6)$$

$$\langle s_D(t)s_D(t') \rangle = \lambda_d \bar{N}(t) \delta(t-t') \quad (2.7)$$

$$\langle s_N(t)s_C(t') \rangle = [\lambda_f \overline{(v_p - 1)v_d} \bar{N}(t) - \mu_c \bar{C}(t)] \delta(t-t') \quad (2.8)$$

$$\langle s_D(t)s_N(t') \rangle = -\lambda_d \bar{N}(t) \delta(t-t') \quad (2.9)$$

$$\langle s_C(t)s_D(t') \rangle = 0 \quad (2.10)$$

If we are dealing with a stationary system, the mean values of the variables in Eqs. (2.1)-(2.10) are independent of time. Writing Eqs. (2.1-2.3) in terms of the fluctuations about the mean values for a stationary system, we have

$$\frac{dn}{dt} = \left[ \lambda_f \bar{v_p} - (\lambda_c + \lambda_d) \right] n + \mu_c c + s_N(t) \quad (2.11)$$

$$\frac{dc}{dt} = \lambda_f \bar{v_d} n - \mu_c c + s_C(t) \quad (2.12)$$

$$d(t) = \lambda_d n + s_D(t) \quad (2.13)$$

where  $n, c, d$  stand for the fluctuations of the neutron number, precursor number and the detection rate over their mean values i.e.  $n(t) = N(t) - \bar{N}$ ,  $c(t) = C(t) - \bar{C}$  and  $d(t) = D(t) - \bar{D}$  respectively.

The Langevin approach can be used for obtaining any noise descriptor but gets more complicated in the time domain if the problem involves several variables. In such cases the Langevin approach is particularly suitable for doing calculations in the frequency domain i.e., for obtaining the power spectral density of detection rate. For this, we recall that according to the Weiner-Khinchin theorem (Van Kampen, 1983), the PSD is proportional to the mod-square of the Fourier transform of the signal, in this case the fluctuation of the detection rate  $d(t)$ . To determine the PSD of  $d(t)$ , we Fourier transform Eq. (2.13) and write

$$\langle d^*(\omega)d(\omega) \rangle = \lambda_d^2 \langle n^*(\omega)n(\omega) \rangle + 2\lambda_d \text{Re}[\langle n^*(\omega)s_D(\omega) \rangle] + \langle s_D^*(\omega)s_D(\omega) \rangle \quad (2.14)$$

Fourier transforming Eq. (2.7) [w.r.t. to the time difference  $t-t'$ ], we get the following contribution (known as the detector noise) to the PSD.

$$\lambda_d \overline{N} \quad (2.15)$$

Fourier transforming Eqs. (2.11) and (2.12) and solving the resulting algebraic equations, we get

$$\begin{aligned} x(\omega) &= (-i\omega + \Lambda)^{-1} s(\omega) \equiv T^* s(\omega) \\ x^*(\omega) &= T s^*(\omega) \end{aligned} \quad (2.16)$$

where  $x$  and  $s$  stand for the vectors  $\begin{pmatrix} n \\ c \end{pmatrix}$  and  $\begin{pmatrix} s_N \\ s_C \end{pmatrix}$  respectively and  $\Lambda$  is the matrix in terms of which Eqs. (2.11) and (2.12) can be written as

$$\frac{dx}{dt} + \Lambda x = s \quad (2.17)$$

i.e.,  $\Lambda = - \begin{pmatrix} \left[ \lambda_f \overline{v_p} - (\lambda_c + \lambda_d) \right] & \mu_c \\ \lambda_f \overline{v_d} & -\mu_c \end{pmatrix}$  and we have written  $T$  for the matrix  $(i\omega + \Lambda)^{-1}$ .

Now we can write the contribution from the first term of (2.14) as

$$\langle n^*(\omega) n(\omega) \rangle = [\langle x^*(\omega) x^t(\omega) \rangle]_{00} = \left[ (i\omega + \Lambda)^{-1} \Sigma(\omega) (-i\omega + \Lambda^t)^{-1} \right]_{00} \quad (2.18)$$

where we have used the index 0 for the neutron variable and 1 for the precursor variable and where  $\Sigma(\omega) = \langle s^*(\omega) s^t(\omega) \rangle$  is spectral density matrix of the NES i.e. the Fourier transform of the covariance matrix of the NES. The individual elements of  $\Sigma(\omega)$  can be simply obtained by taking the Fourier transform of Eqs. (2.5), (2.6) and (2.8) w.r.t.  $\tau = t' - t$  and we get

$$\Sigma = \begin{pmatrix} (\lambda_c + \lambda_d) \overline{N} + \lambda_f \overline{(v_p - 1)^2 N} + \mu_c \overline{C} + \overline{v_s^2 S} & \lambda_f \overline{(v_p - 1) v_d N} - \mu_c \overline{C} \\ \lambda_f \overline{(v_p - 1) v_d N} - \mu_c \overline{C} & \lambda_f \overline{v_d^2 N} + \mu_c \overline{C} \end{pmatrix} \quad (2.19)$$

Finally, we obtain the contribution of the second term of Eq. (2.14). We write,

$$2\lambda_d \text{Re}[\langle n^*(\omega) s_D(\omega) \rangle] = 2\lambda_d \text{Re}[\langle \{T_{00} s_N^*(\omega) + T_{01} s_C^*(\omega)\} s_D(\omega) \rangle] \quad (2.20)$$

The second term in Eq. (2.20) above vanishes in view of Eq. (2.10) while the first term can be written down using (2.9) to yield

$$\begin{aligned} 2\lambda_d \operatorname{Re}[\{T_{00} < s_N^*(\omega)s_D(\omega) >\}] &= -2\lambda_d^2 \bar{N} \operatorname{Re}\{T_{00}\} \\ &= -2\lambda_d^2 \bar{N} \operatorname{Re}[G(i\omega)] \end{aligned} \quad (2.21)$$

as the contribution due to the middle term of Eq (2.14) where  $G(i\omega)$  can be recognized as the zero power transfer function. The PSD of the detection rate is obtained by adding (2.18), (2.21) and the detector noise term (2.15).

The Langevin method described above can be extended to problems of reactor noise including power reactor noise where the noise source is external and moreover may not be white. The white noise source assumption is specific to the internal noise description through the Schottky prescription but is not generic to the Langevin approach. Due to its non-Poisson character, the ADS source cannot be described by the Schottky formulae. However, by choosing the fluctuation character of the source appropriately, it is still possible to use the Langevin approach. This is illustrated in chapter V in both the time and frequency domain.

In the context of zero power noise, some authors (Williams, 1974; Difilippo, 1988) have questioned the validity of the Langevin formulation and the recipes based on the Schottky prescription to give correct results in all situations. While the Langevin approach is less fundamental than the probability balance equation methods (Kolmogorov forward or backward equations, pgf etc) [Williams, 1974], Ackasu and Stolle (1989) have argued that the Schottky prescription is derivable from the Master equation and with a proper vector formulation involving all relevant variables of the problem, yields correct results in all situations for second moments.

## **2..2 Review of noise theories in ADS**

### **2.2.1 Early studies on theory of reactor noise in ADS**

As mentioned earlier, in addition to the well known deterministic methods such as pulsed neutron method and source jerk method, noise techniques were also suggested for monitoring the sub-criticality of ADS (Behringer and Wydler, 1999; Carta and D'Angelo, 1999; Munoz Cobo et al., 2001). In view of this, theoretical studies on various noise techniques for ADS (Pazsit and Yamane, 1998a,b; Kuang and Pazsit, 2000; Degweker, 2000; Behringer and Wydler, 1999; Munoz Cobo et al., 2001) were initiated.

In the earlier publications (Pazsit and Yamane, 1998a,b; Kuang and Pazsit, 2000; Behringer and Wydler, 1999), the authors assumed that the ADS source was a continuous Poisson source and that the main difference from traditional reactors was that in each source event spallation reaction produces a large number of neutrons having a multiplicity distribution with a large mean and a large second factorial moment. Theoretically speaking, such a situation is very similar to that of a spontaneous fission source and has been studied in detail by Munoz Cobo and Difilippo (1988).

However, the principal difference between critical reactor noise and ADS noise is due to the statistical properties of the source. Unlike the source due to radioactive decay present in ordinary reactors, the accelerator produced neutron source in an ADS cannot be assumed to be a Poisson process. Moreover, the source may be pulsed. The initial studies did not account for these effects.

Behringer and Wydler (1999) assumed that the arrival of the protons is Poissonian distributed in time and neglected periodic appearance of source pulses. They also assumed that the number of protons in a pulse is Poisson distributed. They used simple probability balance

equation to derive the formula for variance. It was concluded that, in addition to the fission chain correlations, fluctuations in the burst of spallation neutrons contribute to the increased variance above that for a pure Poissonian process. Pazsit and Yamane (1998a) derived variance to mean formula by using a master equation technique. Source characteristics were assumed to be same as that in the model of Behringer and Wydler. The authors also included the effect of delayed neutrons (Pazsit and Yamane, 1998b; Kuang and Pazsit, 2000). It was shown that in deep subcritical reactors, the large source multiplicity enhances the amplitude of the prompt term of variance to mean formula which can be used for monitoring the reactivity.

### **2.2.2 Studies with periodic pulses**

Periodically pulsed sources were treated by Degweker (2000, 2003), Munoz Cobo et al. (2001), Pazsit et al. (2005) and Kitamura et al. (2005). Munoz Cobo et al. (2001) proposed a method for on line sub critical reactivity monitoring based on the measurement of the cross power spectral density (CPSD) between the proton current signal and a neutron detector signal. They considered the source to be a periodic sequence of delta function pulses with a fixed number of protons per pulse and derived an expression for CPSD. Numerical calculations were done for a typical fast energy amplifier configuration and the value of  $k_{eff}$  was obtained by break frequency method. The results were also compared with Monte Carlo simulations. Pazsit et al. (2005) and Kitamura et al. (2005) also considered the periodicity of the source. They considered the pulse to be of finite width of rectangular and Gaussian shapes. They also included the effect of delayed neutrons.

### 2.2.3 Studies with non-Poisson sources

#### *Basis for the possibility of non-Poisson behavior of the ADS source*

Radioactive sources present in critical reactors consist of large number of radioactive atoms, of which, relatively small number decay independently in the time scales of interest and therefore can be deemed to be stationary Poisson sources (Uhrig, 1970). However, such a description may not necessarily hold for accelerator produced neutron sources. It has been suggested (Pazsit et al., 2004) that since the continuous arrival of charged particles may be treated as a Poisson process, if the same is periodically chopped, the resulting particle stream may be looked upon as a periodically pulsed Poisson source. The argument is valid for a perfectly steady machine. A practical accelerator on the other hand, is expected to show small fluctuations in current which can lead to the non-Poisson distribution of number of particles in a pulse (Degweker and Rana, 2007). Moreover, accelerators produce particles in the form of short bunches at periodic intervals rather than at random. There may also be correlations introduced during production of protons. Thus, irrespective of the type of accelerator used for the purpose, it cannot be tacitly assumed that the source events would constitute a Stochastic Poisson Point Process. To give an empirical evidence of the non-Poisson character of the ADS source, we present below observations on some experimental results.

#### *The TARC experiments*

One of the measurements carried out during the TARC experiment (Abanades et al., 2002) was number of protons per shot; each shot being about 14 s separated from the previous shot. The magnitude of the fluctuations in the number of protons per shot in the experiment was a few percent which is much larger than would be expected for a Poisson source. For small current fluctuations, the accelerator may be treated as linear system with Gaussian current fluctuations having exponential correlation. Simulation of such a process for various

correlation times was carried out by us (Degweker and Rana, 2007) and a comparison with the TARC experiment showed that the measured results appear to be closest to an uncorrelated Gaussian process thereby implying that correlation times if any are short compared to 14 seconds. Thus, the number of protons in a pulse cannot be considered to be Poisson distributed.

#### *The KUCA experiments*

In their paper on the calculation of pulsed Feynman alpha formulae and their experimental verification, Pazsit et al. (2005) have presented experimental results obtained at the KUCA facility showing variation of the Feynman Y function with counting interval for different levels of sub-criticality (or alpha). From this data, it is possible to deduce the asymptotic values (i.e. for large counting intervals on the prompt decay time scale) of the Y function. Fig. 2.1 shows the variation of the asymptotic Y values obtained this way with the inverse of alpha estimated in the above mentioned paper. In the graph (a) we show a power law fit, while in (b) we show a quadratic fit. While both fits are equally good, the power shown is not 2 as is expected on the assumption of a Poisson source. In Fig. 2.1(b), the fitted curve passes through the origin. The quadratic term is due to fission chain correlations while the linear term indicates a non-Poisson source contribution. Since the D-D or D-T reaction produces neutrons in singlets, the origin of the source correlation can be only due to the non-Poisson characteristics of the ion beam.

#### *Other experiments*

A third piece of evidence of the non-Poisson character of accelerator based neutron sources can be seen in the experimental study by Hiroshi Taninaka et al. (2011). The authors have carried out Feynman alpha measurements with a pulsed D-T source. It has been reported that

instabilities in the accelerator current result in a divergent variance to mean ratio and the formula based on Poisson source assumption underestimates the value of alpha.

### ***Theory of ADS noise with non-Poisson sources***

Degweker (2000, 2003) argued that the usual procedure (using forward equation approach or writing down backward equation for single particle induced moments and then using Bartlett formula for source induced moments) for deriving reactor noise formulae are invalid with such sources. The method suggested for treating non-Poisson sources is described below.

Let  $G(z_1, z_2, t)$  be the pgf of detecting counts in a short interval around time 0 and counts in a short interval around time  $\tau$  due to single neutron injected in a source free medium at time  $t$ . If it is assumed that bursts of neutrons appear at times  $t_n$  with a multiplicity distribution  $\rho(v)$  and the last of these bursts occurs at  $t_0$  then the ones prior to this will occur at  $t_0 - 1/f$ ,  $t_0 - 2/f$  and so on. Here  $f$  is the frequency of the accelerator. Using the multiplicative property of pgfs for different source events, the pgf for the case of an arbitrary source is obtained. This property is due to the independent propagation of chains initiated by different source neutrons and is a consequence of the linear character of the neutron transport and multiplication. The resultant pgf is:

$$\prod_{n=0}^{\infty} \sum_v \rho(v) G^v(z_1, z_2, t_0 - n/f) = \prod_{n=0}^{\infty} F_{\rho}(G(z_1, z_2, t_0 - n/f))$$

Since measurement intervals are generally not synchronized with the source pulses,  $t_0$  is a uniformly distributed (between  $\tau - 1/f$  and  $\tau$ ) random variable. Averaging over  $t_0$ , the pgf becomes:

$$g = f \int_{\tau-1/f}^{\tau} \prod_{n=0}^{\infty} F_{\rho}(G(z_1, z_2, t_0 - n/f, \tau)) dt_0$$

By differentiating with respect to  $z_1$  and  $z_2$ , and setting  $z_1 = z_2 = 1$ , one obtains the Rossi alpha formula.

$$f_2(0, \tau) = \frac{f \lambda_d^2}{2\alpha} \left[ \frac{m_1^2}{1 - e^{-\alpha/f}} \left\{ e^{-\alpha/f} e^{\alpha \left( \tau - \frac{\lfloor f\tau \rfloor}{f} \right)} + e^{-\alpha \left( \tau - \frac{\lfloor f\tau \rfloor}{f} \right)} \right\} + (m_2 - m_1^2 + 2m_1 Y_1) e^{-\alpha\tau} \right]$$

The individual pulses were treated as Dirac delta functions, uncorrelated with one another. Various noise descriptors, such as Rossi alpha, Feynman alpha (or variance to mean), Power Spectral Density (PSD), Cross Power Spectral Density (CPSD), were derived. It was shown that the large neutron emission multiplicity of the spallation source is mainly responsible for the enhanced variance compared to critical reactors and the correlated component of the noise is reduced due to regularity of the source pulses. The author (2003) pointed out anomaly in the CPSD formula derived by Munoz Cobo et al. (2001) and showed that if one uses the method of joint pgf for current and neutronic signals, the cross-covariance is identically zero. The scope and content of the noise theory (Degweker, 2000, 2003) has been considerably expanded by us (Degweker and Rana, 2007, 2011; Rana and Degweker, 2009, 2011) and is described in detail in the following chapters.

Later on Ballester and Munoz Cobo et al. (2005, 2006) have also considered the periodic nature of the source and its non-Poisson character. By considering pulsed neutron source along with the spontaneous fissions in the fuel, they derived a generalized relationship between the pgfs of the kernel and the source.

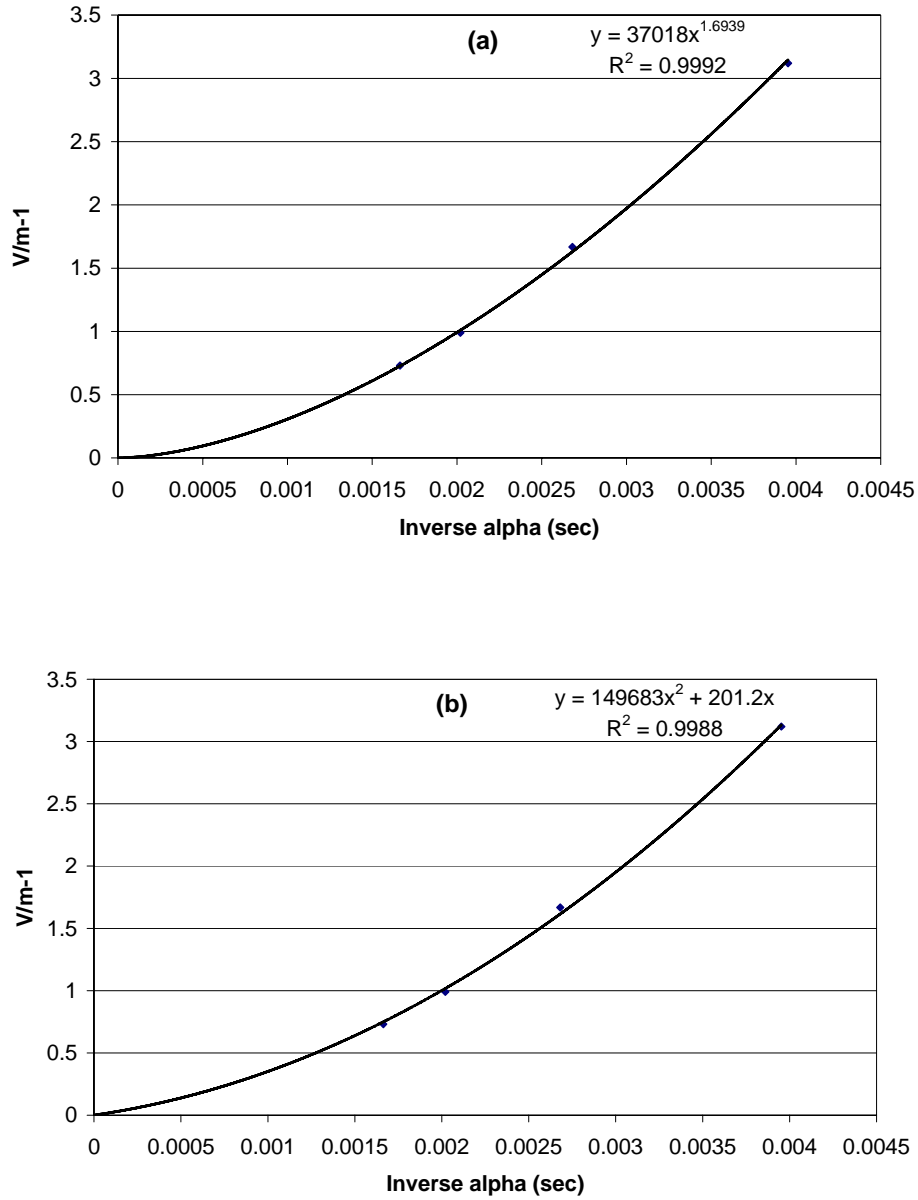


**Fig. 2.1** Variation of the  $v/m$  with inverse of the decay constant. The points are based on the experimental results presented in by Pazsit et al. (2005). In the graph (a) we show a power law fit while in (b) we show a quadratic fit. While both fits are equally good, the power obtained is not 2 as is expected on the assumption of a Poisson source. The quadratic fit passes through the origin and the linear term indicates a non-Poisson source contribution.

# Finite Pulses and Correlations between Different Pulses

As discussed in chapter 2, a theory of Reactor Noise in ADS assuming a general non-Poisson periodically pulsed source of neutrons was constructed by Degweker (2003). In this chapter, we generalize the non-Poisson character of the source to include the possibility of correlations between pulses and derive formulae for Rossi alpha and Feynman alpha. We also take up the case of pulses of finite widths by considering rectangular and Gaussian pulse shapes. We present numerical results based on the derived formulae to illustrate the importance of correlations between pulses in typical experimental conditions. The effect of finite width of source pulses is also illustrated.

Pazsit et al. (2005) have also considered finite width pulses in the context of reactor noise in ADS but for Poisson sources. The formulation in the present chapter is different in that the source is assumed to be non-Poisson with exponential correlation between pulses. In section 3.2, we consider the case of correlated non-Poisson delta function source pulses. The case of finite width pulses is discussed in section 3.3. Our analysis is restricted to the experimental situation in which the counting interval is opened at a time point that is essentially random since this has been shown to be experimentally better for extracting parameters of interest (Pazsit et al., 2005). We do not consider the effect of delayed neutrons. Hence, the formulae are valid only for time scales which are short compared to the delayed neutron precursor lifetimes and all quantities (such as  $k$ ,  $\nu$ , etc.) are to be regarded as prompt.

### 3.1 The doubly stochastic Poisson point process

If  $I(t)$  is the ion current, the probability of a neutron producing event (spallation, D-D or D-T reactions) in a short time  $dt$  can be written as

$$I(t)E(t)dt$$

where,  $E(t)$  is the deterministic variation of the current (periodically occurring pulses). Since this is the probability at any time and independent of any occurrences at other times, we can write for the probability of obtaining  $s$  source events at times  $t_1, t_2, \dots, t_s$  as follows:

$$Q_s(t_1, t_2, \dots, t_s) = E(t_1)I(t_1) \dots E(t_s)I(t_s) \exp\left[-\int_{-\infty}^{+\infty} E(t)I(t)dt\right] \quad (3.1)$$

As mentioned before, we assume  $I(t)$  as an exponentially correlated Gaussian stochastic process. Since, for averaging various functions we have to perform a double averaging; one over the variables  $s$  and  $t_s$  and the second over the stochastic variable  $I(t)$ , we have a doubly stochastic Poisson point process (Saleh, 1978). We shall use such a description in a later section. The explicit form for the functions  $Q_s$  (Van Kampen, 1983) given above will not be required in the subsequent discussions as we shall see that it is only the averages of products of the beam current at various times that will be required.

### 3.2 Correlated Gaussian pulsed source

We assume that the pulses are short compared to all other time scales in the problem and may be represented as a sum of delta functions. Moreover, the neutron source pulses have an exponential correlation in intensity.

### 3.2.1 Rossi alpha formula

We assume that the first count occurs at  $t = 0$  and the second one at  $t = \tau$ . The occurrence of the last source pulse at  $t_0$  is randomly distributed between  $-1/f$  and  $0$ . Following Degweker (2003), the expression for the Rossi alpha can be written as follows:

$$f_2(0, \tau) = f\lambda_d^2 \int_{-1/f}^0 \left[ \frac{\partial^2 F_Q(x, t_0)}{\partial x^2} \frac{\partial G_1(x, \tau)}{\partial x} + \frac{\partial F_Q(x, t_0)}{\partial x} \frac{\partial F_R(x, \tau, t_0)}{\partial x} \right]_{x=1} dt_0 \quad (3.2)$$

where  $F_Q$  and  $F_R$  are the pgfs of the distributions  $P$  and  $R$  defined by Degweker (2003) while  $G_1$  is the pgf of the distribution  $P$  for  $n=1$  and by the independence of neutrons, clearly  $G_1^n(x, \tau)$  is the corresponding pgf for arbitrary  $n$ . We write expressions for  $F_Q$  and  $F_R$  taking into account the fact that there are correlations between pulses, as follows:

$$F_Q(x, t_0) = \sum_{N_0, N_1, \dots, N_\infty} P(N_0, N_1, \dots, N_\infty) \prod_{n=0}^{\infty} \left( G_1(x, -t_0 + \frac{n}{f}) \right)^{N_n} \quad (3.3)$$

$$F_R(x, t_0) = \sum_{N_1, N_2, \dots, N_{[f\tau]}} P(N_1, N_2, \dots, N_{[f\tau]}) \prod_{l=1}^{[f\tau]} \left( G_1(x, \tau - t_0 - \frac{l}{f}) \right)^{N_l} \quad (3.4)$$

where  $P(N_0, N_1, \dots)$  is the joint probability distribution of the source leading to production of  $N_0, N_1, \dots$  etc. neutrons at the corresponding times. We have used the standard notation  $[x]$  to denote the largest integer less than or equal to  $x$ . Using these equations, it is possible to write down the derivatives required in Eq. (3.2) in terms of the derivatives of  $G_1$  evaluated at  $x=1$ .

The pgf  $G_1$  is given by

$$G_1(x, t) = 1 - \frac{e^{-\alpha t}(1-x)}{1 + Y_1(1 - e^{-\alpha t})(1-x)} \quad (3.5)$$

where  $Y_1 = \lambda_f \sqrt{\nu(\nu-1)}/2\alpha$

Using Eq. (3.5), we obtain the following expressions for the first two derivatives of  $G_1$ :

$$G_1'(1, t) = e^{\alpha t} \quad (3.5a)$$

$$G_1''(1, t) = 2Y_1(1 - e^{-\alpha t})e^{-\alpha t} \quad (3.5b)$$

The number of neutrons in a source event is due to the compounding of the number of protons in a bunch and the number of spallation neutrons. The compounded pgf can be written as

$$F_{N_i N_j}(x, y) = F_{p_i, j}[f_{sp}(x), f_{sp}(y)] \quad (3.6)$$

Differentiating with respect to x and y and setting x=y=1, we get

$$\overline{N_i} = \overline{N_{pi}} > \overline{v_{sp}} = m_1 \quad (3.6a)$$

$$\overline{N_i N_j} = \overline{N_{pi} N_{pj}} > \overline{v_{sp}^2} = m_1^2 + \Gamma^2 \exp(-\beta |i - j| / f) \quad (3.6b)$$

$$\overline{N_i(N_i - 1)} = \overline{N_j(N_j - 1)} = \overline{N_{pi}(N_{pi} - 1)} > \overline{v_{sp}^2} + \overline{N_{pi} v_{sp}(v_{sp} - 1)} = m_2 \quad (3.6c)$$

where  $\Gamma^2$  is the variance of the number of neutrons produced in a pulse and  $\beta$  is the decay constant of the source correlations. We obtain,

$$\begin{aligned} f_2(0, \tau) = & f \lambda_d^2 \int_{-1/f}^0 \left[ \sum_{k=0}^{\infty} \left\{ m_2 \exp(2\alpha(t_0 - \frac{k}{f})) + 2m_1 Y_1 \left( 1 - \exp(\alpha(t_0 - \frac{k}{f})) \right) \exp(t_0 - \frac{k}{f}) \right\} e^{-\alpha \tau} dt_0 \right. \\ & + f \lambda_d^2 \int_{-1/f}^0 \left[ \sum_{k=0}^{\infty} \sum_{l \neq k} \left\{ (m_1^2 + \Gamma^2 \exp(-\beta |l - k| / f)) \exp(\alpha(t_0 - \frac{k}{f})) \exp(\alpha(t_0 - \frac{l}{f})) \right\} e^{-\alpha \tau} dt_0 \right. \\ & + f \lambda_d^2 \int_{-1/f}^0 \left[ \sum_{k=0}^{\infty} \sum_{l=1}^{[f\tau]} \left\{ (m_1^2 + \Gamma^2 \exp(-\beta |l + k| / f)) \exp(\alpha(t_0 - \frac{k}{f})) \exp(-\alpha(\tau - t_0 - \frac{l}{f})) \right\} dt_0 \right. \\ & \left. \left. + f \lambda_d^2 \int_{-1/f}^{\tau - \frac{1+[f\tau]}{f}} \left[ \sum_{k=0}^{\infty} \left\{ (m_1^2 + \Gamma^2 \exp(-\beta |lf\tau + k + 1| / f)) \exp(\alpha(t_0 - \frac{k}{f})) \exp(-\alpha(\tau - t_0 - \frac{1+[f\tau]}{f})) \right\} dt_0 \right] \right] \right] \end{aligned} \quad (3.7)$$

Integration and summation are again straight forward and we finally obtain,

$$f_2(0, \tau) = \frac{f \lambda_d^2}{2\alpha} \left[ \frac{m_1^2}{1 - e^{-\alpha/f}} \left\{ e^{-\alpha/f} e^{\alpha \left( \tau - \frac{[f\tau]}{f} \right)} + e^{-\alpha \left( \tau - \frac{[f\tau]}{f} \right)} \right\} + (m_2 - m_1^2 + 2m_1 Y_1) e^{-\alpha\tau} \right. \\ \left. + \Gamma'^2 \left\{ \left( \frac{e^{-(\alpha+\beta)/f} e^{\alpha(\tau - [f\tau]/f)}}{1 - e^{-(\alpha+\beta)/f}} + \frac{e^{-\alpha(\tau - [f\tau]/f)}}{1 - e^{-(\alpha-\beta)/f}} \right) e^{-\beta[f\tau]/f} + \left( \frac{e^{-(\alpha+\beta)/f}}{1 - e^{-(\alpha+\beta)/f}} - \frac{1}{1 - e^{-(\alpha-\beta)/f}} \right) e^{-\alpha\tau} \right\} \right] \quad (3.8)$$

The presence of the last term is due to correlations in the source fluctuations. For  $\beta \gg f$  i.e., for correlation times which are short compared to the time between successive neutron pulses, this term vanishes and the formula reduces to that derived by Degweker (2003). When the frequency  $f$  is large compared to  $\alpha$  and  $\beta$ , the uncorrelated term tends to its usual form for uncorrelated sources while the correlated term remains the same. Thus, for large frequencies we have,

$$f_2(0, \tau) = \frac{f^2 m_1^2 \lambda_d^2}{\alpha^2} + \frac{f \lambda_d^2}{2\alpha} \left[ \left\{ (m_2 - m_1^2 + 2m_1 Y_1) + \frac{2\beta f \Gamma'^2}{\alpha^2 - \beta^2} \right\} \exp(-\alpha\tau) + \frac{2\alpha f \Gamma'^2}{\alpha^2 - \beta^2} \exp(-\beta\tau) \right] \quad (3.9)$$

This shows that even for large frequencies, the above distribution does not reduce to the random source distribution.

### 3.2.2 The Variance to Mean Ratio

The expression for the variance to mean ratio is derived as usual by integration of the expression (3.8) as follows:

$$\frac{v}{m} = 1 - m + \frac{2}{m} \int_0^T (T - \tau) f_2(0, \tau) d\tau \quad (3.10)$$

where  $m$  is the mean given by  $f_1(t)T$ ;  $f_1(t) = m_1 \lambda_d f / \alpha$  being the mean count rate.

We obtain,

$$\begin{aligned}
\frac{v}{m} = & 1 + \frac{\lambda_d m_1}{\alpha^2 T (1 - e^{-\alpha/f})} \left[ \exp\left(\alpha(T - \lfloor fT \rfloor + 1)\right) + \exp\left(-\alpha(T - \lfloor fT \rfloor)\right) + \exp\left(-\alpha(T + \frac{1}{f})\right) - 2e^{-\alpha/f} - e^{-\alpha T} \right] \\
& - \frac{\lambda_d m_1}{\alpha} \left[ fT - 2\lfloor fT \rfloor + \frac{\lfloor fT \rfloor(\lfloor fT \rfloor + 1)}{fT} \right] + \frac{\lambda_d}{m_1 \alpha} \left\{ (m_2 + 2m_1 Y_1) + \Gamma'^2 \left( \frac{e^{-(\alpha+\beta)/f}}{1 - e^{-(\alpha+\beta)/f}} - \frac{1}{1 - e^{-(\alpha-\beta)/f}} \right) \right\} \\
& \left[ \left( 1 - \frac{1 - \exp(-\alpha T)}{\alpha T} \right) + \frac{\lambda_d \Gamma'^2}{m_1 T (1 - e^{-(\alpha-\beta)/f})} \left[ \left( \frac{(\alpha T - 1)(1 - e^{-\alpha/f})}{\alpha^2} + \frac{e^{-\alpha/f}}{\alpha f} \right) \left( \frac{1 - e^{-\beta \lfloor fT \rfloor / f}}{1 - e^{-\beta/f}} \right) - \left( \frac{1 - e^{-\alpha/f}}{\alpha f} \right) \right] \right. \\
& \left. + \frac{\lambda_d \Gamma'^2 e^{-(\alpha+\beta)/f}}{m_1 T (1 - e^{-(\alpha+\beta)/f})} \left[ \left( \frac{(\alpha T + 1)(e^{\alpha/f} - 1)}{\alpha^2} - \frac{e^{\alpha/f}}{\alpha f} \right) \left( \frac{1 - e^{-\beta \lfloor fT \rfloor / f}}{1 - e^{-\beta/f}} \right) - \left( \frac{e^{\alpha/f} - 1}{\alpha f} \right) \right] \right. \\
& \left. + \frac{\lambda_d \Gamma'^2}{\alpha^2 m_1 T} \left( \frac{\left[ \alpha(T - \lfloor fT \rfloor / f) - (1 - e^{-\alpha(T - \lfloor fT \rfloor / f)}) \right]}{(1 - e^{-(\alpha-\beta)/f})} + \frac{e^{-(\alpha+\beta)/f} \left[ e^{\alpha(T - \lfloor fT \rfloor / f)} - 1 - \alpha(T - \lfloor fT \rfloor / f) \right]}{(1 - e^{-(\alpha+\beta)/f})} \right) e^{-\beta \lfloor fT \rfloor / f} \right]
\end{aligned} \tag{3.11}$$

For high frequencies, the above formula reduces to

$$\frac{v}{m} = 1 + \frac{\lambda_d (m_2 - m_1^2 + 2m_1 Y_1 + \frac{2\beta f \Gamma'^2}{\alpha^2 - \beta^2})}{m_1 \alpha} \left( 1 - \frac{1 - \exp(-\alpha T)}{\alpha T} \right) + \frac{2\lambda_d \alpha f \Gamma'^2}{(\alpha^2 - \beta^2) m_1 \beta} \left( 1 - \frac{1 - \exp(-\beta T)}{\beta T} \right) \tag{3.12}$$

The reduction of the variance due to the regularity of the pulses should be noted. The other point worth noting here is the appearance of an enhancement of the variance due to correlations in the number of source neutrons from successive pulses.

### 3.2.3 The ACF and PSD

We visualize the times of absorption of neutrons in a detector as a stochastic point process (Van Kampen, 1983) described by the functions  $Q_s(t_1, t_2, \dots, t_s)$ . Suppose absorption of a neutron in the detector produces a total charge  $q$  which may be a random number and results in a time response given by  $h(\tau)$  (the response function of the detector operating in the

current mode and assumed deterministic), defined such that  $h(\tau)$  is non zero only for  $\tau > 0$

$$\text{and } \int_0^{\infty} h(\tau) d\tau = 1.$$

The mean current and the ACF are then given by

$$\overline{i(t)} = \sum_{s=0}^{\infty} \frac{1}{s!} \int_{-\infty}^{+\infty} \langle [q_1 h(t-t_1) + \dots q_s h(t-t_s)] \rangle Q_s(t_1, \dots, t_s) dt_1 \dots dt_s = \langle q \rangle f_1(t) \quad (3.13)$$

$$\begin{aligned} \overline{i(t)i(t')} &= \sum_{s=0}^{\infty} \frac{1}{s!} \int_{-\infty}^{+\infty} \langle [q_1 h(t-t_1) + \dots q_s h(t-t_s)] [q_1 h(t'-t_1) + \dots q_s h(t'-t_s)] \rangle Q_s(t_1, \dots, t_s) dt_1 \dots dt_s \\ &= \langle q^2 \rangle f_1 h_c(t'-t) + \langle q \rangle^2 \int_{-\infty}^{+\infty} h_c(t'-t-\tau) f_2(\tau) d\tau \end{aligned} \quad (3.14)$$

where the bar indicates overall averaging while  $\langle \rangle$  indicates averaging over the distribution of the number of charges per neutron detection and

$$h_c(t-t') = \int_{-\infty}^{+\infty} h(t-t_1) h(t'-t_1) dt_1 = \int_0^{\infty} h(T) h(t'-t+T) dT \quad (3.15)$$

In writing Eqs. (3.13) and (3.14), we have used the fact that  $f_1(t_1)$  is independent of  $t_1$  while  $f_2(t_2-t_1)$  depends only on  $\tau = t_2-t_1$  due to stationarity of the process. If we use the expression for  $f_2$  [Eq. (3.8)] in Eq. (3.14) and the expression for  $f_1$  (see section 3.2.2 above) in Eq. (3.13), we can write the following formula for the auto covariance:

$$\begin{aligned} \overline{(i(t)-\overline{i(t)})(i(t')-\overline{i(t')})} &= \frac{\langle q^2 \rangle f m_1 \lambda_d^2}{\alpha} h_c(t'-t) - \frac{\langle q \rangle^2 f^2 \lambda_d^2 m_1^2}{\alpha^2} \\ &+ \frac{\langle q \rangle^2 f \lambda_d^2 m_1^2}{2\alpha(1-e^{-\alpha/f})} \int_{-\infty}^{+\infty} h_c(t'-t-\tau) \left\{ e^{-\alpha/f} \exp\left(\alpha\left(\tau - \frac{[f\tau]}{f}\right)\right) + \exp\left(-\alpha\left(\tau - \frac{[f\tau]}{f}\right)\right) \right\} d\tau \\ &+ \frac{\langle q \rangle^2 \Gamma^2 f \lambda_d^2}{2\alpha} \int_{-\infty}^{+\infty} h_c(t'-t-\tau) \left[ \frac{e^{\alpha\left(\tau - \frac{[f\tau+1]}{f} \frac{(\alpha+\beta)}{\alpha}\right)}}{1-e^{-(\alpha+\beta)/f}} + \frac{e^{-\alpha\left(\tau - \frac{[f\tau]}{f} \frac{(\alpha-\beta)}{\alpha}\right)}}{1-e^{-(\alpha-\beta)/f}} \right] d\tau \\ &+ \frac{\langle q \rangle^2 f \lambda_d^2}{2\alpha} \left\{ (m_2 - m_1^2 + 2m_1 Y_1) + \Gamma^2 \left( \frac{e^{-(\alpha+\beta)/f}}{1-e^{-(\alpha+\beta)/f}} - \frac{1}{1-e^{-(\alpha-\beta)/f}} \right) \right\} \int_{-\infty}^{+\infty} h_c(t'-t-\tau) e^{-\alpha\tau} d\tau \end{aligned} \quad (3.16)$$

Taking the Fourier transform of the above equation it is clear that the PSD can be written as follows:

$$G(\omega) = H(\omega) \left[ \frac{\langle q^2 \rangle f m_1 \lambda_d}{\alpha} + \langle q \rangle^2 \wp(\omega) \right] \quad (3.17)$$

where  $H(\omega)$  is the PSD of the detector response and  $\wp(\omega)$  is the Fourier transform of  $f_2(0, \tau) - \bar{i}^2$ . Before taking the Fourier transform of Eq. (3.8) we note that the two terms in the second line of Eq. (3.16) represent a periodic and even function of  $\tau$  having period  $1/f$  and can therefore be expanded into a Fourier cosine series.

$$e^{-\alpha/f} \exp\left(\alpha\left(\tau - \frac{[f\tau]}{f}\right)\right) + \exp\left(-\alpha\left(\tau - \frac{[f\tau]}{f}\right)\right) = (1 - e^{-\alpha/f}) \left( \frac{2f}{\alpha} + \sum_{n=1}^{\infty} \frac{4\alpha f}{\alpha^2 + (2n\pi f)^2} \cos 2n\pi f \tau \right) \quad (3.18)$$

The constant term cancels with  $-\bar{i}^2$ . The other terms give a discrete spectrum i.e. a sum of delta functions at frequencies  $\pm 2n\pi f$  whose strength is given by

$$\frac{4\pi f^2 m_1^2 \lambda_d^2}{\alpha^2 + (2n\pi f)^2} \quad (3.19)$$

Fourier transformation of the other terms is as usual and finally we get the following expression for the PSD

$$G(\omega) = H(\omega) \left[ \frac{\langle q^2 \rangle f m_1 \lambda_d}{\alpha} + \langle q \rangle^2 f \lambda_d^2 \left\{ \sum_{n \neq 0} \frac{4\pi f m_1^2 \delta(\omega - 2n\pi f)}{\alpha^2 + (2n\pi f)^2} + \frac{(m_2 - m_1^2 + 2m_1 Y_1) + \Gamma^2 \left( \frac{e^{-(\alpha+\beta)/f}}{1 - e^{-(\alpha+\beta)/f}} - \frac{1}{1 - e^{-(\alpha-\beta)/f}} \right)}{\omega^2 + \alpha^2} \right\} \right] \\ + H(\omega) \langle q \rangle^2 f \lambda_d^2 \Gamma^2 \frac{\left[ 2(e^{-(\alpha+2\beta)/f} - e^{-\alpha/f}) \cos(\omega/f) + (1 + e^{-2\alpha/f})(1 - e^{-2\beta/f}) \right]}{(\omega^2 + \alpha^2)(1 - 2e^{-\beta/f} \cos(\omega/f) + e^{-2\beta/f})(1 - e^{-(\alpha+\beta)/f})(1 - e^{-(\alpha-\beta)/f})} \quad (3.20)$$

The first term is the usual detector white noise. The second term is a series of discrete lines due to the periodic nature of the uncorrelated terms in the Rossi alpha and autocorrelation

function and is caused by the periodic source pulses. Such a term is not present in the usual PSD method. The third term is the usual response of the reactor to a white noise source and is usually sought to determine alpha. The fourth and fifth terms have the same functional form as the third but are obtained due to the non-Poisson character of the source. The last term is also due to the non-Poisson character of the source and shows the effect of correlations between different source pulses. The magnitude of various terms in the above expression follows the same pattern as that of the Rossi alpha function.

Similarly, expressions for cross correlation function and cross power spectral density can be derived (Degweker and Rana, 2007).

### **3.3 Effect of finite spread of source pulse**

#### **3.3.1 The Rossi alpha formula**

Degweker (2003) has shown that the pulse widths of a source bunch are very short for typical RF proton accelerators producing spallation neutrons to be of any consequence in the noise characteristics of interest. Nevertheless, there could be situations where this might be important. One case is that of an experimental deuteron beam source such as the MUSE facility where the width is significant compared to the die away time. For such situations, Pazsit et al. (2005) have considered Gaussian and rectangular pulse shapes and used the Laplace transform approach to carry out the rather complicated mathematics. For the case of Poisson processes, one can use the Bartlett formula with a source intensity which is time varying in a periodically pulsed fashion. For non Poisson source events, it is not immediately clear how to generalize our approach for delta function pulses to the case of finite pulse widths. We treat the neutron source (spallation) events as a doubly stochastic Poisson point process and derive an expression for  $f_2$ . As regards detailed calculations for obtaining  $f_2$ , and

$v/m$  for Gaussian and rectangular pulses, we use a variant of the approach taken by Pazsit et al. (2005).

The pgf for getting one count in a small interval  $d\tau_0$  at time 0 and another  $d\tau$  at time  $\tau$  due to one neutron at time  $t$  in a source free medium is denoted by  $G(z_1, z_2, t)$ . Then the required pgf is given by

$$\mathfrak{S} = f \int dt_0 \left\langle \sum_s \frac{1}{s!} \int_{-\infty}^{\infty} Q_s(t_1, \dots, t_s) f_{sp}[G(z_1, z_2, t_1)] \dots f_{sp}[G(z_1, z_2, t_s)] dt_1 \dots dt_s \right\rangle \quad (3.21)$$

The required Rossi alpha function can now be written by differentiating successively with respect to  $z_1$  and  $z_2$

$$f_1 d\tau_0 = \frac{\partial \mathfrak{S}}{\partial z_1} = f \int dt_0 \left\langle \sum_s \frac{1}{s!} \int_{-\infty}^{\infty} dt_1 \dots dt_s Q_s(t_1, \dots, t_s) \sum_{i=1}^s \overline{v_{sp}} \frac{\partial G(z_1, z_2, t_i)}{\partial z_1} \Big|_{z_1=1} \right\rangle \quad (3.22)$$

$$\begin{aligned} f_2 d\tau_0 d\tau = \frac{\partial^2 \mathfrak{S}}{\partial z_1 \partial z_2} = f \int dt_0 < \sum_s \frac{1}{s!} \int_{-\infty}^{\infty} dt_1 \dots dt_s Q_s(t_1, \dots, t_s) \left[ \sum_{i=1}^s \sum_{j \neq i} \overline{v_{sp}}^2 \frac{\partial G(z_1, z_2, t_i)}{\partial z_1} \Big|_{z_1=1} \frac{\partial G(z_1, z_2, t_j)}{\partial z_2} \Big|_{z_2=1} \right. \\ \left. + \sum_{i=1}^s \overline{v_{sp}} (\overline{v_{sp}} - 1) \frac{\partial G(z_1, z_2, t_i)}{\partial z_1} \Big|_{z_1=1} \frac{\partial G(z_1, z_2, t_i)}{\partial z_2} \Big|_{z_2=1} + \sum_{i=1}^s \overline{v_{sp}} \frac{\partial^2 G(z_1, z_2, t_i)}{\partial z_1 \partial z_2} \Big|_{z_1=1} \right] > \end{aligned} \quad (3.23)$$

Since  $Q$  is symmetric in the interchange of any of its arguments, we can write the above functions as follows:

$$f_1 d\tau_0 = \frac{\partial \mathfrak{S}}{\partial z_1} = \overline{v_{sp}} f \int dt_0 \int_{-\infty}^{\infty} \varphi_1(t) dt \frac{\partial G(z_1, z_2, t)}{\partial z_1} \Big|_{z_1=1} \quad (3.24)$$

$$\begin{aligned} f_2 d\tau_0 d\tau = \frac{\partial^2 \mathfrak{S}}{\partial z_1 \partial z_2} = f \int dt_0 \int_{-\infty}^{\infty} \varphi_2(t_1, t_2) \overline{v_{sp}}^2 \frac{\partial G(z_1, z_2, t_1)}{\partial z_1} \Big|_{z_1=1} \frac{\partial G(z_1, z_2, t_2)}{\partial z_2} \Big|_{z_2=1} dt_1 dt_2 \\ + f \int dt_0 \int_{-\infty}^{\infty} \varphi_1(t) \left[ \overline{v_{sp}} \frac{\partial^2 G(z_1, z_2, t)}{\partial z_1 \partial z_2} \Big|_{z_1=1} + \overline{v_{sp}} (\overline{v_{sp}} - 1) \frac{\partial G(z_1, z_2, t)}{\partial z_1} \Big|_{z_1=1} \frac{\partial G(z_1, z_2, t)}{\partial z_2} \Big|_{z_2=1} \right] dt \end{aligned} \quad (3.25)$$

where  $\varphi_1$  and  $\varphi_2$  are the average source event rate and the two point source event density respectively given as usual by.

$$\varphi_1(t_1) = \left\langle \sum_s \frac{1}{(s-1)!} \int_{-\infty}^{\infty} dt_2 \dots dt_s Q_s(t_1 \dots t_s) \right\rangle \quad (3.26)$$

$$\varphi_2(t_1, t_2) = \left\langle \sum_s \frac{1}{(s-2)!} \int_{-\infty}^{\infty} dt_3 \dots dt_s Q_s(t_1 \dots t_s) \right\rangle \quad (3.27)$$

It is fairly easy to show that the first and second derivatives of G are given by (Kitamura et al., 2006)

$$G_{z_1}(1,1,t) = \lambda_d e^{\alpha t} d\tau_0, \text{ for } t < 0 \text{ and zero otherwise} \quad (3.27a)$$

$$G_{z_2}(1,1,t) = \lambda_d e^{\alpha(\tau-t)} d\tau, \text{ for } t < \tau \text{ and zero otherwise} \quad (3.27b)$$

$$G_{z_1 z_2}(1,1,t) = 2Y_1 \lambda_d^2 e^{\alpha t} (1 - e^{\alpha t}) e^{-\alpha \tau} d\tau_0 d\tau \text{ for } t < 0 \text{ and zero otherwise.} \quad (3.27c)$$

Introducing (3.1) in (3.26) and (3.27) we can write

$$\varphi_1(t) = E(t) \langle I(t) \rangle = \sum_n \varepsilon(t - t_0 + n/f) \langle I \rangle \quad (3.28)$$

$$\begin{aligned} \varphi_2(t_1, t_2) &= E(t_1) E(t_2) \langle I(t_1) I(t_2) \rangle \\ &= \sum_m \sum_n \varepsilon(t_1 - t_0 + n/f) \varepsilon(t_2 - t_0 + m/f) \langle I(t_1) I(t_2) \rangle \end{aligned} \quad (3.29)$$

where we have written the (deterministic) variation of the current  $E(t)$  as a periodic sum of narrow pulse shape functions  $\varepsilon(t - t_n)$  around  $t_n$ . The latter represents the pulse shape (obtained by chopping or bunching of the ion current). With the assumption of an exponentially correlated process for the current fluctuations, we can rewrite the above expressions for  $f_1$  and  $f_2$  as follows:

$$f_1 = \langle I \rangle \overline{v_{sp}} \lambda_d f \int_{-1/f}^0 dt_0 \sum_{n=0}^{\infty} \varepsilon(t - t_0 + n/f) e^{\alpha t} dt \quad (3.30)$$

$$\begin{aligned}
f_2 = & \overline{v_{sp}}^{-2} \lambda_d^2 f \int_{-1/f}^0 dt_0 \sum_{n=0}^{\infty} \sum_{m=0}^{\infty} \int_{-\infty}^{\infty} \int_{-\infty}^{\infty} \varepsilon(t_1 - t_0 + n/f) \varepsilon(t_2 - t_0 + m/f) \left( \langle I \rangle^2 + \Gamma^2 e^{-\beta|t_1 - t_2|} \right) e^{\alpha t_1} e^{\alpha(t_2 - \tau)} dt_1 dt_2 \\
& + \langle I \rangle \lambda_d^2 f \int_{-1/f}^0 dt_0 \sum_{n=0}^{\infty} \int_{-\infty}^{\infty} \varepsilon(t - t_0 + n/f) \left( 2Y_1 \overline{v_{sp}} e^{\alpha t} (1 - e^{\alpha t}) e^{-\alpha \tau} + \overline{v_{sp}} (\overline{v_{sp}} - 1) e^{\alpha(2t - \tau)} \right) dt
\end{aligned} \tag{3.31}$$

where,  $\Gamma^2 = \langle I^2 \rangle - \langle I \rangle^2$ .

The main difference between non-Poisson bunches and Poisson bunches had been noted by Degweker (2003) and was due to the absence of the  $n = m$  term in the first line of the second of the above two equations whereas here we seem to be summing over all values of  $n$  and  $m$ . To understand this effect, we look at the term representing the correlations between fluctuations in current. If  $1/\beta$  is small compared to time differences within a bunch, we have perfectly uncorrelated (i.e. Poisson) statistics of the protons and as such we get the same results as those by Pazsit et al. (2005). However, for the opposite case, there is an additional contribution to the variance. If we further assume that  $1/\beta$  is small compared to  $1/f$ , then the term is zero for all  $m \neq n$  but is non zero and equal to  $\Gamma^2$  for  $m = n$ . This corresponds to the situation wherein there is no correlation between successive pulses and was considered by Degweker (2003) assuming delta function pulses. Finally, we may have the situation in which  $1/\beta$  is not small compared to  $1/f$ .

Assuming a finite spread in the protons within a bunch and that the bunches are non-Poisson, we evaluate the above integrals for the case of correlation time  $1/\beta$  being much larger than the pulse width but much smaller than  $1/f$ . Evaluations for the other two cases (correlation time much smaller than the pulse width and correlation time much larger than the pulse width) have also been carried out by us (Degweker and Rana, 2007).

### Rectangular pulses

The rectangular pulses are defined by

$$\varepsilon(t) = g / \sigma \text{ for } 0 < t < \sigma; \quad \varepsilon(t) = 0 \text{ otherwise}$$

We assume that the square pulse triggers at time  $t_0$  and has a width of  $\sigma$ . The one time probability or the count rate is simply given by

$$f_1 = \langle I \rangle g \lambda_d \bar{v}_{sp} f \left[ \int_{-1/f}^0 \sum_{n=1}^{\infty} \frac{1}{\sigma} \int_{t_0-n/f}^{t_0-n/f+\sigma} e^{\alpha t} dt dt_0 + \int_{-1/f}^{-\sigma} \frac{1}{\sigma} \int_{t_0}^{t_0+\sigma} e^{\alpha t} dt dt_0 + \int_{-\sigma}^0 \frac{1}{\sigma} \int_{t_0}^0 e^{\alpha t} dt dt_0 \right] \quad (3.32)$$

Thus the integration over one period gives a factor of  $\alpha$  in the denominator:

$$f_1 = \frac{\langle I \rangle g \lambda_d \bar{v}_{sp} f}{\alpha} = \frac{\lambda_d f m_1}{\alpha} \quad (3.33)$$

where  $m_1 = \langle I \rangle g \bar{v}_p$  is the mean number of neutrons per pulse. For finding the two time probability density or Rossi alpha, the integration and summation involved in second line of the expression for  $f_2$  [Eq.(3.31)] is similar to the one for  $f_1$  and we get the following contribution to  $f_2$ .

$$\frac{\langle I \rangle g \lambda_d^2 f}{\alpha} \left[ \frac{\bar{v}_{sp} \nu(\nu-1) \lambda_f}{2\alpha} + \frac{\bar{v}_{sp} (\nu_{sp}-1)}{2} \right] e^{-\alpha \tau} \quad (3.34)$$

In the first line of expression for  $f_2$  [Eq. (3.31)], we have uncorrelated and correlated terms. For the first term (uncorrelated), the integrations over  $t_1$ , and  $t_2$  factorize. Moreover each of these factors which are functions of  $t_0$ , are periodic with period  $1/f$  having a phase difference of  $\delta = ([f\tau] + 1)/f - \tau$ . We can therefore expand each of the factors in a Fourier series. The product is also a Fourier series related to the Fourier series of the individual factors. Integration over  $t_0$  can then be carried out term by term. We write the two factors as  $G(t_0)$  and  $G(t_0 + \delta)$  where  $G(t_0)$  is obtained as follows:

$$G(t_0) = \sum_{n=0}^{\infty} \int_{t_0-n/f}^{t_0-n/f+\sigma} \frac{1}{\sigma} e^{\alpha t} dt = \frac{e^{\alpha t_0} (e^{\alpha \sigma} - 1)}{\alpha \sigma (1 - e^{-\alpha/f})} \quad \text{for } t_0 < -\sigma \quad (3.35a)$$

$$= \sum_{n=1}^{\infty} \int_{t_0-n/f}^{t_0-n/f+\sigma} \frac{1}{\sigma} e^{\alpha t} dt + \int_{t_0}^0 \frac{1}{\sigma} e^{\alpha t} dt = \frac{e^{\alpha t_0} (e^{\alpha \sigma} - 1) e^{-\alpha/f}}{\alpha \sigma (1 - e^{-\alpha/f})} + \frac{1}{\alpha \sigma} (1 - e^{\alpha t_0}) \quad \text{for } t_0 > -\sigma \quad (3.35b)$$

Expanding each of these factors (which are functions of  $t_0$ ) in Fourier series we can integrate over  $t_0$  as follows

$$\begin{aligned} \int_{-1/f}^0 G(t_0) G(t_0 + \delta) dt_0 &= \int_{-1/f}^0 \sum_{n=-\infty}^{\infty} a_n \sum_{m=-\infty}^{\infty} a_m e^{i2n\pi f t_0} e^{i2m\pi f (t_0 + \delta)} dt_0 \\ &= \int_{-1/f}^0 \sum_{n,m} a_n a_m e^{i2m\pi f \delta} e^{i2\pi f t_0 (n+m)} dt_0 \end{aligned} \quad (3.36)$$

Only terms for  $m = -n$  have a non zero value, and hence,

$$\int_{-1/f}^0 G(t_0) G(t_0 + \delta) dt_0 = \frac{2}{f} \sum_{n=1}^{\infty} a_n a_{-n} \cos(2n\pi f \tau) + \frac{a_0^2}{f} \quad (3.37)$$

We can compute the coefficients  $a_n$ ,  $a_0$  using Fourier formula & the above expressions for  $G(t_0)$

$$a_n = f \int_{-1/f}^0 e^{-i2n\pi f t_0} G(t_0) dt_0 \quad (3.38)$$

Integration is straight forward and we get

$$a_n a_{-n} = \frac{f^2}{\sigma^2} \frac{2(1 - \cos(\omega_n \sigma))}{\omega_n^2 (\alpha^2 + \omega_n^2)}, \quad \text{where } \omega_n = 2n\pi f \text{ and} \quad (3.39a)$$

$$a_0^2 = \frac{f^2}{\alpha^2} \quad (3.39b)$$

Substituting the values of  $a_n a_{-n}$  and  $a_0^2$  in Eq. (3.37) and using Eq. (3.31), we get the following contribution from the uncorrelated term:

$$\frac{<I>^2 g^2 \lambda_d^2 \bar{V}_{sp}^2 f}{\alpha^2 \sigma^2} \left[ \sum_{n=1}^{\infty} \frac{4\alpha^2 (1 - \cos(\omega_n \sigma)) \cos(\omega_n \tau)}{\omega_n^2 (\omega_n^2 + \alpha^2)} + \sigma^2 \right] \quad (3.40)$$

As far as the second term (correlated) is concerned, our assumption about the correlation time  $1/\beta$  being much smaller than  $1/f$  implies that terms for which  $n \neq m$  will give zero contribution. For  $n=m$  we can set  $\exp[-|t_1 - t_2|] = 1$ . [Since this case shows no correlations between the number of protons (ions) in successive pulses, it will correspond to the results obtained earlier by Degweker (2003)]. The contribution of this term can then be written as

$$\overline{v_{sp}}^2 \lambda_d^2 \Gamma^2 f \int_{-1/f}^0 dt_0 \sum_{n=0}^{\infty} \int_{-\infty}^{\infty} \int_{-\infty}^{\infty} \varepsilon(t_1 - t_0 + n/f) \varepsilon(t_2 - t_0 + n/f) e^{\alpha t_1} e^{\alpha(t_2 - \tau)} dt_1 dt \quad (3.41)$$

$$= \overline{v_{sp}}^2 \lambda_d^2 \Gamma^2 g^2 f e^{-\alpha \tau} \left[ \int_{-1/f}^0 dt_0 \sum_{n=1}^{\infty} \frac{1}{\sigma} \int_{t_0 - n/f}^{t_0 - n/f + \sigma} e^{\alpha t_1} dt_1 \frac{1}{\sigma} \int_{t_0 - n/f}^{t_0 - n/f + \sigma} e^{\alpha t_2} dt_2 + \int_{-1/f}^{-\sigma} \frac{1}{\sigma} \int_{t_0}^{t_0 + \sigma} e^{\alpha t_1} dt_1 \frac{1}{\sigma} \int_{t_0}^{t_0 + \sigma} e^{\alpha t_2} dt_2 \right. \\ \left. + \int_{-\sigma}^0 \frac{1}{\sigma} \int_{t_0}^0 e^{\alpha t_1} dt_1 \frac{1}{\sigma} \int_{t_0}^0 e^{\alpha t_2} dt_2 \right] \\ = \frac{\overline{v_{sp}}^2 \lambda_d^2 \Gamma^2 g^2 f}{\alpha^2 \sigma} \left[ 1 - \frac{1 - e^{-\alpha \sigma}}{\alpha \sigma} \right] e^{-\alpha \tau} \quad (3.42)$$

Adding (3.34), (3.40) and (3.42), the final expression for  $f_2$  becomes

$$f_2 = \frac{\langle I \rangle^2 g^2 \lambda_d^2 \overline{v_{sp}}^2 f}{\alpha^2 \sigma^2} \left[ \sum_{n=1}^{\infty} \frac{4\alpha^2 (1 - \cos(\omega_n \sigma)) \cos(\omega_n \tau)}{\omega_n^2 (\omega_n^2 + \alpha^2)} + \sigma^2 \right] \\ + \frac{\langle I \rangle g \lambda_d^2 f}{\alpha} \left[ \frac{\overline{v_{sp}} \overline{v(v-1)} \lambda_f}{2\alpha} + \frac{\overline{v_{sp}} (v_{sp} - 1)}{2} \right] e^{-\alpha \tau} + \frac{\overline{v_{sp}}^2 \lambda_d^2 \Gamma^2 g^2 f}{\alpha^2 \sigma} \left[ 1 - \frac{1 - e^{-\alpha \sigma}}{\alpha \sigma} \right] e^{-\alpha \tau} \quad (3.43)$$

The Feynman Y function can be obtained (Degweker and Rana, 2007) from the expression for  $f_2$  using the relation in Eq. (3.10) and we get:

$$Y = \frac{4 \langle I \rangle \lambda_d \overline{v_{sp}} \alpha}{\sigma^2 T f} \left[ \sum_{n=1}^{\infty} \frac{(1 - \cos(\omega_n \sigma)) \sin^2(\omega_n T / 2)}{n^2 \pi^2 \omega_n^2 (\omega_n^2 + \alpha^2)} \right] \\ + \left( \frac{\lambda_d \lambda_f \overline{v(v-1)}}{\alpha^2} + \frac{\lambda_d}{\alpha} \frac{\overline{v_{sp}} (v_{sp} - 1)}{\overline{v_{sp}}} + \frac{2 \Gamma^2 g \lambda_d \overline{v_{sp}}}{\langle I \rangle \alpha} [1 - \alpha \sigma / 3] \right) \left( 1 - \frac{1 - e^{-\alpha T}}{\alpha T} \right) \quad (3.44)$$

### Gaussian pulses

The Gaussian pulses are defined by

$$\varepsilon(t) = \frac{g}{\sqrt{2\pi}\sigma} \exp\left(-\frac{t^2}{2\sigma^2}\right)$$

The pulses are assumed to be centered at  $t_0 + n/f$  and having a width (S.D.)  $\sigma$ . The summation is over all integral values of  $n$  since even pulses which appear later than 0 (or  $\tau$ ) will have leading edges which lie before these times.

$$f_1 = \langle I \rangle g \lambda_d \bar{v}_{sp} f \int_{-1/f}^0 dt_0 \sum_{n=-\infty}^{\infty} \int_{-\infty}^0 \frac{1}{\sqrt{2\pi}\sigma} e^{-\frac{(t-t_0+\frac{n}{f})^2}{2\sigma^2}} e^{\alpha t} dt \quad (3.45)$$

Substituting  $u=t-t_0+n/f$

$$\begin{aligned} f_1 &= \frac{\langle I \rangle g \lambda_d \bar{v}_{sp} f}{\sqrt{2\pi}\sigma} \int_{-\infty}^0 dt \left[ \sum_{n=-\infty}^{\infty} \int_{t+n/f}^{t+(n+1)/f} e^{-\frac{u^2}{2\sigma^2}} du \right] e^{\alpha t} = \frac{\langle I \rangle g \lambda_d \bar{v}_{sp} f}{\sqrt{2\pi}\sigma} \int_{-\infty}^0 \left[ \int_{-\infty}^{\infty} e^{-\frac{u^2}{2\sigma^2}} du \right] e^{\alpha t} dt \\ &= \frac{\langle I \rangle g \lambda_d \bar{v}_{sp} f}{\alpha} = \frac{\lambda_d m_1 f}{\alpha} \end{aligned} \quad (3.46)$$

Thus the integration over one period gives a factor of  $\alpha$  in the denominator.

For finding Rossi alpha formula we note that the integration involved in second part of the expression for  $f_2$  [Eq. (3.31)] is similar to the one for  $f_1$  and gives us the following term

$$\frac{\langle I \rangle g \lambda_d^2 f}{\alpha} \left[ \frac{\lambda_f \bar{v}_{sp} v(v-1)}{2\alpha} + \frac{\bar{v}_{sp} (v_{sp}-1)}{2} \right] e^{-\alpha \tau} \quad (3.47)$$

The uncorrelated component in the first line of the expression for  $f_2$  [Eq. (3.31)] can be written as

$$\langle I \rangle^2 g^2 \lambda_d^2 \bar{v}_{sp}^2 f \int_{-1/f}^0 dt_0 \sum_{n=-\infty}^{\infty} \sum_{m=-\infty}^{\infty} \int_{-\infty}^0 \int_{-\infty}^0 \frac{1}{\sqrt{2\pi}\sigma} e^{-\frac{(t_1-t_0+\frac{n}{f})^2}{2\sigma^2}} e^{\alpha t_1} \frac{1}{\sqrt{2\pi}\sigma} e^{-\frac{(t_2-t_0+\frac{m}{f})^2}{2\sigma^2}} e^{\alpha(t_2-\tau)} dt_1 dt_2 \quad (3.48)$$

For solving Eq. (3.48), we again use the Fourier series expansion technique described in detail for rectangular pulses. In the present case

$$G(t_0) = \frac{1}{\sqrt{2\pi\sigma}} \sum_{m=-\infty}^{\infty} \int_{-\infty}^0 e^{-\frac{(t-t_0+\frac{m}{f})^2}{2\sigma^2}} e^{\alpha t} dt \quad (3.49)$$

and hence we get for  $a_n$ , the Fourier coefficient

$$a_n = f \int_{-1/f}^0 e^{-i2n\pi f t_0} G_1(t_0) dt_0 = f \int_{-\infty}^0 dt \int_{-1/f}^0 dt_0 \sum_{m=-\infty}^{\infty} \frac{1}{\sqrt{2\pi\sigma}} e^{-\frac{(t-t_0+\frac{m}{f})^2}{2\sigma^2}} e^{\alpha t} e^{-i2n\pi f t_0} \quad (3.50)$$

Setting  $u=t-t_0+m/f$ , we can write

$$a_n = f \int_{-\infty}^0 dt \int_{-\infty}^{\infty} du \frac{1}{\sqrt{2\pi\sigma}} e^{-\frac{u^2}{2\sigma^2} + i2n\pi f u} e^{(\alpha t - i2n\pi f t)} = \frac{f}{(\alpha + i\omega_n)} e^{-\frac{(\omega_n \sigma)^2}{2}} \quad (3.51)$$

Thus,

$$a_n a_{-n} = \frac{f^2 e^{-(\omega_n \sigma)^2}}{(\omega_n^2 + \alpha^2)}, \text{ and } a_0^2 = \frac{f^2}{\alpha^2} \quad (3.52)$$

Substituting  $a_n a_{-n}$ , and  $a_0^2$  in Eq. (3.37) and using Eq. (3.31), we get the following contribution:

$$\frac{\langle I \rangle^2 g^2 \lambda_d^2 \bar{V}_{sp}^2 f^2}{\alpha^2} \left[ \sum_{n=1}^{\infty} \frac{2\alpha^2 e^{-(\omega_n \sigma)^2} \cos(\omega_n \tau)}{(\omega_n^2 + \alpha^2)} + 1 \right] \quad (3.53)$$

On making the substitutions  $u = -t_0 + n/f$ ,  $t'_1 = -t_1$  and  $t'_2 = -t_2$  and substituting the Gaussian form for the pulse shape function, the correlated component of  $f_2$  [Eq. (3.41)] after slight algebraic manipulation becomes

$$\frac{\bar{V}_{sp}^2 \lambda_d^2 \Gamma^2 g^2 f}{2\pi\sigma^2} \int_{-\infty}^{\infty} du \int_0^{\infty} dt'_1 \int_{-\tau}^{\infty} dt'_2 \exp\left(-\frac{1}{\sigma^2} \left[ \left(u - \frac{t'_1 + t'_2}{2}\right)^2 + \left(\frac{t'_1 - t'_2}{2}\right)^2 \right]\right) e^{\alpha t_1} e^{\alpha(t_2 - \tau)} \quad (3.54)$$

Performing the integration over  $u$  gives

$$\frac{\overline{\nu_{sp}}^2 \lambda_d^2 \Gamma^2 g^2 f}{\sqrt{4\pi\sigma}} \int_0^\infty dt'_1 \int_{-\tau}^\infty dt'_2 \exp\left(-\left[\frac{(t'_1 - t'_2)^2}{4\sigma^2} + \alpha(t'_1 + t'_2)\right]\right) e^{-\alpha\tau} \quad (3.55)$$

The integrations over  $t'_1, t'_2$  can be carried out using the substitutions  $x = t'_1 + t'_2, y = t'_1 - t'_2$  to give

$$\begin{aligned} & \frac{\overline{\nu_{sp}}^2 \lambda_d^2 \Gamma^2 g^2 f}{2\sqrt{4\pi\sigma}} \left[ \int_{-\infty}^\tau dy e^{-y^2/4\sigma^2} \int_{-y}^\infty dx e^{-\alpha x} + \int_\tau^\infty dy e^{-y^2/4\sigma^2} \int_{y-2\tau}^\infty dx e^{-\alpha x} \right] e^{-\alpha\tau} \\ &= \frac{\overline{\nu_{sp}}^2 \lambda_d^2 \Gamma^2 g^2 f}{2\sqrt{4\pi\sigma\alpha}} \left[ e^{-\alpha\tau} \int_{-\infty}^\tau dy e^{-y^2/4\sigma^2 + \alpha y} + e^{\alpha\tau} \int_\tau^\infty dy e^{-y^2/4\sigma^2 - \alpha y} \right] \end{aligned} \quad (3.56)$$

The expression can be evaluated in terms of the error function to give

$$\frac{\overline{\nu_{sp}}^2 \lambda_d^2 \Gamma^2 g^2 f e^{\alpha^2 \sigma^2}}{4\alpha} \left[ 1 + \text{Erf}\left(\frac{\tau - 2\sigma^2 \alpha}{2\sigma}\right) + \left(1 - \text{Erf}\left(\frac{\tau + 2\sigma^2 \alpha}{2\sigma}\right)\right) e^{2\alpha\tau} \right] e^{-\alpha\tau} \quad (3.57)$$

The final expression for  $f_2$  can be obtained by adding (3.47), (3.53) and (3.57)

$$\begin{aligned} f_2 &= \frac{\langle I \rangle^2 g^2 \lambda_d^2 \overline{\nu_{sp}}^2 f}{\alpha^2} \left[ \sum_{n=1}^\infty \frac{2\alpha^2 e^{-(\omega_n \sigma)^2} \cos(\omega_n \tau)}{(\omega_n^2 + \alpha^2)} + 1 \right] + \frac{\langle I \rangle \lambda_d^2 f}{\alpha} \left[ \frac{\lambda_f \overline{\nu_{sp}} \overline{\nu(\nu-1)}}{2\alpha} + \frac{\overline{\nu_{sp}}(\nu_{sp}-1)}{2} \right] e^{-\alpha\tau} \\ &+ \frac{\overline{\nu_{sp}}^2 \lambda_d^2 \Gamma^2 g^2 f e^{\alpha^2 \sigma^2}}{4\alpha} \left[ 1 + \text{Erf}\left(\frac{\tau - 2\sigma^2 \alpha}{2\sigma}\right) + \left(1 - \text{Erf}\left(\frac{\tau + 2\sigma^2 \alpha}{2\sigma}\right)\right) e^{2\alpha\tau} \right] e^{-\alpha\tau} \end{aligned} \quad (3.58)$$

The corresponding Feynman Y function (Degweker and Rana, 2007) is given as

$$\begin{aligned} Y(T) &= \frac{2\langle I \rangle \lambda_d \overline{\nu_{sp}} \alpha}{fT} \left[ \sum_{n=1}^\infty \frac{e^{-(\omega_n \sigma)^2} \sin^2(\omega_n T/2)}{n^2 \pi^2 (\omega_n^2 + \alpha^2)} \right] + \left[ \frac{\lambda_d \lambda_f \overline{\nu_{sp}} \overline{\nu(\nu-1)}}{\alpha^2} + \frac{\lambda_d}{\alpha} \frac{\overline{\nu_{sp}}(\nu_{sp}-1)}{\overline{\nu_{sp}}} \right] \left( 1 - \frac{1 - e^{-\alpha T}}{\alpha T} \right) \\ &+ \frac{\overline{\nu_{sp}} \lambda_d \Gamma^2 g}{\alpha \langle I \rangle} \left( 1 - \frac{1 - e^{-\alpha T}}{\alpha T} - \alpha^2 \sigma^2 \right) \end{aligned} \quad (3.59)$$

### 3.4 Numerical results

In Fig. 3.1, we show the variation with the delay time  $\tau$  of the Rossi alpha function of Eq. (3.8). The input parameters roughly correspond to the analysis of the MUSE experiment discussed in Ballester and Munoz-Cobo (2005). For spallation, we have taken the TARC

experimental conditions as regards to fluctuations, but adjusted the pulsing rate and source strength to be the same as for the D–T MUSE experiment. Since measurements of the fluctuations of the D+ ion beams are not available, we have assumed for our calculations a  $\sigma/m = 0.01$ , i.e. 1% (and  $\sigma/m = 0.1$ , i.e. 10%) fluctuation in the beam current. The three sets of graphs in the figure correspond to the cases  $\beta \ll \alpha$ ,  $\beta \approx \alpha$  and  $\beta \gg \alpha$ . It is obvious that if  $\alpha$  and  $\beta$  are of about the same magnitude or if  $\beta \ll \alpha$ , it is likely that noise experiments might yield  $\beta$  which may be mistaken for  $\alpha$ ! Only in the case  $\beta \gg \alpha$ , i.e. where the source fluctuations can be treated as white, do we get a variation of the Rossi alpha which will give the correct value of  $\alpha$ .

Finiteness of the pulse width has a smoothening effect on the Rossi alpha function. This is illustrated in Fig. 3.2 which shows a comparison of the uncorrelated part of the Rossi alpha function.

### 3.5 Conclusion

The finiteness of the pulse width adds small corrections to the delta function based formulae. The correlations in the source fluctuations introduce additional terms which could confuse interpretation of alpha measurements by the variance method which is likely to suffer most from the presence of other sources of fluctuations. The Rossi alpha, correlation and spectral density methods might perform better in this case.

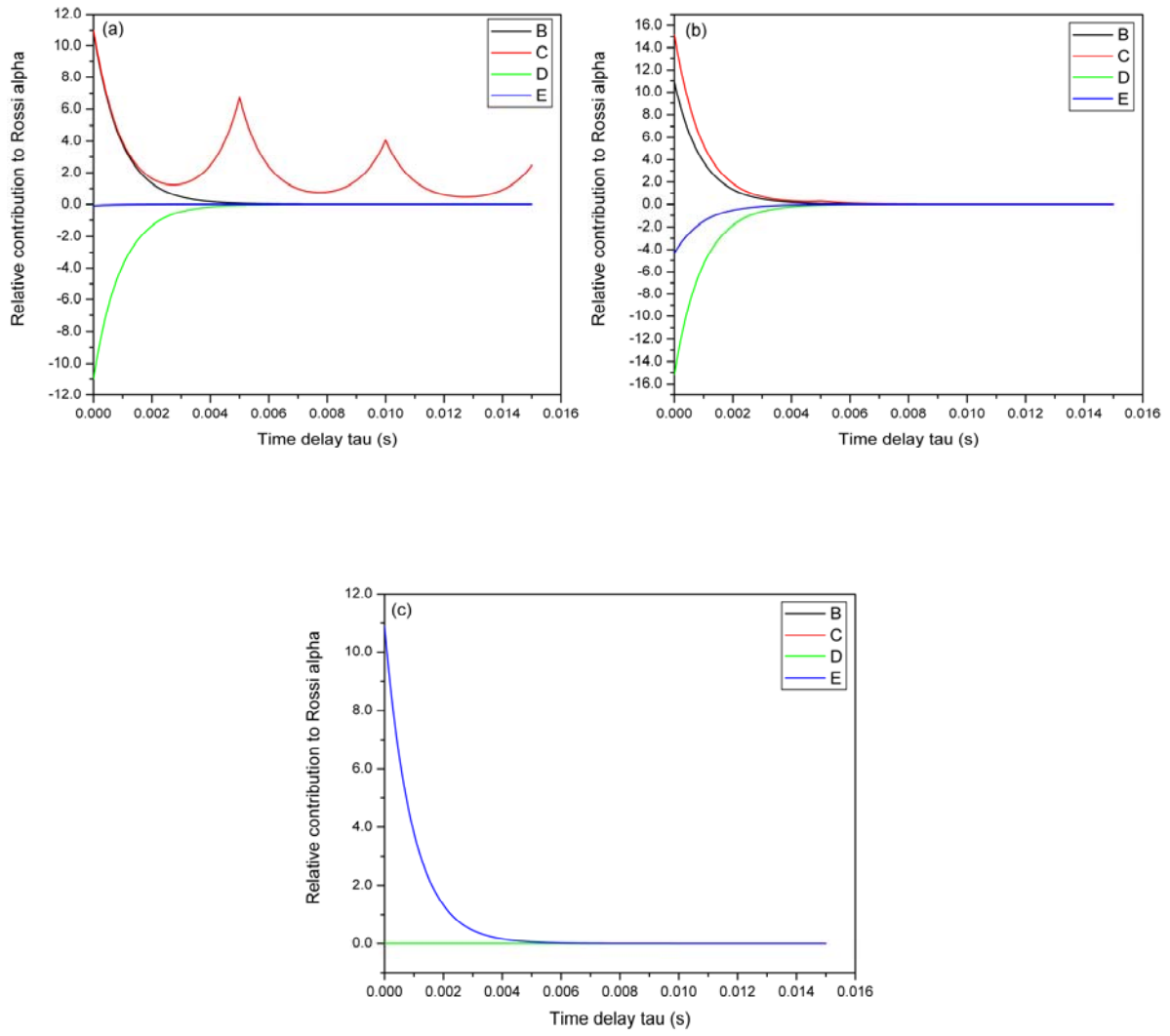


**Figure 3.1:** Variation of different terms of the Rossi alpha formula [Eq. (3.8)] with  $\tau$ . B, C, D, and E refer to the second, the third, the fourth and the sum of the second and fourth terms, respectively. The three sets of graphs (a)–(c) are for  $\beta \ll \alpha$ ,  $\beta \approx \alpha$  and  $\beta \gg \alpha$  respectively.

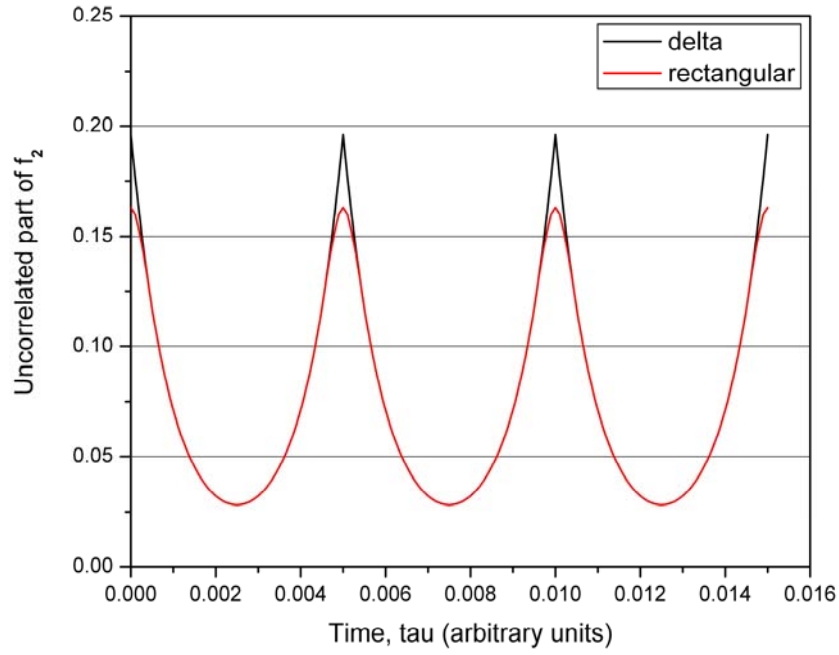


**Figure 3.2:** Comparison of the (uncorrelated part) Rossi alpha formula for delta function and rectangular shaped pulses. The two are identical except close to an integral multiple of the pulse period. In the former we get a sharp cusp whereas for the latter we get a smooth curve in these regions.

# Theory of Reactor Noise in ADS with Delayed Neutrons

In this chapter, we extend the theory of reactor noise in ADS by taking delayed neutrons in to account. We describe the source using non-Poisson periodic delta function pulses and derive formulae for Rossi alpha and Feynman alpha (or variance to mean) by following a method based on resultant pgf of counts (Degweker, 2000). The possibility of correlations between different pulses is also considered. Numerical results based on the derived formulae are presented to illustrate the importance of delayed neutrons in typical experimental conditions.

An earlier study on the effect of delayed neutrons on ADS (driven by a pulsed source) noise characteristics has been performed by Kitamura et al. (2005). This study is based on the use of the Bartlett formula which is valid for Poisson sources. The formulation in the present chapter, as in our earlier chapter, is different in so far as it applies to non-Poisson sources. In section 4.1 we consider the case of un-correlated non-Poisson source pulses. The case of correlated pulses is treated in section 4.2.

### 4.1 No correlation between different pulses

#### 4.1.1 The variance to mean ratio (Feynman alpha) formula

We define  $G(z, t)$  as the pgf of the number of counts in an interval  $[0, T]$ , due to one neutron at time  $t$ . As discussed in section 2.2.3 of chapter 2, if at times  $t_n$  we get bursts of neutrons

having a multiplicity distribution given by  $\rho(\nu)$  and if the last of these bursts occurs at time  $t_0$ , we can write the resultant pgf of counts as follows:

$$f \int_{T-1/f}^T \prod_{n=0}^{\infty} F_{\rho}(G(z, t_0 - n/f, T)) dt_0 \quad (4.1)$$

where  $F_{\rho}(x)$  stands for the pgf of the multiplicity distribution of the number of neutrons produced by a proton bunch i.e. of  $\rho(\nu)$ . Using this pgf, equations for source induced first ( $M_1$ ) and second ( $M_2$ ) factorial moments of the number of counts in the interval 0 to  $T$  can be deduced by repeated differentiation with respect to  $z$  and setting  $z = 1$ . Thus, we obtain

$$m = f m_1 \int_{-\infty}^T G'(1, t) dt \quad (4.2)$$

$$M_2 = f \int_{T-1/f}^T \sum_{n_1 \neq n_2} m_1^2 G'(1, t_0 - n_1/f) G'(1, t_0 - n_2/f) dt_0 + f \int_{-\infty}^T (m_1 G''(1, t) + m_2 G'^2(1, t)) dt \quad (4.3)$$

where  $m_1$  and  $m_2$  stand for the first and second factorial moments of the multiplicity distribution of neutrons produced by a proton bunch and  $f$  is the pulse repetition frequency.

The variance to mean ratio can be obtained as usual from  $m$  and  $M_2$ .

#### *Backward equation for the Green's function $G$*

To evaluate  $m$  and  $M_2$ , we need to have expressions for  $G'(1, t)$  and  $G''(1, t)$ . For this purpose, the backward equation technique for  $G(z, t)$  [Pal 1958] is utilized. The backward equation without delayed neutrons was written down by Degweker (2000). The one with delayed neutrons can be derived along the lines given by Pal (1958). The following equation is a straight generalization to several groups of delayed neutrons.

$$-\frac{\partial G}{\partial t} = -\lambda_a G + \lambda_c + \lambda_d \chi(t) z + \lambda_f f(G(z, t), I_1, \dots, I_N) \quad (4.4)$$

where 
$$I_i = \int_t^T \mu_i e^{-\mu_i(t'-t)} G(z, t') dt' + e^{-\mu_i(T-t)}$$

$f(x, y_1, \dots, y_N)$  is the pgf  $\sum_{n, m_1, \dots, m_N} x^n y_1^{m_1} \dots y_N^{m_N} p(n, m_1, \dots, m_N)$ ;  $p(n, m_i)$  being the probability of finding  $n$  neutrons and  $m_i$  delayed neutron precursors of the  $i^{\text{th}}$  group at time  $t$ ,  $\mu$  is precursors decay constant of the  $i^{\text{th}}$  group and  $\chi(t)$  is unity in the interval  $[0, T]$ , and zero outside.

We get the first and second factorial moments by differentiating with respect to  $z$  and setting  $z = 1$ .

$$-\frac{\partial G'}{\partial t} = -(\lambda_a - \overline{\nu_p} \lambda_f) G' + \lambda_f \sum_i \overline{\nu_{d_i}} \int_t^T \mu_i e^{-\mu_i(t'-t)} G'(1, t') dt' + S_1(t) \quad (4.5)$$

$$-\frac{\partial G''}{\partial t} = -(\lambda_a - \overline{\nu_p} \lambda_f) G'' + \lambda_f \sum_i \overline{\nu_{d_i}} \int_t^T \mu_i e^{-\mu_i(t'-t)} G''(1, t') dt' + S_2(t) \quad (4.6)$$

where,

$$S_1(t) = \lambda_d \chi(t) \quad (4.7)$$

$$S_2(t) = \overline{\nu(\nu-1)_p} \lambda_f G'^2 + 2 \sum_i \overline{\nu_p \nu_{d_i}} \lambda_f G' \int_t^T G'(1, t') \mu_i e^{-\mu_i(t'-t)} dt' + \sum_i \overline{\nu(\nu-1)_{d_i}} \lambda_f \left( \int_t^T G'(1, t') \mu_i e^{-\mu_i(t'-t)} dt' \right)^2 + \sum_i \sum_{j \neq i} \overline{\nu_{d_i} \nu_{d_j}} \lambda_f \left( \int_t^T G'(1, t') \mu_i e^{-\mu_i(t'-t)} dt' \right) \left( \int_t^T G'(1, t') \mu_j e^{-\mu_j(t'-t)} dt' \right) \quad (4.8)$$

where the first two terms on the right hand side are referred to as the prompt-prompt, prompt-delayed correlations, respectively and the last two terms are referred to as delayed-delayed correlations.

If we write  $\overline{\nu(\nu-1)_p} = \overline{\nu(\nu-1)} - \sum_i \overline{\nu(\nu-1)_{d_i}} - \sum_i \sum_{j \neq i} \overline{\nu_{d_i} \nu_{d_j}} - 2 \sum_i \overline{\nu_p \nu_{d_i}}$

then

$$\begin{aligned}
S_2(t') = & \overline{\nu(\nu-1)}\lambda_f G'^2 + 2\sum_i \overline{\nu_p \nu_{d_i}} \lambda_f G' \left( \int_t^T G'(1,t') \mu_i e^{-\mu_i(t'-t)} dt' - G' \right) \\
& + \sum_i \overline{\nu(\nu-1)}_{d_i} \lambda_f \left( \left( \int_t^T G'(1,t') \mu_i e^{-\mu_i(t'-t)} dt' \right)^2 - G'^2 \right) \\
& + \sum_i \sum_{j \neq i} \overline{\nu_{d_i} \nu_{d_j}} \lambda_f \left( \left( \int_t^T G'(1,t') \mu_i e^{-\mu_i(t'-t)} dt' \right) \left( \int_t^T G'(1,t') \mu_j e^{-\mu_j(t'-t)} dt' \right) - G'^2 \right)
\end{aligned} \tag{4.9}$$

It is clear that all terms other than the first are of order  $\beta$  or  $\beta^2$ . Since the contribution of prompt-delayed and delayed-delayed correlations to the final result is negligible, we consider only the first term in the following derivations.

Therefore, we get

$$S_2(t') = \overline{\nu(\nu-1)}\lambda_f G'^2 \tag{4.10}$$

Both  $G'(1,t)$  and  $G''(1,t)$  obey the final condition  $G'(1,T) = G''(1,T) = 0$ .

Note that the last term in Eq. (4.5) and the last three terms in Eq. (4.6) are the adjoint (or backward) equation source terms. The difference between the two equations lies only in these source terms and hence both the equations have a common Green's function given by

$$\sum_j A_j e^{\alpha_j(t-t')} \tag{4.11a}$$

where  $\alpha_j$  are roots of the inhour equation,

$$p \left( \Lambda + \sum_i \frac{\beta_i}{p + \lambda_i} \right) - \rho = 0 \tag{4.11b}$$

and  $\rho = (k_{eff} - 1) / k_{eff}$  and  $\Lambda = l / k_{eff}$  is the generation time.

If we define  $A'_j = A_j / \Lambda$ , we note that the left side of Eq. (4.11b) is the inverse of the zero power transfer function  $G(s)$  and  $A'_i$  are the residues of the transfer function i.e.

$$G(s) = \sum_i \frac{A'_i}{s + \alpha_i} \tag{4.11c}$$

where

$$\frac{1}{G(s)} = s \left( \Lambda + \sum_i \frac{\beta_i}{s + \lambda_i} \right) - \rho \quad (4.11d)$$

From Eq. (4.11c),  $G(0) = \sum_i A_i' / \alpha_i$ . Also, from Eq. (4.11d),  $G(0) = -1 / \rho$ . Combining these

two relations yields

$$\sum_i \frac{A_i'}{\alpha_i} = -1 / \rho \quad (4.11e)$$

Hence it is possible to write the solutions of Eqs. (4.5) and (4.6) as follows

$$G'(1, t) = \sum_j A_j \int_t^T e^{\alpha_j(t-t')} [\lambda_d \chi(t')] dt' \quad (4.12)$$

$$G''(1, t) = \sum_j A_j \int_t^T e^{\alpha_j(t-t')} S_2(t') dt' \quad (4.13)$$

Solving the integral in Eq. (4.12), the result can be shown to be

$$\begin{aligned} G'(1, t) &= \lambda_d \sum_j \frac{A_j}{\alpha_j} e^{\alpha_j t} (1 - e^{-\alpha_j T}) \text{ for } t < 0 \\ &= \lambda_d \sum_j \frac{A_j}{\alpha_j} (1 - e^{-\alpha_j(T-t)}) \text{ for } 0 < t < T \\ &= 0 \end{aligned} \quad (4.14)$$

We will not solve the integral in Eq. (4.13) because the future derivations will not require it.

### *The Feynman alpha formula*

Having written down expressions for the first and second moments of the single neutron pgf  $G'$  and  $G''$ , we now proceed to evaluate the expressions for the source induced moments given by (4.2) and (4.3).

The average number of counts in the interval  $[0, T]$ , or the (source induced) first moment can be written down using Eq. (4.2) and the solution of Eq. (4.5) given above.

$$\begin{aligned}
m &= fm_1 \int_{-\infty}^T G'(1, t, T) dt \\
&= fm_1 \left( \int_{-\infty}^0 \lambda_d \sum_j \frac{A_j}{\alpha_j} e^{\alpha_j t} (1 - e^{-\alpha_j T}) dt + \int_0^T \lambda_d \sum_j \frac{A_j}{\alpha_j} (1 - e^{-\alpha_j (T-t)}) dt \right) \\
&= fm_1 \lambda_d T \sum_j \frac{A_j}{\alpha_j}
\end{aligned} \tag{4.15}$$

Therefore the average count rate is given by

$$f_1(t) = fm_1 \lambda_d \sum_j \frac{A_j}{\alpha_j} \tag{4.16}$$

This expression is similar to the one without delayed neutrons that was obtained in chapter 3.

Before evaluating Eq. (4.3), we make a slight change in it to simplify further calculations.

The double summation in the first term excludes  $n_1 = n_2$ . However, we include this term and subtract it from the second term in Eq. (4.3). With this change, we can rewrite the expression for  $M_2$  given by Eq. (4.3) as a sum of three terms:

$$fm_1 \int_{-\infty}^T G''(1, t) dt + f(m_2 - m_1^2) \int_{-\infty}^T (G'(1, t))^2 dt + f \int_{T-1/f}^T \left[ m_1 \sum_n G'(1, t_0 - n/f) \right]^2 dt_0 \tag{4.17}$$

The three terms in the above expression will be denoted by  $[I]$ ,  $[II]$  and  $[III]$  respectively.

$$[I] = fm_1 \int_{-\infty}^T G''(1, t) dt = fm_1 \int_{-\infty}^T dt \int_t^T dt' \sum_j A_j e^{\alpha_j (t-t')} S_2(t') \tag{4.18}$$

Interchanging the order of integration, we have

$$\begin{aligned}
[I] &= fm_1 \int_{-\infty}^T G''(1, t) dt = fm_1 \int_{-\infty}^T \left( \sum_j \frac{A_j}{\alpha_j} \right) S_2(t') dt' \\
&= fm_1 \overline{v(v-1)} \lambda_f \left( \sum_j \frac{A_j}{\alpha_j} \right) \left( \int_{-\infty}^0 \left[ \lambda_d \sum_j \frac{A_j}{\alpha_j} e^{\alpha_j t'} (1 - e^{-\alpha_j T}) \right]^2 dt' + \int_0^T \left[ \lambda_d \sum_j \frac{A_j}{\alpha_j} (1 - e^{-\alpha_j (T-t')}) \right]^2 dt' \right)
\end{aligned}$$

$$= fm_1 \overline{\nu(\nu-1)} \lambda_f \left( \sum_j \frac{A_j}{\alpha_j} \right) \lambda_d^2 \sum_i \sum_k \frac{A_i A_k}{\alpha_i \alpha_k} \left[ T - \frac{1-e^{-\alpha_k T}}{\alpha_k} - \frac{1-e^{-\alpha_i T}}{\alpha_i} + \frac{2-e^{-\alpha_i T} - e^{-\alpha_k T}}{\alpha_i + \alpha_k} \right] \quad (4.19)$$

The above expression can be written in a form given by Williams (1974)

$$[I] = fm_1 \lambda_f \overline{\nu}^2 \left( \sum_j \frac{A_j}{\alpha_j} \right) \lambda_d^2 T \sum_i Y_i \left( 1 - \frac{1-e^{-\alpha_i T}}{\alpha_i T} \right) \quad (4.20a)$$

where we have introduced the notation  $Y_i$  for

$$Y_i = 2 \frac{\overline{\nu(\nu-1)}}{(\overline{\nu})^2} \frac{A_i G(\alpha_i)}{\alpha_i} \quad (4.20b)$$

$$\begin{aligned} [II] &= f(m_2 - m_1^2) \int_{-\infty}^T (G'(1, t))^2 dt \\ &= f(m_2 - m_1^2) \left( \int_{-\infty}^0 \left[ \lambda_d \sum_j \frac{A_j}{\alpha_j} e^{\alpha_j t} (1 - e^{-\alpha_j T}) \right]^2 dt + \int_0^T \left[ \lambda_d \sum_j \frac{A_j}{\alpha_j} (1 - e^{-\alpha_j(T-t)}) \right]^2 dt \right) \\ &= f(m_2 - m_1^2) \lambda_d^2 \sum_j \sum_k \frac{A_j A_k}{\alpha_j \alpha_k} \left( T - \frac{1-e^{-\alpha_j T}}{\alpha_j} - \frac{1-e^{-\alpha_k T}}{\alpha_k} - \frac{2-e^{-\alpha_j T} - e^{-\alpha_k T}}{(\alpha_j + \alpha_k)} \right) \end{aligned} \quad (4.21)$$

As in Eq. (4.20a), this expression can be written in terms of  $Y_i$  as follows:

$$[II] = \frac{f(m_2 - m_1^2) \overline{\nu}^2 \lambda_d^2 T}{\overline{\nu(\nu-1)}} \sum_i Y_i \left( 1 - \frac{1-e^{-\alpha_i T}}{\alpha_i T} \right) \quad (4.22)$$

$$[III] = f \int_{T-1/f}^T \left[ m_1 \sum_n G'(1, t_0 - n/f) \right]^2 dt_0 \quad (4.23)$$

If  $t_0$  is between  $-1/f$  and 0, then

For  $t < 0$

$$\begin{aligned} \sum_n G'(1, t_0 - n/f) &= \lambda_d \sum_j \frac{A_j}{\alpha_j} \sum_{n=0}^{\infty} (1 - e^{-\alpha_j T}) e^{\alpha_j(t_0 - n/f)} \\ &= \sum_j \frac{A_j \lambda_d}{\alpha_j (1 - e^{-\alpha_j/f})} e^{\alpha_j t_0} (1 - e^{-\alpha_j T}) \end{aligned} \quad (4.24)$$

For  $0 < t_0 - n/f < T$ ,

$$\sum_n G'(1, t_0 - n/f) = \lambda_d \sum_j \frac{A_j}{\alpha_j} \sum_{n=-1}^{-[fT]} \left[ 1 - e^{-\alpha_j(T-(t_0-n/f))} \right];$$

if  $[fT]$  is very close to  $T$  i.e. if  $t_0 + \frac{[fT]+1}{f} > T$

$$= \sum_j \frac{A_j \lambda_d}{\alpha_j} \left[ [fT] - e^{-\alpha_j(T-t_0)} \frac{e^{\alpha_j[fT]/f} - 1}{1 - e^{-\alpha_j/f}} \right] \quad (4.25a)$$

$$= \lambda_d \sum_j \frac{A_j}{\alpha_j} \sum_{n=-1}^{-([fT]+1)} \left[ 1 - e^{-\alpha_j(T-(t_0-n/f))} \right];$$

if  $[fT+1]$  is very close to  $T$  i.e. if  $t_0 + \frac{[fT]+1}{f} < T$

$$= \sum_j \frac{A_j \lambda_d}{\alpha_j} \left[ [fT+1] - e^{-\alpha_j(T-t_0)} \frac{e^{\alpha_j[fT+1]/f} - 1}{1 - e^{-\alpha_j/f}} \right] \quad (4.25b)$$

Thus,

$$\sum_n G'(1, t_0 - n/f) = \lambda_d \sum_j \frac{A_j}{\alpha_j} \left[ \frac{e^{\alpha_j t_0} (1 - e^{-\alpha_j T})}{(1 - e^{-\alpha_j/f})} + [fT] - e^{-\alpha_j(T-t_0)} \frac{e^{\alpha_j[fT]/f} - 1}{1 - e^{-\alpha_j/f}} \right] \quad (4.26a)$$

for  $t_0 + \frac{[fT]+1}{f} > T$

$$\lambda_d \sum_j \frac{A_j}{\alpha_j} \left[ \frac{e^{\alpha_j t_0} (1 - e^{-\alpha_j T})}{(1 - e^{-\alpha_j/f})} + [fT+1] - e^{-\alpha_j(T-t_0)} \frac{e^{\alpha_j[fT+1]/f} - 1}{1 - e^{-\alpha_j/f}} \right] \quad (4.26b)$$

for  $t_0 + \frac{[fT]+1}{f} < T$

Therefore,

$$[III] = \lambda_d^2 m_1^2 f \left( \int_{-1/f}^{T-\frac{1+[fT]}{f}} \left[ \sum_j \frac{A_j}{\alpha_j} \left( \frac{e^{\alpha_j t_0} (1 - e^{-\alpha_j T})}{(1 - e^{-\alpha_j/f})} + [fT+1] - e^{-\alpha_j(T-t_0)} \frac{e^{\alpha_j[fT+1]/f} - 1}{1 - e^{-\alpha_j/f}} \right) \right]^2 dt_0 \right. \\ \left. + \int_{T-\frac{1+[fT]}{f}}^0 \left[ \sum_j \frac{A_j}{\alpha_j} \left( \frac{e^{\alpha_j t_0} (1 - e^{-\alpha_j T})}{(1 - e^{-\alpha_j/f})} + [fT] - e^{-\alpha_j(T-t_0)} \frac{e^{\alpha_j[fT]/f} - 1}{1 - e^{-\alpha_j/f}} \right) \right]^2 dt_0 \right) \quad (4.27a)$$

$$= \lambda_d^2 m_1^2 f \sum_j \sum_k \frac{A_j A_k}{\alpha_j \alpha_k} \left[ \begin{aligned} & \frac{2(1 - e^{-(\alpha_j + \alpha_k)/f})}{(\alpha_j + \alpha_k)(1 - e^{-\alpha_j/f})(1 - e^{-\alpha_k/f})} + T + 2[fT]T - \frac{[fT]}{f}([fT] + 1) \\ & + \frac{1}{\alpha_j(1 - e^{-\alpha_j/f})} \left( \frac{\alpha_k(e^{-\alpha_j(T-[fT]/f)} + e^{\alpha_j(T-([fT]+1)/f})}{\alpha_j + \alpha_k} \right) \\ & + \frac{1}{\alpha_k(1 - e^{-\alpha_k/f})} \left( \frac{\alpha_j(e^{-\alpha_k(T-[fT]/f)} + e^{\alpha_k(T-([fT]+1)/f})}{\alpha_j + \alpha_k} \right) \end{aligned} \right] \quad (4.27b)$$

This expression, as earlier, can be written in terms of  $Y_i$  as follows:

$$[III] = \lambda_d^2 m_1^2 f \left[ \begin{aligned} & \left( \sum_j \frac{A_j}{\alpha_j} \right)^2 \left( T + 2[fT]T - \frac{[fT]}{f}([fT] + 1) \right) \\ & + \frac{\bar{v}^2}{v(v-1)} \sum_i \frac{Y_i}{\alpha_i} \left( \frac{e^{-\alpha_i(T-[fT]/f)} + e^{\alpha_i(T-([fT]+1)/f)} - 1 - e^{-\alpha_i/f}}{1 - e^{-\alpha_i/f}} \right) \end{aligned} \right] \quad (4.28)$$

Now, since variance to mean ratio  $\frac{v}{m} = 1 + \frac{M_2}{m} - m$ , from Eqs. (4.20a), (4.22) and (4.28), the

final expression for variance to mean ratio can be written as follows

$$\begin{aligned} \frac{v}{m} = & 1 + \frac{\bar{v}^2 \lambda_d}{m_1} \sum_i Y_i \left( 1 - \frac{1 - e^{-\alpha_i T}}{\alpha_i T} \right) \left[ m_1 \lambda_f + \frac{(m_2 - m_1^2)}{v(v-1) \sum_j (A_j / \alpha_j)} \right] \\ & + \lambda_d m_1 \left( \sum_j \frac{A_j}{\alpha_j} \right) \left[ \frac{1 + 2[fT] - \frac{[fT]}{fT}([fT] + 1)}{-fT} \right] \\ & + \frac{\bar{v}^2 m_1 \lambda_d}{v(v-1) \sum_j (A_j / \alpha_j)} \sum_i \frac{Y_i}{\alpha_i} \left[ \frac{e^{-\alpha_i(T-[fT]/f)} + e^{\alpha_i(T-([fT]+1)/f)} - 1 - e^{-\alpha_i/f}}{T(1 - e^{-\alpha_i/f})} \right] \end{aligned} \quad (4.29)$$

Replacing  $A_j$  by  $A'_j$  and employing Eq. (4.11e), the final expression for  $\frac{v}{m}$  becomes

$$\begin{aligned} \frac{\bar{\nu}}{m} = 1 + \sum_i Y_i \left( 1 - \frac{1 - e^{-\alpha_i T}}{\alpha_i T} \right) & \left[ 1 - \frac{\bar{\nu} \rho (m_2 - m_1^2)}{m_1 \bar{\nu} (\bar{\nu} - 1)} \right] - \frac{\lambda_d m_1 \Lambda}{\rho} \left[ \frac{1 + 2[fT] - \frac{[fT]}{fT} ([fT] + 1)}{-fT} \right] \\ - \frac{\bar{\nu} m_1 \varepsilon \rho}{\bar{\nu} (\bar{\nu} - 1)} \sum_i \frac{Y_i}{\alpha_i} & \left[ \frac{e^{-\alpha_i (T - [fT]/f)} + e^{\alpha_i (T - ([fT] + 1)/f)} - 1 - e^{-\alpha_i / f}}{T (1 - e^{-\alpha_i / f})} \right] \end{aligned} \quad (4.30)$$

where we have used the relations  $\lambda_d = \varepsilon \lambda_f$  and  $\frac{1}{\bar{\nu} \lambda_f} = \Lambda$

Also we have redefined  $Y_i$  as

$$Y_i = 2\varepsilon \frac{\overline{\bar{\nu}(\bar{\nu} - 1)}}{(\bar{\nu})^2} \frac{A_i' G(\alpha_i)}{\alpha_i}$$

In the above expression, first part of the first term represents the usual uncorrelated component and the second part represents the correlated component. The second and third terms are oscillating in nature and appear due to the periodicity of the source.

It can be seen that the correlated terms have the same form as described by Williams (1974).

The correlated term is different from that for a random source in that it contains the term  $m_2 - m_1^2$  rather than  $m_2$ . The subtraction of the square of  $m_1$  reduces the correlated component of the noise. This reduction may be ascribed to the regularity of the source pulses.

If there are no delayed neutrons, summations are removed,  $A_i = 1 = A_k$ ,  $\alpha_i = \alpha = \alpha_k$  and  $Y_i$  are

replaced by  $\frac{\overline{\bar{\nu}(\bar{\nu} - 1)}}{\bar{\nu}^2 \alpha^2}$

Thus the expression for variance to mean ratio without delayed neutrons becomes

$$\begin{aligned} \frac{\bar{\nu}}{m} = 1 + \frac{\bar{\nu}^2 \lambda_d}{m_1} \frac{\overline{\bar{\nu}(\bar{\nu} - 1)}}{\bar{\nu}^2 \alpha^2} \left( 1 - \frac{1 - e^{-\alpha T}}{\alpha T} \right) & \left[ m_1 \lambda_f + \frac{(m_2 - m_1^2)}{\bar{\nu}(\bar{\nu} - 1)(1/\alpha)} \right] + \frac{\lambda_d m_1}{\alpha} \left[ \frac{1 + 2[fT] - \frac{[fT]}{fT} ([fT] + 1)}{-fT} \right] \\ + \frac{\bar{\nu}^2 m_1 \lambda_d}{\bar{\nu}(\bar{\nu} - 1)(1/\alpha)} \frac{\overline{\bar{\nu}(\bar{\nu} - 1)}}{\bar{\nu}^2 \alpha^3} & \left[ \frac{e^{-\alpha (T - [fT]/f)} + e^{\alpha (T - ([fT] + 1)/f)} - 1 - e^{-\alpha / f}}{T (1 - e^{-\alpha / f})} \right] \end{aligned}$$

$$\begin{aligned}
&= 1 + \frac{\lambda_d (m_2 + 2m_1 Y_1)}{m_1 \alpha} \left( 1 - \frac{1 - e^{-\alpha T}}{\alpha T} \right) - \frac{\lambda_d m_1}{\alpha} \left[ fT - 2[fT] + \frac{[fT]}{fT} ([fT] + 1) \right] \\
&+ \frac{\lambda_d m_1}{\alpha} \left[ \frac{e^{-\alpha(T - [fT]/f)} + e^{\alpha(T - ([fT] + 1)/f)} + e^{-\alpha(T + 1/f)} - 2e^{-\alpha/f} - e^{-\alpha T}}{T\alpha(1 - e^{-\alpha/f})} \right]
\end{aligned} \tag{4.31}$$

Where we have used  $Y_1 = \overline{\lambda_f \nu(\nu - 1) / 2\alpha}$

Thus, in the absence of delayed neutrons, the expression for variance to mean ratio reduces to the form derived earlier by Degweker (2003), as it should.

In Appendix I, we have derived expression for the  $v/m$  ratio taking into account the terms involving prompt-delayed and delayed–delayed neutron correlations. There are six additional terms in the variance formulae having a functional variation with time similar to the usual variance formula, corresponding to the six precursor decay constants.

#### 4.1.2 The two time probability density (Rossi alpha) formula

We introduce the pgf  $G(z_1, z_2, t)$  of detecting counts in a short interval around time 0 and counts in a short interval around time  $\tau$  due to one neutron at time  $t$ . This obeys the backward equation. The Rossi-alpha formula can be derived by introducing the Master equation technique for  $G(z_1, z_2, t)$  [Kitamura et al., 2005].

$$-\frac{\partial G}{\partial t} = -\lambda_a G + \lambda_c + \lambda_d \sum_{i=1}^2 (z_i - 1) \chi_i(t) + \lambda_f f(G(z_1, z_2, t), I_i) \tag{4.32}$$

where

$$I_i = \int_t^\tau \mu_i e^{-\mu_i(t'-t)} G(z, t') dt' + e^{-\mu_i(\tau-t)}$$

$$\chi_1(t) = 1, \text{ in an interval } dt_0 \text{ around } t = 0$$

and

$$\chi_2(t) = 1, \text{ in an interval } d\tau \text{ around } t = \tau$$

Since the short interval is infinitesimal, we only consider the possibility that there are either 0 or 1 counts in these intervals.

We get the first and second factorial moments by differentiating with respect to  $z_1$  and  $z_2$  and setting  $z_1 = 1$  and  $z_2 = 1$  respectively.

$$-\frac{\partial G_{z_1}}{\partial t} = -(\lambda_a - \overline{\nu_p} \lambda_f) G_{z_1} + \lambda_f \overline{\nu_d} \int_t^\tau \mu e^{-\mu(t'-t)} G_{z_1}(1, t') dt' + \lambda_d \chi_i(\tau) \quad (4.33)$$

$$-\frac{\partial G_{z_1 z_2}}{\partial t} = -(\lambda_a - \overline{\nu_p} \lambda_f) G_{z_1 z_2} + \lambda_f \sum_i \overline{\nu_{d_i}} \int_t^\tau \mu_i e^{-\mu_i(t'-t)} G_{z_1 z_2}(1, 1, t') dt' + S_2(t) \quad (4.34a)$$

$$\begin{aligned} S_2(t) &= \overline{\nu(\nu-1)}_p \lambda_f G_{z_1} G_{z_2} + \sum_i \overline{\nu_p \nu_{d_i}} \lambda_f G_{z_1} \int_t^\tau G_{z_2}(1, 1, t') \mu_i e^{-\mu_i(t'-t)} dt' \\ &+ \sum_i \overline{\nu_p \nu_{d_i}} \lambda_f G_{z_2} \int_t^\tau G_{z_1}(1, 1, t') \mu_i e^{-\mu_i(t'-t)} dt' \\ &+ \sum_i \overline{\nu(\nu-1)}_{d_i} \lambda_f \left( \int_t^\tau \mu_i G_{z_1}(1, 1, t') e^{-\mu_i(t'-t)} dt' \right) \left( \int_t^\tau \mu_i G_{z_2}(1, 1, t') e^{-\mu_i(t'-t)} dt' \right) \\ &+ \sum_i \sum_{j \neq i} \overline{\nu_{d_i} \nu_{d_j}} \lambda_f \left( \int_t^\tau G_{z_1}(1, 1, t') \mu_i e^{-\mu_i(t'-t)} dt' \right) \left( \int_t^\tau G_{z_2}(1, 1, t') \mu_j e^{-\mu_j(t'-t)} dt' \right) \end{aligned} \quad (4.34b)$$

As described earlier, neglecting the prompt-delayed and delayed-delayed correlations

$$S_2(t) = \overline{\nu(\nu-1)}_p \lambda_f G_{z_1} G_{z_2}$$

The solution of (4.33) can be shown to be

$$\begin{aligned} G_{z_1} &= \lambda_d \sum_j A_j e^{\alpha_j t} \quad \text{for } t < 0 \\ &= 0 \quad \text{otherwise} \end{aligned}$$

and

$$\begin{aligned} G_{z_2} &= \lambda_d \sum_j A_j e^{\alpha_j(t-\tau)} \quad t < \tau \\ &= 0 \quad \text{otherwise} \end{aligned}$$

$$G_{z_1 z_2}(1, t) = \sum_j A_j \int_t^\tau e^{\alpha_j(t-t')} S_2(t') dt'$$

To get the source induced moments, we simply replace Eq. (4.1) with the following

$$f \int_{\tau-1/f}^{\tau} \prod_{n=0}^{\infty} F_{\rho} \left( G(z_1, z_2, t_0 - n/f, T) \right) dt_0$$

On differentiating with respect to  $z_1$  and  $z_2$  and setting  $z_1=z_2=1$ , we get the following expression for the Rossi alpha

$$\begin{aligned} & fm_1 \int_{-\infty}^{\tau} G_{z_1 z_2}(1, t) dt + f(m_2 - m_1^2) \int_{-\infty}^{\tau} G_{z_1} G_{z_2} dt' \\ & + fm_1^2 \int_{\tau-1/f}^{\tau} \left[ \left( \sum_{n_1} G_{z_1}(1, t_0 - n_1/f) \right) \left( \sum_{n_2} G_{z_2}(1, t_0 - n_2/f) \right) \right] dt_0 \end{aligned} \quad (4.35)$$

The three terms that are required to be evaluated for calculating the (source induced) second moment become

$$\begin{aligned} [I] &= fm_1 \int_{-\infty}^{\tau} G_{z_1 z_2}(1, t) dt = fm_1 \int_{-\infty}^{\tau} \left( \sum_j \frac{A_j}{\alpha_j} \right) S_2(t') dt' \\ &= fm_1 \left( \sum_j \frac{A_j}{\alpha_j} \right) \overline{\nu(\nu-1)} \lambda_f \lambda_d^2 \sum_i \sum_k \frac{A_i A_k}{\alpha_i + \alpha_k} e^{-\alpha_k \tau} \\ &= fm_1 \left( \sum_j \frac{A_j}{\alpha_j} \right) \frac{\lambda_f \lambda_d^2 \bar{\nu}^2}{2} \sum_i \alpha_i Y_i e^{-\alpha_i \tau} \end{aligned} \quad (4.36)$$

From Eq. (4.35),

$$\begin{aligned} [II] &= f(m_2 - m_1^2) \int_{-\infty}^{\tau} G_{z_1} G_{z_2} dt' = f(m_2 - m_1^2) \lambda_d^2 \sum_i \sum_k e^{-\alpha_k \tau} \left( \frac{A_i A_k}{\alpha_i + \alpha_k} \right) \\ &= \frac{\bar{\nu}^2 f(m_2 - m_1^2) \lambda_d^2}{2\nu(\nu-1)} \sum_i \alpha_i Y_i e^{-\alpha_i \tau} \end{aligned} \quad (4.37)$$

From Eq. (4.35),

$$\begin{aligned}
[III] &= fm_1^2 \int_{\tau-1/f}^{\tau} \left[ \left( \sum_{n_1} G_{z_1}(1, t_0 - n_1 / f) \right) \left( \sum_{n_2} G_{z_2}(1, t_0 - n_2 / f) \right) \right] dt_0 \\
&= fm_1^2 \left( \int_{\tau-\frac{[f\tau]+1}{f}}^{\frac{0}{f}} \left[ \left( \sum_{n_1=0}^{\infty} G'_{z_1}(1, t_0 - n_1 / f) \right) \left( \sum_{n_2=-[f\tau]}^{\infty} G'_{z_2}(1, t_0 - n_2 / f) \right) \right] dt_0 \right. \\
&\quad \left. + \int_{\frac{1}{f}}^{\tau-\frac{[f\tau]+1}{f}} \left[ \left( \sum_{n_1=0}^{\infty} G'_{z_1}(1, t_0 - n_1 / f) \right) \left( \sum_{n_2=-([f\tau]+1)}^{\infty} G'_{z_2}(1, t_0 - n_2 / f) \right) \right] dt_0 \right) \\
&= fm_1^2 \lambda_d^2 \sum_i \sum_k \frac{A_i A_k e^{-\alpha_k(\tau-[f\tau]/f)}}{(1-e^{-\alpha_i/f})(1-e^{-\alpha_k/f})} \left( \frac{(1-e^{-\alpha_i/f}) + (1-e^{-\alpha_k/f}) e^{(\alpha_i+\alpha_k)(\tau-[f\tau]/f)-\alpha_i/f}}{\alpha_i + \alpha_k} \right) \\
&= \frac{fm_1^2 \lambda_d^2 \bar{\nu}^{-2}}{2\nu(\nu-1)} \left[ \sum_i \frac{\alpha_i Y_i}{(1-e^{-\alpha_i/f})} \left( e^{-\alpha_i(\tau-[f\tau]/f)} + e^{\alpha_i(\tau-([f\tau]+1)/f)} \right) \right] \tag{4.38}
\end{aligned}$$

From Eqs. (4.36), (4.37) and (4.38), the final expression for Rossi-alpha with delayed neutrons becomes

$$\begin{aligned}
f_2 &= \frac{f \lambda_d^2 \bar{\nu}^{-2}}{2} \sum_i \alpha_i Y_i e^{-\alpha_i \tau} \left[ m_1 \lambda_f \left( \sum_j \frac{A_j}{\alpha_j} \right) + \frac{(m_2 - m_1^2)}{\nu(\nu-1)} \right] \\
&\quad + \frac{\bar{\nu}^{-2}}{2\nu(\nu-1)} fm_1^2 \lambda_d^2 \sum_i \frac{\alpha_i Y_i}{(1-e^{-\alpha_i/f})} \left( e^{-\alpha_i(\tau-[f\tau]/f)} + e^{\alpha_i(\tau-([f\tau]+1)/f)} \right) \tag{4.39}
\end{aligned}$$

Replacing  $A_j$  by  $A'_j$  and employing Eq. (4.11e), the final expression for Rossi Alpha becomes

$$\begin{aligned}
f_2 &= \frac{f \varepsilon}{2} \sum_i \alpha_i Y_i e^{-\alpha_i \tau} \left[ -\frac{m_1 \lambda_f}{\rho} + \frac{(m_2 - m_1^2)}{\nu(\nu-1)} \right] \\
&\quad + \frac{f \varepsilon m_1^2}{2\nu(\nu-1)} \sum_i \frac{\alpha_i Y_i}{(1-e^{-\alpha_i/f})} \left( e^{-\alpha_i(\tau-[f\tau]/f)} + e^{\alpha_i(\tau-([f\tau]+1)/f)} \right) \tag{4.40}
\end{aligned}$$

Again, as in the case of variance to mean ratio, we have the term  $m_2 - m_1^2$ , arising due to non-Poisson character of the source, and the oscillating terms due to the periodic nature of the source.

If there are no delayed neutrons, the above expression reduces to

$$\begin{aligned}
f_2 &= \frac{f\lambda_d^2 \bar{\nu}^2}{2} \frac{e^{-\alpha\tau}}{\alpha} \frac{\bar{\nu}(\bar{\nu}-1)}{\bar{\nu}^2} \left[ \frac{m_1\lambda_f}{\alpha} + \frac{(m_2-m_1^2)}{\bar{\nu}(\bar{\nu}-1)} \right] \\
&+ \frac{\bar{\nu}^2}{2\bar{\nu}(\bar{\nu}-1)} f m_1^2 \lambda_d^2 \frac{\bar{\nu}(\bar{\nu}-1)}{\bar{\nu}^2 \alpha (1-e^{-\alpha/f})} \left( e^{-\alpha(\tau-[f\tau]/f)} + e^{\alpha(\tau-([f\tau]+1)/f)} \right) \\
&= \frac{f\lambda_d^2}{2\alpha} \left[ (2m_1Y_1 + m_2 - m_1^2) e^{-\alpha\tau} + \frac{m_1^2}{1-e^{-\alpha/f}} \{ e^{-\alpha/f} e^{\alpha(\tau-[f\tau]/f)} + e^{-\alpha(\tau-([f\tau]+1)/f)} \} \right] \quad (4.41)
\end{aligned}$$

Thus, we see that the Rossi alpha expression (4.39) reduces to the form derived earlier by Degweker (2003).

In Appendix II, we have derived expression Rossi alpha taking into account the terms involving prompt-delayed and delayed-delayed neutron correlations. It appears from these formulae that in the Rossi-alpha formula, in addition to the well known exponentials with decay constants given by the roots of the inhour equation, there are six other exponentials corresponding to the six delayed neutron precursor decay constants.

#### 4.1.3 Numerical Results

We have done calculations of the Feynman alpha and Rossi alpha for typical ADS experimental parameters given in Table 4.1.

Figs. 4.1-4.3 show the variation of  $\nu/m$  with the length of the counting interval. Fig. 4.1(a) shows the results on prompt neutron time scale while Fig. 4.1(b) shows the results on the delayed neutron time scale. On the latter scale, we see a prompt jump followed by a slower rise. From these graphs it can be seen that the contribution of delayed neutrons is significant. Fig 4.1(c) shows the contribution due to source correlations. The magnitude of this term is small compared to that due to fission chain correlations for the parameters assumed and the level of sub-criticality. However, under different circumstances, this could become large and

even the dominant contributor to the Feynman Y function. Fig. 4.1(d) represents the contribution of the oscillatory term due to the periodicity of the source.

The same sets of graphs are shown in Fig. 4.2 but with a prompt neutron lifetime of about 1 ms, typical of a heavy water reactor. The important point to note is that the prompt and delayed neutron time scales overlap; they are not distinctly separated like in case of Fig. 4.1. As a result we do not see a sharp prompt jump in the  $v/m$  on delayed neutron time scales. The significance of this is that in trying to extract  $\alpha$  from a plot of  $v/m$  or Y versus counting interval, it is necessary to include corrections due to delayed neutron terms. The four sets of graphs in Fig 4.3 again correspond to the case of a heavy water reactor but with lower level of sub-criticality. Here once again the two time scales overlap and the important point to note is that the magnitude of  $v/m$  is more as it should be.

In Figs. 4.4-4.6, we show for different sets of parameters listed in table 4.1, the magnitude of various terms of the Rossi Alpha formula with delay time. An interesting feature is that a plot of the logarithm of the correlated term with time separation results in two sharply defined lines for the light water case where the prompt and delayed time scales are well separated but for the heavy water case, there is a smooth transition from the prompt to the delayed region. It can be seen from Fig. 4.4(c) that in this particular case, the magnitude of the term arising due to source correlations is very small compared to other terms which is why the contribution of this term appears negligible when plotted along with other terms (see Figs. 4.4(a), 4.5(a), and 4.6(a)).

## **4.2 Correlation between different pulses**

### **4.2.1 The two time probability density (Rossi alpha) formula**

The counting gate system assumed for deriving the Rossi alpha formula is shown in Figure 4.7. If at times  $t_n$  we get bursts of neutrons having a multiplicity distribution given

by  $\rho(v_1, v_2, \dots, v_N)$  and if the last of these bursts occurs at time  $t_0$ , we can write the resultant pgf of counts, to get the source induced moments, as follows:

$$f \int_{\tau-1/f}^{\tau} \sum_{v_1, v_2, \dots, v_N} \rho(v_1, v_2, \dots, v_N) G^{v_1}(z_1, z_2, t_0 - 1/f) G^{v_2}(z_1, z_2, t_0 - 2/f) \dots G^{v_N}(z_1, z_2, t_0 - N/f) dt_0$$

On differentiating w.r.t.  $z_1$  and  $z_2$  and setting  $z_1=z_2=1$  we get the following expression for the Rossi alpha

$$f_2(0, \tau) = f \int_{\tau-1/f}^{\tau} \left[ \sum_{n=0}^{\infty} m_2 G_{z_1}(1, t_0 - n/f) G_{z_2}(1, t_0 - n/f) + m_1 G_{z_1 z_2}(1, t_0 - n/f) + \sum_{n_1 \neq n_2} \left( m_1^2 + \Gamma^2 e^{-\varsigma|n_1 - n_2|/f} \right) G_{z_1}(1, t_0 - n_1/f) G_{z_2}(1, t_0 - n_2/f) \right] dt_0 \quad (4.42)$$

where  $\Gamma^2$  is the variance of the number of neutrons produced in a pulse and  $\varsigma$  is the decay constant of the source correlations.

The  $n_1 \neq n_2$  term can be written as

$$\sum_{n_1=0}^{\infty} \sum_{n_2=0}^{\infty} \left( m_1^2 + \Gamma^2 e^{-\varsigma|n_1 - n_2|/f} \right) G_{z_1}(1, t_0 - n_1/f) G_{z_2}(1, t_0 - n_2/f) - \sum_{n=0}^{\infty} \left( m_1^2 + \Gamma^2 \right) G_{z_1}(1, t_0 - n/f) G_{z_2}(1, t_0 - n/f) \quad (4.43)$$

First summation in the above equation, can be written as

$$I = \sum_{n_1=0}^{\infty} \sum_{n_2=0}^{n_1} \left( m_1^2 + \Gamma^2 e^{-\varsigma(n_1 - n_2)/f} \right) G_{z_1}(1, t_0 - n_1/f) G_{z_2}(1, t_0 - n_2/f) + \sum_{n_1=0}^{\infty} \sum_{n_2=n_1+1}^{\infty} \left( m_1^2 + \Gamma^2 e^{-\varsigma(n_2 - n_1)/f} \right) G_{z_1}(1, t_0 - n_1/f) G_{z_2}(1, t_0 - n_2/f)$$

Changing order of summation in the first summation, we can write

$$I = \sum_{n_2=0}^{\infty} \sum_{n_1=n_2}^{\infty} \left( m_1^2 + \Gamma^2 e^{-\varsigma(n_1 - n_2)/f} \right) G_{z_1}(1, t_0 - n_1/f) G_{z_2}(1, t_0 - n_2/f) + \sum_{n_1=0}^{\infty} \sum_{n_2=n_1+1}^{\infty} \left( m_1^2 + \Gamma^2 e^{-\varsigma(n_2 - n_1)/f} \right) G_{z_1}(1, t_0 - n_1/f) G_{z_2}(1, t_0 - n_2/f)$$

In first of the above summations, substituting  $n_1 = n_2 + m$  and in the second one  $n_2 = n_1 + m$ , we get

$$\begin{aligned}
I = & \sum_{n_2=0}^{\infty} \sum_{m=0}^{\infty} \left( m_1^2 + \Gamma^2 e^{-\zeta m/f} \right) G_{z_1}(1, t_0 - (n_2 + m)/f) G_{z_2}(1, t_0 - n_2/f) \\
& + \sum_{n_1=0}^{\infty} \sum_{m=0}^{\infty} \left( m_1^2 + \Gamma^2 e^{-\zeta m/f} \right) G_{z_1}(1, t_0 - n_1/f) G_{z_2}(1, t_0 - (n_1 + m)/f) \\
& - \sum_{n=0}^{\infty} \left( m_1^2 + \Gamma^2 \right) G_{z_1}(1, t_0 - n/f) G_{z_2}(1, t_0 - n/f)
\end{aligned}$$

Thus from Eq. (4.43), the  $n_1 \neq n_2$  term becomes

$$\begin{aligned}
& \sum_{n_2=0}^{\infty} \sum_{m=0}^{\infty} \left( m_1^2 + \Gamma^2 e^{-\zeta m/f} \right) G_{z_1}(1, t_0 - (n_2 + m)/f) G_{z_2}(1, t_0 - n_2/f) \\
& + \sum_{n_1=0}^{\infty} \sum_{m=0}^{\infty} \left( m_1^2 + \Gamma^2 e^{-\zeta m/f} \right) G_{z_1}(1, t_0 - n_1/f) G_{z_2}(1, t_0 - (n_1 + m)/f) \\
& - 2 \sum_{n=0}^{\infty} \left( m_1^2 + \Gamma^2 \right) G_{z_1}(1, t_0 - n/f) G_{z_2}(1, t_0 - n/f)
\end{aligned}$$

Substituting this in Eq. (4.42), the expression for Rossi alpha becomes

$$\begin{aligned}
f_2(0, \tau) = & f m_1 \int_{-\infty}^{\tau} G_{z_1 z_2}(1, t) dt + f m_2 \int_{-\infty}^{\tau} G_{z_1} G_{z_2} dt + f \int_{-\infty}^{\tau} \sum_{m=0}^{\infty} \left( m_1^2 + \Gamma^2 e^{-\zeta m/f} \right) G_{z_1}(1, t_0 - m/f) G_{z_2}(1, t_0) dt_0 \\
& + f \int_{-\infty}^{\tau} \sum_{m=0}^{\infty} \left( m_1^2 + \Gamma^2 e^{-\zeta m/f} \right) G_{z_1}(1, t_0) G_{z_2}(1, t_0 - m/f) dt_0 - 2f \left( m_1^2 + \Gamma^2 \right) \int_{-\infty}^{\tau} G_{z_1} G_{z_2} dt
\end{aligned} \tag{4.44}$$

The first, second and fifth terms have been solved in section 4.1.2 and are as follows

$$f m_1 \int_{-\infty}^{\tau} G_{z_1 z_2}(1, t) dt = f m_1 \left( \sum_j \frac{A_j}{\alpha_j} \right) \frac{\lambda_f \lambda_d^2 \bar{v}^{-2}}{2} \sum_i \alpha_i Y_i e^{-\alpha_i \tau} \tag{4.45}$$

$$f m_2 \int_{-\infty}^{\tau} G_{z_1} G_{z_2} dt = \frac{\bar{v}^{-2} f m_2 \lambda_d^2}{2\nu(\nu-1)} \sum_i \alpha_i Y_i e^{-\alpha_i \tau} \tag{4.46}$$

$$2f \left( m_1^2 + \Gamma^2 \right) \int_{-\infty}^{\tau} G_{z_1} G_{z_2} dt = \frac{\bar{v}^{-2} f \left( m_1^2 + \Gamma^2 \right) \lambda_d^2}{\nu(\nu-1)} \sum_i \alpha_i Y_i e^{-\alpha_i \tau} \tag{4.47}$$

where we have used  $Y_i = 2 \frac{\overline{\nu(\nu-1)}}{(\bar{\nu})^2} \frac{A_i G(\alpha_i)}{\alpha_i}$

$G(s)$  is zero power transfer function and  $A_i$  are the residues of the transfer function i.e.

$$G(s) = \sum_i \frac{A_i}{s + \alpha_i}$$

The third term in Eq. (4.44) can be written as

$$f \sum_{m=0}^{\infty} \left[ \int_{-\infty}^0 \left( m_1^2 + \Gamma^2 e^{-\zeta m/f} \right) G_{z_1}(1, t_0 - m/f) G_{z_2}(1, t_0) dt_0 \right. \\ \left. + \int_0^{\tau} \left( m_1^2 + \Gamma^2 e^{-\zeta m/f} \right) G_{z_1}(1, t_0 - m/f) G_{z_2}(1, t_0) dt_0 \right]$$

Since  $\frac{[f\tau]+1}{f} > \tau$  and keeping in mind the fact that  $G_{z_1}(1, t)$  is non zero only for  $t < 0$ , the

second term in the above expression is split in two parts and the final form of the third term in Eq. (4.44) becomes

$$\begin{aligned} & f \int_{-\infty}^0 \sum_{m=0}^{\infty} \left( m_1^2 + \Gamma^2 e^{-\zeta m/f} \right) G_{z_1}(1, t_0 - m/f) G_{z_2}(1, t_0) dt_0 \\ & + \sum_{m=[f\tau]+1}^{\infty} \int_0^{\tau} \left( m_1^2 + \Gamma^2 e^{-\zeta m/f} \right) G_{z_1}(1, t_0 - m/f) G_{z_2}(1, t_0) dt_0 \\ & + \sum_{m=0}^{[f\tau]} \int_0^{m/f} \left( m_1^2 + \Gamma^2 e^{-\zeta m/f} \right) G_{z_1}(1, t_0 - m/f) G_{z_2}(1, t_0) dt_0 \\ & = f \lambda_d^2 \sum_{j,k} \frac{A_j A_k}{\alpha_j + \alpha_k} e^{-\alpha_k \tau} \left[ \frac{m_1^2}{1 - e^{-\alpha_j/f}} + \frac{\Gamma^2}{1 - e^{-(\alpha_j + \zeta)/f}} \right] \\ & + f \lambda_d^2 \sum_{j,k} \frac{A_j A_k}{\alpha_j + \alpha_k} \left( e^{\alpha_j \tau} - e^{-\alpha_k \tau} \right) \left[ m_1^2 \frac{e^{-\alpha_j([f\tau]+1)/f}}{1 - e^{-\alpha_j/f}} + \Gamma^2 \frac{e^{-(\alpha_j + \zeta)([f\tau]+1)/f}}{1 - e^{-(\alpha_j + \zeta)/f}} \right] \\ & + f \lambda_d^2 \sum_{j,k} \frac{A_j A_k}{\alpha_j + \alpha_k} e^{-\alpha_k \tau} \left[ m_1^2 \left\{ \frac{1 - e^{\alpha_k([f\tau]+1)/f}}{1 - e^{\alpha_k/f}} - \frac{1 - e^{-\alpha_j([f\tau]+1)/f}}{1 - e^{-\alpha_j/f}} \right\} \right. \\ & \left. + \Gamma^2 \left\{ \frac{1 - e^{(\alpha_k - \zeta)([f\tau]+1)/f}}{1 - e^{(\alpha_k - \zeta)/f}} - \frac{1 - e^{-(\alpha_j + \zeta)([f\tau]+1)/f}}{1 - e^{-(\alpha_j + \zeta)/f}} \right\} \right] \end{aligned} \quad (4.48)$$

Similarly, the fourth term in Eq. (4.44) can be written as

$$f \int_{-\infty}^0 \sum_{m=0}^{\infty} \left( m_1^2 + \Gamma^2 e^{-\zeta m/f} \right) G_{z_1}(1, t_0) G_{z_2}(1, t_0 - m/f) dt_0$$

$$= f \lambda_d^2 \sum_{j,k} \frac{A_j A_k}{\alpha_j + \alpha_k} e^{-\alpha_k \tau} \left[ \frac{m_1^2}{1 - e^{-\alpha_k / f}} + \frac{\Gamma^2}{1 - e^{-(\alpha_k + \varsigma) / f}} \right] \quad (4.49)$$

Substituting Eq. (4.45)-(4.49) in Eq. (4.44) and simplifying, we get the following expression for Rossi-alpha

$$\begin{aligned} f_2(0, \tau) = & \frac{f \lambda_d^2 \bar{\nu}^2}{2} \sum_i \alpha_i Y_i e^{-\alpha_i \tau} \left[ m_1 \lambda_f \left( \sum_j \frac{A_j}{\alpha_j} \right) + \frac{(m_2 - m_1^2)}{\nu(\nu - 1)} \right] \\ & + \frac{\bar{\nu}^2}{2\nu(\nu - 1)} f m_1^2 \lambda_d^2 \sum_i \frac{\alpha_i Y_i}{(1 - e^{-\alpha_i / f})} \left( e^{-\alpha_i(\tau - [f\tau]/f)} + e^{\alpha_i(\tau - ([f\tau] + 1)/f)} \right) \\ & + \Gamma^2 \frac{f \lambda_d^2 \bar{\nu}^2}{2\nu(\nu - 1)} \sum_i \alpha_i Y_i \left[ e^{-\alpha_i \tau} \left( \frac{e^{-(\alpha_i + \varsigma)/f}}{1 - e^{-(\alpha_i + \varsigma)/f}} - \frac{1}{1 - e^{-(\alpha_i - \varsigma)/f}} \right) \right. \\ & \left. + \left( \frac{e^{-(\alpha_i + \varsigma)/f} e^{\alpha_i(\tau - [f\tau]/f)}}{1 - e^{-(\alpha_i + \varsigma)/f}} + \frac{e^{-\alpha_i(\tau - [f\tau]/f)}}{1 - e^{-(\alpha_i - \varsigma)/f}} \right) e^{-\varsigma[f\tau]/f} \right] \end{aligned} \quad (4.50)$$

The first term has two parts one coming from the source multiplicity and the second due to the chain multiplication. The second term is the uncorrelated term i.e. coming from two neutrons unrelated to one another. It however has a periodic character rather than the usual constant form due to the periodicity of the source. The presence of the last term is due to correlations in the source fluctuations. For  $\varsigma \gg f$ , i.e., for correlation times which are short compared to the time between successive neutron pulses, this term vanishes and the formula reduces to that derived in section 4.1.2.

If there are no delayed neutrons, summations are removed,  $A_i = 1 = A_k$ ,  $\alpha_i = \alpha = \alpha_k$  and  $Y_i$  are

replaced by  $\frac{\nu(\nu - 1)}{\bar{\nu}^2 \alpha^2}$

Thus the expression for Rossi-alpha without delayed neutrons becomes

$$f_2(0, \tau) = \frac{f\lambda_d^2}{2\alpha} \left[ \frac{m_1^2}{1 - e^{-\alpha/f}} \left\{ e^{-\alpha/f} e^{\alpha\left(\tau - \frac{\lfloor f\tau \rfloor}{f}\right)} + e^{-\alpha\left(\tau - \frac{\lfloor f\tau \rfloor}{f}\right)} \right\} + (m_2 - m_1^2 + 2m_1 Y_1) e^{-\alpha\tau} \right. \\ \left. + \Gamma^2 \left\{ \left( \frac{e^{-(\alpha+\zeta)/f} e^{\alpha(\tau - \lfloor f\tau \rfloor / f)}}{1 - e^{-(\alpha+\zeta)/f}} + \frac{e^{-\alpha(\tau - \lfloor f\tau \rfloor / f)}}{1 - e^{-(\alpha-\zeta)/f}} \right) e^{-\zeta \lfloor f\tau \rfloor / f} + \left( \frac{e^{-(\alpha+\zeta)/f}}{1 - e^{-(\alpha+\zeta)/f}} - \frac{1}{1 - e^{-(\alpha-\zeta)/f}} \right) e^{-\alpha\tau} \right\} \right] \quad (4.51)$$

where  $Y_1 = \lambda_f \overline{\nu(\nu-1)}/2\alpha$ .

Thus, in absence of delayed neutrons, the expression for the Rossi-alpha reduces to the form [Eq. (3.8)] derived in chapter 3, as it should.

#### 4.2.2 The variance to mean ratio (Feynman alpha) formula

The expression for the variance to mean ratio (the counting gate system is shown in Figure 4.10) is derived as usual by integration of the expression for Rossi alpha [Eq. (4.50)], as follows:

$$\frac{v}{m} = 1 - m + \frac{2}{m} \int_0^T (T - \tau) f_2(0, \tau) d\tau \quad (4.52)$$

where  $m$  is average number of counts in the interval  $[0, T]$ , or the (source-induced) first moment and, as described in section 4.1.1, is given as

$$m = f m_1 \lambda_d T \sum_j \frac{A_j}{\alpha_j} \quad (4.53)$$

The integration is somewhat tricky since  $f_2$  is a piecewise continuous function and has to be handled by breaking the range into periods of size  $1/f$ . All the terms of the Feynman formula will be same as in our previous paper but for the term arising due to source correlations i.e. the  $\Gamma^2$  term of  $f_2$ .

As discussed in section 4.1.1 earlier, the contribution of first two terms of  $f_2$  to the Feynman formula is as follows:

$$\begin{aligned}
& \frac{\bar{\nu}^{-2} \lambda_d}{m_1} \sum_i Y_i \left( 1 - \frac{1 - e^{-\alpha_i T}}{\alpha_i T} \right) \left[ m_1 \lambda_f + \frac{(m_2 - m_1^2)}{\nu(\nu-1) \sum_j (A_j / \alpha_j)} \right] + \lambda_d m_1 \left( \sum_j \frac{A_j}{\alpha_j} \right) \left[ \frac{1 + 2[fT] - \frac{[fT]([fT]+1)}{fT}}{-fT} \right] \\
& + \frac{\bar{\nu}^{-2} m_1 \lambda_d}{\nu(\nu-1) \sum_j (A_j / \alpha_j)} \sum_i \frac{Y_i}{\alpha_i} \left[ \frac{e^{-\alpha_i(T-[fT]/f)} + e^{\alpha_i(T-([fT]+1)/f)} - 1 - e^{-\alpha_i/f}}{T(1 - e^{-\alpha_i/f})} \right]
\end{aligned} \tag{4.54}$$

Let us consider the  $\Gamma^2$  term of  $f_2$  i.e.

$$\frac{f \lambda_d^2 \bar{\nu}^{-2}}{2\nu(\nu-1)} \sum_i \alpha_i Y \left[ e^{-\alpha_i \tau} \left( \frac{e^{-(\alpha_i + \varsigma)/f}}{1 - e^{-(\alpha_i + \varsigma)/f}} - \frac{1}{1 - e^{-(\alpha_i - \varsigma)/f}} \right) + \left( \frac{e^{-(\alpha_i + \varsigma)/f}}{1 - e^{-(\alpha_i + \varsigma)/f}} + \frac{e^{-\alpha_i(\tau - [f\tau]/f)}}{1 - e^{-(\alpha_i - \varsigma)/f}} \right) e^{-\varsigma[f\tau]/f} \right] \tag{4.55}$$

The integration of the first term is straightforward and gives the following contribution to v/m :

$$\frac{\lambda_d \bar{\nu}^{-2}}{\nu(\nu-1) m_1 \left( \sum_j A_j / \alpha_j \right)} \sum_i Y_i \left( 1 - \frac{1 - \exp(-\alpha_i T)}{\alpha_i T} \right) \left( \frac{e^{-(\alpha_i + \varsigma)/f}}{1 - e^{-(\alpha_i + \varsigma)/f}} - \frac{1}{1 - e^{-(\alpha_i - \varsigma)/f}} \right) \tag{4.56}$$

For integrating the second term in Eq. (4.55), we break the integration range as follows

$$\sum_{m=1}^{[fT]} \int_{(m-1)/f}^{m/f} (T - \tau) f_2(0, \tau) d\tau + \int_{[fT]/f}^T (T - \tau) f_2(0, \tau) d\tau$$

Integration leads to the following contribution to the Feynman formula

$$\begin{aligned}
& \frac{\lambda_d \bar{\nu}^{-2}}{\nu(\nu-1)m_1 T \left( \sum_j A_j / \alpha_j \right)} \sum_i Y_i \frac{e^{-(\alpha_i + \varsigma)/f}}{(1 - e^{-(\alpha_i + \varsigma)/f})} \left[ \left\{ \left( \frac{(\alpha_i T + 1)(e^{\alpha_i/f} - 1)}{\alpha_i} - \frac{e^{\alpha_i/f}}{f} \right) \left( \frac{1 - e^{-\varsigma[fT]/f}}{1 - e^{-\varsigma/f}} \right) \right. \right. \\
& \left. \left. - \left( \frac{e^{\alpha_i/f} - 1}{f} \right) \left( \frac{e^{-\varsigma/f} (1 - e^{-\varsigma[fT]/f})}{(1 - e^{-\varsigma/f})^2} - \frac{[fT] e^{-\varsigma[fT]/f}}{1 - e^{-\varsigma/f}} \right) \right\} \right. \\
& \left. + \frac{e^{-\varsigma[fT]/f}}{\alpha_i} \left\{ e^{\alpha_i(T - [fT]/f)} - 1 - \alpha_i (T - [fT]/f) \right\} \right] \\
& + \frac{\lambda_d \bar{\nu}^{-2}}{\nu(\nu-1)m_1 T \left( \sum_j A_j / \alpha_j \right)} \sum_i Y_i \frac{1}{(1 - e^{-(\alpha_i - \varsigma)/f})} \left[ \left\{ \left( \frac{(\alpha_i T - 1)(1 - e^{-\alpha_i/f})}{\alpha_i} + \frac{e^{-\alpha_i/f}}{f} \right) \left( \frac{1 - e^{-\varsigma[fT]/f}}{1 - e^{-\varsigma/f}} \right) \right. \right. \\
& \left. \left. - \left( \frac{1 - e^{-\alpha_i/f}}{f} \right) \left( \frac{e^{-\varsigma/f} (1 - e^{-\varsigma[fT]/f})}{(1 - e^{-\varsigma/f})^2} - \frac{[fT] e^{-\varsigma[fT]/f}}{1 - e^{-\varsigma/f}} \right) \right\} \right. \\
& \left. + \frac{e^{-\varsigma[fT]/f}}{\alpha_i} \left\{ \alpha_i (T - [fT]/f) - (1 - e^{-\alpha_i(T - [fT]/f)}) \right\} \right]
\end{aligned} \tag{4.57}$$

From Eq. (4.54), (4.56) and (4.57), the final expression for the Feynman formula becomes

$$\begin{aligned}
\frac{\nu}{m} = 1 + \frac{\bar{\nu}^2 \lambda_d}{m_1} \sum_i Y_i \left( 1 - \frac{1 - e^{-\alpha_i T}}{\alpha_i T} \right) & \left[ m_1 \lambda_f + \frac{(m_2 - m_1^2)}{\nu(\nu-1) \sum_j (A_j / \alpha_j)} \right. \\
& \left. + \frac{\Gamma^2}{\nu(\nu-1) \left( \sum_j A_j / \alpha_j \right)} \left( \frac{e^{-(\alpha_i + \zeta)/f}}{1 - e^{-(\alpha_i + \zeta)/f}} - \frac{1}{1 - e^{-(\alpha_i - \zeta)/f}} \right) \right] \\
& + \lambda_d m_1 \left( \sum_j \frac{A_j}{\alpha_j} \right) \left[ \frac{1 + 2[fT] - \frac{[fT]}{fT} ([fT] + 1)}{-fT} \right] \\
& + \frac{\bar{\nu}^2 m_1 \lambda_d}{\nu(\nu-1) \sum_j (A_j / \alpha_j)} \sum_i \frac{Y_i}{\alpha_i} \left[ \frac{e^{-\alpha_i(T-[fT])/f} + e^{\alpha_i(T-[fT]+1)/f} - 1 - e^{-\alpha_i/f}}{T(1 - e^{-\alpha_i/f})} \right] \\
& + \frac{\lambda_d \bar{\nu}^2 \Gamma^2}{\nu(\nu-1) m_1 T \left( \sum_j A_j / \alpha_j \right)} \sum_i Y_i \left[ \frac{e^{-(\alpha_i + \zeta)/f}}{(1 - e^{-(\alpha_i + \zeta)/f})} \left\{ \left( \frac{(\alpha_i T + 1)(e^{\alpha_i/f} - 1)}{\alpha_i} - \frac{e^{\alpha_i/f}}{f} \right) \left( \frac{1 - e^{-\zeta[fT]/f}}{1 - e^{-\zeta/f}} \right) \right. \right. \\
& \left. \left. - \left( \frac{e^{\alpha_i/f} - 1}{f} \right) \left( \frac{e^{-\zeta/f} (1 - e^{-\zeta[fT]/f})}{(1 - e^{-\zeta/f})^2} - \frac{[fT] e^{-\zeta[fT]/f}}{1 - e^{-\zeta/f}} \right) \right\} \right. \\
& \left. + \frac{e^{-\zeta[fT]/f}}{\alpha_i} \left\{ e^{\alpha_i(T-[fT])/f} - 1 - \alpha_i (T - [fT]/f) \right\} \right] \\
& + \frac{1}{(1 - e^{-(\alpha_i - \zeta)/f})} \left\{ \left( \frac{(\alpha_i T - 1)(1 - e^{-\alpha_i/f})}{\alpha_i} + \frac{e^{-\alpha_i/f}}{f} \right) \left( \frac{1 - e^{-\zeta[fT]/f}}{1 - e^{-\zeta/f}} \right) \right. \\
& \left. - \left( \frac{1 - e^{-\alpha_i/f}}{f} \right) \left( \frac{e^{-\zeta/f} (1 - e^{-\zeta[fT]/f})}{(1 - e^{-\zeta/f})^2} - \frac{[fT] e^{-\zeta[fT]/f}}{1 - e^{-\zeta/f}} \right) \right\} \\
& \left. + \frac{e^{-\zeta[fT]/f}}{\alpha_i} \left\{ \alpha_i (T - [fT]/f) - (1 - e^{-\alpha_i(T-[fT])/f}) \right\} \right] \right]
\end{aligned} \tag{4.58}$$

If there are no delayed neutrons, summations are removed,  $A_i = 1 = A_k$ ,  $\alpha_i = \alpha = \alpha_k$  and  $Y_i$  are

replaced by  $\frac{\nu(\nu-1)}{\bar{\nu}^2 \alpha^2}$

Thus, the expression for Feynman formula without delayed neutrons becomes

$$\begin{aligned}
\frac{v}{m} = & 1 + \frac{\lambda_d m_1}{\alpha^2 T (1 - e^{-\alpha/f})} \left[ \exp\left(\alpha\left(T - \frac{[fT] + 1}{f}\right)\right) + \exp\left(-\alpha\left(T - \frac{[fT]}{f}\right)\right) + \exp\left(-\alpha\left(T + \frac{1}{f}\right)\right) - 2e^{-\alpha/f} - e^{-\alpha T} \right] \\
& - \frac{\lambda_d m_1}{\alpha} \left[ fT - 2[fT] + \frac{[fT]([fT] + 1)}{fT} \right] + \frac{\lambda_d}{m_1 \alpha} \left\{ \frac{(m_2 + 2m_1 Y_1)}{+ \Gamma^2 \left( \frac{e^{-(\alpha+\varsigma)/f}}{1 - e^{-(\alpha+\varsigma)/f}} - \frac{1}{1 - e^{-(\alpha-\varsigma)/f}} \right)} \right\} \left( 1 - \frac{1 - \exp(-\alpha T)}{\alpha T} \right) \\
& + \frac{\lambda_d \Gamma^2}{m_1 T (1 - e^{-(\alpha-\varsigma)/f})} \left[ \left( \frac{(\alpha T - 1)(1 - e^{-\alpha/f})}{\alpha^2} + \frac{e^{-\alpha/f}}{\alpha f} \right) \left( \frac{1 - e^{-\varsigma[fT]/f}}{1 - e^{-\varsigma/f}} \right) - \left( \frac{1 - e^{-\alpha/f}}{\alpha f} \right) \left( \frac{1 - e^{-\varsigma[fT]/f}}{(1 - e^{-\varsigma/f})^2} - \frac{[fT]e^{-\varsigma[fT]/f}}{1 - e^{-\varsigma/f}} \right) \right] \\
& + \frac{\lambda_d \Gamma^2 e^{-(\alpha+\varsigma)/f}}{m_1 T (1 - e^{-(\alpha+\varsigma)/f})} \left[ \left( \frac{(\alpha T + 1)(e^{\alpha/f} - 1)}{\alpha^2} - \frac{e^{\alpha/f}}{\alpha f} \right) \left( \frac{1 - e^{-\varsigma[fT]/f}}{1 - e^{-\varsigma/f}} \right) - \left( \frac{e^{\alpha/f} - 1}{\alpha f} \right) \left( \frac{1 - e^{-\beta[fT]/f}}{(1 - e^{-\beta/f})^2} - \frac{[fT]e^{-\varsigma[fT]/f}}{1 - e^{-\varsigma/f}} \right) \right] \\
& + \frac{\lambda_d \Gamma^2}{\alpha^2 m_1 T} \left( \frac{\left[ \alpha(T - [fT]/f) - (1 - e^{-\alpha(T - [fT]/f)}) \right]}{(1 - e^{-(\alpha-\varsigma)/f})} + \frac{e^{-(\alpha+\varsigma)/f} \left[ e^{\alpha(T - [fT]/f)} - 1 - \alpha(T - [fT]/f) \right]}{(1 - e^{-(\alpha+\varsigma)/f})} \right) e^{-\varsigma[fT]/f}
\end{aligned}$$

Thus, in the absence of delayed neutrons, the expression for the Feynman formula reduces to the form [Eq. (3.11)] derived in chapter 3, as it should.

### 4.2.3 Numerical results

We show in Figs. 4.8 and 4.9 the variation with the delay time  $\tau$  of the Rossi alpha function for light water and heavy water systems respectively. The parameters used to plot Figure 4.8 are taken from Kitamura et al. (2006) and are given in set 1 of table-4.2. The parameters  $m_2 - m_1^2$  and  $\Gamma^2$  (defined as  $\Gamma^2 = m_2 - m_1^2 + m_1$ ) are evaluated by considering fluctuations in ion current. Here in all the cases, current fluctuations are about 1%. It can be seen from the figure that Rossi alpha function oscillates with time and has a decaying part in the beginning which later on becomes non-decaying. Since strength of the external source is very small, source fluctuations are close to Poisson and hence have negligible contribution.

Figs. 4.9(a), 4.9(b) and 4.9(c) correspond to three different cases viz.  $\varsigma \ll \alpha$ ,  $\varsigma \sim \alpha$  and  $\varsigma \gg \alpha$  respectively. The assumed parameters, corresponding to a typical heavy water system, are listed under set 2 in Table 4.2. The source characteristics correspond to a typical D-T

source (Soule et al., 2004). Figs. 4.9(a) and 4.9(b) show that if  $\zeta \sim \alpha$  or  $\zeta \ll \alpha$ , it is likely that noise Experiments might yield  $\zeta$  which may be mistaken for  $\alpha$ ! Only in the case of  $\zeta \gg \alpha$  i.e. where source fluctuations can be treated as white do we get Rossi Alpha which will give correct  $\alpha$ ..

Fig. 4.9(d) shows the contribution to Rossi alpha due to correlations in the source fluctuations and that due to source multiplicity plus fission chain. From the figure it can be seen that if we have heavy water systems, correlations in the source fluctuations will be particularly important if their correlation time is comparable or larger than that of prompt neutrons. For short correlation times this effect is not important.

Figs. 4.11(a) and 4.11(b) show variation of total and different terms of the  $\nu/m$  formula with the length of the counting interval on prompt and delayed neutron lifetime scales respectively. The parameters used to plot the graphs are listed under set 1 of Table 4.2 and correspond to a typical light water system. From Figure 4.11(a), it is seen that the  $\nu/m$  appears to saturate and hence use of formula with only prompt neutrons may be adequate for analyzing the experimental results. In Figure 4.11(b), the contribution of delayed neutrons is however seen.

Figs. 4.12(a) and 4.12(b) show variation of total and different terms of the  $\nu/m$  formula with the length of the counting interval on prompt and delayed neutron lifetime scales respectively. The parameters used to plot the graphs are listed under set 3 of Table 4.2 and correspond to a typical heavy water system. From the Fig. 4.12(b) it can be seen that, unlike Fig. 4.11(b), the prompt and delayed neutron lifetime scales are not distinctly separable. Thus if one tries to extract alpha from a plot of  $\nu/m$  versus counting interval, it is necessary to include corrections due to delayed neutron terms.

### 4.3 Conclusion

The importance of the delayed neutron contributions will be most clearly felt in those situations where the prompt and delayed time scales are not very distinct and the formulae derived by us would serve as corrections even on prompt neutron time scales. While the periodic variation with the period of the driving source is similar to that obtained by other authors, the source correlation term has a different magnitude. This is due to the non-Poisson character of the source.

If correlation (between the number of neutrons emitted in different pulses) times are greater than or of the order of the prompt neutron decay times, it will be difficult to use methods such as Rossi alpha. It is therefore important to study the current fluctuation statistics of ion beams from accelerators, either theoretically or experimentally.

**Table 4.1: Numerical parameters used to plot Figures (4.1) through (4.6)**

Parameters	Values		
	Set 1 Light water system	Set 2 Heavy water system	Set 3 Heavy water system
$\lambda_d$	$3.3485 \times 10^2$	6.1164	6.1788
$\lambda_f$	$2.1686 \times 10^4$	$3.9612 \times 10^2$	$4.0016 \times 10^2$
$\alpha_1$	$1.4438 \times 10^3$	$2.1066 \times 10^1$	$1.1139 \times 10^1$
$\alpha_2$	$6.0676 \times 10^{-2}$	1.2106	1.1445
$A_1$	$5.3650 \times 10^4$	$9.7682 \times 10^2$	$9.7707 \times 10^2$
$A_2$	0.7181	3.17852	$1.2928 \times 10^1$
$\langle \nu \rangle$	2.4740	2.4740	2.4740
$\langle \nu(\nu - 1) \rangle$	4.8965	4.8965	4.8965
$m_1$	$5.0000 \times 10^1$	$5.0000 \times 10^1$	$5.0000 \times 10^1$
$m_2$	$3.0040 \times 10^1$	$3.0040 \times 10^1$	$3.0040 \times 10^1$
$f$	$5.0000 \times 10^2$	7.0000	7.0000
$\Lambda$	$1.8639 \times 10^{-5}$	$1.0204 \times 10^{-3}$	$1.0101 \times 10^{-3}$
$\beta$	$6.5000 \times 10^{-3}$	$1.0200 \times 10^{-3}$	$1.0200 \times 10^{-3}$
$\lambda$	0.0800	1.2750	1.2750
$\rho$	-0.0204	-0.0204	-0.0101

**Table 4.2: Numerical parameters used to plot Figures (4.8), (4.9), (4.11) and 4.12)**

Parameters	Values		
	Set 1 Light water system	Set 2 Heavy water system	Set 3 Heavy water system
$\lambda_d$	334.85	6.24	6.24
$\lambda_f$	21686	404.2	404.2
$\alpha_1$	1566.3	29.149	29.149
$\alpha_2$	0.0608	0.061	0.061
$A_1$	53762.8	999.338	999.338
$A_2$	0.66	0.662	0.662
$\bar{\nu}$	2.4740	2.4740	2.4740
$\overline{\nu(\nu-1)}$	4.8965	4.8965	4.8965
$m_1$	50.0	$3.0 \times 10^6$	$3.0 \times 10^6$
$m_2 - m_1^2$	0.25	$9.0 \times 10^8$	$9.0 \times 10^8$
$\Gamma^2$	50.25	$9.03 \times 10^8$	$9.03 \times 10^8$
$f$	500.0	10.0	500.0
$\Lambda$	$1.86 \times 10^{-5}$	$1.0 \times 10^{-3}$	$1.0 \times 10^{-3}$
$\beta$	$7.0 \times 10^{-3}$	$7.0 \times 10^{-3}$	$7.0 \times 10^{-3}$
$\lambda$	0.08	0.08	0.08
$\rho$	-0.02213	-0.02213	-0.02213

## Appendix I

### Additional terms in the Feynman alpha formula due to prompt-delayed and delayed-delayed correlations

In the main text we had evaluated only the first term in the integral for obtaining the source induced second moment

$$[I] = fm_1 \left( \sum_j \frac{A_j}{\alpha_j} \right) \int_{-\infty}^T S_2(t) dt$$

where

$$\begin{aligned} S_2(t) = & \overline{\nu(\nu-1)} \lambda_f G'^2 + 2 \sum_i \overline{\nu_p \nu_{d_i}} \lambda_f G' \left( \int_t^T G'(1, t') \mu_i e^{-\mu_i(t'-t)} dt' - G' \right) \\ & + \sum_i \overline{\nu(\nu-1)}_{d_i} \lambda_f \left( \left( \int_t^T G'(1, t') \mu_i e^{-\mu_i(t'-t)} dt' \right)^2 - G'^2 \right) \\ & + \sum_i \sum_{j \neq i} \overline{\nu_{d_i} \nu_{d_j}} \lambda_f \left( \left( \int_t^T G'(1, t') \mu_i e^{-\mu_i(t'-t)} dt' \right) \left( \int_t^T G'(1, t') \mu_j e^{-\mu_j(t'-t)} dt' \right) - G'^2 \right) \end{aligned} \quad (A.1)$$

For evaluating the integral over the source for the other three terms we must first obtain

$$I = \int_t^T G'(1, t') \mu_i e^{-\mu_i(t'-t)} dt' \quad (A.2)$$

Instead of using explicitly the form (4.14) we use the form (4.12) and write the above integral as

$$I = \int_t^T \mu_i e^{-\mu_i(t'-t)} dt' \sum_j A_j \int_t^T e^{\alpha_j(t'-t'')} [\lambda_d \chi(t'')] dt'' \quad (A.3)$$

Interchanging the order of integration makes the evaluation easier and we finally obtain

$$\begin{aligned} I(t) = & \lambda_d \sum_j \frac{A_j}{(\alpha_j - \mu_i)} e^{\mu_i t} (1 - e^{-\mu_i T}) - \lambda_d \sum_j \frac{A_j \mu_i}{\alpha_j (\alpha_j - \mu_i)} e^{\alpha_j t} (1 - e^{-\alpha_j T}) \quad \text{for } t < 0 \\ = & \lambda_d \sum_j \frac{A_j}{(\alpha_j - \mu_i)} (1 - e^{-\mu_i(T-t)}) - \lambda_d \sum_j \frac{A_j \mu_i}{\alpha_j (\alpha_j - \mu_i)} (1 - e^{-\alpha_j(T-t)}) \quad \text{for } 0 < t < T \end{aligned} \quad (A.4)$$

Due to the formal similarity between (4.14) and expression (A.4) for  $I(t)$ , the evaluation of the integral over the source becomes easier. With a little algebraic manipulation it is possible to write the combined contribution of all the above source terms to the variance as follows

$$\lambda_d \lambda_f \bar{v}^2 \sum_i (Y_i^{pp} - Y_i^{pd} - Y_i^{dd}) \left( 1 - \frac{1 - e^{-\alpha_i T}}{\alpha_i T} \right) + \lambda_d \lambda_f \bar{v}^2 \sum_l (Z_l^{pd} + Z_l^{dd}) \left( 1 - \frac{1 - e^{-\mu_l T}}{\mu_l T} \right) \quad (\text{A.5})$$

where

$$Y_i^{pp} = 2 \frac{\overline{\nu(\nu-1)}}{(\bar{\nu})^2} \frac{A_i G(\alpha_i)}{\alpha_i},$$

$$Y_i^{pd} = \frac{4}{\bar{\nu}^2} \sum_l \frac{\overline{\nu_p \nu_{dl} \mu_l^2} A_i G(\alpha_i)}{\alpha_i (\alpha_i^2 - \mu_l^2)},$$

$$Y_i^{dd} = \frac{2}{\bar{\nu}^2} \sum_{j,k,l} \frac{\overline{\nu_{dk} \nu_{dl} \mu_k \mu_l} A_i G(\alpha_i)}{(\alpha_i + \mu_k)(\alpha_i - \mu_l) \alpha_i} + \frac{2}{\bar{\nu}^2} \sum_{j,k} \frac{\overline{\nu_{dk} (\nu_{dk} - 1) \mu_k^2} A_i A_j}{(\alpha_i - \mu_k)(\alpha_i + \alpha_j)(\alpha_i + \mu_k) \alpha_i},$$

$$Z_i^{pd} = \frac{2}{\bar{\nu}^2} \overline{\nu_p \nu_{dl}} G(-\mu_l) G(\mu_l),$$

and

$$Z_i^{dd} = \frac{2}{\bar{\nu}^2} \sum_k \frac{\overline{\nu_{dk} \nu_{dl} \mu_k}}{(\mu_k + \mu_l)} G(-\mu_l) G(\mu_l) + \frac{2}{\bar{\nu}^2} \sum_k \frac{\overline{\nu_{dk} (\nu_{dk} - 1)}}{2} G(-\mu_l) G(\mu_l).$$

The expression (A.5) should replace the term due to induced fission chain correlations (first term) of Eq. (4.29)

## Appendix II

### Additional terms in the Rossi alpha formula due to prompt-delayed and delayed-delayed correlations

In this case since the  $G_{z_1}$  and  $G_{z_2}$  are simpler, the evaluation of various contributions is more straightforward. In addition to the prompt-prompt correlation term given in the main text, we get the following terms which must be added to the RHS of Eq. (4.39)

$$\begin{aligned}
& \frac{f m_1 \lambda_f \lambda_d^2 \Lambda}{-\rho} \sum_i G(\mu_i) G(-\mu_i) \mu_i \left\{ \overline{v_p v_{di}} + \frac{\overline{v_{di} (v_{di} - 1)}}{2} + \sum_l \frac{\overline{v_{di} v_{dl} \mu_l}}{\mu_i + \mu_l} \right\} \exp(-\mu_i \tau) \\
& - \frac{f m_1 \lambda_f \lambda_d^2 \Lambda}{-\rho} \sum_j \left[ \sum_i \frac{2 \overline{v_p v_{di}} A_j \mu_i^2 G(\alpha_j)}{\alpha_j^2 - \mu_i^2} + \sum_{i \neq l} \frac{\overline{v_{dl} v_{di}} A_j \mu_i \mu_l G(\alpha_j)}{(\alpha_j + \mu_l)(\alpha_j - \mu_i)} + \sum_i \frac{\overline{v_{di} (v_{di} - 1)} A_j \mu_i^2 G(\alpha_j)}{(\alpha_j^2 - \mu_i^2)} \right] \exp(-\alpha_j \tau)
\end{aligned}
\tag{A.6}$$

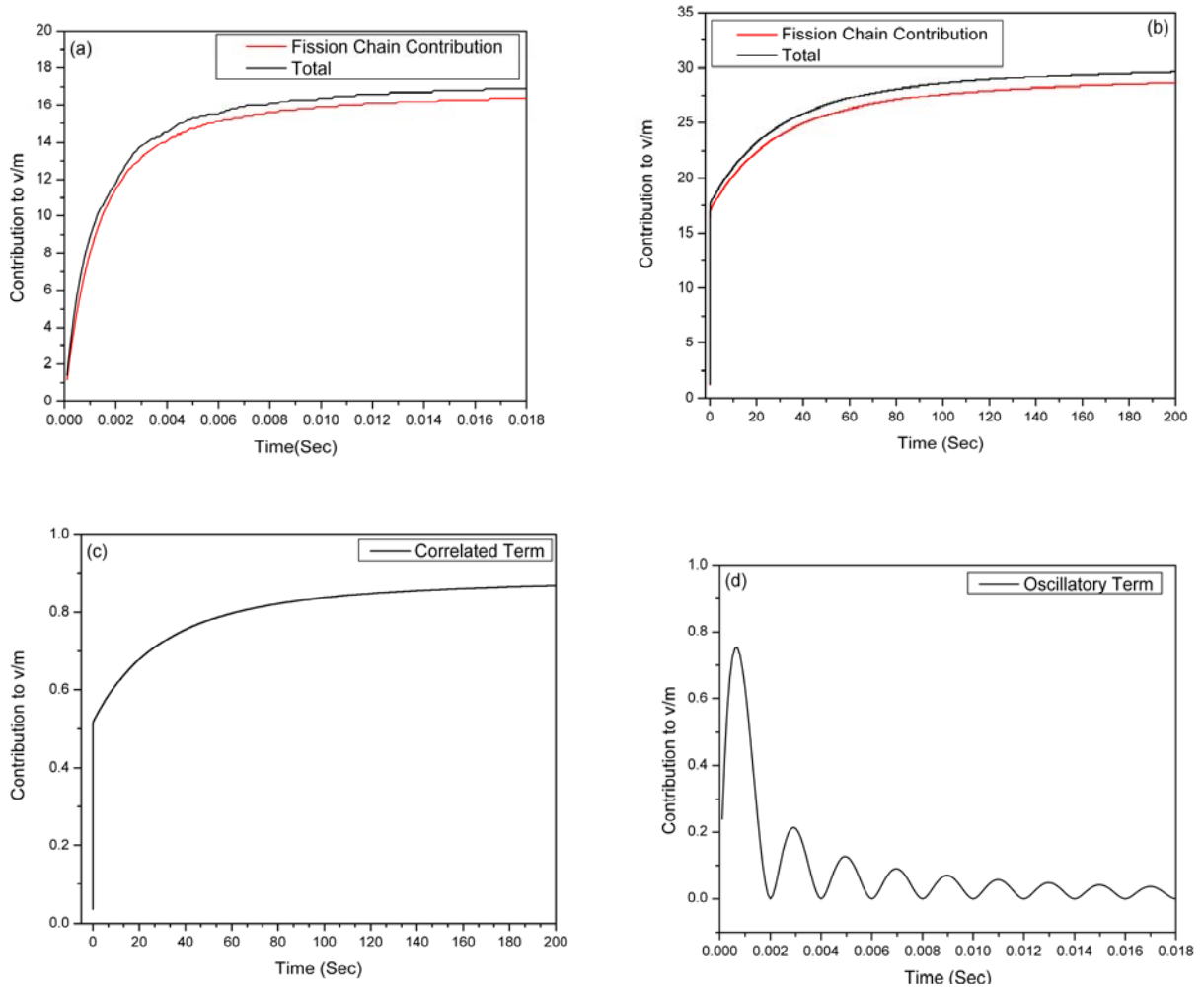


**Fig. 4.1** Variation of different terms of the  $v/m$  formula with the length of the counting interval. The parameters used to plot the graphs are listed under set 1 in table 4.1. (a) Fission chain contribution on prompt neutron lifetime scale; (b) Fission chain contribution on delayed neutron lifetime scale; the contribution of delayed neutrons is to be noticed; (c) Contribution due to source correlations; (d) Oscillatory term due to the periodicity of the source.

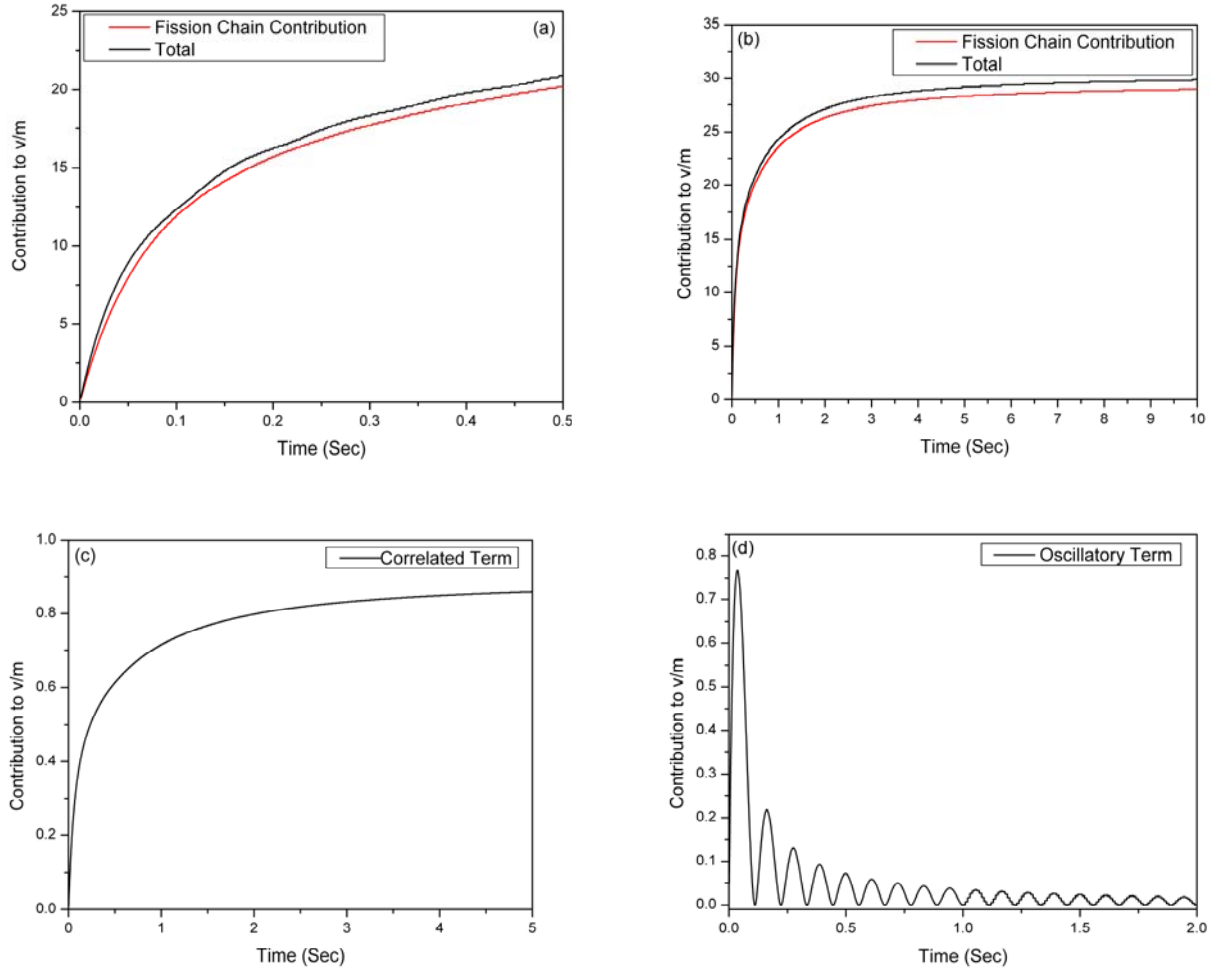


**Fig. 4.2** Variation of different terms of the  $v/m$  formula with the length of the counting interval. The parameters used to plot the graphs are listed under set 2 in table 4.1. (a) Fission chain contribution on prompt neutron lifetime scale; (b) Fission chain contribution on delayed neutron lifetime scale; this being a heavy water reactor case, the two scales can be seen overlapping; (c) Contribution due to source correlations; (d) Oscillatory term due to the periodicity of the source

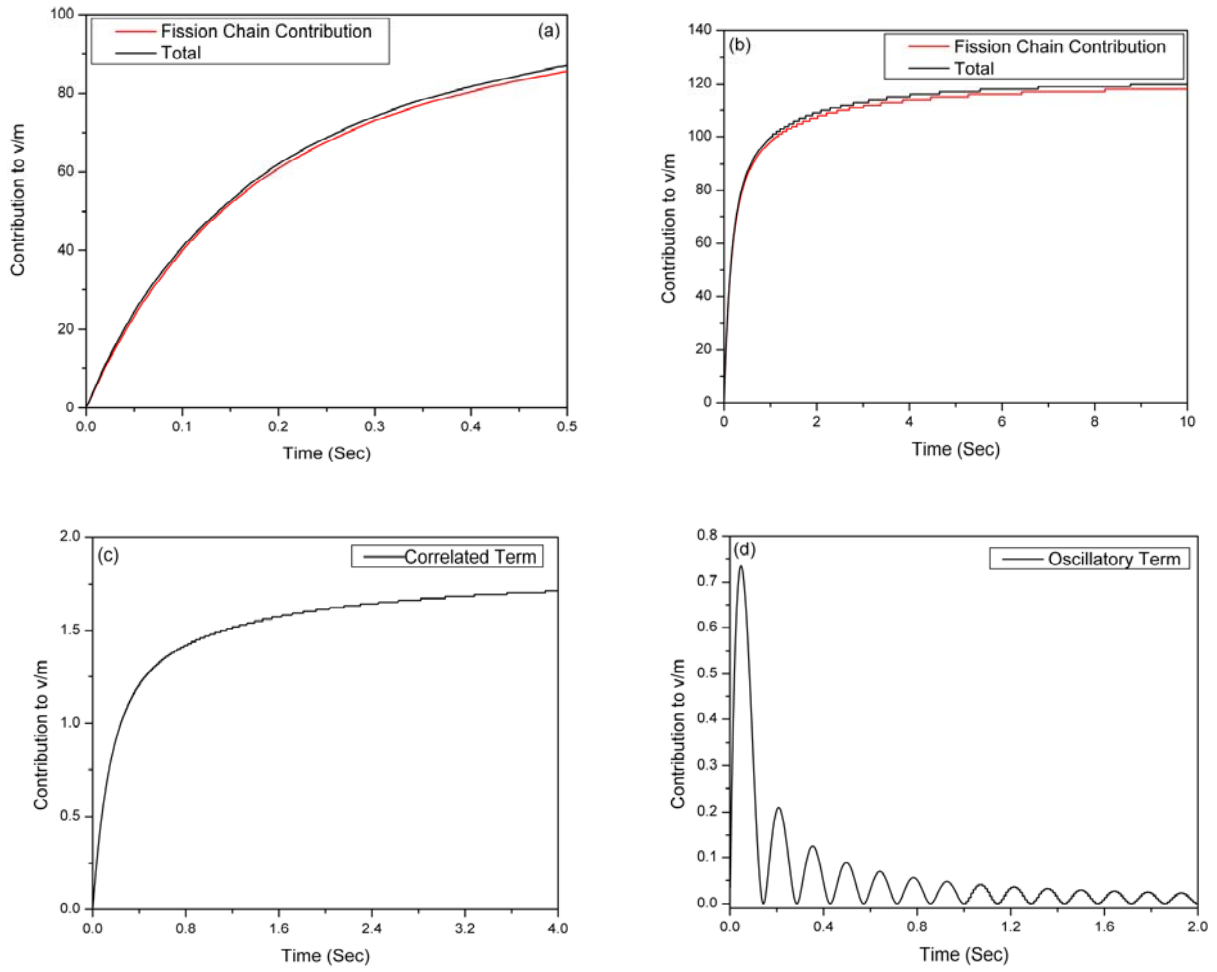


**Fig. 4.3** Variation of different terms of the  $v/m$  formula with the length of the counting interval. The parameters used to plot the graphs are listed under set 3 in table 4.1. (a) Fission chain contribution on prompt neutron lifetime scale; (b) Fission chain contribution on delayed neutron lifetime scale; again this being a heavy water reactor case, the two scales can be seen overlapping, also the magnitude is more than that in Fig. 2 because of lesser sub-criticality level; (c) Contribution due to source correlations; (d) Oscillatory term due to the periodicity of the source

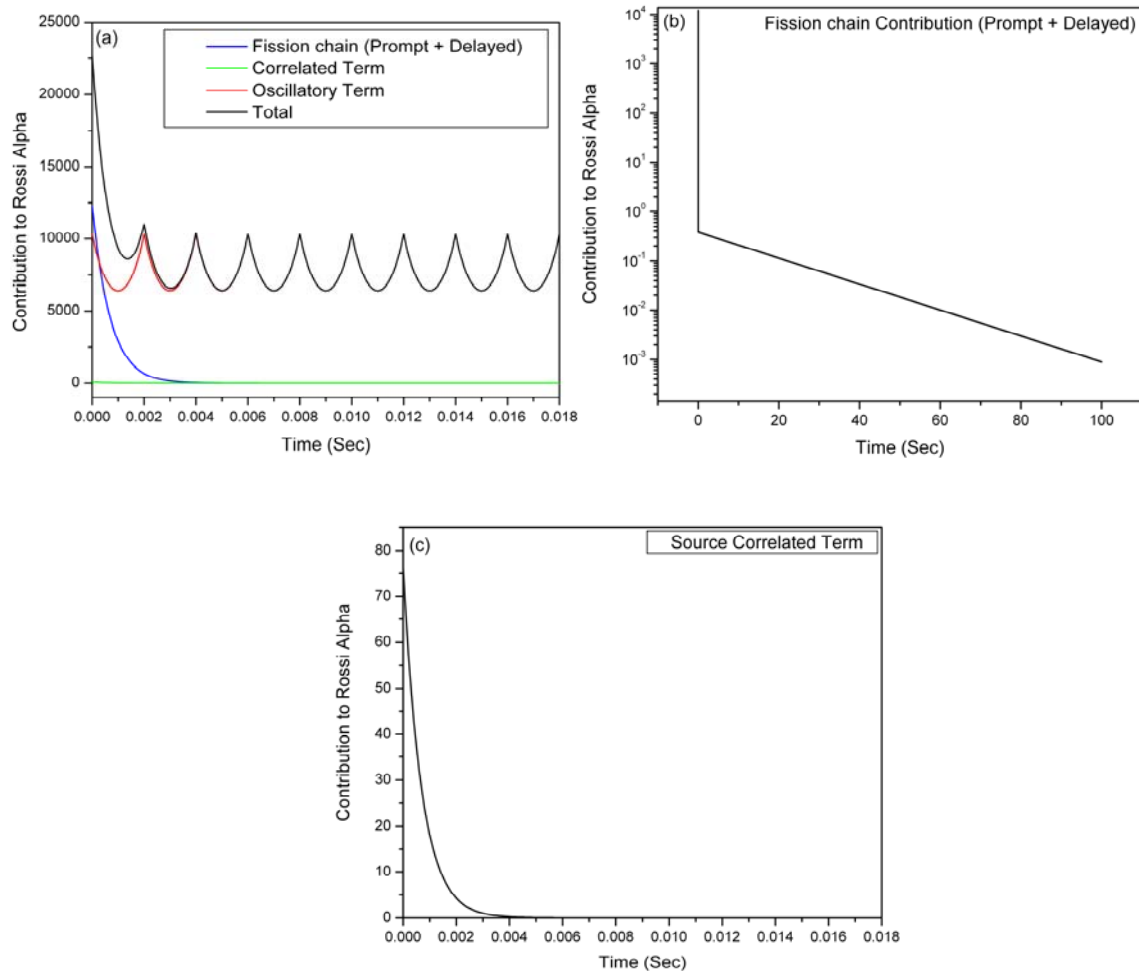


**Fig. 4.4** Variation of different terms of the Rossi Alpha formula with delay time. The parameters used to plot the graphs are listed under set 1 in table 4.1. (a) on prompt neutron lifetime scale; (b) on delayed neutron lifetime scale; (c) term arising due to source correlations.

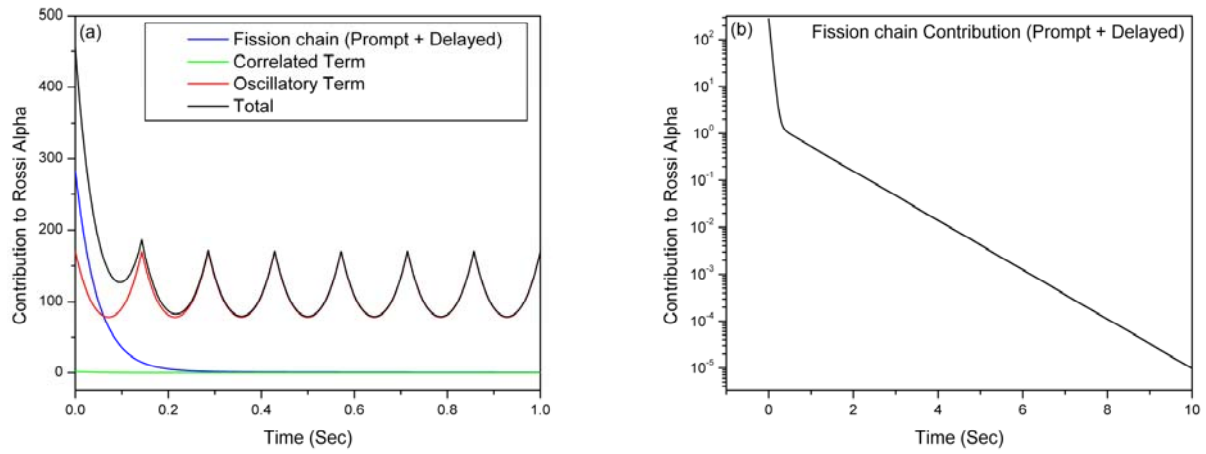


**Fig. 4.5** Variation of different terms of the Rossi Alpha formula with delay time. The parameters used to plot the graphs are listed under set 2 in table 4.1. (a) on prompt neutron lifetime scale; (b) on delayed neutron lifetime scale.

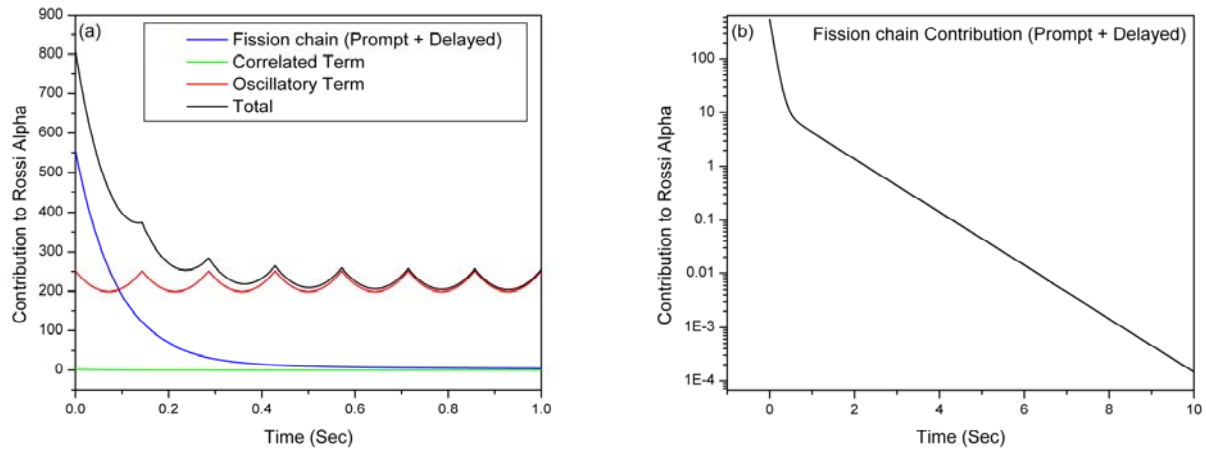


**Fig. 4.6** Variation of different terms of the Rossi Alpha formula with delay time. The parameters used to plot the graphs are listed under set 3 in table 4.1. (a) on prompt neutron lifetime scale; (b) on delayed neutron lifetime scale.

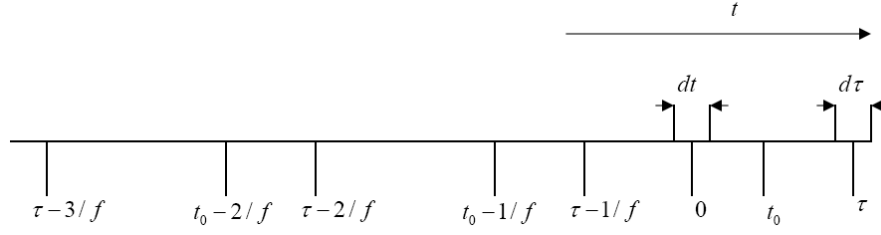


**Fig. 4.7:** Counting gate system for Rossi alpha measurements. The first count occurs in the interval  $dt$  around  $t = 0$  and the second in the interval  $d\tau$  around  $t = \tau$ . The last source pulse that contributes to the counts occurs at  $t_0$  and the ones prior to this will occur at  $t_0 - 1/f$ ,  $t_0 - 2/f$ , ... etc.  $t_0$  is a random variable and has equal probability of occurrence between  $\tau - 1/f$ ,  $\tau$ . Correspondingly, the earlier pulse will lie between  $\tau - 2/f$  and  $\tau - 1/f$  and so on.

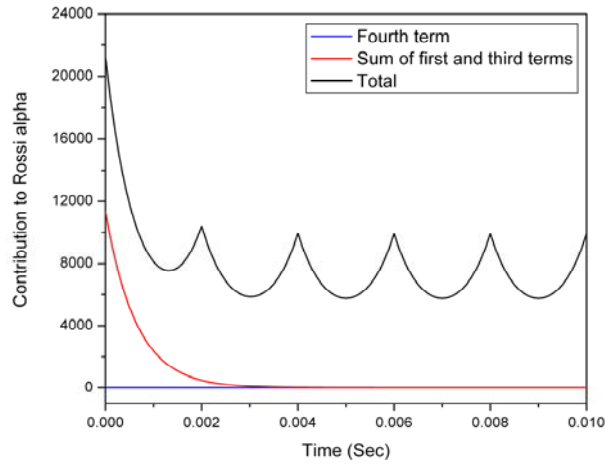


**Fig. 4.8:** Variation of different terms of the Rossi alpha formula (Eq. 4.50) with  $\tau$  on prompt neutron lifetime scale. The parameters used to plot the graphs are listed under set 1 in Table 4.2 corresponding to light water systems. Also shown is the Rossi alpha function oscillates with time and has a decaying part in the beginning which later on becomes non-decaying. The correlated component (due to fission chain, source multiplicity and correlations in the source fluctuations) of Rossi alpha function falls exponentially. The contribution of the fourth term of the Rossi alpha function i.e. oscillating part of the term arising due to correlations in the source fluctuations is rather small to be significant in this case.

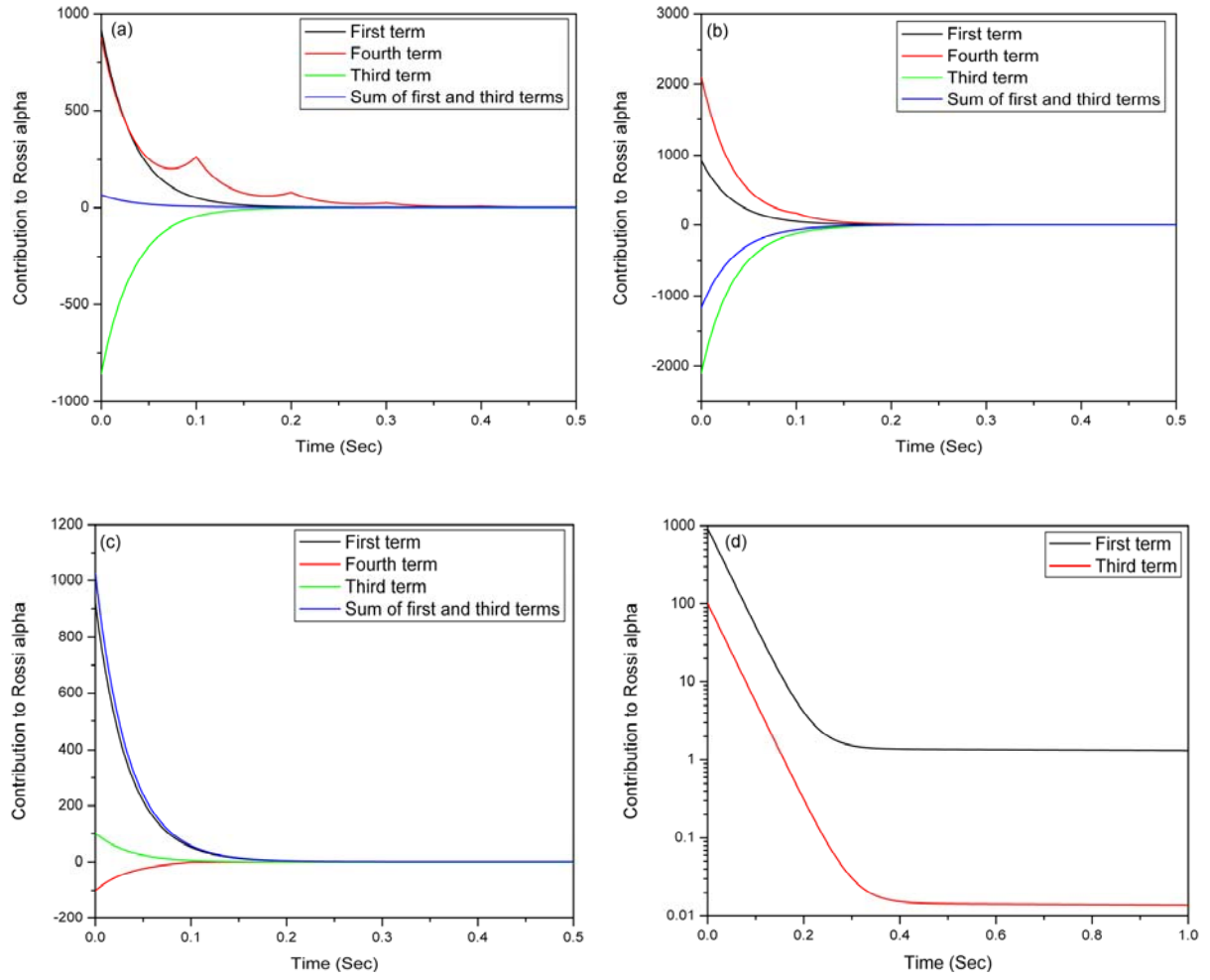


**Fig. 4.9:** Variation of different terms of the Rossi alpha formula with  $\tau$ . The graphs a-c are for  $\zeta \ll \alpha$ ,  $\zeta \sim \alpha$  and  $\zeta \gg \alpha$  respectively. If  $\zeta \sim \alpha$  or  $\zeta \ll \alpha$ , it is likely that noise experiments might yield  $\zeta$  which may be mistaken for  $\alpha$ ! Only in the case of  $\zeta \gg \alpha$  i.e. where source fluctuations can be treated as white do we get Rossi alpha which will give correct  $\alpha$ . Fig. 4.9 (d) shows contribution to Rossi alpha due to correlations in the source fluctuations and that due to source multiplicity plus fission chain. The parameters used to plot the graphs are listed under set 2 in Table 4.2 corresponding to heavy water systems.

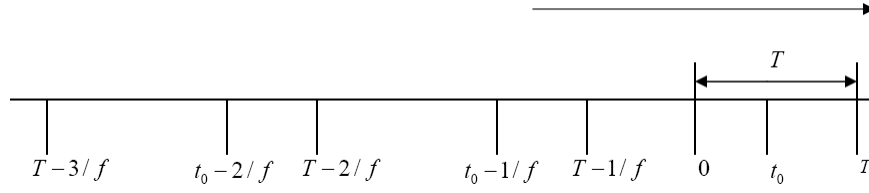


**Fig. 4.10:** Counting gate system for  $\nu/m$  measurements. The counting interval is  $[0, T]$ . The last source pulse that contributes to the counts occurs at  $t_0$  and the ones prior to this will occur at  $t_0 - 1/f$ ,  $t_0 - 2/f$ , ...etc.  $t_0$  is a random variable and has equal probability of occurrence between  $T - 1/f$ ,  $T$ . Correspondingly, the earlier pulse will lie between  $T - 2/f$  and  $T - 1/f$  and so on.

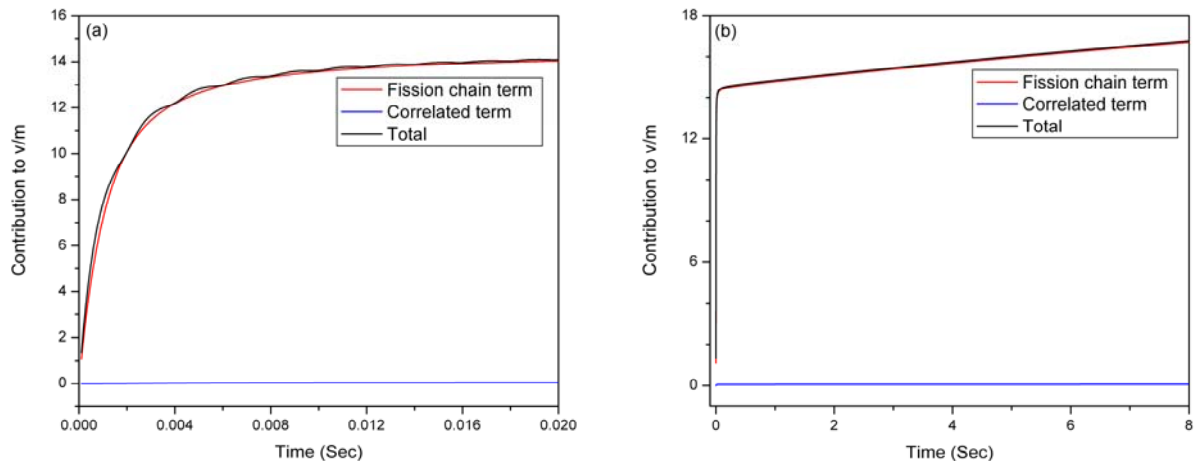


**Fig. 4.11:** Variation of total and different terms of the  $\nu/m$  formula with the length of the counting interval. The parameters used to plot the graphs are listed under set 1 in Table 4.2. (a) On prompt neutron life time scale. It is seen that the  $\nu/m$  appears to saturate and hence use of formula with only prompt neutrons may be adequate for analyzing the experimental results. (b) On delayed neutron life time scale; the contribution of delayed neutrons is however seen.

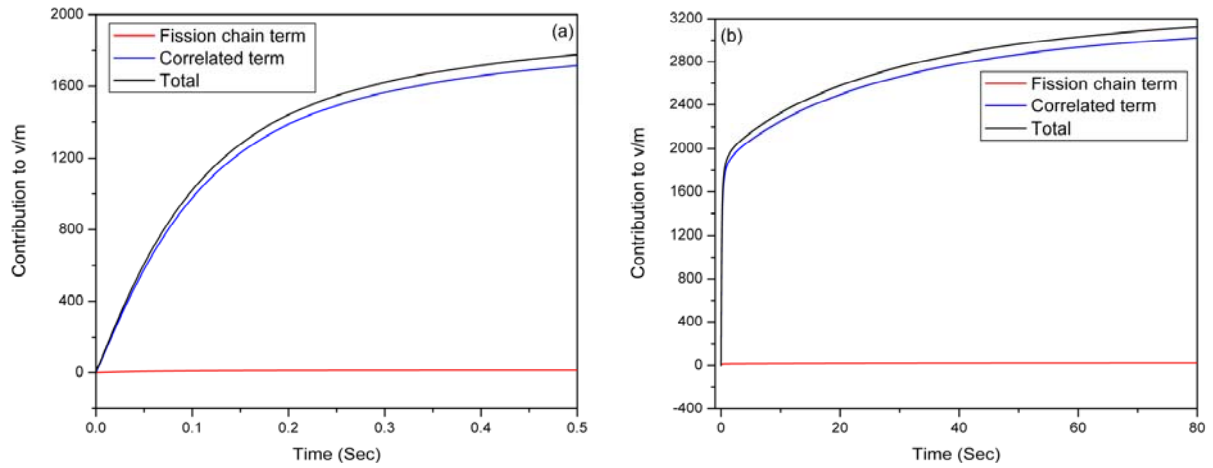


**Fig. 4.12:** Variation of total and different terms of the  $\nu/m$  formula with the length of the counting interval. The parameters used to plot the graphs are listed under set 3 in Table 4.2 corresponding to heavy water systems. Here the prompt and delayed scales are not very distinct and corrections due to delayed neutron terms will be necessary for analyzing experimental results. (a) On short life time scale. (b) On delayed neutron life time scale.

### **The Langevin Approach to Reactor Noise in ADS**

In chapter 3, we described the non-Poisson source as a periodic sequence of delta function pulses with correlations between different pulses and derived expressions for Rossi alpha and Feynman alpha functions. Pulses of finite widths were also considered. By considering rectangular and Gaussian pulse shapes, Rossi alpha and Feynman alpha formulae were derived. However, the study was limited to the case of prompt neutrons. In chapter 4, we extended the theory of reactor noise in ADS by including delayed neutrons. The source was described using non-Poisson periodic delta function pulses and formulae for Rossi alpha and Feynman alpha were derived. The possibility of correlations between different pulses was also considered. The further extension of the theory to the more general case of correlated non-Poisson pulsed sources with finite pulse width including delayed neutrons becomes difficult as it involves mathematical complexity. Hence, we develop a simpler approach to reactor noise in ADS based on the Langevin method. We first demonstrate that it is possible to obtain the correct expressions for various noise descriptors using the Langevin approach with Schottky prescription for fission, detector, and capture events but with a separate treatment for ADS source fluctuations. We carry out the demonstration for one of the models of the source studied by us earlier. It is shown that our earlier results by the more rigorous method of pgf are reproduced. The method is then applied to treat the more general problem of zero power ADS noise as described above.

Behringer and Wydler (1999) have considered the Langevin approach for ADS noise, but they use a modified Schottky prescription to include the noise equivalent (NES) source for source fluctuations. Pazsit and Arzhanov (1999) have presented a treatment of source

fluctuations based on the Langevin approach in the context of power reactor ADS noise which also includes spatial effects. Kitamura et al. (2005), in their study on the effect of delayed neutrons on ADS noise, have treated finite width pulses. However, the study is based on the assumption of Poisson sources. We examine the possibility of treating zero power neutron fluctuations in an ADS with non-Poisson source using the Langevin formulation. We show that this is possible and for this purpose, the external source fluctuations cannot be treated only as a noise equivalent source or only as an external parametric fluctuation but rather as a combination of an internal noise described by the Schottky formula and as an external fluctuating function. This way, non-Poisson sources of all kinds can be treated.

## 5.1 The Langevin theory of noise measurements

### 5.1.1 Un-correlated delta pulsed source

In this section, we assume that the pulses are short compared to all other time scales in the problem and may be represented as a sum of delta functions. We assume no correlation between the pulses and that all neutrons are prompt. We assume that the counting intervals are not deliberately correlated with the incoming source pulses; i.e., we consider the case of stochastic pulsing. This means that the various noise descriptors are averaged over one period of the pulsed neutron source in addition to normal averaging due to the stochastic nature of the variables. This is the model Degweker (2003) had developed in detail using the pgf method and is described in section 2.2.3 of chapter 2. We write down the following Langevin equations for the number of neutrons  $N(t)$  at time  $t$  and the detection rate  $D(t)$  [or number of detected particles  $Z(t)$  in the interval 0 to  $t$ ]:

$$\frac{dN}{dt} = -\alpha N + \sum_{n=-\infty}^{\infty} S_n \delta(t - n / f - t_0) + s_N(t) \quad (5.1)$$

$$D(t) = \frac{dZ}{dt} = \lambda_d N + s_D(t) \quad (5.2)$$

where

$S_n$  = random variable representing number of neutrons in the  $n^{\text{th}}$  pulse

$s_N(t)$  = NES for neutrons and includes capture and fission events

$s_D(t)$  = NES for detection

$\alpha$  = prompt neutron decay constant

$t_0$  = arrival time of one of the pulses

$\lambda_d$  = probability per unit time of detection

Due to the assumption of stochastic pulsing, all quantities are to be averaged with respect to  $t_0$  over one period  $T_0 = 1/f$ . Note however that we do not treat the fluctuations in source events by the Schottky prescription. Instead, we treat it as an external source of noise with the properties described in section 3.2.1 of chapter 3. The properties of the various noise sources are as follows:

$$\langle s_N(t) \rangle = \langle s_D(t) \rangle = 0 \quad (5.3)$$

$$\begin{aligned} \langle s_N(t)s_N(t') \rangle &= [(\lambda_c + \lambda_d)\bar{N} + (\nu - 1)^2\lambda_f\bar{N}]\delta(t - t') \\ &= [\alpha + \nu(\nu - 1)\lambda_f]\bar{N}\delta(t - t') \end{aligned} \quad (5.4)$$

$$\langle s_D(t)s_D(t') \rangle = \lambda_d\bar{N}\delta(t - t') \quad (5.5)$$

$$\langle s_N(t)s_D(t') \rangle = -\lambda_d\bar{N}\delta(t - t') \quad (5.6)$$

$$\langle s_N(t)S_n \rangle = \langle s_D(t)S_n \rangle = 0 \quad (5.7)$$

$$\langle S_n \rangle = S = m_1 \quad (5.8)$$

$$\langle S_n S_m \rangle = S^2 + \langle \delta S^2 \rangle \delta_{nm} = m_1^2 + (m_2 + m_1 - m_1^2)\delta_{nm} \quad (5.9)$$

where

$\lambda_f, \lambda_c$  = probabilities per unit time of fission and capture respectively

$m_1$  = mean number of neutrons produced in one pulse

$m_2$  = second factorial moment of  $m_1$

Eqs. (5.4), (5.5) and (5.6) are the usual Schottky formulae for vector Langevin method (Ackasu and Stolle, 1989) while Eqs. (5.7) through (5.9) are substituted for the external noise source due to source fluctuations in place of the Schottky formula for the source fluctuations. We may note in passing that if we had used the usual Schottky prescription for the source fluctuations, we would get the same results as for a Poisson source, i.e. what would be obtained by the forward Kolmogorov equation or by use of the Bartlett formula.

Another important point to be noted is that, in the Schottky prescription, the average quantities such as  $\overline{N}$  are (generally speaking) a function of  $t$  if we are dealing with nonstationary processes. Since the periodically pulsed source produces a nonstationary process, we should have a similar time dependence on the averaged values of the variables shown in Eqs. (5.4), (5.5) and (5.6). However, as noted above, the measurements are made with randomly triggered intervals, which implies a further averaging of all measured quantities, e.g., the ACF over one pulsing period. For this reason, as is shown below, only averages over one pulse period of the variables on the right side of Eqs. (5.4), (5.5) and (5.6) are required. Hence, all such averaged quantities, e.g.,  $\overline{N} = f \int_0^{1/f} \overline{N}(t) dt$ , that are independent of time are deemed to be used on the right side of Eqs. (5.4), (5.5) and (5.6).

Integrating Eqs. (5.1) and (5.2), we write:

$$N(t) = \int_{-\infty}^t \exp[-\alpha(t-t')] \left[ \sum_n S_n \delta(t'-t_n) + s_N(t') \right] dt' \quad (5.10)$$

$$= \sum_{n=-\infty}^M S_n \exp[-\alpha(t - \frac{n}{f} - t_0)] + \int_{-\infty}^t \exp[-\alpha(t-t')] s_N(t') dt'$$

$$Z(t) = \int_0^T [\lambda_d N(t') + s_D(t')] dt' \quad (5.11)$$

The summation in (5.10) extends to  $M = [ft]$  for  $t_0 > t - ([ft] + 1)/f$  and to  $M = [ft] + 1$  for  $t_0 < t - ([ft] + 1)/f$ . Taking averages of Eqs. (5.10) and (5.11), we get

$$\langle N(t) \rangle = S \sum_{n=-\infty}^M \exp[-\alpha(t - \frac{n}{f} - t_0)] \quad (5.12)$$

$$\langle Z(T) \rangle = \int_0^T \lambda_d N(t') dt' \quad (5.13)$$

*The average neutron count rate and number of counts in an interval*

On averaging over the location of the counting interval vis-à-vis the periodic pulses, we can write for the average number of neutrons at any randomly chosen point of time as

$$\overline{N} = f \int_{-1/f}^0 \langle N(t | t_0) \rangle dt_0 = \frac{fm_1}{\alpha} \quad (5.14)$$

Hence, the mean count rate at a randomly chosen time point and the mean number of counts in a randomly triggered interval of length  $T$  are given by

$$\begin{aligned} \overline{D} &= \lambda_d \overline{N} = \frac{\lambda_d fm_1}{\alpha} \\ \overline{Z} &= \frac{\lambda_d fm_1 T}{\alpha} \end{aligned} \quad (5.15)$$

*The Autocorrelation Function*

To obtain the ACF, we first compute  $\langle D(t_1)D(t_2) \rangle$  by averaging over  $t_0$  as follows:

$$\langle D(t_1)D(t_2) \rangle = f \int_{-1/f}^0 dt_0 \left[ \lambda_d^2 \langle N(t_1)N(t_2) \rangle + \lambda_d \langle N(t_1)s_D(t_2) \rangle + \lambda_d \langle N(t_2)s_D(t_1) \rangle + \langle s_D(t_1)s_D(t_2) \rangle \right] \quad (5.16)$$

The last of the four terms in the integrand in Eq. (5.16) is a delta function and is simply written using Eq. (5.5) as

$$\lambda_d \overline{N} \delta(t_1 - t_2) = \frac{fm_1 \lambda_d}{\alpha} \delta(t_1 - t_2) \quad (5.17)$$

Of the two middle terms in the integrand in Eq. (5.16), the first can be evaluated using the form (5.10) for  $N(t)$  and the fact that the external source and the internal noise equivalent sources are uncorrelated:

$$\begin{aligned} f \lambda_d^2 \int_{-1/f}^0 dt_0 \langle N(t_1) s_D(t_2) \rangle &= f \lambda_d^2 \int_{-1/f}^0 dt_0 \int_{-\infty}^{t_1} \exp[-\alpha(t_1 - t')] \langle s_N(t') s_D(t_2) \rangle dt' \\ &= -f \lambda_d^2 \bar{N} \int_{-1/f}^0 dt_0 \exp[-\alpha(t_1 - t_2)] = -\lambda_d^2 \bar{N} \exp[-\alpha(t_1 - t_2)] \end{aligned} \quad (5.18)$$

For  $t_1 > t_2$ . In the first line of Eq. (5.18), we have used the relation (5.6) after averaging over one period. For  $t_1 < t_2$ , the delta function gives a zero contribution and the above expression is zero. Likewise, we can show that the second of the middle terms in the integrand in Eq. (5.16) gives a contribution

$$-\lambda_d^2 \bar{N} \exp[-\alpha(t_2 - t_1)] \quad (5.19)$$

for  $t_1 < t_2$  and zero for  $t_1 > t_2$ . Eq. (5.18) and expression (5.19) together imply a total contribution

$$-\lambda_d^2 \bar{N} \exp[-\alpha |t_2 - t_1|] = -\frac{f m_1 \lambda_d^2}{\alpha} \exp[-\alpha |t_2 - t_1|] \quad (5.20)$$

The first term in the integrand in Eq. (5.16) can be evaluated using the form in Eq. (5.10) for  $N(t)$ , and because the external and internal sources are uncorrelated, we obtain only the following two terms:

$$\begin{aligned} f \lambda_d^2 \int_{-1/f}^0 dt_0 \left[ \sum_{n=-\infty}^{\lfloor f t_1 \rfloor} \sum_{m=-\infty}^{\lfloor f t_2 \rfloor} \langle S_n S_m \rangle \exp[-\alpha(t_2 - \frac{m}{f} - t_0)] \exp[-\alpha(t_1 - \frac{n}{f} - t_0)] \right] \\ + f \lambda_d^2 \int_{-1/f}^0 dt_0 \int_{-\infty}^{t_1} dt' \int_{-\infty}^{t_2} dt'' \exp[-\alpha(t_1 - t')] \exp[-\alpha(t_2 - t'')] \langle s_N(t') s_N(t'') \rangle \end{aligned} \quad (5.21)$$

Before proceeding, we note that we can, without loss of generality, assume that  $t_2 > t_1, t_1 = 0$  and  $\tau = t_2 - t_1$ . The summation over  $n$  is then up to 0 while the summation over  $m$  goes up to the last source pulse before  $t_2$  which could be either  $\lfloor f t_2 \rfloor$  or  $\lfloor f t_2 + 1 \rfloor$  depending upon the

value of  $t_0$ . We split the first term into two parts. In the first, we have a double summation with the  $n = m$  term excluded. The second part has the term with  $n = m$ . The two terms can then be written using Eq. (5.9). As regards the second term, the evaluation is straight forward using the properties of the NES corresponding to neutrons. The expression (5.21) thus becomes

$$f \lambda_d^2 \int_{-1/f}^0 dt_0 \left[ \sum_{n \neq m, m=-\infty}^{\lfloor ft_0 \rfloor} m_1^2 \exp[-\alpha(t_2 - \frac{m}{f} - t_0)] \exp[-\alpha(-\frac{n}{f} - t_0)] + \sum_{n=-\infty}^0 (m_2 + m_1) \exp[-\alpha(t_2 - \frac{2n}{f} - 2t_0)] \right] + \frac{\lambda_d^2 [\alpha + \overline{\nu(\nu-1)} \lambda_f] N}{2\alpha} \exp(-\alpha t_2) \quad (5.22)$$

Expression (5.22) is evaluated by Degweker (2003) [in fact most of the terms can be recognized as being the same], and we obtain

$$\frac{f \lambda_d^2}{2\alpha} \left[ \frac{m_1^2}{1 - e^{-\alpha/f}} \left\{ e^{-\alpha/f} \exp\left(\alpha\left(\tau - \frac{\lfloor f\tau \rfloor}{f}\right)\right) + \exp\left(-\alpha\left(\tau - \frac{\lfloor f\tau \rfloor}{f}\right)\right) \right\} + (m_2 + 2m_1(1 + Y_1) - m_1^2) e^{-\alpha\tau} \right] \quad (5.23)$$

where  $Y_1 = \lambda_f \overline{\nu(\nu-1)}/2\alpha$  and we have written  $\tau = |t_1 - t_2|$ . The final expression for the auto-correlation function is obtained by adding (5.17), (5.20) and (5.23).

$$\frac{f m_1 \lambda_d}{\alpha} \delta(t - t') + \frac{f \lambda_d^2}{2\alpha} \left[ \frac{m_1^2}{1 - e^{-\alpha/f}} \left\{ e^{-\alpha/f} \exp\left(\alpha\left(\tau - \frac{\lfloor f\tau \rfloor}{f}\right)\right) + \exp\left(-\alpha\left(\tau - \frac{\lfloor f\tau \rfloor}{f}\right)\right) \right\} + (m_2 + 2m_1 Y_1 - m_1^2) e^{-\alpha\tau} \right] \quad (5.24)$$

A number of points are worth noting. If  $t_2 < t_1$ , we get a formula similar to (5.24) for the ACF with  $\tau = t_1 - t_2$ . In other words, the ACF is symmetric with respect to  $t_2$ ,  $t_1$  and depends on the absolute value of  $\tau = t_1 - t_2$ . Secondly, expression (5.24) for the ACF is the same as the equation for the function  $f_2$  described in section 2.2.3 of chapter 2 apart from the first delta function term representing the detector noise. Since the Rossi alpha formula is interpreted in terms of the probability of getting a second count in a (infinitesimally) short time interval around  $t_2$  given a count at  $t_1$ , rather than averages of the product of the number of counts in

short intervals, the detector noise term is absent from the Rossi alpha formula. Thus, we also interpret (5.24) [minus the detector noise term] to be the expression for  $f_2$ .

### *The Variance to mean*

From the expression for  $f_2$ , the variance can thus be derived in the same way as by Degweker (2003) and we expect to obtain the same result. The variance can also be obtained from (5.24) noting that

$$\frac{v}{m} = \frac{\overline{Z^2} - \overline{Z}^2}{\overline{Z}} = \frac{\int_0^T \int_0^T \langle D(t_1)D(t_2) \rangle dt_1 dt_2 - \left( \int_0^T \langle D(t) \rangle dt \right)^2}{\int_0^T \langle D(t) \rangle dt} \quad (5.25)$$

The detector noise term in (5.24) contributes unity to the variance to mean, and thus, we can look upon the unity in the  $v/m$  formula as being due to the detector noise. We have therefore demonstrated the applicability of the Langevin approach to Reactor Noise in ADS provided the external source is modeled explicitly rather than as an internal noise source given by the Schottky prescription.

### **5.1.2 Correlated finite pulsed source including delayed neutrons**

We now consider the general case of correlated non-Poisson pulsed source with finite pulse width including delayed neutrons. As is well known, the Langevin approach is the simplest in the frequency domain and we exploit this simplicity. Hence, we restrict ourselves to the frequency domain and obtain the power spectral density as the mathematics for the time domain is rather intractable. We continue to make the assumption of stochastic pulsing in this section.

The Langevin equations for this model can be written as follows

$$\frac{dN}{dt} = \left[ \lambda_f \overline{\nu_p} - (\lambda_c + \lambda_d + \lambda_f) \right] N + \sum_i \mu_i C_i + S(t) + s_N(t) \quad (5.26)$$

$$\frac{dC_i}{dt} = \lambda_f \overline{\nu_{di}} N - \mu_i C_i + s_{C_i}(t) \quad (5.27)$$

$$\frac{dZ}{dt} = \lambda_d N + s_D(t) \quad (5.28)$$

where  $\mu_i$ ,  $C_i$ ,  $\nu_{di}$  and  $s_{C_i}(t)$  are decay constant, concentration, yield and NES respectively of  $i^{\text{th}}$  group of delayed neutron precursors. The other symbols have the same meaning as in the previous section.

The NESs are assumed to have the following statistical properties

$$\langle s_N(t) \rangle = \langle s_{C_i}(t) \rangle = \langle s_D(t) \rangle = 0 \quad (5.29)$$

$$\langle s_N(t) s_N(t') \rangle = [(\lambda_c + \lambda_d) \overline{N} + \lambda_f (\overline{\nu_p} - 1)^2 \overline{N} + \mu_i \overline{C_i} + \overline{\nu_{sp}^2 S}] \delta(t - t') \quad (5.30)$$

$$\langle s_D(t) s_D(t') \rangle = \lambda_d \overline{N} \delta(t - t') \quad (5.31)$$

$$\langle s_D(t) s_N(t') \rangle = -\lambda_d \overline{N} \delta(t - t') \quad (5.32)$$

$$\langle s_N(t) s_{C_i}(t') \rangle = [\lambda_f (\overline{\nu_p} - 1) \overline{\nu_{di}} \overline{N} - \mu_i \overline{C_i}] \delta(t - t') \quad (5.33)$$

$$\langle s_{C_i}(t) s_{C_i}(t') \rangle = [\lambda_f \overline{\nu_{di}^2} \overline{N} + \mu_i \overline{C_i}] \delta(t - t') \quad (5.34)$$

$$\langle s_{C_i}(t) s_{C_j}(t') \rangle = \lambda_f \overline{\nu_{di}} \overline{\nu_{dj}} \overline{N} \delta(t - t') \quad (5.35)$$

$$\langle s_{C_i}(t) s_D(t') \rangle = 0 \quad (5.37)$$

The inclusion of the last term in Eq. (5.30) for the correlation function of the noise equivalent source for the neutronic variable is to account for the fact that the source produces neutrons randomly even if it were a constant function rather than a periodically modulated stochastic process.

The external source is defined such that  $S(t)dt$  represents the probability of a spallation event occurring in time  $dt$ . To describe the source, we add one more equation for the number of protons (ions) in the target.

$$\frac{dP}{dt} = -\lambda P + E(t)I(t) + s_p(t) \quad (5.38)$$

where  $\lambda$  is the probability per unit time for a proton (ion) to induce a spallation (neutron producing) reaction in the target,  $E(t)$  is shape function for periodic sequence of pulses,  $I(t)$  is randomly fluctuating proton current and  $s_p(t)$  is noise equivalent source for protons. Thus, the first term is the removal of protons by spallation while the second represents the addition of protons in the target region due to the incoming beam current. The last term represents a noise term corresponding to the proton removal process whose characteristics are given by the Schottky formula as follows:

$$\langle s_p(t) \rangle = 0 \quad (5.39)$$

$$\langle s_p(t)s_p(t') \rangle = \lambda \bar{P} \delta(t-t') \quad (5.40)$$

$$\langle s_p(t)s_N(t') \rangle = -\lambda \bar{\nu}_s \bar{P} \delta(t-t') \quad (5.41)$$

The justification for the last of these equations is that removal of a proton leads to the production of  $\nu_s$  spallation neutrons. As in chapter 3, the incoming current is modeled as the product of a periodically varying function consisting of narrow pulses of any shape (Gaussian or rectangular) and a stationary stochastic process.

$$E(t)I(t) = \sum_n \varepsilon(t-t_0 + nT_0)I(t) \quad (5.42)$$

$$I(t) = \langle I \rangle + i(t)$$

$i(t)$  has zero mean and we assume that it has an exponential auto correlation function i.e.

$$\langle i(t) \rangle = 0$$

$$\langle i(t)i(t') \rangle = \Gamma^2 \exp(-\beta |t-t'|) \quad (5.43)$$

Eq. (5.38) can be easily solved to give

$$S(t) = \lambda P(t) = \int_{-\infty}^t \lambda \exp[-\lambda(t-t')] \{E(t')I(t') + s_p(t')\} dt' \quad (5.44)$$

Since the time given by the inverse of  $\lambda$  is very short compared to all other times, we can replace the kernel in Eq. (5.44) by a delta function to finally yield

$$S(t) = E(t)I(t) + s_p(t) \quad (5.45)$$

The functional form for these pulses is such that each of the pulses has an area (integral over time) equal to  $g$  so that the average source event rate is  $\bar{S} = \lambda \bar{P} = g \langle I \rangle / T_0$ .

### *The PSD of the detection rate*

If we write  $D(t) = dZ / dt$  for the detection rate, then the measured quantity is the auto-covariance function:

$$\langle d(t)d(t') \rangle = \langle D(t)D(t') \rangle - \langle D(t) \rangle^2$$

or its Fourier transform, the PSD. Fourier transforming Eq. (5.28), we can write the PSD as

$$\langle d^*(\omega)d(\omega) \rangle = \lambda_d^2 \langle n^*(\omega)n(\omega) \rangle + 2\lambda_d \text{Re}[\langle n^*(\omega)s_D(\omega) \rangle] + \langle s_D^*(\omega)s_D(\omega) \rangle \quad (5.46)$$

### *Contribution from the (Internal) NESs*

The PSD corresponding to the last term in Eq. (5.46) is simply written down using Eq. (5.31):

$$\lambda_d \bar{N} \quad (5.47)$$

which is the white noise contribution from the detector. Using Eq. (5.32), the PSD due to the middle term in Eq. (5.46) is

$$-2\lambda_d^2 \bar{N} \text{Re}(G(i\omega)) \quad (5.48)$$

Following Ackasu and Stolle (1989) [see section 2.1.2.5 of chapter 2], we write the PSD of the first term in Eq. (5.46) due to the noise equivalent sources as follows:

$$\left[ (i\omega + \Lambda)^{-1} \Sigma' (-i\omega + \Lambda^t)^{-1} \right]_{00} \quad (5.49)$$

where  $\Sigma'$  is the spectral density matrix of NES and external source and can be written as a sum of three parts. The first is due to the internal NESs (neutronic and precursor) and the second due to the external source. Since the latter is not at all correlated with the former, there are no cross terms. The third part is due to the proton noise equivalent source and its correlation with the neutronic noise equivalent source as given by Eqs. (5.40) and (5.41). We write the three parts explicitly as follows:

$$\begin{aligned}\Sigma'(\omega) &= \langle s^*(\omega)s^t(\omega) \rangle = \langle \text{col}(S_N^*(\omega) + S(\omega), S_{C_1}^*(\omega) \dots S_{C_6}^*(\omega)) (S_N(\omega) + S(\omega) S_{C_1}(\omega) \dots S_{C_6}(\omega)) \rangle \\ &= \Sigma + \Sigma_1 + \Sigma_2 \\ [\Sigma_1]_{00} &= \langle I^*(\omega)I(\omega)E^*(\omega)E(\omega) \rangle \\ [\Sigma_2]_{00} &= \langle S_N^*(\omega)S_p(\omega) + S_p^*(\omega)S_N(\omega) + S_p^*(\omega)S_p(\omega) \rangle = \lambda \bar{P}(1 - 2\bar{\nu}_s) \\ [\Sigma_1]_{ij} &= [\Sigma_2]_{ij} = 0, \forall i, j \neq 0\end{aligned}$$

where

$\Sigma$  = spectral density matrix of NES coming from the neutron and precursor contributions (section 5.1.2.5 of chapter 2)

$\Sigma_1$  = spectral density matrix due to the external source fluctuations

$\Sigma_2$  = spectral density matrix due to the proton NES (and its correlation with the neutrons)

The matrix  $\Lambda$  defines the system of linear differential equations (5.26) and (5.27). The explicit forms of  $\Sigma$  and  $\Lambda$  are as follows:

$$\Sigma_{00} = (\lambda_c + \lambda_d)\bar{N} + \lambda_f(\bar{\nu}_p - 1)^2\bar{N} + \mu_i\bar{C}_i + \bar{\nu}_s^2\bar{S} \quad (5.50)$$

$$\Sigma_{ii} = \lambda_f\bar{\nu}_{di}^2\bar{N} + \mu_i\bar{C}_i \quad (i \neq 0) \quad (5.51)$$

$$\Sigma_{0i} = \Sigma_{i0} = \lambda_f(\bar{\nu}_p - 1)\bar{\nu}_{di}\bar{N} - \mu_i\bar{C}_i \quad (5.52)$$

$$\Sigma_{ij} = \lambda_f\bar{\nu}_{di}\bar{\nu}_{dj}\bar{N} \quad (i \neq j) \quad (5.53)$$

$$\Lambda_{00} = -[\lambda_f\bar{\nu}_p - (\lambda_c + \lambda_d)] = \alpha_p \quad (5.54)$$

$$\Lambda_{0j} = -\mu_j \quad (5.55)$$

$$\Lambda_{i0} = -\lambda_f \overline{v_{di}} = -\alpha_{di} \quad (5.56)$$

$$\Lambda_{ij} = \mu_i \delta_{ij} \quad (5.57)$$

It is fairly easy to write down the inverse of the matrix  $(i\omega + \Lambda)^{-1} = T$ , and we obtain

$$T_{00} = \frac{1}{D} \prod_k (i\omega + \mu_k) = G(i\omega) \quad (5.58)$$

$$T_{0j} = \alpha_{dj} \frac{1}{D} \prod_{k \neq j} (i\omega + \mu_k) = \frac{\alpha_{dj} G(i\omega)}{(i\omega + \mu_j)} \quad (5.59)$$

$$T_{i0} = -\mu_i \frac{1}{D} \prod_{k \neq i} (i\omega + \mu_k) = \frac{-\mu_i G(i\omega)}{(i\omega + \mu_i)} \quad (5.60)$$

With this, we can evaluate the first part of (5.49) to finally yield

$$|G(i\omega)|^2 \left( \Sigma_{00} + \sum_k \frac{\Sigma_{kk} \alpha_{dk}^2 + 2\Sigma_{0k} \mu_k \alpha_{dk}}{\omega^2 + \mu_k^2} + 2 \sum_{k,l} \frac{\Sigma_{kl} \alpha_{dk} \alpha_{dl} (\mu_k \mu_l + \omega^2)}{(\omega^2 + \mu_k^2)(\omega^2 + \mu_l^2)} \right) \quad (5.61)$$

where  $G$  is the zero power transfer function.

#### *Contribution from the (External) source fluctuations*

The matrix multiplication corresponding to the second part, namely, the contribution due to the external source  $\Sigma_1$ , is easily carried out since most of the elements are zero, and one obtains

$$\wp(\omega) |G(i\omega)|^2 \quad (5.62)$$

where  $\wp(\omega) = [\Sigma_1]_{00}$  is the PSD of the external source averaged over one pulse period, which can be written as

$$\begin{aligned}
\wp(\omega) &= \frac{1}{T_0} \int_{-T_0}^0 dt_0 \int_{-\infty}^{\infty} \langle S(t)S(t+\tau) \rangle \exp(i\omega\tau) d\tau \\
&= \int_{-\infty}^{\infty} \exp(i\omega\tau) d\tau \sum_{n,m} \frac{1}{T_0} \int_{-T_0}^0 \varepsilon(t-t_0+nT_0) \varepsilon(t+\tau-t_0+mT_0) \left[ \langle I(t)I(t+\tau) \rangle - \langle I(t) \rangle^2 \right] dt_0 \\
&= \int_{-\infty}^{\infty} \exp(i\omega\tau) d\tau \sum_{n,m} \frac{1}{T_0} \int_{-T_0}^0 \varepsilon(t-t_0+nT_0) \varepsilon(t+\tau-t_0+mT_0) \Gamma^2 \exp(-\beta|\tau|) dt_0 \quad (5.63)
\end{aligned}$$

### Gaussian Pulses

We assume a narrow Gaussian form for the pulse shape having variance  $\sigma^2$ . The two Gaussians in the product will overlap significantly for only that value of  $m$  which is different from  $n$  by  $[f\tau]+1$ . Integration over  $t_0$  gives us a periodic function of  $\tau$  whose form within one period is another Gaussian somewhat broader with a variance equal to  $2\sigma^2$ . The PSD is thus given by

$$\sum_{n=-\infty}^{\infty} \int_{-\infty}^{\infty} \frac{1}{\sqrt{4\pi\sigma^2}} \exp\left(-\frac{(\tau-nT_0)^2}{4\sigma^2}\right) \Gamma^2 \exp(-\beta|\tau|) \exp(i\omega\tau) d\tau \quad (5.64)$$

We write the periodic function as a Fourier series:

$$\sum_{n=-\infty}^{\infty} \frac{1}{\sqrt{4\pi\sigma^2}} \exp\left(-\frac{(\tau-nT_0)^2}{4\sigma^2}\right) = \sum_{n=-\infty}^{\infty} \frac{\exp(2n\pi i\tau/T_0)}{T_0 \sqrt{4\pi\sigma^2}} \int_{-T_0/2}^{T_0/2} \exp\left[-\left(\frac{2n\pi i\tau}{T_0} + \frac{\tau^2}{4\sigma^2}\right)\right] d\tau \quad (5.65)$$

Since the pulses are narrow compared to the pulsing period, the limits of integration on the RHS can be replaced by  $\pm\infty$  which then becomes the Fourier transform of a Gaussian.

Hence, we obtain

$$\sum_{n=-\infty}^{\infty} \frac{1}{\sqrt{4\pi\sigma^2}} \exp\left(-\frac{(\tau-nT_0)^2}{4\sigma^2}\right) = \frac{1}{T_0} \sum_{n=-\infty}^{\infty} \exp[-((2n\pi\sigma/T_0)^2)] \exp(2n\pi i\tau/T_0) \quad (5.66)$$

The PSD of Eq. (5.64) is now easily written as

$$\wp(\omega) = \frac{2\beta\Gamma^2}{T_0} \sum_{n=-\infty}^{\infty} \frac{\exp[-(2n\pi\sigma/T_0)^2]}{(\omega + 2n\pi/T_0)^2 + \beta^2} \quad (5.67)$$

### Rectangular Pulses

Here we assume a rectangular pulse of width  $\sigma$  and height  $1/\sigma$ . The result of averaging over  $t_0$  finally gives us a periodic function of  $\tau$  whose form within one period is a triangular pulse extending from (say)  $-\sigma$  to  $\sigma$  and having a height of  $1/\sigma$ . The PSD is thus given by

$$\begin{aligned} & \sum_{n=-\infty}^{\infty} \int_{nT_0-\sigma}^{nT_0} \left( \frac{\tau}{\sigma^2} - \frac{(nT_0-\sigma)}{\sigma^2} \right) \Gamma^2 \exp(-\beta |\tau|) \exp(i\omega\tau) d\tau \\ & + \sum_{n=-\infty}^{\infty} \int_{nT_0}^{nT_0+\sigma} \left( -\frac{\tau}{\sigma^2} + \frac{(nT_0+\sigma)}{\sigma^2} \right) \Gamma^2 \exp(-\beta |\tau|) \exp(i\omega\tau) d\tau \end{aligned} \quad (5.68)$$

where as before we can expand the periodic function in a Fourier series and we obtain an expression for the PSD similar to (5.67) with a different Fourier coefficient:

$$\wp(\omega) = \frac{4\beta\Gamma^2}{T_0} \sum_{n=-\infty}^{\infty} \frac{1 - \cos(2n\pi\sigma/T_0)}{(2n\pi\sigma/T_0)^2 [(\omega + 2n\pi/T_0)^2 + \beta^2]} \quad (5.69)$$

### Contribution from the proton NESs

In a manner similar to that used for obtaining (5.62), the proton NES and the correlation term with the neutronic NES corresponding to the matrix  $\Sigma_2$  give the following contribution [the third of expression (5.49)]:

$$\lambda \bar{P} (1 - 2\bar{\nu}_s) |G(i\omega)|^2 \quad (5.70)$$

### Final Expression for the PSD

The PSD of the detected signal can now be written by adding (5.47), (5.48), (5.61), (5.62), & (5.70):

$$\begin{aligned} & |G(i\omega)|^2 \left( \wp(\omega) + (1 - 2\bar{\nu}_s) \lambda \bar{P} + \Sigma_{00} + \sum_k \frac{\Sigma_{kk} \alpha_{dk}^2 + 2\Sigma_{0k} \mu_k \alpha_{dk}}{\omega^2 + \mu_k^2} + 2 \sum_{k,l} \frac{\Sigma_{kl} \alpha_{dk} \alpha_{dl} (\mu_k \mu_l + \omega^2)}{(\omega^2 + \mu_k^2)(\omega^2 + \mu_l^2)} \right) \\ & - 2\lambda_d^2 \bar{N} \operatorname{Re}(G_{00}(i\omega)) + \lambda_d \bar{N} \end{aligned} \quad (5.71)$$

where it may be noted that the quantities  $\overline{N}, \overline{C_i}, \overline{S}, \overline{P}$  appearing in Eq. (5.71) [through the  $\Sigma$  matrix defined by Eqs. (5.50) through (5.53)] are not independent but are related to each other through the stationary solution of Eqs. (5.26) and (5.27) for the averages as follows:  $\overline{N} = \overline{\nu_{sp}} \overline{S} / (\lambda_c + \lambda_d - \lambda_f \overline{\nu})$ ,  $\overline{C_i} = \lambda_f \overline{\nu_{di}} \overline{N} / \lambda_i$  and  $\overline{S} = \lambda \overline{P} = g \langle I \rangle / T_0$

The PSD for the general ADS noise problem given by Eq. (5.71) has not been obtained by us by the first principle methods due to the mathematical difficulties involved. The Langevin formulation makes it fairly tractable. Eq. (5.71) thus represents a new result not presented earlier.

## 5.2 Conclusion

The Langevin approach is capable of correctly describing the non-Markov process resulting from a non-Poisson source. We have shown that a complete description of the spallation neutron source is possible by treating it as a combination of an internal noise given by the Schottky prescription and another that is of external origin arising from the proton beam. We have obtained the PSD of the Reactor Noise in ADS by considering delayed neutrons, finite pulsed width and correlations if any between proton pulses.

# **Simulation of Noise Experiments in Sub-critical Systems by Diffusion Theory Based Analogue Monte Carlo**

Low power sub-critical experiments are being planned (Rasheed et al., 2010) to be carried out at the Bhabha Atomic Research Centre (BARC) with the aim of demonstrating pulsed neutron and noise methods for measuring the sub-critical reactivity of ADS. Another aim of the experiments is to verify the theory of reactor noise in ADS developed by us and interpret the results in terms of the theory. The system planned is a natural uranium sub-critical assembly moderated by water or high density polyethylene and driven by a D-D or D-T neutron generator. The maximum  $k_{\text{eff}}$  of the assembly is expected to be about 0.9. At such a low value of  $k_{\text{eff}}$  while it may be possible to carry out pulsed neutron experiment successfully, noise experiments for determining alpha are likely to face difficulties in interpretation due to much greater modal contamination effects. By the time the higher modes have died out and the fundamental mode decay of the correlation sets in, very few correlated counts remain and the background noise dominates. However, for both types of experiments, it is possible to select certain detector positions where the modal contamination of many of the higher modes immediately above the fundamental mode can be eliminated. In view of these difficulties, it is necessary to simulate the experiments and get an idea of the kind of results that might be expected with different detector locations and counting and analyzing setups. Simulations with standard code packages (MCNP, 1987; Gupta, 1991) are not appropriate because of several non-analogue features built into such codes. These need to be

modified into completely analogue simulation codes. Munoz Cobo et al. (2001) coupled the high energy code LAHET with another Monte Carlo code MCNP-DSP and simulated cross power spectral density between the proton current signal and a neutron detector signal for a typical fast energy amplifier configuration. While LAHET simulates the spallation process and transport of charged particles, MCNP-DSP is used to simulate the counting statistics from neutrons counters. Pozzi et al. (2012) have developed a variant of MCNP, called MCNP-PoliMi. The code can simulate correlated statistics of neutrons and photons. It can also handle the effect of delayed neutrons. However, completely analogue computations are very time consuming. There have been attempts to remedy (Máté Szieberth and Gergely Klujber, 2010) some of these problems by special methods of correcting tallies which give not only the correct value of the first moment but also of the second moment. The simulation is still having many time reducing features and takes less time compared to purely analogue simulations.

In this chapter, we describe an alternate method of time reduction in analogue Monte Carlo through the development of a diffusion theory based analogue Monte Carlo simulator. The simulator generates a detailed time history of counts in the detector so that any method of analysis can be carried out. While few-group diffusion theory may not be as accurate as exact Monte Carlo simulations, it will be adequate for the purpose mentioned above. We discuss the basic theory of the simulation method and the results of our simulations on a simplified model of one of the proposed assemblies. In section 6.1, we describe a simple reactor model for which analytical diffusion kernel can be used very effectively to get some of the required results. Our approach is well suited to the study of few group time dependent diffusion equations. In section 6.2, we describe a numerical approach based on the finite differenced diffusion equation. The approach is general enough to be applicable to all problems of interest. In section 6.3, we discuss modal effects on noise experiments by following the

backward stochastic transport equation approach and expanding the probability generating functions in terms of the alpha modes of the adjoint equations. Results of our simulations are discussed in section 6.4 and in section 6.5 we present our conclusions.

## **6.1 Analytical diffusion theory kernels**

### **6.1.1 Infinite medium kernel**

At the outset, we note that while the transport theory simulation by Monte Carlo is possible by using the transport kernel, the same is not easy in diffusion theory using the diffusion kernel. In transport, theory we are looking at the next collision and subsequently at what happens at the collision site. In diffusion theory, we are looking at the next significant event which is removal (an absorption or slowing down to the next group). A large number of intermediate transport steps would have been covered in the process (including diffusion in two or more neighboring media) before the final event. This is the reason that the diffusion kernel approach is faster but this is also the reason that it is more difficult to implement, since the particle does not follow a simple path. However, there are certain situations in which diffusion kernel can be used very effectively to reduce the number of simulation steps and hence the computing time. Suppose we have a reactor consisting of a number of large sized homogeneous zones such as core regions with different enrichments or core and reflector. Each of the regions is assumed to be large compared to the slowing down length or the diffusion length in that group. In such a situation, at most of the points of the reactor, the neutron is likely to diffuse in a single region before absorption or slowing down and the infinite medium kernel is approximately valid. In this sub-section, we obtain the infinite medium kernel and in subsequent sub-section, we derive simple corrections for a finite medium.

The quantity of interest in Monte Carlo simulation is the probability that a neutron will undergo removal in the small space-time interval  $dx dy dz dt$ . This can be obtained (Rana et al., 2013) by solving the one group time dependent diffusion equation with a single neutron (assumed to be located at  $x = y = z = t = 0$ ):

$$P(x, y, z, t) dx dy dz dt = \frac{1}{l(4\pi Dvt)^{3/2}} \exp\left(-\frac{x^2 + y^2 + z^2}{4Dvt}\right) \exp(-t/l) dx dy dz dt \quad (6.1)$$

The marginal distribution for the time variable can be obtained by integrating over the space coordinates:

$$\frac{1}{l} \exp(-t/l) dt \quad (6.2)$$

The conditional distribution for the space variables for a given value of time is obtained by dividing (6.1) by (6.2) to give:

$$\frac{1}{(4\pi Dvt)^{3/2}} \exp\left(-\frac{x^2 + y^2 + z^2}{4Dvt}\right) dx dy dz \quad (6.3)$$

Eq. (6.3) indicates that the distribution can be written as a product of three Gaussians for the three coordinates each having zero mean and  $2Dvt$  as variance. Eqs. (6.2) and (6.3) suggest the following algorithm for obtaining the next time and position of a removal event. We sample the time as an exponential distribution (having mean  $l$ ) and for the sampled value of the time, we sample the position coordinates as three independent Gaussians each with zero mean and  $2Dvt$  as the variance.

### 6.1.2 Finite medium kernel: Method of images for bare homogenous reactor

#### *Rectangular parallelepiped*

While Eq. (6.1) is valid for an infinite medium, it is possible to use it also for a finite bare homogeneous reactor. For this, we recall the method of images for obtaining the potential due to a charge in a finite region bounded by an earthed conducting plane. Specifically, we refer

to the case of an infinite earthed plane P shown in Fig. 6.1. The presence of the image charge of equal magnitude and opposite sign at an equal distance behind the plane neutralizes the potential due to the real charge on the conducting plane and results in a zero potential at the plane and hence the correct solution on the left of P.

In the case of a bare homogenous reactor, of rectangular geometry, we need to have a zero flux boundary condition at the reactor (extrapolated) boundary i.e. at all six faces of the parallelepiped. Such a geometry in electrostatics requires an infinite number of image charges due to the long range nature of the interaction. In the case of diffusion theory, since the reactor dimensions are usually much larger than a diffusion length, multiple images contribute very little and it is possible to do with one, three or seven images depending upon whether the point is near a face, edge or corner as illustrated in Fig. 6.2. For the simplest case of the source being near a face, the probability density for points inside the medium (to the left of the system boundary) can be written as:

$$P(\vec{r}, t) = \frac{1}{l(4\pi Dvt)^{3/2}} \left[ \exp\left(-\frac{|\mathbf{r} - \mathbf{r}'|^2}{4Dvt}\right) - \exp\left(-\frac{|\mathbf{r} - \mathbf{r}''|^2}{4Dvt}\right) \right] \exp(-t/l), \quad (6.4)$$

where  $\mathbf{r}'$  and  $\mathbf{r}''$  are the coordinates of the source point and image point respectively.

Note that on the boundary plane  $|\vec{r} - \vec{r}'|^2 = |\vec{r} - \vec{r}''|^2$  and hence the above expression vanishes identically as it should and thus simulates the zero flux boundary condition. The random variables  $x, y, z$  and  $t$  can be sampled for the distribution given by Equation (6.4) by first sampling  $x, y, z$  and  $t$  according to Eqs. (6.1-6.3) and then using a rejection technique. If the sampled point falls outside the medium, the history is terminated. If it falls inside the medium, it is accepted with probability  $1 - \exp\left(-\frac{(x - x'')^2 - (x - x')^2}{4Dvt}\right)$  else the history is terminated.

## 6.2 Finite difference diffusion theory kernels

The method described in the previous section works best for bare homogeneous reactors and can possibly be extended to situations involving one or two core zones and a reflector. Where there are several regions interwoven in a complex manner, the method described above will not work well. For such complicated problems involving several regions, numerical methods have to be used to obtain solution of the diffusion equations. The finite difference method is one of the commonly used techniques for the purpose. Using this method, the following equation for the finite difference form of the multi-group time dependent diffusion equation can be derived (see the derivation in Appendix I):

$$\begin{aligned} \frac{1}{v} \frac{d\varphi_{i,j,k}}{dt} = & (\Sigma_a + \Sigma_s) \varphi_{i,j,k} \\ & + \frac{1}{h_i} \left\{ \frac{2D_{i,j,k}(D_{i-1,j,k}\varphi_{i,j,k} - D_{i-1,j,k}\varphi_{i-1,j,k})}{(D_{i-1,j,k}h_{(i)} + D_{i,j,k}h_{(i-1)})} - \frac{2D_{i+1,j,k}(D_{i,j,k}\varphi_{i+1,j,k} - D_{i,j,k}\varphi_{i,j,k})}{(D_{i+1,j,k}h_{(i)} + D_{i,j,k}h_{(i+1)})} \right\} \\ & + \frac{1}{h_j} \left\{ \frac{2D_{i,j,k}(D_{i,j-1,k}\varphi_{i,j,k} - D_{i,j-1,k}\varphi_{i,j-1,k})}{(D_{i,j-1,k}h_{(j)} + D_{i,j,k}h_{(j-1)})} - \frac{2D_{i,j+1,k}(D_{i,j,k}\varphi_{i,j+1,k} - D_{i,j,k}\varphi_{i,j,k})}{(D_{i,j+1,k}h_{(j)} + D_{i,j,k}h_{(j+1)})} \right\} \\ & + \frac{1}{h_k} \left\{ \frac{2D_{i,j,k}(D_{i,j,k-1}\varphi_{i,j,k} - D_{i,j,k-1}\varphi_{i,j,k-1})}{(D_{i,j,k-1}h_{(k)} + D_{i,j,k}h_{(k-1)})} - \frac{2D_{i,j,k+1}(D_{i,j,k}\varphi_{i,j,k+1} - D_{i,j,k}\varphi_{i,j,k})}{(D_{i,j,k+1}h_{(k)} + D_{i,j,k}h_{(k+1)})} \right\}, \quad (6.5) \end{aligned}$$

where we have written  $\Sigma_s$  for the slowing down cross section. The equation is simply a statement of the decrease in number of neutrons in a mesh due to removal from the mesh by absorption, slowing down or diffusion leakage. We can rewrite the above equation in terms of the number of particles  $N_{ijk}$  in a mesh and using probabilities per unit time in place of macroscopic cross sections ( $\lambda_x = v\Sigma_x$ ) as follows:

$$\begin{aligned} \frac{dN_{ijk}}{dt} = & -(\lambda_a + \lambda_s)N_{ijk} - (\lambda_r + \lambda_l + \lambda_f + \lambda_b + \lambda_u + \lambda_d)N_{ijk} \\ & + (\lambda_l N_{i+1,j,k} + \lambda_r N_{i-1,j,k} + \lambda_b N_{i,j+1,k} + \lambda_f N_{i,j-1,k} + \lambda_d N_{i,j,k+1} + \lambda_u N_{i,j,k-1}), \quad (6.6) \end{aligned}$$

where

$$N_{ijk} = V_{ijk} \varphi_{i,j,k} / v$$

and

$$\lambda_r = D_{ijk} D_{i+1,jk} v / [h_{(i)} (D_{i+1,j,k} h_{(i)} + D_{i,j,k} h_{(i+1)})]$$

is the probability per unit time for a particle to diffuse out of the mesh to the mesh on the right. It may be noted that the various  $\lambda$ s are mesh dependent quantities though we have suppressed the mesh indices for the purpose of clarity. Similar equations for the other lambdas can be written down. By using a similar procedure, it is possible to obtain an equation like (6.6) for meshes which lie on the outer boundary of the reactor and have some missing neighbors from the finite differenced form of the diffusion equation for such meshes around them.

If a large number of particles are present in each of the meshes, the first term on the right hand side of Eq. (6.6) represents the average rate of absorption and second set of six terms, the diffusion of particles from the central mesh (under consideration) to the neighboring meshes (the subscripts  $r, l, f, b, u$  and  $d$  indicating right, left, front, back, top and bottom respectively of the given mesh) while the third set of terms represents the rate of return of particles from the neighboring meshes to the central mesh. With a single particle, clearly we can reinterpret Eq. (6.6) as a probability balance equation with the coefficients giving the probability per unit time of absorption, diffusion out of the central mesh into the neighboring meshes and vice versa.

$$\begin{aligned} \frac{dP_{ijk}}{dt} = & -(\lambda_a + \lambda_s)P_{ijk} - (\lambda_r + \lambda_l + \lambda_f + \lambda_b + \lambda_u + \lambda_d)P_{ijk} \\ & + (\lambda_l P_{i+1,jk} + \lambda_r P_{i-1,jk} + \lambda_b P_{ij+1k} + \lambda_f P_{ij-1k} + \lambda_d P_{ijk+1} + \lambda_u P_{ijk-1}) \end{aligned} \quad (6.7)$$

This probabilistic interpretation suggests the following algorithm for carrying out the analogue Monte Carlo simulation. We sample a random number from an exponential distribution  $[\exp(-\lambda_t t)]$ ;  $\lambda_t = \lambda_a + \lambda_s + \lambda_r + \lambda_l + \lambda_f + \lambda_b + \lambda_u + \lambda_d$  being the total probability of interaction per unit time] to get the time of the next event. Whether it is an absorption, slowing down or diffusion out to the neighboring meshes is decided by the relative

probabilities (e.g.  $\lambda_a / \lambda_t$ ). In a typical multi-group scheme, the mesh indices and energy group of the source neutron would be sampled according to the space-energy distribution of the source. The neutron is then followed till it finally gets absorbed or leaks out of the system.

It may be noted that the algorithm described in this section is somewhat different from that of Sadiku et al. (2006), wherein space and time are both treated by finite differences.

Before concluding this section, we make a comment on the time savings expected in the diffusion Monte Carlo approach over the traditional transport Monte Carlo. The number of collisions required for a neutron to be removed is typically 25, 50 and 100 for light water, fast and heavy water reactors respectively. In transport Monte Carlo, these many collisions must be followed for each history. In the analytical approach of the previous sub-section, a single sampling of the distribution is enough and a very substantial saving in computer time is expected. In the numerical approach, the savings will depend upon the number of samplings required which will depend on how fine is the mesh and the number of energy groups and would not be as spectacular as in the analytical approach.

### **6.3 Modal effects in noise experiments**

The space and energy dependence of neutron flux in a reactor gives rise to higher modes. These modes are responsible for contamination of measured values of alpha by noise experiments. A lot of theoretical studies have been carried out in the past (Munoz-Cobo et al., 2011; Yamamoto, 2011) to investigate the effect of higher modes on noise measurements. Munoz-Cobo et al. (2011) have derived Feynman alpha and Rossi alpha formulae for stochastic and continuous neutron sources by taking higher alpha modes into account. The derived formulae are then compared with the point kinetics formulae in the fundamental mode approximation to deduce spatial correction factors. They have also included the

delayed neutrons. The derived formulae are validated experimentally. Yamamoto (2011) has estimated the Feynman alpha function by considering the higher alpha modes obtained by diffusion approximation and applying transport correction to low order modes. The results are compared with the values obtained by Monte Carlo simulation of the Feynman alpha method. It is concluded that in a deeply sub-critical system, variance to mean ratio is seriously contaminated by the higher order modes, and applying the conventional Feynman-alpha formula may give a completely wrong result.

Since the source is usually located at the centre of a symmetric reactor, it might appear that the anti-symmetric modes would not be present in the flux distribution and these would be automatically eliminated. While this is true in pulsed neutron experiments, a careful modal analysis of the noise method shows that elimination of the anti-symmetric modes requires also that the detectors be placed symmetrically. Moreover to eliminate the next higher symmetric modes, we locate the detectors at the intersection (common zeros) of the zeros of the symmetric modes. This way, all the first set of symmetric and first and second set of anti-symmetric modes are eliminated and the first higher mode contributing to the detected noise signal is from the second set of symmetric modes. In what follows, we make an explicit mathematical demonstration of this result.

Let  $p(\mathbf{r}, \mathbf{\Omega}, E, t; n_1, n_2)$  be the probability of the number of detections in two intervals of length  $\Delta t_1$  and  $\Delta t_2$  around the times  $t_1$  and  $t_2$  ( $t_2 > t_1$ ) due to a neutron injected at  $(\mathbf{r}, \mathbf{\Omega}, E, t)$ .

The corresponding pgf is given by the following equation:

$$G(\mathbf{r}, \mathbf{\Omega}, E, t; z_1, z_2) = \sum_{n_1, n_2=0}^{\infty} p(\mathbf{r}, \mathbf{\Omega}, E, t; n_1, n_2) z_1^{n_1} z_2^{n_2} \quad (6.8)$$

The pgf obeys the backward stochastic transport equation (Pazsit and Pal, 2007; Bell, 1965; Pal, 1958):

$$\begin{aligned}
& -\frac{1}{v} \frac{\partial G}{\partial t} - \mathbf{\Omega} \cdot \nabla G + \Sigma G = \Sigma_c + z_1 \Sigma_{d1} + z_2 \Sigma_{d2} + \int \Sigma_s(\mathbf{\Omega}, E \rightarrow \mathbf{\Omega}', E') G(\mathbf{r}, \mathbf{\Omega}', E', t; z_1, z_2) d\mathbf{\Omega}' dE' \\
& + \Sigma_f f \left[ \int \frac{\chi(E')}{4\pi} G(\mathbf{r}, \mathbf{\Omega}', E', t; z_1, z_2) d\mathbf{\Omega}' dE' \right]
\end{aligned} \tag{6.9}$$

In equation (6.9),  $f$  stands for the pgf of the number of neutrons in a fission reaction.

If  $S(\mathbf{r}, \mathbf{\Omega}, E)$  is a steady source of the Poisson type, the pgf  $G_s(z_1, z_2)$  with the source is given by the Bartlett formula (Bartlett, 1955):

$$G_s(z_1, z_2) = \exp \left[ - \int \{ S(\mathbf{r}, \mathbf{\Omega}, E) G(\mathbf{r}, \mathbf{\Omega}, E, t; z_1, z_2) - 1 \} d\mathbf{r} d\mathbf{\Omega} dE dt \right] \tag{6.10}$$

The Rossi alpha formula is obtained by differentiating (6.10) twice with respect to  $z_1$  and  $z_2$  and setting  $z_1 = z_2 = 1$ :

$$\begin{aligned}
P(t_1, t_2) dt_1 dt_2 &= \int S(\mathbf{r}, \mathbf{\Omega}, E) G_{z_1 z_2}(\mathbf{r}, \mathbf{\Omega}, E, t; 1, 1) d\mathbf{r} d\mathbf{\Omega} dE dt \\
&+ \left( \int S(\mathbf{r}, \mathbf{\Omega}, E) G_{z_2}(\mathbf{r}, \mathbf{\Omega}, E, t; 1, 1) d\mathbf{r} d\mathbf{\Omega} dE dt \right) \left( \int S(\mathbf{r}, \mathbf{\Omega}, E) G_{z_1}(\mathbf{r}, \mathbf{\Omega}, E, t; 1, 1) d\mathbf{r} d\mathbf{\Omega} dE dt \right)
\end{aligned} \tag{6.11}$$

On differentiating (6.9) with respect to  $z_1$  (or  $z_2$ ) and twice with respect to  $z_2$  and  $z_1$ , and setting  $z_1 = z_2 = 1$ , we obtain the following equations for these derivatives i.e. the first and second moments:

$$L^\dagger G_{z_1} = \Sigma_{d1} \tag{6.12}$$

$$L^\dagger G_{z_2} = \Sigma_{d2} \tag{6.13}$$

$$L^\dagger G_{z_1 z_2} = \overline{\nu(\nu-1)} \Sigma_f \left( \int \frac{\chi(E')}{4\pi} G_{z_1}(\mathbf{r}, \mathbf{\Omega}', E', t; 1, 1) d\mathbf{\Omega}' dE' \right) \left( \int \frac{\chi(E')}{4\pi} G_{z_2}(\mathbf{r}, \mathbf{\Omega}', E', t; 1, 1) d\mathbf{\Omega}' dE' \right) \tag{6.14}$$

The equation for the flux due to the source can be written as follows:

$$L\phi = S \tag{6.15}$$

In Eqs. (6.12-6.15), we have used the symbols  $L$  and  $L^\dagger$  for the time dependent backward (adjoint) and forward transport operators defined below:

$$\begin{aligned}
L^\dagger G_{z_1} &= -\frac{1}{v} \frac{\partial G_{z_1}}{\partial t} + H^\dagger G_{z_1} = -\frac{1}{v} \frac{\partial G_{z_1}}{\partial t} - \mathbf{\Omega} \cdot \nabla G_{z_1} + \Sigma G_{z_1} - \int \Sigma_s(\mathbf{\Omega}, E \rightarrow \mathbf{\Omega}', E') G_{z_1}(\mathbf{r}, \mathbf{\Omega}', E', t; 1, 1) d\mathbf{\Omega}' dE' \\
&- \bar{v} \Sigma_f \int \frac{\chi(E')}{4\pi} G_{z_1}(\mathbf{r}, \mathbf{\Omega}', E', t; 1, 1) d\mathbf{\Omega}' dE'
\end{aligned} \tag{6.16}$$

$$\begin{aligned}
L\phi &= \frac{1}{v} \frac{\partial \phi}{\partial t} + H\phi = \frac{1}{v} \frac{\partial \phi}{\partial t} + \mathbf{\Omega} \cdot \nabla \phi + \Sigma \phi - \int \Sigma_s(\mathbf{\Omega}', E' \rightarrow \mathbf{\Omega}, E) \phi(\mathbf{r}, \mathbf{\Omega}', E', t) d\mathbf{\Omega}' dE' \\
&- \chi(E) \int \frac{\bar{v} \Sigma_f}{4\pi} \phi(\mathbf{r}, \mathbf{\Omega}', E', t) d\mathbf{\Omega}' dE'
\end{aligned} \tag{6.17}$$

and where  $H$  and  $H^\dagger$  are the corresponding time independent transport operators. Using the fact that the various terms on the RHS in Eq. (6.11) are scalar products between the source and the functions  $G_{z_1}$  etc., and Eqs. (6.12), (6.13) and (6.14), and the properties of mutually adjoint operators, we can rewrite (6.11) as follows:

$$\begin{aligned}
P(t_1, t_2) dt_1 dt_2 &= \left( \int \Sigma_{d1} \phi(\mathbf{r}, \mathbf{\Omega}, E) d\mathbf{r} d\mathbf{\Omega} dE dt \right) \left( \int \Sigma_{d2} \phi(\mathbf{r}, \mathbf{\Omega}, E) d\mathbf{r} d\mathbf{\Omega} dE dt \right) \\
&+ \int \phi(\mathbf{r}, \mathbf{\Omega}, E) \overline{\bar{v}(\bar{v}-1) \Sigma_f} \left[ \left( \int \frac{\chi(E')}{4\pi} G_{z_1}(\mathbf{r}, \mathbf{\Omega}', E', t; 1, 1) d\mathbf{\Omega}' dE' \right) \right. \\
&\left. \left( \int \frac{\chi(E')}{4\pi} G_{z_2}(\mathbf{r}, \mathbf{\Omega}', E', t; 1, 1) d\mathbf{\Omega}' dE' \right) \right] d\mathbf{r} d\mathbf{\Omega} dE dt,
\end{aligned} \tag{6.18}$$

where we have omitted the time variable for the flux, as we are considering a stationary Poisson source. The first term in Eq. (6.18) is merely the product of the average number of counts in the two intervals and is the uncorrelated term whereas the second term is due to fission chain correlations. It is this term that allows the estimation of  $\alpha$  from Rossi alpha [or Auto Correlation Function (ACF)] measurements. We expand the function  $G_{z_1}$ , in terms of the alpha modes  $\phi_n^\dagger$  of the adjoint equations obeying:

$$H^\dagger \phi_n^\dagger = \frac{\alpha_n}{v} \phi_n^\dagger \tag{6.19}$$

and that of the forward equation obeying

$$H \phi_n = \frac{\alpha_n}{v} \phi_n \tag{6.20}$$

as follows:

$$G_{z_1}(\mathbf{r}, \mathbf{\Omega}, E, t; 1, 1) = \sum_n a_n(t) \varphi_n^\dagger(\mathbf{r}, \mathbf{\Omega}, E) \quad (6.21)$$

and similarly the detector cross section(s):

$$\Sigma_{d_1} = \delta(t - t_1) \sum_n d_n \varphi_n^+(\mathbf{r}, \mathbf{\Omega}, E) \quad (6.22)$$

The coefficients can be written down using bi-orthogonality relation  $(\varphi_n^\dagger, \frac{1}{v} \varphi_n) = \delta_{nm}$  of the eigen-functions to yield:

$$\Sigma_{d_1} = \delta(t - t_1) \sum_n \frac{(\varphi_n^\dagger, \frac{1}{v} \Sigma_{d_1})}{(\varphi_n^\dagger, \frac{1}{v} \varphi_n)} \varphi_n^+(\mathbf{r}, \mathbf{\Omega}, E) \quad (6.23)$$

Substituting the expansions of Eqs. (6.21) and (6.22) in Eq. (6.12) and using Eq. (6.19), we get the following equation for  $a_n(t)$  :

$$\frac{da_n(t)}{dt} = \alpha_n a_n(t) + \frac{(\varphi_n^\dagger, \frac{1}{v} \Sigma_{d_1})}{(\varphi_n^\dagger, \frac{1}{v} \varphi_n)} \delta(t - t_1) \quad (6.24)$$

Solving the above equation, we finally obtain:

$$G_{z_1}(\mathbf{r}, \mathbf{\Omega}, E, t; 1, 1) = \sum_n \frac{(\varphi_n^\dagger, \frac{1}{v} \Sigma_{d_1})}{(\varphi_n^\dagger, \frac{\alpha_n}{v} \varphi_n^\dagger)} \varphi_n^\dagger \exp[-\alpha_n(t_1 - t)] \quad (6.25)$$

If the detectors are symmetrically located and at the intersection of the zeros of the first set of symmetric forward eigen-functions, it is clear that in (6.22), all anti-symmetric modes and the first set of symmetric modes do not contribute. Thus to a very good approximation we can write:

$$G_{z_1}(\mathbf{r}, \mathbf{\Omega}, E, t; 1, 1) = \frac{(\varphi_0^\dagger, \frac{1}{v} \Sigma_{d_1})}{(\varphi_0^\dagger, \frac{\alpha_0}{v} \varphi_0^\dagger)} \varphi_0^\dagger \exp[-\alpha_0(t_1 - t)] \quad (6.26)$$

Similarly we can obtain the following expression for  $G_{z_2}(\mathbf{r}, \mathbf{\Omega}, E, t; 1, 1)$

$$G_{z_2}(\mathbf{r}, \mathbf{\Omega}, E, t; 1, 1) = \frac{(\varphi_0, \frac{1}{v} \Sigma_{d_2})}{(\varphi_0, \frac{\alpha_n}{v} \varphi_0^\dagger)} \varphi_0^\dagger \exp[-\alpha_0(t_2 - t)] \quad (6.26a)$$

Using Eqs. (6.26) and (6.26a), the second term of Eq. (6.18) becomes

$$\frac{\overline{\nu(\nu-1)}}{\alpha_0^2} \int F(\mathbf{r}) [I_0(\mathbf{r})]^2 d\mathbf{r} \left[ \frac{(\varphi_0, \frac{\Sigma_{d_1}}{v})}{(\varphi_0, \frac{\varphi_0^\dagger}{v})} \right]^2 \int_{-\infty}^{t_1} \exp[-\alpha_0(t_1 - t)] \exp[-\alpha_0(t_2 - t)] dt, \quad (6.27)$$

where

$$I_0(\mathbf{r}) = \int \frac{\chi(E')}{4\pi} \varphi_0^\dagger(\mathbf{r}, \mathbf{\Omega}', E') d\mathbf{\Omega}' dE' \quad (6.28)$$

and

$$F(\mathbf{r}) = \int \Sigma_f \varphi(\mathbf{r}, \mathbf{\Omega}, E) d\mathbf{\Omega} dE \quad (6.29)$$

The time integration is carried out easily and we obtain the traditional Rossi alpha type expression:

$$\frac{\overline{\nu(\nu-1)}}{2\alpha_0^3} \int F(\mathbf{r}) [I_0(\mathbf{r})]^2 d\mathbf{r} \left[ \frac{(\varphi_0, \frac{\Sigma_{d_1}}{v})}{(\varphi_0, \frac{\varphi_0^\dagger}{v})} \right]^2 \exp(-\alpha_0 |t_1 - t_2|) \quad (6.30)$$

What if the detectors are not located symmetrically though the source is symmetrically located? To answer the question, we examine Eq. (6.18). The second term has a spatial integral over the flux and the product of two neutron importance functions. Since the detector is not symmetrically located, each of these factors would have anti-symmetric modal contributions. With regard to the product, two anti-symmetric factors give a symmetric factor and hence its integral weighted over the symmetric flux function does not vanish. Hence the time response would contain higher exponentials due to the anti-symmetric modes. Therefore, unlike in the pulsed neutron experiment, we cannot assume that if the source is located at the centre of a symmetrical reactor, the anti-symmetric modes would automatically

vanish. In the following section, we show confirmation of this result by simulation using the diffusion theory based simulator described in previous sections.

## 6.4 Results

### *Analytical diffusion theory kernel method*

We study the problem of suitable location of the neutron detectors to avoid contamination due to contribution from higher modes as much as possible. We assume a bare homogeneous reactor in the shape of a rectangular parallelepiped which is described by one group diffusion theory with the source located at the centre. The dimensions (inclusive of extrapolation distance) and other properties are listed in Table-6.1 and are chosen to roughly correspond to natural uranium fuelled and High Density Poly Ethylene (HDPE) moderated assembly likely to be used in the first phase of the experiments. For the bare assembly, the points of intersection of the zeros of the first set of symmetric modes are easily seen to be at the coordinates  $(\pm 14, \pm 14, \pm 20)$ . For actual geometries, the problem of obtaining these locations is more complex and can be solved using the code developed by Singh et al. (2009).

Fig. 6.4a shows a plot of the auto-covariance with eight detectors centered at the coordinates  $(\pm 14, \pm 14, \pm 20)$ . We see that barring the first point all others fall on a single exponential. Fitting an exponential to the remaining points gives us a value of  $\alpha = 3897 \text{ s}^{-1}$ , which is close to the theoretical value of  $3746 \text{ s}^{-1}$ . The small difference between the estimated and theoretical values appears to be due to small but non-zero contributions from higher modes which are probably not fully suppressed by placement of the detectors. The first point, which is clearly an outlier, might be due to contribution from the second set of symmetric modes which are not at all suppressed by placement of detectors. Fig. 6.4b shows the ratio of variance to mean with counting interval. In Figs. 6.5a and 6.5b we show the results of the same simulation including the effect of delayed neutrons. We see from Fig. 6.5a

that beyond a separation time of about 1 ms i.e. about  $4/\alpha$ , the ACF is mostly on account of delayed neutrons and is approximately constant on the prompt neutron time scale. Subtracting the constant value gives us Fig. 6.5b. Again after leaving out the first point, we get an almost single exponential with  $\alpha = 3723 \text{ s}^{-1}$ . Thus, we clearly see that with the detectors located symmetrically at the intersection of the zeros the Rossi alpha or ACF response is almost entirely due to the fundamental mode.

On the other hand in Fig. 6.6a, we locate the detectors symmetrically but at  $(\pm 10, \pm 10, \pm 0)$  i.e. not at the zeros of the symmetric modes. We see that a single exponential does not fit the data well and moreover the computed value of alpha is also not close to the theoretical value. In Fig. 6.6b, we locate the detector at the zero of the symmetric modes but only in one quadrant. Due to the reduced efficiency, the data are not as good as in Fig. 6.4 & 6.5 but more than that we see that neither a single exponential fits the data well nor the value of alpha, so derived, is anywhere near the theoretical value. The important point to be noted is that by the time we reach a time separation where the fundamental mode dominates, the correlations have more or less died out and the ACF is weak. Moreover delayed neutron effects start playing an important role and these have to be corrected for. This introduces additional uncertainty. The suppression of higher modes by proper selection of detector locations constitutes an important study for determining the sub-criticality in highly sub-critical systems.

### *Finite difference method*

We study the problem of bare homogeneous reactor, described above, by finite diffusion theory based analogue Monte Carlo as mentioned in section 6.2. Simulations were carried out for meshes of two different sizes. In one case, coarse meshes of about 5 to 6 cm size were chosen while in other case fine meshes of about 2.5-3.5 size were considered.

Figs. 6.7a, 6.7b show a plot of the auto-covariance with eight detectors centered at the coordinates  $(\pm 14, \pm 14, \pm 20)$  for coarse and fine mesh structures respectively. Fitting an exponential to the data points gives us values of alpha to be 3902 and 3788 for coarse and fine mesh schemes respectively. Thus, the value of alpha obtained by fine mesh scheme is closer to the theoretical value. Figs. 6.8a and 6.8b show the ratio of variance to mean with counting interval for the coarse and fine mesh structure respectively. In Fig. 6.9 we show a comparison of the results (for fine mesh structure) with those obtained by analytical diffusion theory based kernels. It can be seen that the two are in agreement within  $\pm 4\%$ . It may again be noted that mesh size does have an impact on the shape and maximum size of variance to mean ratio and the small difference can be ascribed to this effect.

In Table 6.2, we show a comparison of simulation results for various parameters obtained using analytical kernel and finite difference kernels with exact values.

By following the method described in section 6.3, it can be shown that maximum value of variance to mean ratio is given as:

$$\frac{\overline{\nu(\nu-1)} \int \Sigma_f(\mathbf{r}, E) \phi_s(\mathbf{r}, E) [I(\mathbf{r})]^2 d\mathbf{r} dE}{\int \phi_s(\mathbf{r}, E) \Sigma_a(\mathbf{r}, E) d\mathbf{r} dE},$$

where

$$I(\mathbf{r}) = \int \chi(E') \phi_s^*(\mathbf{r}, E') dE'.$$

Thus, to get an estimate of the maximum value of variance to mean ratio, direct and adjoint fluxes were calculated by running the finite difference diffusion theory code. The above expression was then used to estimate the maximum value.

The maximum value of variance to mean ratio thus obtained was 2.09 (corresponding value of Feynman Y function i.e. Y-inf is 1.09) for fine mesh structure. Using the (input) value of alpha given in Table-6.1, together with this value for Y-inf, we find that the value of Y at 10

ms is 1.06 which may be compared with the value obtained by the (finite difference) simulator i.e. 1.064. Similarly, the value obtained for the coarse mesh structure was 2.19 which corresponds to a value of 1.16 for Y at 10 ms. This may be compared with the value obtained by the (finite difference) simulator i.e. 1.12.

### *Dead time effects*

In this section, we study effect of detector dead-time on variance to mean ratio for the problem described in the previous section. Two types of detector dead-times have been considered namely non-paralyzable and paralyzable. Figure-6.10 shows the variance to mean ratios for non-paralyzable dead-times of 2 and 4 micro seconds. The effect of dead-time can clearly be seen on the maximum value of variance to mean ratio. For a dead time of 2 micro seconds, the maximum value of variance to mean ratio is about 1.968 as compared to the value of 2.064 without dead-time effect. The count rate also reduces from 5070 to 4974 cps. In case of 4 micro seconds, the maximum value of variance to mean ratio reduces further to 1.892 and the corresponding count rate is 4912 cps.

Figure-6.11 shows the variance to mean ratios for paralyzable dead-times of 2 and 4 micro seconds. For a dead time of 2 micro seconds, the maximum value of variance to mean ratio is about 1.965 as compared to the corresponding value of 1.970 for non-paralyzable dead-time. The count rate in this case is 4972 cps. In case of 4 micro seconds, the maximum value of variance to mean ratio is 1.887 and the corresponding count rate is 4884 cps.

## **6.5 Conclusion**

The few group diffusion theory based analogue Monte Carlo simulator gives a fairly realistic picture of the kind of results that may be expected with regard to the errors and the accuracy that may be expected from actual measurements.

Simulations of proposed Purnima sub-critical assemblies show that proper location of detectors gives an almost single exponential (fundamental mode) response making alpha measurements by the noise methods possible even in deeply sub-critical systems.

## Appendix I

### Derivation of flux at the boundary of a mesh

The multi-group time dependent diffusion equation can be written as:

$$D_g \nabla^2 \varphi_g - \Sigma_{ag} \varphi_g - \sum_{h \neq g} \Sigma_{g \rightarrow h} \varphi_g + \sum_{h \neq g} \Sigma_{h \rightarrow g} \varphi_h + \chi_g \sum_h \nu \Sigma_{fh} \varphi_h + S_{ext} = \frac{1}{v_g} \frac{\partial \varphi}{\partial t} \quad (A.1)$$

The first term on the left hand side is the (negative of) neutron leakage, while the second and third terms are removal by absorption and by transfer to other groups respectively. The fourth, fifth and sixth terms are sources due to -transfer from other groups, -fission and -external source respectively. All the quantities are per unit volume and per unit time around the point under consideration. To convert the diffusion equation into a finite difference equation, we introduce a rectangular mesh such that the nuclear properties within a mesh are constant. We label a mesh by its indices i, j and k along the x, y and z directions respectively and the various nuclear properties such as diffusion coefficients, and various cross sections for absorption, fission, scattering accompanied by slowing down to lower energy groups will be labeled by the corresponding mesh indices.  $h_i, h_j, h_k$  are the lengths of the sides of the rectangular mesh (i, j, k). By integrating over a mesh volume, the above equation becomes (using the divergence theorem for the leakage term):

$$\sum_{m=1}^6 \int \left( -D_g \frac{\partial \varphi_g}{\partial n_m} \right) dS_m + V_{i,j,k} \left[ -\Sigma_{ag} \varphi_g - \sum_{h \neq g} \Sigma_{g \rightarrow h} \varphi_g + \sum_{h \neq g} \Sigma_{h \rightarrow g} \varphi_h + \chi_g \sum_h \nu \Sigma_{fh} \varphi_h + S_{ext} \right] = \frac{1}{v_g} \frac{\partial \varphi}{\partial t} V_{i,j,k}, \quad (A.2)$$

where  $V_{i,j,k} = h_i h_j h_k$  is the volume of the mesh (i, j, k), the integration is over all the six surfaces of a mesh and  $n$  is a unit vector normal to the surface. Each of the six integrals can

be written as the product of the average normal component of the current at the surface with the area of the surface. If there is no source (external, fission or slowing down), the above equation then becomes:

$$\frac{1}{v_{i,j,k}} \sum_{m=1}^6 \left( -D_g \frac{\partial \varphi_g}{\partial n_m} \right) S_m + \left[ -\Sigma_{ag} \varphi_g - \sum_{h \neq g} \Sigma_{g \rightarrow h} \varphi_g \right] = \frac{1}{v_g} \frac{\partial \varphi}{\partial t} \quad (\text{A.3})$$

Henceforth we drop group indices as they are no longer required. To obtain expressions for the average currents on the six surfaces, we consider the mesh arrangements in the reactor as shown in Fig. 6.3. Each mesh is a rectangular region with uniform material properties. Material properties in the neighboring meshes might however be different. The average flux in the mesh (i, j, k) is denoted by  $\phi_{i,j,k}$  and the same is assumed to be the flux at the centre of the mesh. The corresponding average fluxes at the boundaries of the mesh are as indicated in the figure. Continuity of current is ensured by the flowing equation:

$$J_r = -\frac{D_{i+1,j,k}(\phi_{i+1,j,k} - \psi_2)}{h_{(i+1)}/2} = -\frac{D_{i,j,k}(\psi_2 - \phi_{i,j,k})}{h_{(i)}/2} \quad (\text{A.4})$$

The same value of the flux at the boundary ( $\psi_2$ ) is used on the left and right side of the above equation to ensure continuity of the flux.

From eq. (A.4), the following expression for the flux at the boundary is obtained:

$$\psi_2 = \frac{D_{i+1,j,k} h_{(i)} \phi_{i+1,j,k} + D_{i,j,k} h_{(i+1)} \phi_{i,j,k}}{D_{i+1,j,k} h_{(i)} + D_{i,j,k} h_{(i+1)}} \quad (\text{A.5})$$

Substituting this expression on the LHS of (A.4), current on the right edge ( $J_r$ ) is given as:

$$J_r = -\frac{2D_{i+1,j,k} (D_{i,j,k} h_{(i+1)} \phi_{i+1,j,k} - D_{i,j,k} h_{(i+1)} \phi_{i,j,k})}{h_{(i+1)} (D_{i+1,j,k} h_{(i)} + D_{i,j,k} h_{(i+1)})} \quad (\text{A.6})$$

Similarly currents on all the six edges can be evaluated which in turn are used for getting expressions for leakages in x, y and z directions. By substituting the expressions for currents on the six faces, we obtain the following equation:

$$\begin{aligned}
& (\sum_a + \sum_s) \varphi_{i,j,k} + \\
& \frac{1}{h_i} \left\{ \frac{2D_{i,j,k} (D_{i-1,j,k} h_{(i)} \varphi_{i,j,k} - D_{i-1,j,k} h_{(i)} \varphi_{i-1,j,k})}{h_{(i)} (D_{i-1,j,k} h_{(i)} + D_{i,j,k} h_{(i-1)})} - \frac{2D_{i+1,j,k} (D_{i,j,k} h_{(i+1)} \varphi_{i+1,j,k} - D_{i,j,k} h_{(i+1)} \varphi_{i,j,k})}{h_{(i+1)} (D_{i+1,j,k} h_{(i)} + D_{i,j,k} h_{(i+1)})} \right\} \\
& + \frac{1}{h_j} \left\{ \frac{2D_{i,j,k} (D_{i,j-1,k} h_{(j)} \varphi_{i,j,k} - D_{i,j-1,k} h_{(j)} \varphi_{i,j-1,k})}{h_{(j)} (D_{i,j-1,k} h_{(j)} + D_{i,j,k} h_{(j-1)})} - \frac{2D_{i,j+1,k} (D_{i,j,k} h_{(j+1)} \varphi_{i,j+1,k} - D_{i,j,k} h_{(j+1)} \varphi_{i,j,k})}{h_{(j+1)} (D_{i,j+1,k} h_{(j)} + D_{i,j,k} h_{(j+1)})} \right\} \\
& + \frac{1}{h_k} \left\{ \frac{2D_{i,j,k} (D_{i,j,k-1} h_{(k)} \varphi_{i,j,k} - D_{i,j,k-1} h_{(k)} \varphi_{i,j,k-1})}{h_{(k)} (D_{i,j,k-1} h_{(k)} + D_{i,j,k} h_{(k-1)})} - \frac{2D_{i,j,k+1} (D_{i,j,k} h_{(k+1)} \varphi_{i,j,k+1} - D_{i,j,k} h_{(k+1)} \varphi_{i,j,k})}{h_{(k+1)} (D_{i,j,k+1} h_{(k)} + D_{i,j,k} h_{(k+1)})} \right\} \\
& = \frac{1}{v} \frac{d\varphi_{i,j,k}}{dt}
\end{aligned} \tag{A.7}$$

**Table 6.1: Bare homogeneous reactor: geometrical and nuclear data**

Width and height (a, b)	84 cm
Length (c)	120 cm
Migration area $M^2$	36 cm <sup>2</sup>
k-inf	0.982
k-eff	0.873
k-eff (p)	0.867
Infinite medium lifetime ( $l_\infty$ )	40 $\mu$ s
Neutron lifetime ( $l$ )	35.5 $\mu$ s
$\beta$	0.0065
$\alpha$	3746 s <sup>-1</sup>

**Table 6.2: Comparison of various parameters obtained using analytical kernel  
and finite difference kernels with exact values**

Parameter	Exact	Analytical	FD (coarse)	FD (fine)
$K_{eff} (p)$	0.8673	$0.8676 \pm 0.0009$	$0.8706 \pm 0.0003$	$0.8676 \pm 0.0003$
$\alpha (s^{-1})$	3746	$3897 \pm 35.4$	$3902 \pm 52.81$	$3788 \pm 55.68$
$l (\mu s)$	35.5	34.1	33.0	35.4

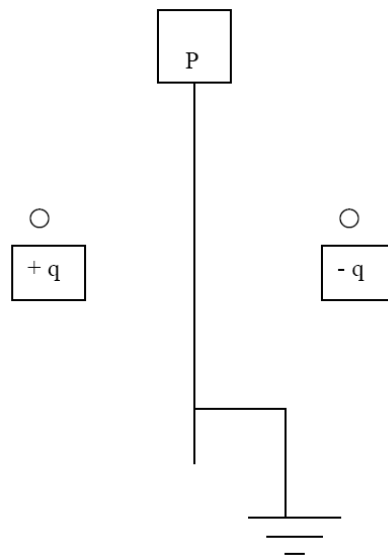


**Fig. 6.1:** The problem of determining the potential (to the left of the plane P) due to a positive charge  $+q$  near the conducting plane P which is earthed can be solved by adding an image charge  $-q$  at an equal distance behind the plane.

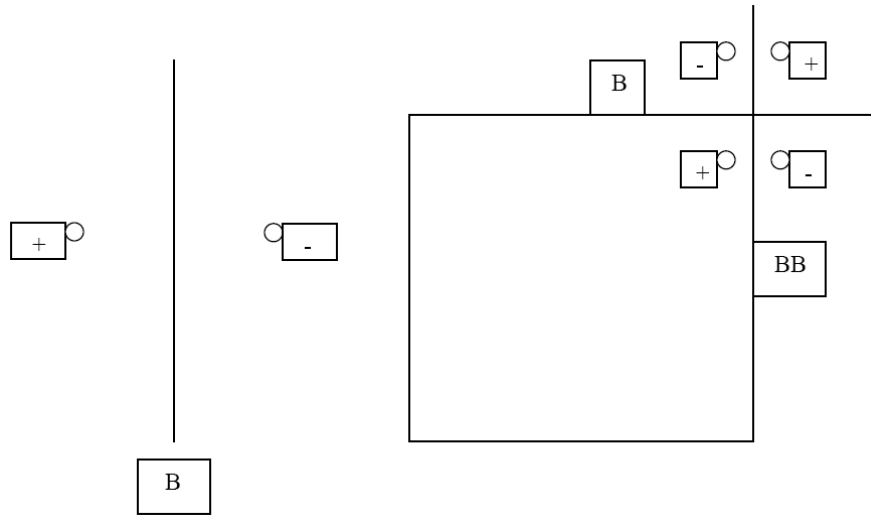


**Fig. 6.2:** On the left we show the case of a single plane boundary with the medium on the left and vacuum on the right. A single negative image source on the right at the same distance from the boundary as the original source reproduces the zero flux boundary condition on B. For the two dimensional case shown on the right, we need three image sources to reproduce the zero flux boundary condition on B and BB.

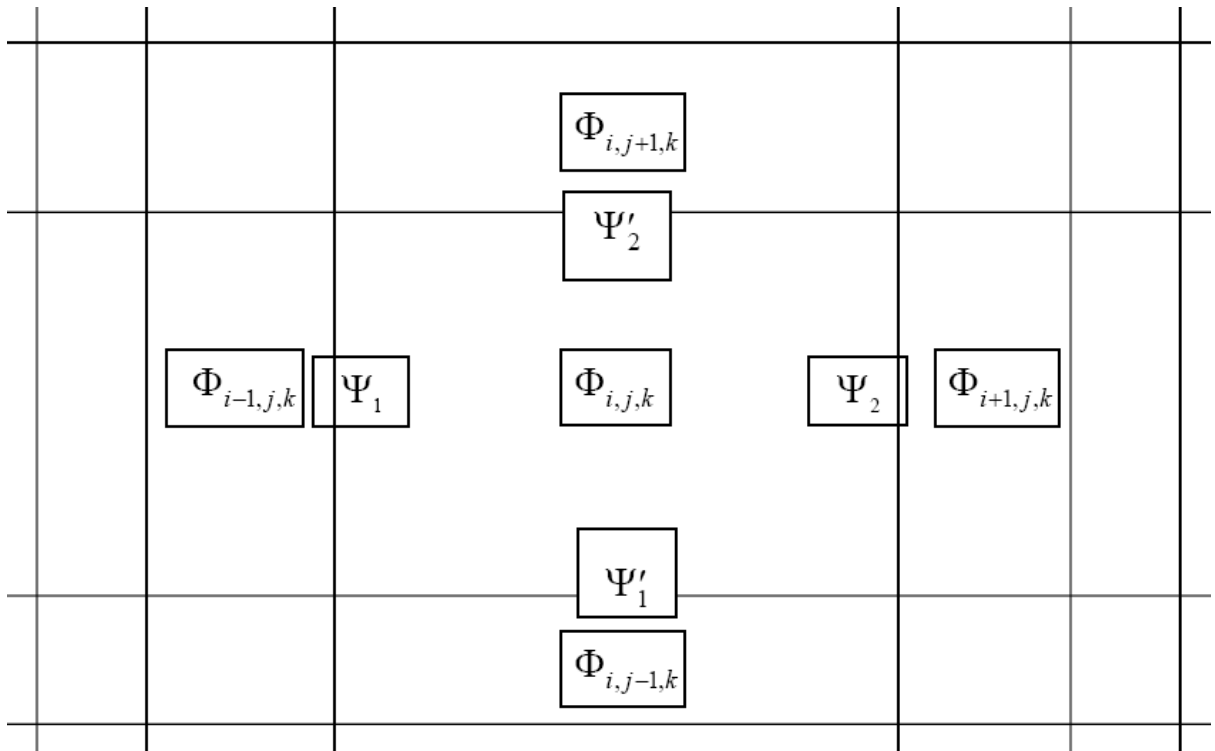
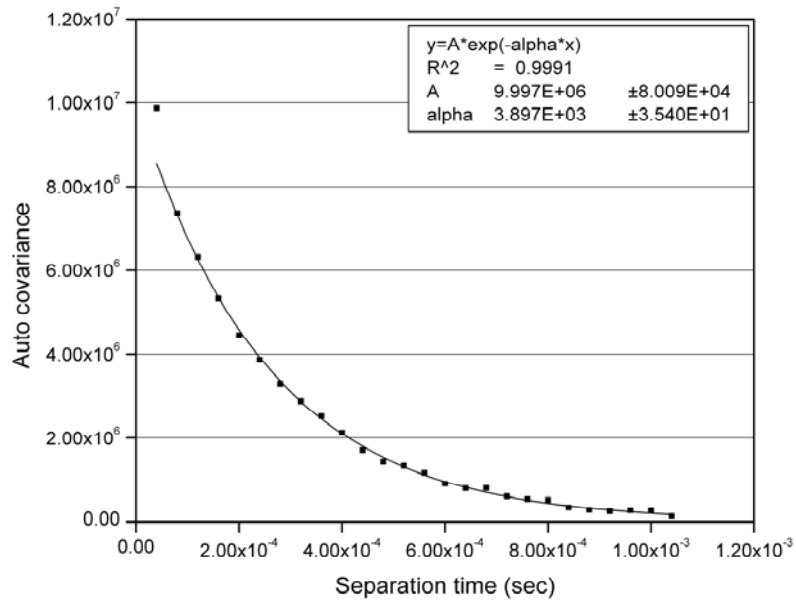
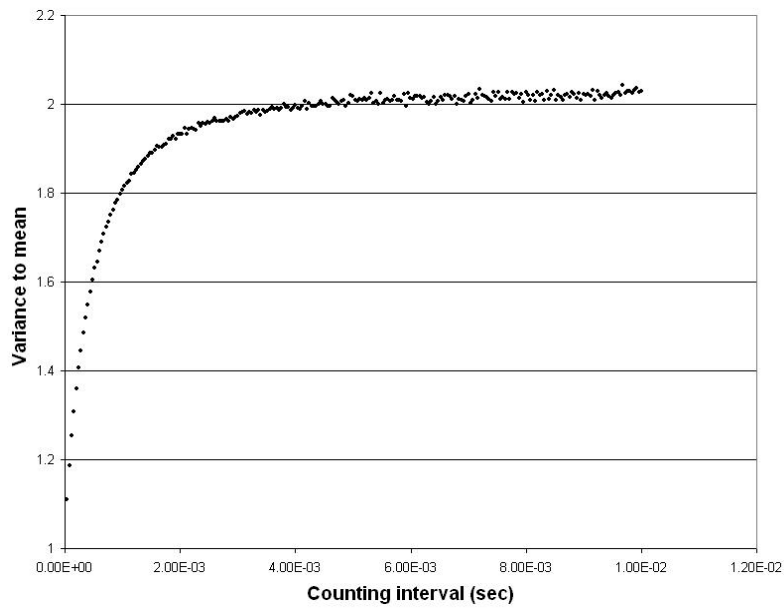


**Fig. 6.3:** Mesh arrangement in finite differencing scheme

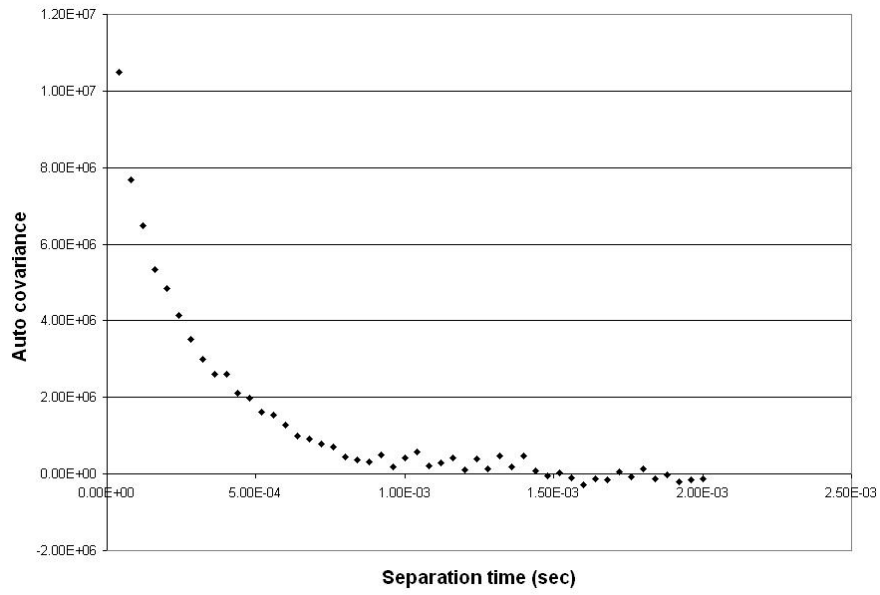


(a)

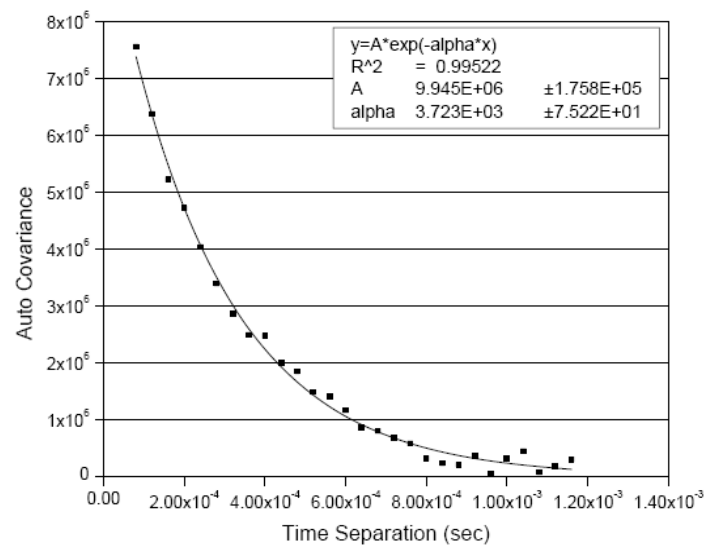


(b)

**Fig. 6.4** (a) Plot of the auto covariance of the count rate with the time separation with symmetrically placed detectors at the zeros of the first symmetric harmonics. After removing the first point, the single exponential fit is almost exact and gives a value of  $\alpha$  close to the expected value. (b) Plot of the variance to mean ratio with the counting interval length with symmetrically placed detectors at the zeros of the first symmetric harmonics.

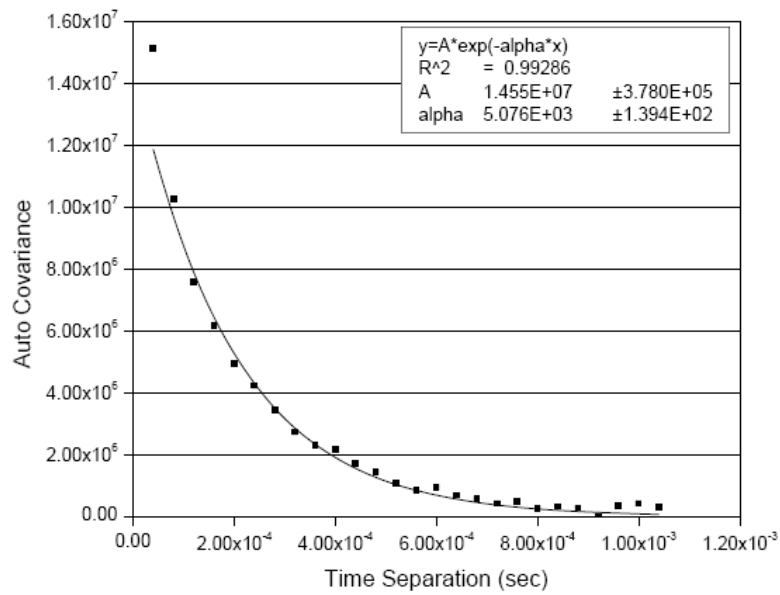


(a)

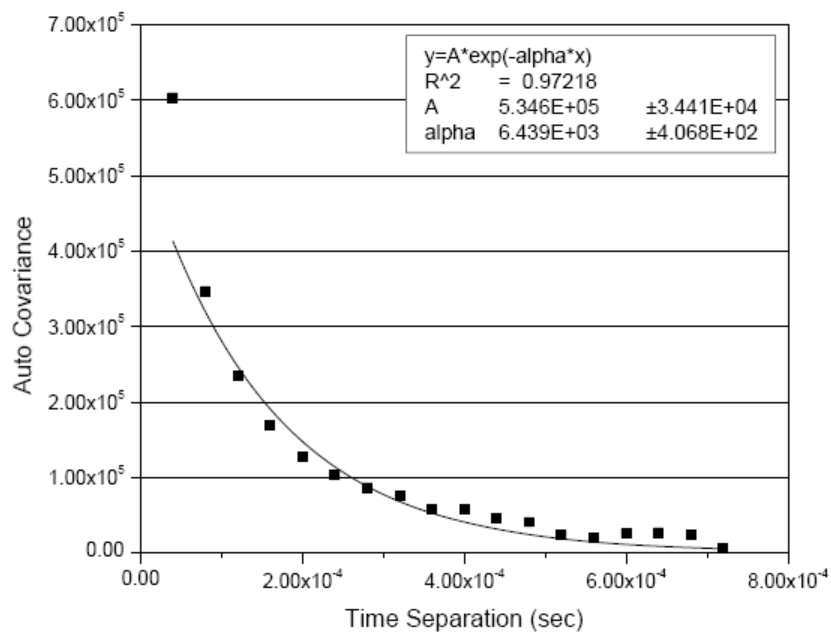


(b)

**Fig. 6.5** (a) Plot of the auto covariance of the count rate with the time separation with symmetrically placed detectors at the zeros of the first symmetric harmonics with inclusion of delayed neutrons. Note that the auto covariance reaches an approximately constant value after 1 ms due to delayed neutrons. (b) Plot of the auto covariance of the count rate with the time separation with symmetrically placed detectors at the zeros of the first symmetric harmonics after subtracting the delayed neutron contribution. The exponential fit is good and gives a value of alpha close to the expected value.

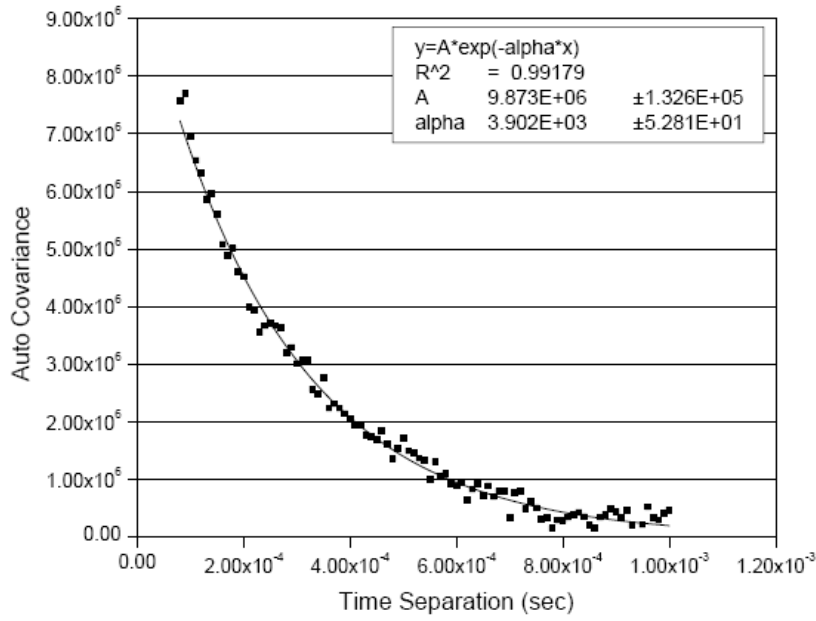


(a)

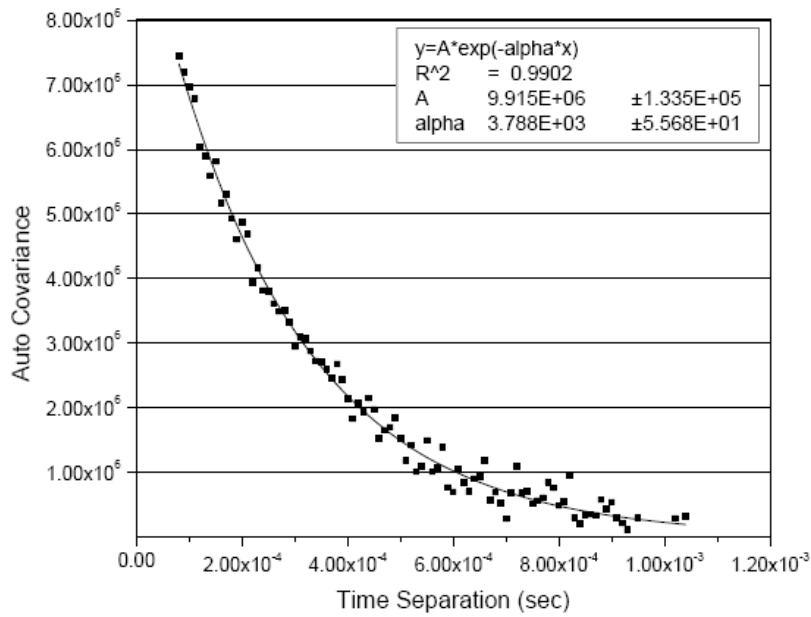


(b)

**Fig. 6.6** (a) Plot of the auto covariance of the count rate with the time separation with detectors placed symmetrically but away from the zeros of the first symmetric harmonics. The exponential fit is not good nor does it give a value of  $\alpha$  close to the expected value. (b) Plot of the auto covariance of the count rate with the time separation with detectors placed at the zeros of the first symmetric harmonics but in a single quadrant. The exponential fit is not good nor does it give a value of  $\alpha$  close to the expected value.

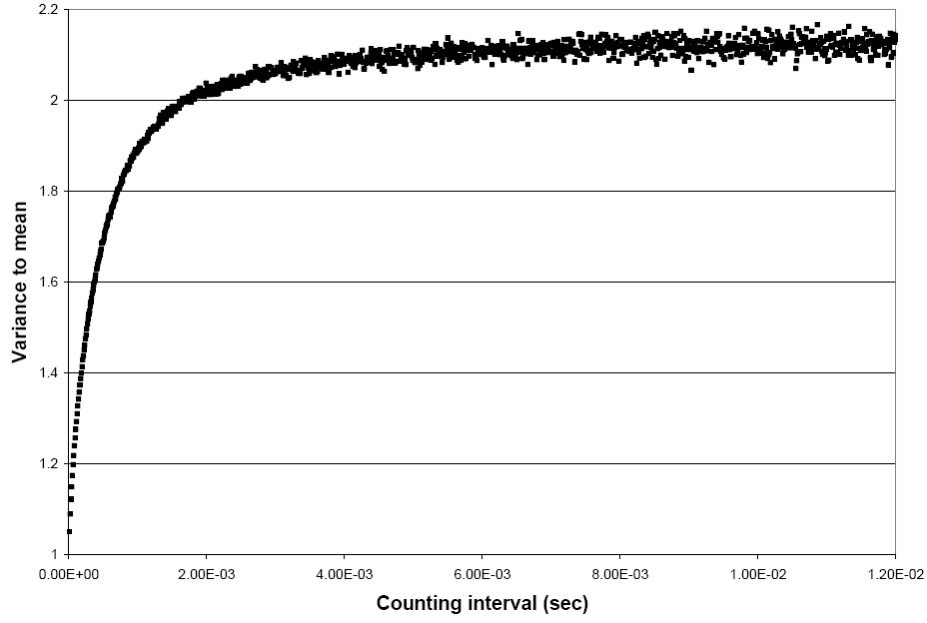


(a)

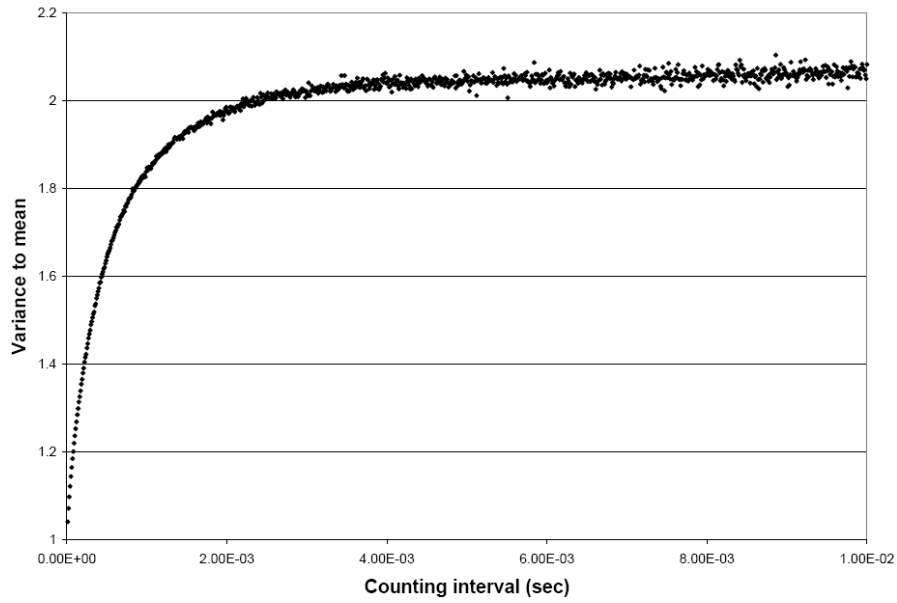


(b)

**Fig. 6.7** (a) Plot of the auto covariance of the count rate with the time separation with symmetrically placed detectors at the zeros of the first symmetric harmonics as simulated by few group diffusion theory based analogue Monte Carlo code with coarse mesh size. (b) Plot of the auto covariance of the count rate with the time separation with symmetrically placed detectors at the zeros of the first symmetric harmonics as simulated by few group diffusion theory based analogue Monte Carlo code with fine mesh size.



(a)



(b)

**Fig. 6.8** (a) Plot of the variance to mean ratio with the counting interval length with symmetrically placed detectors at the zeros of the first symmetric harmonics as simulated by few group diffusion theory based analogue Monte Carlo code with coarse mesh size. (b) Plot of the variance to mean ratio with the counting interval length with symmetrically placed detectors at the zeros of the first symmetric harmonics as simulated by few group diffusion theory based analogue Monte Carlo code with fine mesh size.

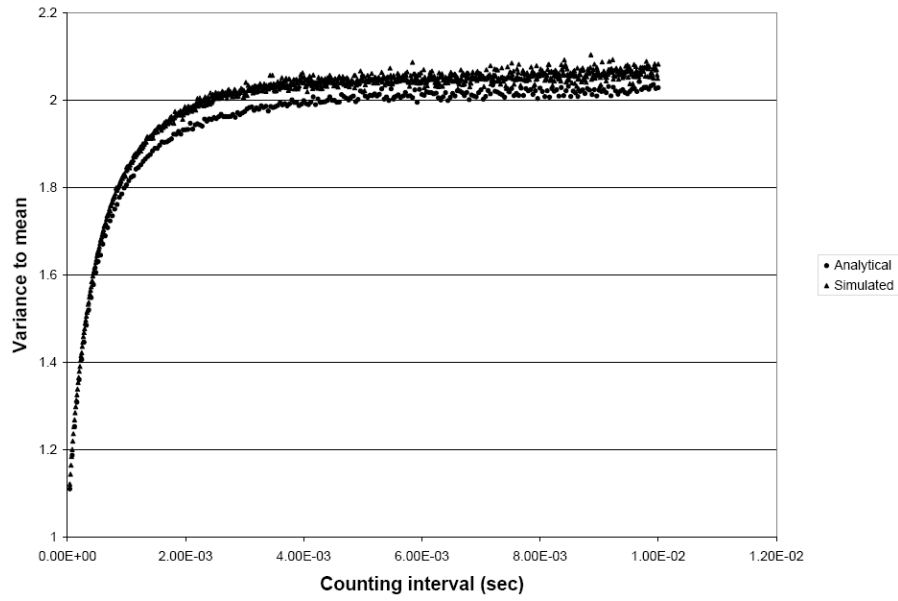


**Fig. 6.9:** Plot of the variance to mean ratio with the counting interval length with symmetrically placed detectors at the zeros of the first symmetric harmonics- a comparison of the results obtained by analytical diffusion theory based kernels and simulation (for fine mesh structure) by few group diffusion theory based analogue Monte Carlo code.

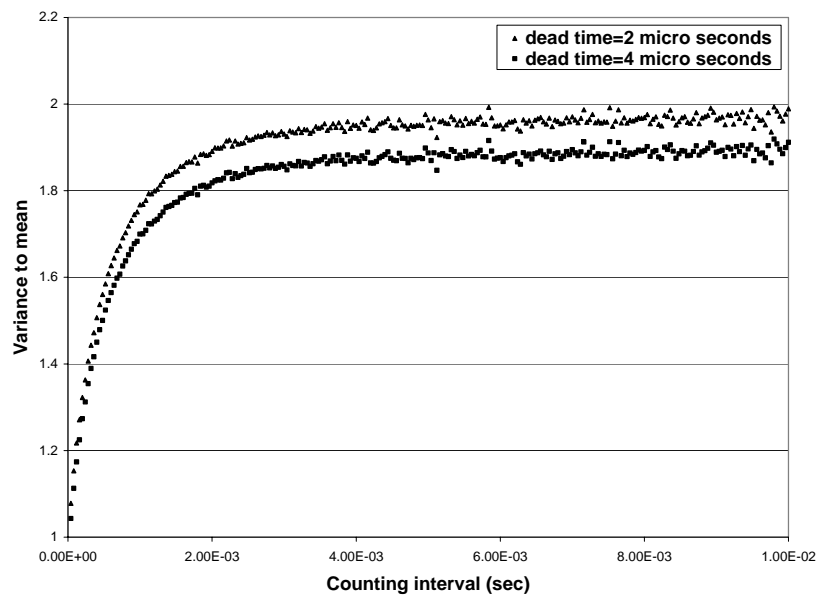


**Fig. 6.10** Variance to mean ratios for non-paralyzable dead-times of 2 and 4 micro seconds

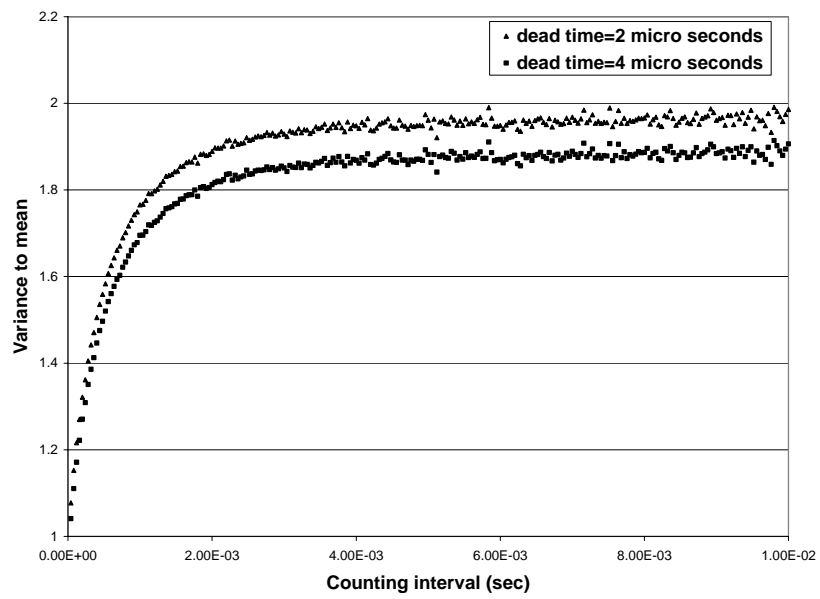


**Fig. 6.11** Variance to mean ratios for paralyzable dead-times of 2 and 4 micro seconds

### Summary and Conclusions

As part of our program on R & D of ADS, we have carried out theoretical studies on the development of reactor noise methods for measuring sub-criticality of such systems. The principal difference between reactor noise in ADS and traditional reactors, as also between our approach and that followed by other authors (Pazsit and Yamane, 1998a,b; Kuang and Pazsit, 2000; Behringer and Wydler, 1999; Munoz-Cobo et al., 2001), lies in the characteristics of the external source. As elaborated in section 2.2.3 of chapter 2, there are reasons to believe that the accelerator produced neutron source cannot be assumed to be a Poisson process. An immediate consequence of this is that the commonly used approaches in traditional reactor noise theory such as the Kolmogorov forward equation and the Bartlett formula are not applicable to the study of reactor noise in ADS.

Thus, it is necessary to have a different theoretical approach to the subject. In view of this, a theory of reactor noise in ADS considering periodically pulsed source and its non-Poisson character was developed earlier by Degweker (2000, 2003). The theory has been further developed in the thesis as outlined below.

In chapter 3, we have characterized the non-Poisson source by considering exponentially correlated Gaussian statistics of the proton beam intensity. We have also treated pulses of finite widths by considering rectangular and Gaussian pulse shapes. Expressions for various noise descriptors have been obtained. In chapter 4, we have extended the theory to include the effect of delayed neutrons. The source is considered to be a periodic sequence of delta function pulses with non-Poisson character. Two cases have been considered. In one case it is

assumed that there is no correlation between different source pulses while in the other case we have considered a specific model viz. exponential correlation between the proton pulses. We have derived expressions for Rossi alpha and Feynman alpha formulae. For further extension of the theory of reactor noise in ADS to the more general case of correlated non-Poisson pulsed sources with finite pulse width including delayed neutrons, we have followed the Langevin approach in chapter 5. We have obtained the PSD of the reactor noise in ADS for the general case described above.

Experimental studies are planned (Rasheed et al., 2010) to be carried out in the upcoming Purnima sub-critical facility at BARC to study pulsed neutron and noise methods for measuring the sub-critical reactivity of ADS and to interpret the results in the light of the above theory. As a part of the planning of these experiments, we have developed a few group diffusion theory based analogue Monte Carlo code for simulating the proposed experimental set-up. The simulator incorporates delayed neutron effects and dead time effects. The development of the simulator and some results obtained are described in chapter 6.

The main conclusions of our studies are as follows.

The correlations in the source fluctuations introduce additional terms which could confuse interpretation of alpha measurements by the variance method. The variance method is likely to suffer most from the presence of other sources of fluctuations. The Rossi alpha, correlation and spectral density methods might perform better in this case. On the other hand, correlations between the numbers of neutrons emitted in different pulses give rise to extra terms. Calculation of Rossi alpha shows that if correlation times are greater than or of the order of the prompt neutron decay times, it will be difficult to use methods such as Rossi alpha. The importance of the delayed neutron contributions will be most clearly felt in those situations where the prompt and delayed time scales are not very distinct and the formulae

derived by us would serve as corrections even on prompt neutron time scales. The Langevin approach is capable of correctly describing the non-Markov process resulting from a non-Poisson source. We have shown that a complete description of the spallation neutron source is possible by treating it as a combination of an internal noise given by the Schottky prescription and another that is of external origin arising from the proton beam. With such a description, we have obtained the PSD of ADS reactor noise complete with delayed neutrons, finite pulsed width, and correlations if any between proton pulses. The simulator gives a fairly realistic picture of the kind of results that may be expected with regard to the errors and the accuracy that may be expected from actual measurements. Simulations of proposed Purnima sub-critical assemblies show that proper location of detectors gives an almost single exponential (fundamental mode) response making alpha measurements by the noise methods possible even in deeply sub-critical systems.

Further studies on the subject can be carried out along the lines given below.

If noise methods are to be used for sub-criticality measurements, experimental studies on the statistical characteristics of the proton bunches should be carried out. Since the Feynman alpha method has been studied in several experimental facilities, it would be worthwhile to look for non-Poisson behavior of the source. A study of the variation of the Feynman Y function with the degree of sub-criticality would bring out the relative contributions from the external source and from the fission source. It is also important to study the current fluctuation statistics of ion beams from accelerators, either theoretically or experimentally. Our treatment of reactor noise in ADS is limited to very low power systems and we have completely disregarded the effects of thermal hydraulic feedbacks and other noise sources which are expected to be important in an operating power reactor. It will be worthwhile to investigate these effects. Finally, development of a robust procedure for diffusion in multi-media, and which does not use numerical approximations such as finite differencing, remains

an interesting problem which needs to be studied further. A more accurate simulation of the process using time dependent analogue Monte Carlo is being attempted (Singh and Degweker).

## References:

**Abanades, A. et al. (2002)**, “Results from the TARC experiment: spallation neutron phenomenology in lead and neutron-driven nuclear transmutation by adiabatic resonance crossing,” *Nucl. Instr. Meth. A*, **478(3)**, 577

**Abbondanno, U. et al. (2002)**, “Neutron capture measurements at the CERN-nTOF facility for ADS applications,” [http://dababneh.com/Articles/csgrs11\\_proc\\_FG.pdf](http://dababneh.com/Articles/csgrs11_proc_FG.pdf)

**Abderahim, H. A. (2005)**, “Myrrha Project – ADS Related R&D and Nuclear Data,” *DAE-BRNS National Workshop on Nuclear Data for Reactor Technology and Fuel Cycle, Mumbai, India*

**Abderrahim, H. A. et al. (2001)**, “MYRRHA: A multipurpose accelerator driven system for research & development,” *Nucl. Instr. Meth. A*, **487**

**Ackasu, A. Z. and Stolle, A. (1989)**, “Comments on the Noise Equivalent Source in the Langevin Technique,” *Ann. Nucl. Energy*, **16(10)**, 493

**Ackasu, A. Z. and Osborn, R. K. (1966)**, “Application of Langevin’s Technique to Space- and Energy-Dependent Noise Analyses,” *Nucl. Sci. Eng.*, **26**, 13

**Ackerman, J. P. et al. (1997)**, “Treatment of wastes in the IFR fuel cycle,” *Prog. Nucl. Energy*, **31 (1-2)** 141

**Adonai Herrera-Martínez et al. (2007)**, “Transmutation of nuclear waste in accelerator-driven systems: Fast spectrum,” *Ann. Nucl. Energy*, **34(7)**, 564

**Albrecht, R. W. (1962)**, “The Measurement of Dynamic Nuclear Reactor Parameters Using the Variance of the Number of Neutrons Detected,” *Nucl. Sci. Eng.*, **14**, 153

- Andriamonje, S. et al. (1995)**, “Experimental determination of the energy generated in nuclear cascades by a high energy beam,” *Physics letters B*, **348**, 697-709
- Arcipiani, B. and Pacilio, N. (1980)**, “A discussion of the forward and backward Kolmogorov equations for multiplying systems,” *Ann. Nucl. Energy*, **7**, 553
- Babala, D. (1967)**, “Point-reactor theory of Rossi-alpha experiment,” *Nucl. Sci. Eng.*, **28**, 237
- Babala, D. (1966)**, “Neutron counting statistics in nuclear reactors,” *Report KR-114*
- Baeten, P. et al. (2010)**, “Determination of the sub-criticality level using the  $\text{Cf}^{252}$  source-detector method,” *Ann. Nucl. Energy*, **37**, 740
- Ballester, D. and Munoz-Cobo, J. L. (2006)**, “The Pulsing CPSD Method for Subcritical Assemblies Driven by Spontaneous and Pulsed Sources,” *Ann. Nucl. Energy*, **33**, 281
- Ballester, D. and Munoz-Cobo, J. L. (2005)**, “Feynman-Y function for a subcritical assembly with intrinsic spontaneous fissions driven by external pulsed sources,” *Ann. Nucl. Energy*, **32**, 493
- Bays, S. et al. (2009)**, “Minor Actinide Recycle in Sodium Cooled Fast Reactors Using Heterogeneous Targets,” *INL/CON-09-15505, Advances in Nuclear Fuel Management IV*, South Carolina, USA
- Bartholomew, G. A. (1965)**, “The AECL Symposium on the Generation of Intense Neutron Fluxes,” *AECL-2177, Chalk River, Ontario*
- Bartlett, M. S. (1955)**, “An introduction to stochastic processes,” *Cambridge University Press, Cambridge*
- Beaman, S. L., and Aitken, E. A. (1976)**, “Feasibility Studies of Actinide Recycle in LMFBR's as a Waste Management alternative,” *ANS annual meeting, Toronto, Canada*
- Beck, J. M. and Pincock, L. F. (2011)**, “High Temperature Gas-Cooled Reactors Lessons Learned Applicable to the Next Generation Nuclear Plant,” *INL/EXT-10-19329*

- Behringer, K. and Wydler, P. (1999),** “On the Problem of Monitoring Neutron Parameters of the Fast Energy Amplifier,” *Ann. Nucl. Energy*, **26**, 1131
- Bell, G. I. (1965),** “On the stochastic theory of neutron transport,” *Nucl. Sci. Eng.*, **21**, 390
- Beller, D. (2004),** “Overview of the Reactor-Accelerator Coupling Experiments (RACE) project,” [http://www.oecd-nea.org/pt/docs/iem/lasvegas04/11\\_Session\\_V/S5\\_04.pdf](http://www.oecd-nea.org/pt/docs/iem/lasvegas04/11_Session_V/S5_04.pdf)
- Bennett, E. F. (1960),** “The Rice formulation of pile noise,” *Nucl. Sci. Eng.*, **8**, 53
- Bergelson, B. R. et al. (2007),** “Operation of CANDU power reactor in thorium self-sufficient fuel cycle,” *Pramana-J. Phys.*, **68** (2), 143
- Billebaud, A. et al. (2009),** “The GUINEVERE Project for Accelerator Driven System Physics,” *International conference GLOBAL 2009 “The Nuclear Fuel Cycle: Sustainable Options and Industrial Perspectives,” Paris, France*
- Bowman, C. D. (1992),** “Nuclear energy generation and waste transmutation using intense thermal neutron source,” *Nucl. Instr. Meth. A*, **320**, 336
- Bowman, C. D. and Venneri, F. (1993),** “Options for weapons-plutonium burning using molten salt accelerator-driven sub-critical systems or reactors,” *18th session of the Erice International seminars on planetary emergencies, Italy*
- Bowman, C. D. (1997),** “Los Alamos National Laboratory ADS projects,” *Accelerator driven systems: Energy generation and transmutation of nuclear waste, Status Report, IAEA TECDOC 985*
- Bowman, C. D. (2000),** “Once-through thermal-spectrum accelerator-driven light water reactor waste destruction without reprocessing,” *Nucl. Tech.*, **132**, 66–93
- Bowman, C. D. (2011),** “Accelerators for sub-critical molten salt reactors,” *Proceedings of 2011 Particle Accelerator Conference, New York, USA*
- Breunlich, W. H. et al. (1989),** “Muon-Catalyzed Fusion,” *Annual Review of Nuclear and Particle Science*, **39**, 311

- Brolly, A. and Vertes, P. (2004)**, “Concept of an electron accelerator driven molten salt sub-critical reactor,” [http://www.oecd-neo.org/pt/iempt8/abstracts/Abstracts/Vertes\\_concabs.doc](http://www.oecd-neo.org/pt/iempt8/abstracts/Abstracts/Vertes_concabs.doc)
- Brunson, G. S. et al. (1957)**, “Measuring the prompt period of a reactor,” *Nucleonics*, **15(11)**, 132
- Carl-Magnus Persson et al. (2005)**, “Analysis of reactivity determination methods in the sub-critical experiment Yalina,” *Nucl. Instr. Meth. A*, **554**, 374
- Carta, M. and D’Angelo, A. (1999)**, “Sub-criticality level evaluation in accelerator driven systems by harmonic modulation of the external source,” *Nucl. Sci. Eng.*, **133**, 282
- Catsaros, N. et al. (2009)**, “Criticality qualification of a new Monte Carlo code for reactor core analysis,” *Ann. Nucl. Energy*, **36(11–12)**, 1689
- Cheol Ho Pyeon et al. (2011)**, “Preliminary study on the thorium-loaded accelerator-driven system with 100 MeV protons at the Kyoto University Critical Assembly,” *Ann. Nucl. Energy*, **38**, 2298
- Cisneros, A. et al. (2012)**, “Feasibility of Once Through Subcritical Cores Driven by an Accelerator Spallation Neutron Source,” *Fus. Sci.Tech.*, **61(1T)**, 431-435
- Claiborne, H. C. (1972)**, “Neutron-Induced Transmutation of High-Level Radioactive Waste,” *ORNL-TM- 3964*, Oak Ridge National Laboratory, Oak Ridge, TN
- Coates, David J. and Parks, G. T. (2010)**, “Actinide evolution and equilibrium in fast thorium reactors,” *Ann. Nucl. Energy*, **37**, 1076
- Cohn, C. E. (1960)**, “A simplified theory of pile noise,” *Nucl. Sci. Eng.*, **7**, 472
- Courant, E. D. and Wallace, P. R. (1947)**, “Fluctuations of the Number of Neutrons in a Pile,” *Physical Review*, **72(11)**, 1038
- Croff, A. G. et al. (1980)**, “Actinide Partitioning-Transmutation Program Final Report I. Overall Assessment,” *ORNL-5566*, Oak Ridge National Laboratory, Oak Ridge, TN

- Dalfes, A. (1966),** “The random processes of a nuclear reactor and their detection,” *Nukleonik*, **8**, 94
- Davidenko, V. A. (1970),** “On Electronuclear Breeding,” *translated from Atomnaya Energiya*, **29(3)** 158–162
- Degweker, S. B. (1994),** “A forward equation for stochastic neutron transport”, *Ann. Nucl. Energy*, **21(9)**, 531
- Degweker, S. B. et al. (1999),** “Accelerator driven sub-critical systems with enhanced neutron multiplication,” *Ann. Nucl. Energy*, **26(2)**, 123-140 (1999)
- Degweker, S. B. (2000),** “Some Variants of the Feynman Alpha Method in Critical and Accelerator Driven Sub-critical Systems,” *Ann. Nucl. Energy*, **27(14)**, 1245
- Degweker, S. B. (2001a),** “Accelerator driven energy production: a comment,” *Ann. Nucl. Energy*, **28(14)**, 1477
- Degweker, S. B. et al. (2001b),** “Sub-critical Reactor for Accelerator Driven Systems,” *Twelfth Annual Conference of the Indian Nuclear Society (INSAC-2001)*, Indore, India
- Degweker, S. B. et al. (2010),** “Neutronic Studies for Thorium Utilization in Accelerator Driven Systems,” *International Workshop on Accelerator Driven Sub-critical Systems and Thorium Utilization*, Virginia Tech, Blacksburg, Virginia
- Degweker, S. B. (2003),** “Reactor Noise in Accelerator Driven Systems,” *Ann. Nucl. Energy*, **30(2)**, 223
- Degweker, S. B. and Rana, Y. S. (2007),** “Reactor Noise in Accelerator Driven Systems-II,” *Ann. Nucl. Energy*, **34(6)**, 463
- Degweker, S. B. and Rana, Y. S. (2011),** “The Langevin Approach to Reactor Noise in Accelerator Driven Systems,” *Nucl. Sci. Eng.* **169**, 296
- Devan, K. et al. (2006),** “Photo-Neutrons Produced at the Pohang Neutron Facility Based on an Electron Linac,” *Journal of the Korean Physical Society*, **49(1)**, 89

- Difilippo, F. C. (1988)**, “Correlation of the Signals from Detectors in the Presence of a Stochastic Neutron Field,” *Nucl. Sci. Eng.*, **99**, 28-35
- Dragt, J. B. (1966a)**, “Accurate reactor noise measurements in a low power critical reactor,” *Nukeonik*, **8(4)**, 188
- Dragt, J.B. (1966b)**, “Reactor noise analysis by means of polarity correlation,” *Nukleonik*, **8(4)**, 225
- Ferrari, A. and Sala, P. R. (1996)**, “The Physics of High-energy Reactions,” Proceedings of the *Workshop on Nuclear Reaction Data and Nuclear Reactors Physics, Design and Safety, Trieste, Italy*
- Feynman, R. P. et al. (1956)**, “Dispersion of the neutron emission in  $U^{235}$  fission,” *J. Nucl. Energy*, **3**, 64
- Furukawa, K. et al. (1997)**, “Thorium cycle implementation through plutonium incineration by thorium molten-salt nuclear energy synergetics,” *IAEA-TECDOC-1319*
- Gandini, A. and Salvatores, M. (2002)**, “The Physics of Subcritical Multiplying Systems,” *J. Nucl. Sci. Tech.*, **39(6)**, 673
- Gandini, A. (1997)**, “Sensitivity analysis of source driven subcritical systems by the HGPT methodology,” *Ann. Nucl. Energy*, **24**, 1241
- Ghosh, Biplab and Degweker, S. B. (2004)**, “McBurn: A Continuous Energy Monte Carlo Burnup Code for Critical and Accelerator Driven Systems,” *Report, BARC/ThPD/594*
- Goeckerman, R. H. and Perlman, I. (1948)**, “Characteristics of Bismuth Fission with High Energy Particles,” *Phys. Rev.*, **73**, 1127
- Gohar, Y. et al. (2004)**, “Accelerator-Driven Sub-critical assembly: concept development and analyses,” *The RERTR-2004 international meeting on reduced enrichment for research and test reactors, Vienna*

**Gohar Y. and Smith D. L. (2010)**, “YALINA Facility A Sub-Critical Accelerator-Driven System (ADS) for Nuclear-Energy Research Facility Description and an Overview of the Research Program (1997-2008),” *ANL-10/05*

**Gregory, M. V. and Steinberg, M. (1967)**, “A Nuclear Transmutation System for Disposal of Long-Lived Fission Product Waste in an Expanding Nuclear Power Economy,” *BNL-11915, Brookhaven National Laboratory, Upton, NY*

**Gupta, H. C. (1991)**, “MONALI – Rev.1 “A Monte Carlo code for analyzing fuel assemblies of nuclear reactors,” *Report BARC-1543*

**Haubenreich, Paul N. and Engel, J. R. (1970)**, “Experience with the Molten-Salt Reactor Experiment,” *Nucl. Ap. & Tech.*, **8**

**Hiroshi Taninaka et al. (2011)**, “Feynman- $\alpha$  analysis for a thermal sub-critical reactor system driven by an unstable 14 MeV neutron source,” *J. Nucl. Sci. Tech.*, **48(9)**, 1272

**IAEA TECDOC 1319 (2002)**, “Thorium fuel utilization: Options and trends”

**IAEA Technical Reports Series No. 435 (2004)**, “Implications of Partitioning and Transmutation in Radioactive Waste Management”

**IAEA-TECDOC-1319**, “Thorium fuel utilization: Options and trends”

**IAEA Safety Standard Series No. GSG-1 (2009)**, “Classification of radioactive waste”

**Imel, G. et al. (2004)**, “The TRADE source multiplication experiments,” *PHYSOR 2004*

**Juraj Breza et al. (2010)**, “Study of thorium advanced fuel cycle utilization in light water reactor VVER-440,” *Ann. Nucl. Energy*, **37**, 685

**Kadi, Y. and Adonai Herrera-Martínez (2006)**, “Energy amplifier systems: simulation and experiments in the field,” *Nucl. Instr. Meth. A*, **562**, 573–577

**Kakodkar, A. (2008)**, “Evolving Indian Nuclear Programme: Rationale and Perspectives,” *Public Lecture, Indian Acad. Sci., Bangalore*, <http://www.dae.gov.in/lecture/iasc.pdf>

- Kapoor, S. S. (2001)**, “Roadmap for development of Accelerator Driven Sub-critical Reactor Systems,” *BARC/2001/R/004*
- Keepin, G. R. (1965)**, “Physics of Nuclear Kinetics,” *Addison Wesley, Reading, MA*
- Kitamura, Y. et al. (2005)**, “Calculation of the pulsed Feynman- and Rossi-alpha formulae with delayed neutrons,” *Ann. Nucl. Energy*, **32**, 671
- Kitamura, Y. et al. (2006)**, “Calculation of the stochastic pulsed Rossi-alpha formula and its experimental verification,” *Prog. Nucl. Energy*, **48**, 37
- Kobayashi, K. and Nishihara, K. (2000)**, “Definition of Subcriticality Using the Importance Function for the Production of Fission Neutrons,” *Nucl. Sci. Eng.*, **136(2)**, 272
- Kobayashi, K. (2005)**, “A rigorous weight function for neutron kinetics equations of the quasi-static method for subcritical systems,” *Ann. Nucl. Energy*, **32**, 763
- Koning, A. J. et al. (2007)**, “New Nuclear Data Libraries for Lead and Bismuth and Their Impact on Accelerator-Driven Systems Design,” *Nucl. Sci. Eng.*, **156(3)**, 357
- Kuang, Z. F. and Pazsit, I. (2000)**, “A Quantitative Analysis of the Feynman- and Rossi-Alpha Formulas with Multiple Emission Sources,” *Nucl. Sci. Eng.*, **136**, 305
- Kumawat, H. and Barashenkov, V. S. (2005)**, “Development of the Monte Carlo model CASCADE-2004 of high-energy nuclear interactions,” *Euro. Phys. J., A* **26**, 61
- Kuramoto, R. Y. R. et al. (2007)**, “Kinetic parameters determination through power spectral densities measurements using pulse-type detectors in the IPEN/MB-01 research reactor,” *International Nuclear Atlantic Conference - INAC 2007, Santos, SP, Brazil*
- Lindley, Benjamin A. and Parks, G. T. (2012)**, “Near-complete transuranic waste incineration in a thorium fuelled pressurized water reactor,” *Ann. Nucl. Energy*, **40**, 106
- Makai, M. (2008)**, “Comments on the Kinetic Parameters for Source-Driven Systems,” *Transport Theory and Statistical Physics*, **37(5 – 7)**, 550

- Mansani, L. et al. (2002)**, “Proposed sub-criticality level for an 80 MW<sub>th</sub> lead-bismuth cooled ADS,” *Seventh Information Exchange Meeting on Actinide and Fission Product Partitioning and Transmutation, Jeju, Republic of Korea*
- Matthes, W. (1962)**, “Statistical Fluctuations and their correlation in reactor neutron distributions,” *Nukleonik*, **4**, 213
- Matthes, W. (1966)**, “Theory of fluctuations in neutron fields,” *Nukleonik*, **8**, 87
- “MCNP — A General Monte Carlo N-Particle Transport Code,” *Report LA-UR-03-1987*
- Mihalczo, J. T. (1974)**, “The use of Californium-252 as a randomly pulsed neutron source for prompt neutron decay measurements,” *Nucl. Sci. Eng.*, **53**, 393
- Mihalczo, J. T. et al. (1990)**, “Dynamic sub-criticality measurements using the Cf<sup>252</sup>-source-driven noise analysis method,” *Nucl. Sci. Eng.*, **104**, 314
- Moore, M. N. (1964)**, “The Role of Reactor Dispersion Function in the Noise Field of a Reactor,” *Trans. Am. Nucl. Soc.*, **6(2)**, 213
- Mukaiyama, T. et al. (2001)**, “Review of research and development of accelerator-driven system in Japan for transmutation of long-lived nuclides,” *Prog. Nucl. Energy*, **38 (1-2)** 107
- Munoz-Cobo, J.L. and Verdu, G. (1987)**, “Neutron stochastic transport theory with delayed neutrons,” *Ann. Nucl. Energy*, **14(7)**, 327
- Munoz Cobo, J.L. and Difilippo, F. C. (1988)**, “Noise and Nonlinear Phenomena in Nucl. Systems,” *Proc. NATO Adv. Res. Wksp. Plenum, NY*
- Munoz Cobo J.L. et al. (2001)**, “Sub-critical Reactivity Monitoring in Accelerator Driven Systems,” *Ann. Nucl. Energy*, **28**, 1519
- Munoz-Cobo, J.L. et al. (2011)**, “Feynman-alpha and Rossi-alpha formulas with spatial and modal effects,” *Ann. Nucl. Energy*, **38**, 590
- NEA-OECD (1999)**, “Status and assessment report on actinide and fission product partitioning and transmutation”

- NEA-OECD (2002)**, “Accelerator-driven Systems (ADS) and Fast Reactors (FR) in Advanced Nuclear Fuel Cycles”
- Nifenecker, H. et al. (2001)**, “Basics of accelerator driven sub-critical reactors,” *Nucl. Instr. Meth. A*, **463(3)** 428
- Nifenecker, H. et al. (2003)**, “Accelerator Driven Sub-critical Reactors,” *IOP Publishing*
- Nomura, T. (1966)**, “Reactivity Measurements by Reactor Noise Analysis using Two-Detector Correlation Method,” *J. Nucl. Sci. Tech.*, **3(1)**, 14
- Norelli, F. et al. (1975)**, “Stochastic kinetics: Analytical solutions of detailed probability balance equations,” *Ann. Nucl. Energy*, **2**, 67
- Nuttin, A. et al. (2012)**, “Comparative analysis of high conversion achievable in thorium-fueled slightly modified CANDU and PWR reactors,” *Ann. Nucl. Energy*, **40**, 171
- Orndoff, J. D. (1957)**, “Prompt neutron periods of metal critical assemblies,” *Nucl. Sci. Eng.*, **2**, 450
- Pacilio, N. et al. (1976)**, “Toward a unified theory of reactor neutron noise analysis techniques,” *Ann. Nucl. Energy*, **3 (5-6)**
- Pal, L. (1958)** “On the theory of stochastic processes in nuclear reactors,” *Il Nuovo Cimento*, **7 (Suppl.)**, 25-42
- Pazsit, I. (1987)**, “Duality in transport theory,” *Ann. Nucl. Energy*, **14(1)**, 25
- Pazsit, I. and Yamane, Y. (1998a)**, “The Variance-to-Mean Ratio in Subcritical Systems Driven by a Spallation Source,” *Ann. Nucl. Energy*, **25(9)**, 667
- Pazsit, I. and Yamane, Y. (1998b)**, “Theory of neutron fluctuations in source driven sub-critical systems,” *Nucl. Instr. Meth. A*, **403**, 431
- Pazsit, I. and Arzhanov, V. (1999)**, “Theory of Neutron Noise Induced by Source Fluctuations in Accelerator Driven Sub-critical Reactors,” *Ann. Nucl. Energy*, **26**, 1371

- Pazsit, I. et al. (2004)**, “Theory and Analysis of the Feynman-Alpha Method for Deterministically and Randomly Pulsed Neutron Sources,” *Nucl. Sci. Eng.*, **148 (1)**, 67
- Pazsit, I. et al. (2005)**, “Calculation of the pulsed Feynman alpha formulae and their experimental verification,” *Ann. Nucl. Energy*, **32(9)**, 986
- Pazsit, I. and Pal, L. (2007)**, “Neutron fluctuations: a treatise on the physics of branching processes,” *Elsevier Ltd.*
- Pozzi, S. A. et al. (2012)**, “MCNPX-PoliMi for nuclear nonproliferation applications,” *Nucl. Instr. Meth. A*, **694(2)** 119
- Prael, R. E. and Madland, D. G. (2000)**, “The LAHET code system with LAHET2.8,” *Report, LA-UR-00-2140*
- Rana, Y. S. and Degweker, S. B. (2009)**, “Feynman Alpha and Rossi Alpha Formulae with Delayed Neutrons for Sub-critical Reactors Driven by Pulsed Non-Poisson Sources,” *Nucl. Sci. Eng.*, **162**, 117
- Rana, Y. S. and Degweker S. B. (2011)**, “Feynman-Alpha and Rossi-Alpha Formulas with Delayed Neutrons for Subcritical Reactors Driven by Pulsed Non-Poisson Sources with Correlation Between Different Pulses,” *Nucl. Sci. Eng.*, **169**, 98
- Rana Y. S. et al. (2013)**, “Diffusion Theory Based Analogue Monte Carlo for Simulating Noise Experiments in sub-critical Systems,” *Nucl. Sci. Eng.*, **174**, 245
- Rasheed, K. K. et al. (2010)**, “Proposed Experiments at BARC with Natural Uranium- Light Water Sub-critical Assembly Driven by 14 Mev Neutrons,” *presented at 4th Research Coordination Meeting of the Coordinated Research Project on Analytical and Experimental Benchmark Analyses of Accelerator Driven Systems, Mumbai, India*
- Ridikis, D. and Mitting, W. (1998)**, “Neutron production and energy generation by energetic projectiles: protons or deuterons?,” *Nucl. Instr. Meth. A*, **418(2-3)** 449

- Rosenthal, M. W. (1970)**, “Molten salt reactors: history, status, and potential,” *Nucl. Ap. & Tech.*, **8**
- Rubia, C. et al. (1995)**, “Conceptual Design of a Fast Neutron Operated High Power Energy Amplifier,” *Report CERN/AT/95-44 (ET)*
- Rugama, Y. et al. (2003)**, “Preliminary measurements of the prompt neutron decay constant in MASURCA,” *Prog. Nucl. Energy*, **43(1-4)**, 421
- Sa. Kondo et al. (1992)**, “SIMMER-III: An Advanced Computer Program for LMFBR Severe Accident Analysis,” *Proc. Int. Conference on Design and Safety of Advanced Nuclear Power Plants (ANP'92)*, Tokyo, Japan
- Sadiku, M. N. O. et al. (2006)** “Monte Carlo Analysis of Time Dependent Problems,” *Southeastcon Proceedings of the IEEE*
- Saito, K. (1967)**, “Noise-equivalent source in nuclear reactors,” *Nucl. Sci. Eng.*, **28**, 384
- Saito, K. (1979)**, “Source papers in reactor noise,” *Prog. Nucl. Energy*, **3**, 157
- Saleh, B. (1978)**, “Photoelectron Statistics,” *Springer, Berlin*
- Sandra Dulla et al. (2006)**, “Kinetic Parameters for Source Driven Systems,” *PHYSOR-2006, ANS Topical Meeting on Reactor Physics*
- Sheff, J. R. and Albrecht, R. W. (1966)**, “The space dependence of reactor noise-I (Theory),” *Nucl. Sci. Eng.*, **24**, 246; *see also* **Sheff, J. R. and Albrecht, R. W. (1966)**, “The space dependence of reactor noise-II (Calculations),” *Nucl. Sci. Eng.*, **26**, 207
- Si Shengyi (2009)**, “Roadmap Design for Thorium-Uranium Breeding Recycle in PWR,” *IAEA-CN-164-5S09*
- Shvedov, O. V. et al. (1997)**, “ADS Program in Russia,” *Status report on Accelerator driven systems: Energy generation and transmutation of nuclear waste, IAEA-TECDOC 985, D.4*, 313

**Singh, K. P. et al. (2009)**, “Iterative schemes for obtaining dominant alpha-modes of the neutron diffusion equation,” *Ann. Nucl. Energy*, **36** (8), 1086

**Singh, K. P. et al. (2011)**, “Iterative method for obtaining the prompt and delayed alpha-modes of the diffusion equation,” *Ann. Nucl. Energy*, **38** (9), 1996

**Singh, K. P. and Degweker, S. B.**, “Transport Theory Based Analogue Monte Carlo for Simulating Noise Experiments in sub-critical Systems,” *to be published*

**Sjostrand, N. G. (1956)**, “Measurements on a subcritical reactor using a pulsed neutron source,” *Arkiv for physic*, **11**(13), 233

**Soule, R. et al. (2004)** “Neutronic Studies in Support of ADS: The MUSE Experiments in the MASURCA Facility,” *Nucl. Sci. Eng.*, **148**, 124-152

**Srinivasan, M. (1967)**, “On the measurement of alpha by a simple dead time method,” *Nukleonik*, **10**, 224

**Srinivasan, M. and Sahni, D. C. (1967)**, “Modified statistical technique for the measurement of alpha in fast and intermediate reactor assemblies,” *Nukleonik*, **9**, 155

**Steinberg, M. et al. (1979)**, ‘The Linear Accelerator Fuel Enricher Regenerator (LAFER) and Fission Product Transmutor (APEX),” *BNL-26951, Brookhaven National Laboratory, Upton, NY.*

**Stribel, T. (1963)**, “Neutron lifetime and reactivity measurements in thermal reactors with the help of the Rossi-alpha method,” *Nukleonik*, **5**, 170

**Sugawara, T. et al. (2011)**, “Nuclear data sensitivity/uncertainty analysis for XT-ADS,” *Ann. Nucl. Energy*, **38** (5), 1098

**Suzuki, T. et al. (2005)**, “Transient analyses for accelerator driven system PDS-XADS using the extended SIMMER-III code,” *Nucl. Eng. Design*, **235**(24), 2594

**Suzuki, E. (1966)**, “A Method for Measuring Absolute Reactor Power through Neutron Fluctuation,” *J. Nucl. Sci. Tech.* **3**(3), 98

- Szuta, M. and Wojciechowski, A. (2010)**, “Once through thorium based fuel cycle analysis of accelerator driven system for energy production and radioactive waste transmutation-impact on economy improvement,” *XX International Baldin Seminar on High Energy Physics Problems-“Relativistic Nuclear Physics & Quantum Chromodynamics,” Dubna, Russia*
- Tommasi, J. et al. (1995)**, “Long-lived waste transmutation in reactors,” *Nucl. Tech.*, **111**, 133
- Uhrig, R. E. (1970)**, “Random noise techniques in nuclear reactor systems,” *The Ronald press company, New York*
- Van Atta, C. M. (1977)**, “A brief history of the MTA project,” *UCRL-79151*
- Van Kampen, N. G. (1983)**, “Stochastic Processes in Physics and Chemistry,” *North Holland, Amsterdam*
- Veltman, B.P.T. and Kwakernaak, H. (1961)**, *Regelungstechnik* **9**, 357
- Venneri, F. et al. (1993)**, “Accelerator-Driven Transmutation of Waste (ATW): A new method for reducing the long-term radioactivity of commercial nuclear waste,” *Physics World*, **6**, 40
- Viatcheslav V. Anisimov et al. (2001)**, “A 14-MeV Intense Neutron Source Based on Muon-Catalyzed Fusion - I: An Advanced Design,” *Fus. Sci. Tech.*, **39 (2)** 198
- Wakabayashi, T. et al. (1997)**, “Feasibility studies of plutonium and minor actinide burning in fast reactors,” *Nucl. Tech.*, **118**, 14
- Williams, M. M. R. (1974)**, “Random Processes in Nuclear Reactors,” *Pergamon Press, Oxford*
- Yamamoto, T. (2011)**, “Higher order mode analyses in Feynman-alpha method,” *Ann. Nucl. Energy*, **38**, 1231

## LIST OF PUBLICATIONS

1. **Degweker, S. B. and Rana, Y. S. (2007)**, “Reactor Noise in Accelerator Driven Systems-II,” *Ann. Nucl. Energy*, **34(6)**, 463
2. **Rana, Y. S. and Degweker, S. B. (2009)**, “Feynman Alpha and Rossi Alpha Formulae with Delayed Neutrons for Sub-critical Reactors Driven by Pulsed Non-Poisson Sources,” *Nucl. Sci. Eng.*, **162**, 117
3. **Rana, Y. S. and Degweker, S. B. (2011)**, “Feynman-Alpha and Rossi-Alpha Formulas with Delayed Neutrons for Subcritical Reactors Driven by Pulsed Non-Poisson Sources with Correlation Between Different Pulses,” *Nucl. Sci. Eng.*, **169**, 98
4. **Degweker, S. B. and Rana, Y. S. (2011)**, “The Langevin Approach to Reactor Noise in Accelerator Driven Systems,” *Nucl. Sci. Eng.*, **169**, 296
5. **Rana Y. S., Singh, Arun and Degweker, S. B. (2013)**, “Diffusion Theory Based Analogue Monte Carlo for Simulating Noise Experiments in sub-critical Systems,” *Nucl. Sci. Eng.*, **174**, 245